Firing Dynamics of Thalamic Neurones During Genetically Determined Experimental Absence Seizures

A thesis submitted to Cardiff University for the

degree of Doctor of Philosophy

by

Cian McCafferty BSc (Hons)

School of Biosciences, Cardiff University, February 2014

Declaration and Statements

No portion of this thesis has been submitted in substance for any other degree or award at this or any other university or place of learning, nor is being submitted concurrently in candidature for any degree or other award.

Signed ……. (candidate) Cian McCafferty

This thesis is the result of my own work except where otherwise indicated by specific reference, and any views expressed are my own.

Signed ……. (candidate) Cian McCafferty

I hereby give permission for my thesis, if accepted, to be made available for photocopying and for inter-library loan, and for the title and summary to be made available to outside organisations.

Signed ……. (candidate) Cian McCafferty

Summary

Absence seizures (ASs) are the predominant form of seizure featuring in the idiopathic generalised epilepsies, and are the only seizure type of childhood absence epilepsy. They are characterised by behavioural arrest, impairment of consciousness and an electrographic signature of spike-and-wave discharges (SWDs) and are associated with psychosocial and cognitive impairment of development. The seizures are known to arise in the thalamocortical network, but the firing dynamics of thalamic neurones during seizure is not known. *In vivo* and *in vitro* studies have yielded contradictory results, suggesting predominant silence and regular burst firing respectively, but no studies have previously recorded from intact, single thalamic neurones in a freely moving model of absence epilepsy.

In this thesis it has been shown that, in Genetic Absence Epilepsy Rats from Strasbourg, thalamocortical (TC) neurones are mostly either silent or fire single spikes irregularly but synchronously during AS. T-type calcium channel-mediated bursts in neurones of the reticular thalamic nucleus (nRT) were frequently observed during full seizure expression. These cells expressed varied firing patterns ranging from regular burst firing to predominant silence, with similarly varying degrees of synchrony. It is also suggested that the nRT burst firing observed may be required for seizure generation. T-type calcium channel-mediated burst firing of TC neurones is neither necessary for, nor commonly observed in, the full generation or propagation of absence seizures

These results suggest that TC neurones are predominantly silent during AS. This is compatible with the idea of a cortical seizure initiator and driver, as suggested by the cortical initiation site and cortical abnormalities observed in multiple experimental AS models. The observations herein also confirm that the temporal relationship between thalamic firing and SWDs previously observed in anaesthetised animals is maintained in the freely moving condition, but suggest that there is a greater incidence of asynchronous thalamic activity during AS (particularly of nRT neurones) than previously suggested.

The firing dynamics of thalamic neurones observed are a crucial step towards understanding TC network activity during AS, and provide a significant insight into the role of the thalamus in alterations of sensation, movement, and consciousness associated with these seizures.

Collaborations

Animal implantations and data collection in Chapter 3 were performed together with Dr. François David.

Acknowledgements

I wish to thank the people who have helped me over the course of my PhD.

Firstly I would like to thank my supervisor Vincenzo Crunelli, who has always been generous with his time and resources as well as conscientious in his supervision and scientific direction, for the opportunity to undertake this PhD.

All the members of the Crunelli lab for their help and advice on scientific issues, particularly Bill for statistics and experimental design, Hannah for surgical practice and treats as I was writing up, and François for TC network dynamics and spike sorting.

Marcello and Joscha for being willing to talk about anything and everything with me, and for reviving my interest in scientific enquiry at times when it was flagging – I would have been far less involved in, and less rewarded by my PhD without them.

Tim for always being up for a chat, impressing me with his competitive dedication to cycling, and for all his work as our lab manager.

Everyone who spent some time working in the lab, particularly Nihan and Brittany, for bringing some perspective of the wider world of neuroscience.

My parents, brother Rory, and the rest of my family for their constant support and interest in my somewhat esoteric chosen field of study, as well as their ability to put things in context and take the pressure off me when I needed that.

Finally and most importantly I would like to thank Gabster. For not letting me run away when I was writing up, for keeping me going with superhuman levels of positivity and support (and food), for making sure the last four years of my life would have been the best whatever I happened to be doing, and for generally being a better person than I could have ever realistically hoped to meet.

Table of Contents

Abbreviations

aCSF	Artificial cerebrospinal fluid
AMPA	α-amino-3-hydroxy-5-methyl-isoxazolepropionic acid
AP	Action potential
AS	Absence seizure
CAE	Childhood absence epilepsy
CNS	Central nervous system
dLGN	Dorsal lateral geniculate nucleus
EPSC	Excitatory postsynaptic current
EPSP	Excitatory postsynaptic potential
EEG	Electroencephalogram
$eGABA_AR$	Extrasynaptic $GABA_A$ receptor
ETX	Ethosuximide
FFT	Fast Fourier transform
fMRI	Functional magnetic resonance imaging
FPGE	Feline penicillin generalised epilepsy
GABA	γ-aminobutyric acid
$GABA_AR$	γ-aminobutyric acid receptor type A
$GABA_BR$	γ-aminobutyric acid receptor type B
GAERS	Genetic absence epilepsy rats from Strasbourg
GAT-1	GABA transporter type 1
GAT-3	GABA transporter type 3

GBL	γ-butyrolactone
GHB	γ-hydroxybutyrate
GHBR	γ-hydroxybutyrate receptor
GPCR	G-protein coupled receptor
HVA	High voltage activated
IGE	Idiopathic generalised epilepsy
ILAE	International League Against Epilepsy
i.m.	Intra-muscular
IPSC	Inhibitory postsynaptic current
IPSP	Inhibitory postsynaptic potential
i.p.	Intra-peritoneal
I_h	Hyperpolarisation-activated current
I_T	T-type Ca^{2+} current
JAE	Juvenile absence epilepsy
JME	Juvenile myoclonic epilepsy
KCl	Potassium chloride
KO	Knock-out
LFP	Local field potential
lh	Lethargic mutant mouse
LTCP	Low-threshold calcium potential
LVA	Low voltage activated
MoCtx	Motor cortex

mGluR	Metabotropic glutamate receptor
NEC	Non-epileptic control
NMDA	N-methyl-D-aspartate
nRT	Nucleus reticularis thalami
PET	Positron emission tomography
PTZ	Pentylenetetrazol
S1	Somatosensory cortex area 1
S2	Somatosensory cortex area 2
SSADH	Succinic semialdehyde dehydrogenase
stg	Stargazer mutant mouse
SWC	Spike-and-wave complex
SWD	Spike-and-wave discharge
tg	Tottering mutant mouse
TC	Thalamocortical
TTX	Tetrodotoxin
TM	Transmembrane
WAG/Rij	Wistar albino Glaxo rats from Rijswijk
WT	Wild-type
VB	Ventrobasal complex
VPL	Ventroposterolateral nucleus
VPM	Ventroposteromedial nucleus

Chapter 1 – Introduction

This section will introduce the scientific background informing the experiments undertaken in this thesis by discussing ASs, the TC network that plays a critical role in these seizures, the experimental models used to investigate the specifics of that role, and the current knowledge of the pathophysiology of ASs.

1.1 Absence Seizures

An epileptic seizure is defined as excessive and synchronous electrical activity among neurones (Blume et al., 2001). Seizures are classified into types according to two properties: their electroencephalographic signature, and their clinical behaviour. Structural imaging can also be used to distinguish between certain types of seizure (Wang et al., 2013). Both of these can include ictal and inter-ictal components. Epilepsies are neurological disorders featuring persistent recurrence of one or more seizure types as primary or sole symptoms. An epilepsy featuring multiple seizure types is defined as a syndrome (Engel, 2001). Such disorders are diagnosed not just according to the seizure types involved but also considering other factors including presence and scale of brain damage, comorbid disorders, and age of the patient.

Classifications of epileptic seizures by the International League Against Epilepsy divide them along two primary lines: focal versus generalized onset and idiopathic versus symptomatic pathogenesis (Engel, 2006a, 2006b; Berg et al., 2010). The former separates seizures that originate in a particular brain area from those that appear to initiate simultaneously across the neocortical surface as measured by the EEG. Focal seizures tend to be symptomatic and generalised to be idiopathic. However, not only are there exceptions to this association, but there are many seizures and syndromes that defy simple classification (ILAE, 1981, 1989; Blume et al., 2001; Engel, 2001; Leutmezer et al., 2002). The focal or generalised nature of a seizure is more of a continuum than a dichotomy, as exemplified by recent evidence indicating an initiation site in ASs [Fig. 1.1], the prototypical idiopathic generalised epilepsy (IGE) (Holmes et al., 2004; Gotman et al., 2005; Bai et al., 2010).

A typical AS is a non-convulsive seizure involving impairment of consciousness, loss of directed movement, and a 2.5 – 4Hz generalised spike-and-wave discharge (SWD) electrographic signature (Panayiotopoulos et al., 1989a). ASs are the sole symptom of childhood absence epilepsy (CAE) as well as a primary symptom of juvenile absence epilepsy (JAE) and juvenile

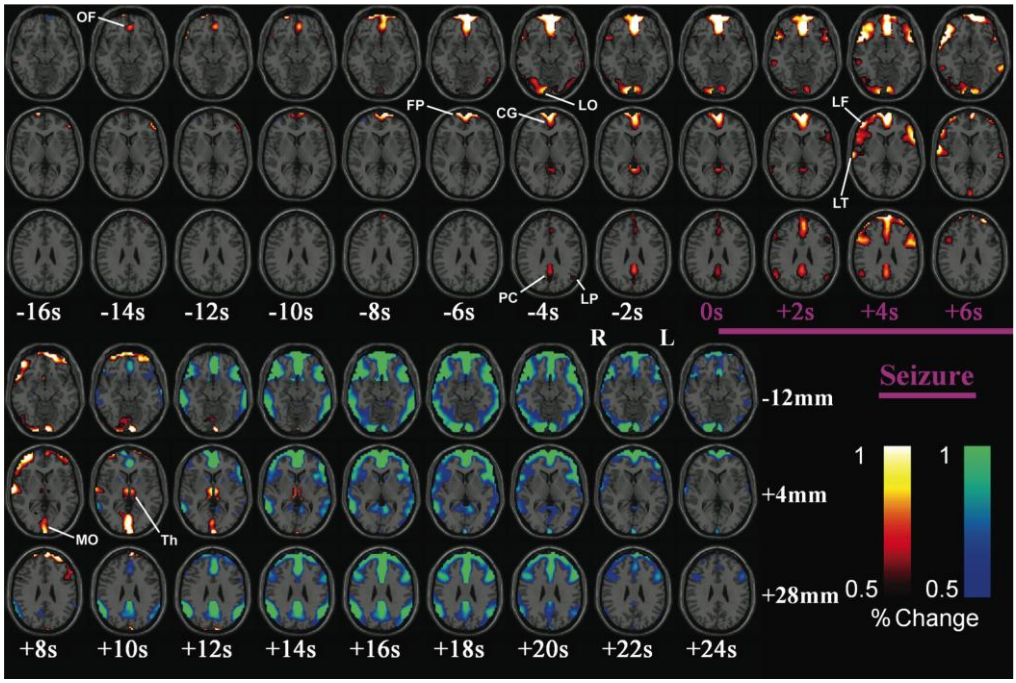

Figure 1.1 Initiation sites in AS –fMRI evidence

Positive signal changes are observed in BOLD fMRI in medial orbital frontal (OF) and frontal polar (FP) cortex more than 5 seconds before the onset of SWDs in 8 patients with CAE, with other increases in cingulate (CG), lateral parietal (LP), precuneus (PC), and lateral occipital (LO) cortex also preceding SWD onset. Thalamic (Th) increases were not observed until after seizure end. Warm colours denote fMRI percentage increases while cool colours denote decreases (taken from Bai et al., 2010).

myoclonic epilepsy (JME), all of which are categorised as IGEs. Of all the seizure types observed in IGEs, ASs are the most common, and also present as a primary symptom of myoclonic absence epilepsy (MAE), which is classed as symptomatic rather than idiopathic (Duncan, 1997; Janz, 1997) [TABLE 1.1].

The cellular and network mechanisms of ASs in their pure form can be studied in isolation in CAE, due to the lack of comorbid neurological conditions (ILAE, 1989). For this reason, the following description of ASs will primarily confine its clinical references to CAE and use this disease to explore the relevant properties of experimental models of ASs. Other syndromes that feature ASs as part of a more complex phenotype (Duncan, 1997) will be briefly mentioned when relevant. Certain experimental models may have particular significance for one or more of these diseases, and this will also be indicated when relevant.

1.1.1 Childhood Absence Epilepsy (CAE)

1.1.1.1 Clinical Features

CAE is an idiopathic generalised epilepsy occurring in pre-pubescent children. Absences are its sole seizure type, and begin between the ages of 2 and 8 years with a peak occurrence at approximately 6 years of age (ILAE, 1989). An AS lasts between 4 and 30 seconds, typically less than 15, with no preceding aura or post-ictal state. Its principle behavioural feature is an apparent loss of consciousness, which manifests itself as an interruption of on-going directed activity. There may be some limited automatisms, usually facial twitches or rapid blinking (Dreifuss, 1990; Duncan, 1997; Panayiotopoulos, 1997). Incidences per day range from a few to several hundred and are found preferentially in periods of inactivity or emotional stress (Horita et al., 1991) as well as appearing more frequently during transitions between (Baldy-Moulinier, 1992; Niedermeyer, 1996; Horita, 2001; Halász et al., 2002), and in states of, light wakefulness and superficial sleep (Kellaway et al., 1980; Kellaway, 1985; Halász et al., 2002). The relationship between ASs and sleep is a significant and controversial one (Kostopoulos, 2000; Beenhakker and Huguenard, 2009; Leresche et al., 2012), varying between and sometimes within epilepsy syndromes and animal models (see section 1.2). Ictal events are often inducible by hyperventilation (Duncan, 1997; Panayiotopoulos, 1997).

General consensus is that, during a seizure, patients are unresponsive to stimuli and suffer absolute abolition of directed motion. However, there is evidence that impairment of both motor output and sensory input is variable, with their extent depending on the patient, the particular episode, and on the complexity of the input/output in question (Blumenfeld, 2005).

Table 1.1 Generalised seizures

Generalised seizure type	Clinical features	EEG signature
Typical absence seizures	Loss of consciousness for 4-30 seconds, no aura, no postictal state, few automatisms	Spike-and-wave discharges (SWDs)
Tonic seizures	Sudden onset, tonic extension (rigidity) of head and trunk that lasts several seconds	Beta 'buzz'
Myoclonic seizures	Brief (<1sec) arrhythmic jerks that cluster within a few minutes, may evolve into clonic	Fast polyspike & slow wave complexes
Atonic seizures	Brief loss of postural tone	Beta 'buzz'
Generalised tonic-clonic seizures	Grand mal epilepsy: tonic then clonic seizures, prolonged postictal confusion	Bilateral complexes of spikes, polyspikes and slow waves

Modified from ILAE Commission: classification of epileptic syndromes (1989) and Engel (2001).

It has been established that, in certain cases, a sensory stimulus of sufficient potency terminates an AS. In fact, it may be argued that ASs range from complete abolition of sensory input and directed movement to 'sub-clinical' events with no obvious clinical impairment but subtle impairments of reaction time and motor performance (Blumenfeld, 2005; Sadleir et al., 2006). Thus, the loss of consciousness that is generally considered a critical feature of ASs is not necessarily absolute or even major.

ASs that are involved in other IGEs as one of multiple seizure types have been proposed to differ from those of CAE (Panayiotopoulos et al., 1989b). However, current evidence is that age, arousal and multiple other factors affect a patient's seizures and that these effects are sufficiently large to completely confound or mask any possible causative link between syndrome and seizure properties (Sadleir et al., 2008, 2009).

There are no other developmental or neurological abnormalities associated with pure CAE; neither are there any AS-related morphological alterations to the brain (Loiseau and Duche, 1995; Duncan, 1997; Panayiotopoulos, 1997; Woermann et al., 1998).

1.1.1.2 EEG Features

The EEG signature of an AS is considered one of the primary diagnostic features (Panayiotopoulos et al., 1989a; Duncan, 1997; Panayiotopoulos, 1997) and consists of bilaterally synchronous SWDs, with an apparently generalised origin, on a normal inter-ictal background. A SWD is so called due to its pattern of distinctively-shaped high-amplitude voltage deflections with a frequency of approximately 3 Hz [Fig. 1.2] (Williams, 1953; Panayiotopoulos, 1997; Stefan and Snead, 1997). The very start of a SWD is usually fast with an irregular waveform, and there is a gradual and smooth decline in frequency towards the end while the waveform remains regular (Panayiotopoulos et al., 1989a; Sadleir et al., 2006).

Studies suggest that EEG features and behavioural symptoms of ASs have variable temporal relationships. Cases have been reported of behavioural effects being restricted to the central section of a SWD (Shimazono et al., 1953; Goldie and Green, 1961; Mirsky and Van Buren, 1965), as well as initiating simultaneously with (Browne et al., 1974) or before the SWD (Mirsky and Van Buren, 1965).

The theory that ASs are not truly generalized but rather start in certain cortical regions before others was first suggested by the identification of an initiation site in the Wistar Albino Glaxo rat from Rijswijk (WAG/Rij) polygenic rat model, since confirmed in Genetic Absence Epilepsy

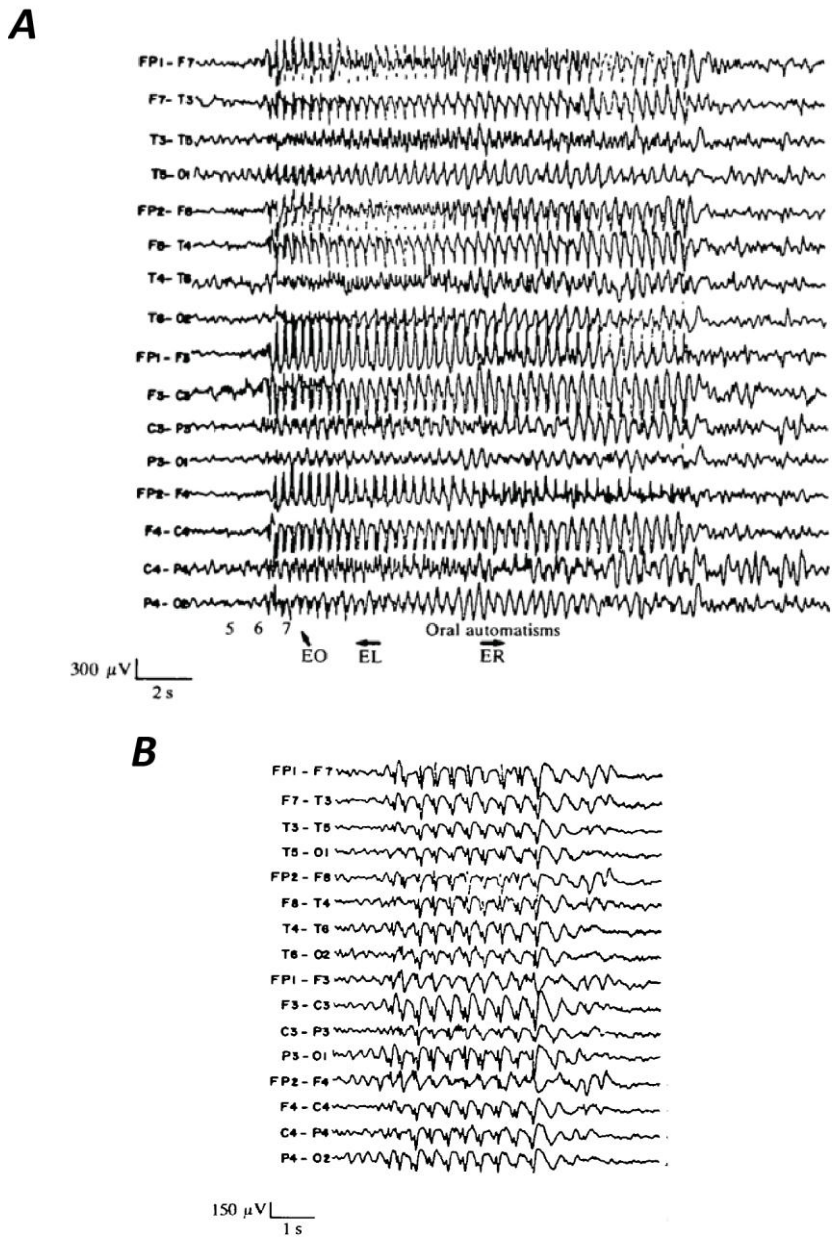

Figure 1.2 Appearance of a SWD

A EEG recording of a typical SWD from an 8-year-old girl with CAE. The seizure was induced by hyperventilation. Numbers at the bottom indicate breaths counted, with one breath counted after initiation of SWD. ***B*** Trace with expanded time scale showing spike-and-wave complexes (SWCs). Both from Panayiotopoulos et al (1989).

Rats from Strasbourg (GAERS) (Meeren et al., 2002; Polack et al., 2007, see section 1.2.3). Holmes et al., (2004) used dense-array EEG to identify consistent activation of the dorsolateral and orbital frontal lobe at the start of SWDs in humans. This study, carried out on ASs which were part of mixed IGE syndromes in adults, was later supported by EEG and fMRI studies (Bai et al., 2010; Berman et al., 2010; Szaflarski et al., 2010) showing similar dorsolateral and orbital frontal as well as some parietal activity before the start of seizure proper in CAE. Notably, location of the leading site varied between individuals (Gotman et al., 2005).

SWDs are also present in the thalamus during ASs (Williams, 1953; Velasco et al., 1989), and between this electrographic evidence and imaging studies (Prevett et al., 1995; Iannetti et al., 2001; Bai et al., 2010; Berman et al., 2010) there has formed widespread consensus that ASs are generated and/or propagated via dysfunctional behaviour in the TC network (reviewed in Crunelli and Leresche, 2002b; Kostopoulos, 2001; Blumenfeld, 2002). Therefore, although the contribution of other regions, such as the brainstem, to seizures has been identified in some studies (Feucht et al., 1998; Yeni et al., 2000), the TC network is the most promising area for investigation of neuronal activity relating to ASs (Crunelli and Leresche, 2002a).

1.1.1.3 Epidemiology & Aetiology

CAE has an incidence of between 2 and 8 children in 100,000 under 15 years of age (Loiseau et al., 1990; Sander, 1995), and between 2 and 10% of children with any other form of epilepsy will also have CAE (Desguerre et al., 1994). The disease is considered to be genetically determined, albeit with a complex and polygenic inheritance pattern. Concordance is from 70 to 85% between genetically identical monozygotic twins and 33% between first-degree relatives. There is a 16-45% positive family history (Bianchi and Italian LAE Collaborative Group, 1995; Berkovic, 1997; Berkovic et al., 1998).

Genes associated with CAE, whether by proband or association analysis studies, have tended to be involved either with GABAergic neurotransmission or with T-type Ca^{2+} channels. The few genetic mutations in probands with a CAE phenotype that have been identified so far have corresponded to genes or proteins known to be significant in animal models of ASs. However, association analysis in multiple ethnic groups has demonstrated that none of these mutations are essential for CAE development, and thus reinforced the idea of a complex, polygenic origin. This latter type of study has highlighted multiple susceptibility loci, some of which are lent greater significance by animal studies or related specific proband mutations (reviewed by Crunelli and Leresche, 2002a; Yalçın, 2012).

Two separate mutations in the *GABRG2* gene, which codes for the modulatory γ2 subunit of the $GABA_A$ receptor ($GABA_AR$), have been found in different families with CAE and febrile seizures (Wallace et al., 2001; Kananura et al., 2002). Although mimicking the first-discovered mutation causes an AS phenotype in mice (Tan et al., 2007), and both mutations impair protein function (Kananura et al., 2002; Kang and Macdonald, 2004), association analysis in Japanese and Chinese populations revealed no link of the *GABRG2* gene to CAE (Lu et al., 2002; Ito et al., 2005). A single CAE proband with a *GABRA1* mutation, coding for a truncated version of the α1 subunit of $GABA_AR$, has also been identified (Maljevic et al., 2006). Again there are no positive links from genome-wide association scans thus far (Ito et al., 2005).

There is significant evidence that the β3 subunit of the $GABA_AR$, encoded by *GABRB3*, can contribute to a CAE phenotype. As well as specific proband studies showing multiple mutations in this gene in Mexican families with CAE (Tanaka et al., 2008), association analysis has suggested a possible link with CAE sufferers from some, but not all, ethnic groups (Feucht et al., 1999; Urak et al., 2006; Hempelmann et al., 2007). As with *GABRG2*, mice with the same mutation exhibit ASs but only as part of a complex phenotype featuring multiple seizure types and bearing a resemblance to Angelman syndrome in humans (DeLorey et al., 1998).

Mutations in Ca^{2+} channels related to CAE are of particular interest to this thesis. A pair of mutations in *CACNA1A*, the α1A subunit of P/Q-type high voltage-activated Ca^{2+} channels (see section 1.4.1.1), has been found in patients with ASs comorbid with ataxia (Jouvenceau et al., 2001; Imbrici et al., 2004). Both mutations have been shown to reduce high voltage-activated (HVA) Ca^{2+} current to different degrees, which is mimicked in mouse models of ataxia and absence (tottering and leaner, see section 1.2.2) with *CACNA1A* mutations (Fletcher et al., 1996; Doyle et al., 1997; Wakamori et al., 1998; Fletcher and Frankel, 1999). Significantly, the HVA impairment in these mouse models as well as in a specific *CACNA1A* knockout mouse was shown to cause an increase in LVA T-type Ca^{2+} current in thalamic neurones, upon which the absence phenotype was apparently dependent (Zhang et al., 2002; Song et al., 2004).

CACNA1G, *CACNA1H*, and *CACNA1I,* which code for the three variants of the α1 subunit of T-type Ca^{2+} channels, have not been directly linked to any CAE probands but have had varying degrees of association demonstrated through genome-wide scans. *CACNA1G*, which is expressed in TC and cortical neurones among others (see section 1.4), has had both positive and negative associations with CAE in different populations (Chen et al., 2003b; Singh et al., 2007), as has the thalamic reticular nucleus (nRT)-expressed *CACNA1H* (Chen et al., 2003a; Heron et al., 2004; Khosravani et al., 2005; Chioza et al., 2006; Liang et al., 2006, 2007). This

suggests that, while the gene may be capable of playing a role in development of the phenotype, it is neither necessary nor sufficient on its own. In both cases animal model (Kim et al., 2001; Ernst et al., 2009; Powell et al., 2009) and cell line (Khosravani et al., 2004; Vitko et al., 2005, 2007) experiments, the former of which will be discussed in section 1.2, have suggested possible cellular and network effects of mutations in these genes.

The significant post-transcriptional splicing of *CACNA1H* appears to be related to its association with CAE (Zhong et al., 2006). Alternative splicing can create α1H proteins with varying degrees of functionality, as well as completely dysfunctional channels, some of which could contribute to the pathogenesis of ASs. *CACNA1I*, also expressed in the nRT, has been reported to have no associations with CAE as yet (Wang et al., 2006).

In summary, while there have been multiple genes associated with CAE either by detection of genetic variants in specific probands or by population-wide association analyses, no single gene has been ubiquitously linked with the disease. It thus appears certain that CAE is a disease of polygenic origin, and it cannot be ruled out that multiple, distinct underlying genetic dysfunctions may result in the expression of the same disease. This may or may not also be associated with phenotypical variation in the disease itself. Given the lack of concrete implication of any one gene, animal studies may usefully be taken into account when considering strength of association and suitability for further investigation.

1.1.1.4 Treatment

Ethosuximide (ETX) and sodium valproate (valproic acid) are the first choice treatments for ASs. Although historically there has been a consensus that both achieve high levels of success (between 70% and 80%) in treating seizures (Richens, 1995; Schachter, 1997), and this is supported by a recent retrospective study (Hwang et al., 2012), there has been a lack of methodologically sound, randomised controlled and double-blind trials (RCT) of efficacy. A systematic Cochrane review of clinical studies in 2010 concluded that there was insufficient evidence from well-designed trials to make any recommendations regarding clinical practice (Posner et al., 2010). Since the publication of this review, a large-scale (~150 subjects per group) RCT in CAE patients has suggested an efficacy after 16 weeks of therapy of only 53% for ETX and 58% for valproic acid, considerably lower than previous estimates. ETX was still recommended as the initial monotherapy in CAE due to the emergence of attentional deficits in a higher proportion of those patients receiving valproate (Glauser et al., 2010). These

deficits persisted in a 12-month follow up study, at which point the success rates of ETX and valproic acid were 45% and 44% respectively (Glauser et al., 2012).

Patients unresponsive to ETX can be prescribed sodium valproate, the less-effective lamotrigine, or a combination of two of the three (Schachter, 1997; Glauser et al., 2010). Each medication has its own adverse effects and interaction profile with other anti-epileptics and unrelated drugs (Patsalos and Perucca, 2003a, 2003b; French and Pedley, 2008). Medication used to treat convulsive seizures, including phenytoin, carbamazepine, vigabatrin and tiagabine, has been found to exacerbate (Panayiotopoulos et al., 1997; Schachter, 1997; Parker et al., 1998; Perucca et al., 1998) and even sometimes to induce (Schapel and Chadwick, 1996; Ettinger et al., 1999) ASs. Vigabatrin prevents GABA catabolism while tiagabine blocks its uptake from the synapse, both increasing the effective pool of GABA available to the synapse. Exacerbation of ASs by an increase in GABA would tend to suggest that theories involving a simple decrease in GABAergic neurotransmission being capable of generating ASs, either clinically or experimentally, are simplistic.

1.1.1.5 Prognosis

Prognosis is generally considered good for sufferers of CAE, although reported long-term remission rates are variable. All studies report high remission rates of CAE primary symptoms by the end of adolescence in children who do not develop generalised tonic-clonic seizures (GTCSs) before this point (Loiseau, 1992; Richens, 1995; Bouma et al., 1996; Callenbach et al., 2009). However, the tendency to develop GTCSs is increased when CAE is developed later in childhood (past 8 years of age), and some studies indicate an overall risk as high as 50% of such GTCS development (Bouma et al., 1996). There is also evidence that there can be long-term psychosocial and educational impairment after the remission of CAE itself in children who never suffered GTCSs (Wirrell et al., 1997; Pavone et al., 2001). Medication is usually withdrawn gradually after 2 seizure-free years (Panayiotopoulos, 1997).

1.1.2 Summary of human absence seizures

ASs are a type of non-convulsive epileptic seizures featuring in many IGEs. EEG and functional imaging evidence suggests a thalamocortical basis with a particular cortical site of origin. Aetiology is largely unknown, all methods of genetic analysis employed thus far having significant limitations. GABAergic neurotransmission and Ca^{2+} channels are implicated, but not conclusively. Treatment efficacy and remission rates are encouraging but there is evidence

that both have been over-reported. The pathophysiological mechanisms of the disease are still unknown, but are very likely to involve aberrant activity within the thalamocortical network.

1.2 Functional Anatomy of the Thalamocortical System

The TC system refers to particular neuronal populations of the thalamus and cortex that communicate by varied pathways and modes of synaptic organisation. All functions of the thalamus involve its relationship to the cortex while the majority of cortical afferents are thalamic in origin, and thus the functional connectivity between the two structures is of great significance to both. The primary role of the thalamocortical network, and therefore that of the thalamus itself, is considered to be in the processing of sensory and motor information originating from the peripheral nervous system, either en route to cortex or as part of a reciprocal communication with one or more cortical areas. The thalamus is also known to have a role in the modulation of arousal and consciousness (Schiff, 2008). Such functionality is likely to be related to, and inter-dependent with, its first- and higher-order sensory relay and processing.

Note: the following discussion will be concerned with the functional anatomy of both rat and human thalamocortical systems. The greater emphasis is on that of the rat as this information has direct implications for experimental design and interpretation of results. When aspects of the human thalamocortical network are being discussed or contrasted this will be indicated. It will also focus on thalamic neurones, the central subject of the thesis, and deal briefly with cortical neurones and connectivity as they relate to the thalamus,

1.2.1 Overview of the network

The neuronal populations of the network are the TC, historically known as relay, neurones, thalamic nuclei intrinsic interneurones, neurones of the nRT, cortical thalamo-recipient neurones, and corticothalamic projection neurones. Cortical interneurones and other cortico-cortical connections, though significant influences on network activity via their modulation of corticothalamic activity, are generally not considered part of the thalamocortical network. Nevertheless, cortical processing does need to be considered holistically in order to understand the relationship between thalamocortical input and corticothalamic output. In this thesis the somatosensory nuclei of the thalamus and the corresponding primary somatosensory cortex are of particular interest due to their association with experimental ASs

and the characterisation of their role in experimental models of the disease (see section 1.1.1.2, 1.3, and below).

1.2.2 Thalamus

Exact definitions and nomenclature of the thalamus have been mutable and confusing due to changing understanding of the developmental and functional relationships of the components of the diencephalon. The diencephalon, or midbrain, is divided into several primary nuclear groups. These groups have multiple naming systems. For the purposes of this thesis the terms thalamus, ventral thalamus, epithalamus and hypothalamus will be employed as names of the primary groups. 'Thalamus' now most commonly refers to the single primary nuclear group that was historically known as the dorsal thalamus. This is the portion of the diencephalon from which the cerebral cortex receives the majority of its subcortical input and the foremost portion of interest in this discussion of the thalamocortical network. The nRT, while developmentally derived from the ventral thalamus, is functionally associated with the dorsal thalamus and so will be discussed here also.

The various cortical and subcortical projection nuclei of the dorsal thalamus can be divided in multiple ways according to different anatomical, functional and developmental criteria. A useful distinction for our purpose is that of specific from diffusely projecting nuclei. The former category is of particular interest to this thesis, containing as it does the primary thalamocortical projection neurones which link peripheral sensory organs of particular modality to their corresponding cortical region, as well as receiving reciprocal connections from this region [Fig. 1.3]. The diffusely projecting nuclei consist of multiple distinct intralaminar (located within the internal medullary lamina) and midline (located in the mediolateral centre of the diencephalon) nuclei. They send information to a variety of cortical and subcortical areas, receiving input of varied origin in turn, and are thought to mediate arousal and attentional mechanisms.

Somatosensory nuclei are not entirely limited to focused, single-region connectivity and do not fulfil the simple 1:1 sensory input to cortical output relay function once attributed to them. Their cortical afferents can also be as or more numerous than their efferents, and are not solely reciprocal (Jones, 1985; Deschênes et al., 1998). Indeed specific thalamic nuclei are thought to mediate multi-modal sensory integration and association as well as uni-modal relay (Groenewegen and Witter, 2004). The divergent nature of some of their efferents, as well as of some corticothalamic efferents, is central to some theories of both physiological and

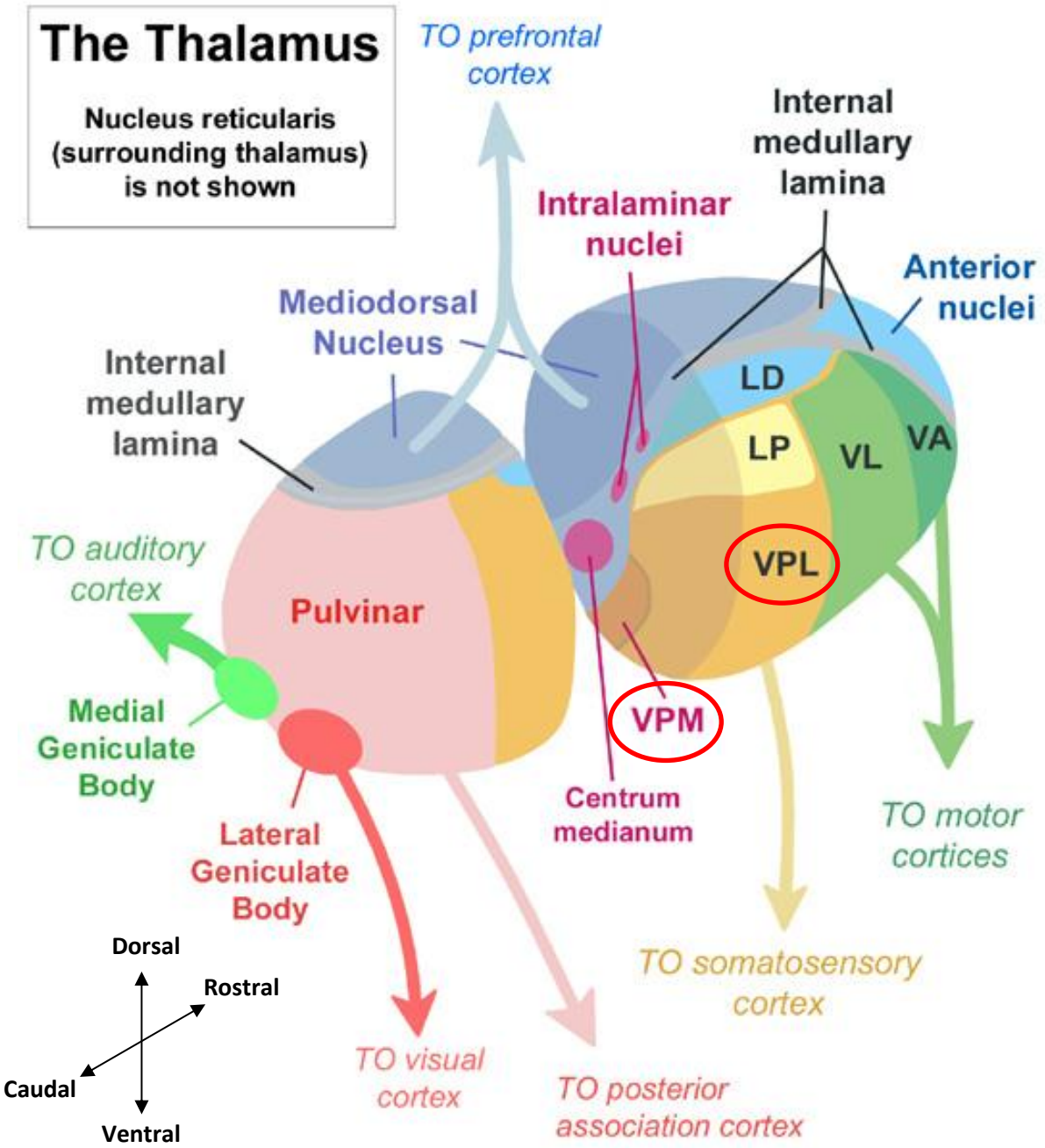

Figure 1.3 Gross organisation of the thalamus

A representation of one side of the human thalamus showing nuclear groups and major recipients of projections. The divisions into major nuclear portions is less clear, but can be seen by following the internal medullary lamina which divides the anterior, medial, and lateral portions. The latter is further subdivided into dorsal and ventral tiers. The dorsal tier includes the pulvinar, laterodorsal and lateral posterior nuclear groups. The ventral tier includes the ventral anterior, ventrolateral, ventroposteromedial and ventroposterolateral. These last two nuclear groups, circled in red above, together compose the ventrobasal complex, which is the somatosensory portion of the thalamus. Modified from medlibes online medical library.

pathophysiological network activity (see section 1.4). However, as distinct from intralaminar and midline nuclei, they do have predominant roles in one or more sensory modality and predominant communications with well-characterised cortical areas. They also completely lack the subcortical projections that originate from nonspecific nuclei.

The specific nuclei are named according to a roughly two-tiered scheme incorporating the spatial relationship of the secondary nuclear group to which they belong to the internal medullary lamina, and their own position within that group. [Fig. 1.3]. For example, the ventrolateral nuclear group contains the ventroposteromedial and ventroposterolateral somatosensory nuclei. The geniculate nuclei, conveying special sensory information (auditory and visual), are located in the posterior group at the caudal end of the thalamus.

1.2.2.1 Ventrobasal nucleus of the thalamus

The most important somatosensory nuclei of the rat, responsible for the majority of nociception and touch, are located within the ventrobasal (sometimes known as ventral posterior) complex (VB). This complex includes the ventroposteromedial (VPM) and ventroposterolateral (VPL) nuclei, which receive input from the contralateral head and the contralateral body respectively (Groenewegen and Witter, 2004; Tracey, 2004). The importance of vibrissal sensation to the rat is reflected by the large relative size and barreloid organisation of both the VPM and the peri-oral somatosensory cortex to which it is reciprocally connected. This cortical area in the rat has been implicated in the initiation of absence seizures in GAERS and WAG/Rij models (see section 1.2.3).

Neurones of the rat VB are almost invariably medium sized TC neurones. The lack of GABAergic interneurones contrasts with their presence in the somatosensory thalamic nuclei of other species, including humans (Harris and Hendrickson, 1987). The VPL is somatotopically organised. As mentioned, the majority of the VPM has a barreloid organisation, representing individual vibrissae (whiskers) functionally and spatially at the thalamic level. There exists the potential for communication between neurones of different barreloids (Van Der Loos, 1976; Desîlets-Roy et al., 2002). The remainder of the nucleus is organised somatotopically, similarly to the VPL, and deals with nociceptive and tactile information from the rest of the face and head (Groenewegen and Witter, 2004). A minority of the neurones in the VB, namely the small (parvicellular) neurones at the medial extremities of both VPL and VPM, receives gustatory and visceral sensory information (Cechetto and Saper, 1987). This thin sheet is sometimes known as the ventral posterior parvicellular nucleus (VPPC) (Groenewegen and Witter, 2004).

Some other thalamic nuclei also deal with primary somatosensory information but this is primarily nociceptive and is not relevant to this thesis (Tracey, 2004).

1.2.2.2 Reticular thalamic nucleus

The nRT contrasts from the nuclei derived from the dorsal thalamus in that it contains solely GABAergic neurones, which do not project to cortex. Rather, they provide intra-nRT and nRT to TC inhibitory modulation [Fig. 1.4]. The nRT migrates dorsally during development and ends up as a thin sheet of neurones wrapping around the dorsal thalamus laterally, anteriorly and partially posteriorly and ventrally. This position between the external medullary lamina of the dorsal thalamus and the internal capsule (the primary white matter tract to and from the cortex) means that all dorsal thalamic afferents and efferents must pass through the nRT, and many of these passing fibres sprout collaterals that synapse within the extensive dendritic trees of nRT neurones (Pinault, 2004).

Neurones of the nRT are spatially organised according to the area of the dorsal thalamus to which they project, and there are subsets of nRT neurones modulating communication of information in nearly all sensory and motor modalities via the dorsal thalamus (Pinault and Deschênes, 1998; Pinault, 2004). Although divergence of nRT -> dorsal thalamus projections from the modally corresponding regions/nuclei appears to be limited primarily to functionally related nuclei (Pinault and Deschênes, 1998; Varga et al., 2002), it may be significant in facilitating communication between thalamic nuclei that have no other similarly direct means of influencing each other's activity (Crabtree et al., 1998). TC-nRT and nRT-TC projections are reciprocal, and corticothalamic projections with nRT collaterals are also from the cortical region of corresponding modality [Fig. 1.4]. The nRT is also innervated by the basal forebrain and brainstem.

Intra-nRT synaptic inhibition exists, although the exact role it plays in different states of thalamocortical network activity is unknown (Destexhe et al., 1996; Fuentealba and Steriade, 2005; Schofield et al., 2009). More detail on synapses between neurones of the nRT is to be found in section 1.2.4.

1.2.3 Somatosensory cortex

While almost all of the sensory neocortex receives the majority of its input from the thalamus, this review will deal solely with the somatosensory cortex as it is both archetypal of other primary sensory cortical areas and their participation in thalamocortical networks, and of

particular interest and relevance to experimental ASs. The primary targets of projections from the somatosensory thalamus are located in cortical area SI.

All areas of the rat somatosensory cortex consist of the 6 cortical layers standard to neocortex. Granule cells in layer IV are the recipients of thalamic input (although recent studies show significant TC projections directly to cortical layers 5/6 (Constantinople and Bruno, 2013), and the thickness of this layer varies between cortical regions. The other cellular layers of the cortex receive input from layer IV and innervate both other cortical areas (in the cases of layers II, III) and subcortical regions (layers V, VI). This latter category of projections includes reciprocal innervation of thalamus (Amaral, 2000; Tracey, 2004).

1.2.4 Thalamic neurone connectivity

Together with intrinsic cellular properties, patterns of connectivity and synaptic properties at each point of connection determine cellular and network activity.

1.2.4.1 Anatomical connections of thalamic neurones

The fundamental anatomy of the thalamocortical network involves the following projections.

1) Thalamocortical: specific (and diffuse) thalamic nuclei to layer IV (primarily) of associated cortical region.
2) Intracortical connections, inter-layer (IV to II/III, IV to V/VI) and inter-region (II/III to II/III, II/III to V/VI).
3) Corticothalamic: layers V and VI to specific and non-specific thalamic nuclei, the majority being precise reciprocals of 1) but a significant minority being diffuse.
4) Intrathalamic connections: extent & significance unknown. Limited primarily to 6) in rat VB complex.
5) Thalamoreticular & corticoreticular: collaterals from 1) and 3) innervating nRT en route to associated cortical & thalamic region respectively.
6) Reticulothalamic: sole projections of nRT, inhibiting originator cells of 1) in a particular thalamic nucleus.
7) Intrareticular: inhibitory communications between neurones of the nRT [Fig. 1.4]

Thus the network takes the form of a primary mutually excitatory loop between related regions of cortex and thalamus, and a secondary loop nested within it providing negative feedback via the nRT (again mostly region-specific). The rule of reciprocal region specificity is

broken to a limited extent. This may be significant given recent information suggesting the spread of ASs from a focal origin throughout the entire network (see section 1.1). There is evidence from primates that TC neurones in specific nuclei are in fact divided into core and matrix groups, with the former projecting in a focused, faithfully reciprocal fashion, primarily to layers III and IV of the cortex, while the latter project more diffusely and terminate more in superficial cortical layers. Corticothalamic neurones similarly are divided into focused, reciprocal layer VI and more diffuse layer V. It has been proposed that this variety of neurones acts to reinforce oscillatory behaviour while simultaneously allowing it to spread throughout the network (Jones, 2002).

The anatomical connections of the thalamocortical network should be considered in the context of the extrinsic major afferents to each of the participatory cell types, as these are directly or indirectly capable of modulating activity in any component neuronal population of the network. Thalamocortical neurones receive their primary driver input from sensory neurones, and may also be disynaptically inhibited by the same neurones via thalamic interneurones (where those exist). NRT neurones project only within the network, while extra-network cortical and thalamic efferents are not of particular interest in this thesis. It should be acknowledged, however, that modulatory cholinergic, adenosinergic, histaminergic, noradrenergic, and serotonergic input from the brainstem and basal forebrain are potential determinants of thalamic activity (McCormick, 1992) and hence (to varying degrees) of cortical state and arousal level (Hirata and Castro-Alamancos, 2010; Constantinople and Bruno, 2011; Kagan et al., 2013; Pifl et al., 2013; Wester and Contreras, 2013; Yang et al., 2013).

- Thalamocortical network-extrinsic input: sensory drivers (direct and via interneurones), subcortical regions (raphe nucleus, parabrachial, brainstem)
- Corticothalamic network-extrinsic input: intracortical, direct and indirect connections from the entire subcortical structure.
- nRT network-extrinsic input: basal forebrain, brainstem.

In the VB the sensory, cortical and reticular afferents synapse at different locations on the cell. Glutamatergic sensory afferent synapses are located on large, clear boutons within glomeruli on medial dendrites of the TC neurones (Salt, 1987; Steriade et al., 1997; Groenewegen and Witter, 2004). Corticofugal axons from layers V and VI, which comprise an even greater proportion of excitatory input, tend to synapse more distally (Jones and Powell, 1969; Liu et al., 1995; Zhang and Deschenes, 1997, and reviewed in Guillery, 1995; Sherman and Guillery, 1996) than the sensory input. GABAergic synapses of nRT axons are mainly

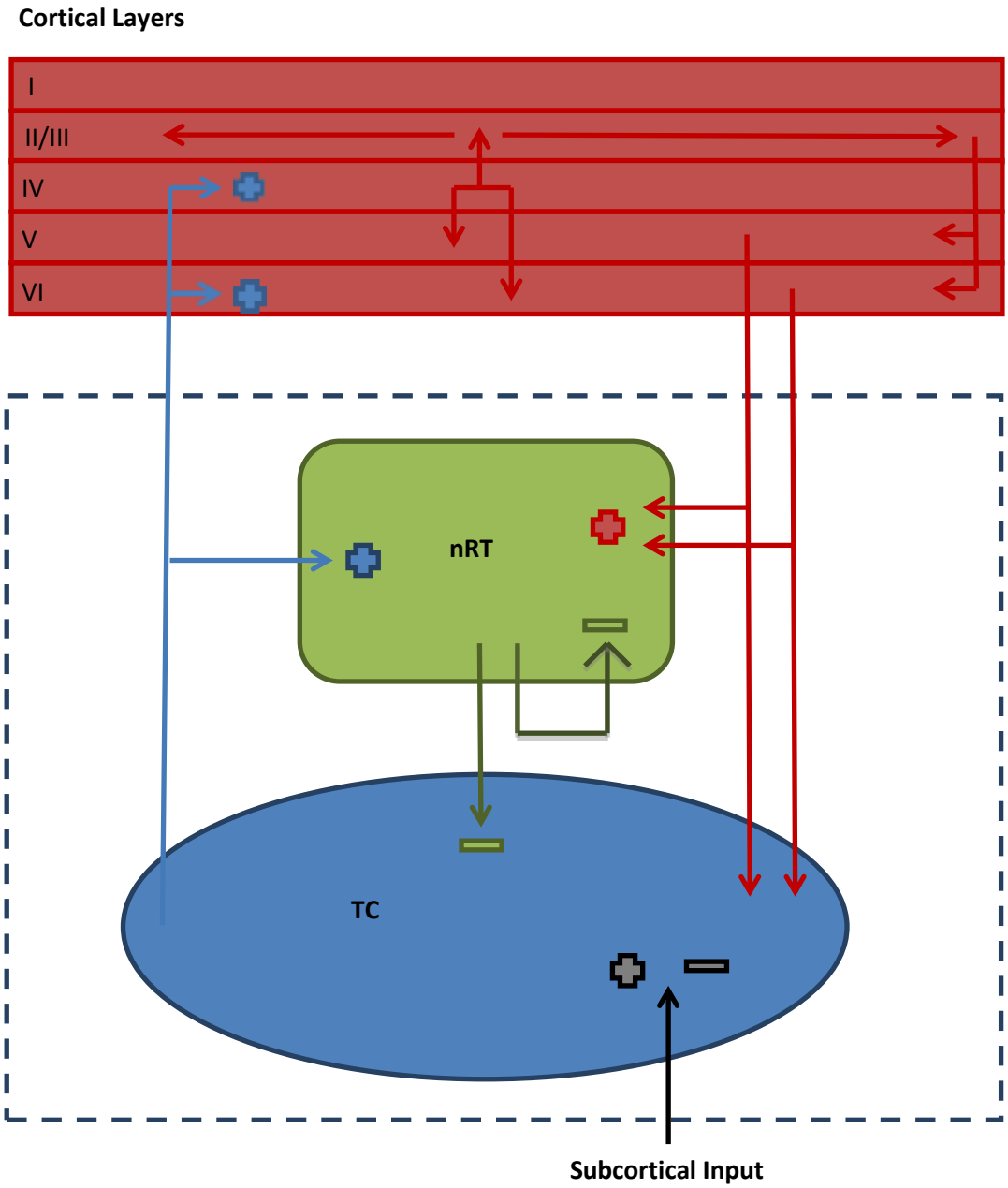

Figure 1.4 Thalamocortical network connectivity – schematic representation

The principle connections within the thalamocortical network are represented by arrowheads, with **+** indicating excitatory and **-** inhibitory synapses. Also contains a simplified view of intracortical communication. Branches do not imply collateral innervations.

distributed among proximal dendrites and the soma (Sherman and Guillery, 1996; Groenewegen and Witter, 2004). As mentioned above, nRT -> TC projections are primarily reciprocal on the level of nuclei, but it has been demonstrated that this not the case down to the single-neuron level (Pinault and Deschênes, 1998). Neuromodulatory synapses are dendritically distributed in both TC and nRT neurones (McCormick, 1992).

Within the reticular nucleus synaptic inputs are also spatially segregated but to a lesser extent, with cortical input predominantly distal and thalamic more proximal among the dendritic tree (Liu and Jones, 1999). Cortical axons give rise to approximately 60% of all nRT input while thalamic afferents provide another 25%. The remaining input is predominantly inhibitory (Jones, 2002). The extent and physiological function of communication between nRT neurones is unknown; considerable dendro-dendritic synaptic connectivity has been observed (Pinault et al., 1997; Schofield et al., 2009) and is capable of suppressing thalamic oscillatory behaviour *in vitro* (Sohal and Huguenard, 2003) while no conclusive evidence has been provided for the functional significance of electrical gap junction communication between the neurones (Haas and Landisman, 2011; Haas et al., 2011).

TC axons primarily synapse on the dendritic trees of layer IV neurones, which are distributed exclusively within that layer (Lübke et al., 2000), but can possibly also directly activate layer V/VI neurones (Constantinople and Bruno, 2013). These neurones then pass information to all the other layers of the cortex, either directly via their axon collaterals to layers II/III or indirectly via intracortical communication between layers II/III and IV or II/III and V/VI of different functional columns (Lübke et al., 2000).

Layers V and VI of the cortex project to the thalamus, as well as to other subcortical and distal cortical regions. Approximately 45% of layer VI pyramidal cells are corticothalamic; these cells also send collaterals to layer IV neurones within their own functional column (Zhang and Deschênes, 1997). Layer V also has some thalamic projections. It is less dedicated in this regard than layer VI, and these projections do not send collaterals to the nRT (Veinante et al., 2000), but may play a significant role in oscillations that, like SWDs, are spread throughout the entire thalamocortical network. This is because of the more diffuse nature of its dorsal thalamic efferents relative to those of layer VI.

1.2.4.2 Synaptic properties of thalamic neurones

The somatosensory thalamocortical network features glutamate and GABA as its principle excitatory and inhibitory neurotransmitters respectively [Fig. 1.4]. Glutamate acts on ionotropic receptors (both fast AMPA/kainate and slow NMDA) on corticothalamic (both TC and nRT), thalamocortical, and pre-thalamic afferents (Jones, 2002). It also acts on metabotropic receptors (mGluRs) from groups I and III (mediating slow excitatory and inhibitory responses respectively) on both TC and nRT neurones. Group II mGluRs are predominantly nRT-located and generate slow hyperpolarisations (Cox and Sherman, 1999; Lourenço Neto et al., 2000). The group I ($mGluR_1$ and $mGluR_5$) postsynaptic expression on TC & nRT neurones and their activation by corticofugal fibres may be of particular significance to network activity (Hughes et al., 2002; Blethyn et al., 2006; Zhu et al., 2006; Crunelli and Hughes, 2010). Group III ($mGluR_7$ and $mGluR_8$) presynaptic expression on nRT-TC and CT-nRT synapses can induce short-term depression (Kyuyoung and Huguenard, 2014).

GABAergic inhibition within the rat somatosensory thalamus invariably originates from the nRT. These nRT-TC synapses feature both ionotropic $GABA_A$ and metabotropic $GABA_B$ receptors (Ohara, 1988; Ohara and Lieberman, 1993; Ulrich and Huguenard, 1997; Zhang et al., 1997). The dendro-dendritic intra-nRT synapses feature mostly $GABA_A$ receptors (Ulrich and Huguenard, 1996a; Sanchez-Vives et al., 1997), but a significant physiological contribution of $GABA_B$ should not be ruled out (Ulrich and Huguenard, 1996b).

As well as synaptic, there also exist extrasynaptic $GABA_A$ receptors, which generate a persistently active current that contributes to resting membrane potential. This is due to the higher sensitivity and slower desensitisation of $GABA_A$ receptors containing the δ subunit, and to their extrasynaptic localisation where they are exposed to low ambient concentrations of GABA rather than transiently high synaptic concentrations. Extrasynaptic $GABA_A$Rs are present in cortical pyramidal cells and TC neurones as well as cortical inhibitory interneurones (Cope et al., 2005; Farrant and Nusser, 2005; Jia et al., 2005; Glykys and Mody, 2007).

The presence of this continuously-active Cl^- current influences the responsiveness of TC neurones both by direction of the resting membrane potential away from the activation thresholds of both Na^+ and Ca^{2+} potentials and, to a greater extent, by increasing membrane conductance (Cope et al., 2005, 2009).

1.2.5 Intrinsic membrane currents of thalamocortical network neurones

Complex interactions of the ion channel-mediated currents expressed in TC, nRT and cortical neurones dictate their response to synaptic input.

1.2.5.1 Na^+ currents

All neurones fire Na^+-mediated action potentials (APs) in response to depolarisation past a threshold. The underlying Na^+ channels are fast activating, fast inactivating and selectively blocked by TTX (Jahnsen and Llinás, 1984a, 1984b). There is also evidence of a small amplitude persistent, i.e. non-inactivating, Na^+ current in both TC (Parri and Crunelli, 1998), and nRT (Deschênes et al., 1984; Pinault and Deschênes, 1992) neurones. This I_{NaP} has been shown to activate at potentials more negative than those necessary to initiate both APs and low-threshold $Ca2^+$ potentials (LTCPs), suggesting a possible contribution to both of these potentials *in vivo* (Parri and Crunelli, 1998). Importantly, the anti-absence drug ETX is capable of reducing I_{NaP} in both cortical and thalamic neurones (Crunelli and Leresche, 2002b), while sodium valproate can inhibit fast Na^+ currents (Ragsdale and Avoli, 1998).

1.2.5.2 K^+ currents

All CNS neurones express K^+ currents, which vary across neuronal types and are mediated by a large array of ion channels. These include both voltage- and ion-dependent channels, but all K^+ currents tend to play variations on the same prevailing role: persistent homeostatic direction of the membrane potential towards its electrostatic reversal potential. This modulation is crucial in maintaining resting membrane potential at a hyperpolarised level relative to that necessary for AP initiation. The most common role of voltage-gated K^+ channels is to activate upon depolarisation and thus repolarise the membrane potential after an AP. TC neurones feature both fast and slowly activating Ca^{2+}-dependent K^+ conductances (Jahnsen and Llinás, 1984b; Budde et al., 1992). The fast-activating, fast-inactivating voltage-gated I_A is also significant in TC neurones: it has a similar voltage dependence of activation to I_T and is capable of modulating LTCP rise time and amplitude as part of the interplay of currents involved in rhythmic burst firing (Huguenard et al., 1991; Pape et al., 1994) as well as being involved in some forms of tonic firing (Jahnsen and Llinás, 1984b; Huguenard et al., 1991; Budde et al., 1992; McCormick and Huguenard, 1992).

TC neurones also have a leak K^+ current (I_{leak}) that maintains the membrane in a relatively hyperpolarised state (Lee and McCormick, 1997; Salt et al., 1999; Turner and Salt, 2000). There

is a single inward-rectifiying K^+ current in TC neurones, I_{KIR}, that's activated by membrane hyperpolarisation and may help de-inactivate T-type Ca^{2+} channels (Williams et al., 1997b). K^+ currents of the nRT can interact with I_T to mediate rhythmic bursting (such as the Ca^{2+}-dependent I_{KCa} as described by Bal and McCormick, 1993), as well as fulfilling other functions such as inducing hyperpolarisation after prolonged tonic or burst firing (Kim and McCormick, 1998).

1.2.5.3 Hyperpolarisation-activated mixed cation current

I_h has been observed in both thalamocortical (McCormick and Pape, 1990a; Soltesz et al., 1991) and nRT neurones (Blethyn et al., 2006; Rateau and Ropert, 2006). This current, carried by both K^+ and Na^+ ions, is activated when the membrane is hyperpolarised beyond approximately -60mV. It doesn't inactivate and only slowly deactivates. This slow deactivation results in the current persisting even after the membrane potential is no longer within its range of activation and thus generating a depolarising 'overshoot' (McCormick and Pape, 1990a, 1990b; Soltesz et al., 1991; Spain et al., 1991; Williams et al., 1997b).

1.2.5.4 Ca^{2+}-activated mixed cation current

Another player in TC neurones membrane potential dynamics is the Ca^{2+}-activated non-specific cation current, I_{CAN}. It is also present in nRT neurones (Bal and McCormick, 1993) and in neurones beyond the thalamocortical network (Partridge and Swandulla, 1988; Hasuo et al., 1990; Zhu et al., 1999). As it is activated by Ca^{2+} entry through T-type Ca^{2+} channels (Hughes et al., 2002) and inactivates slowly, producing a prolonged current, it can modify the shape and duration of any Ca^{2+}-dependent depolarising potential, and dictate the membrane state after the termination of that potential (Bal and McCormick, 1993).

1.2.5.5 Ca^{2+} currents

Both HVA and low voltage activated (LVA) Ca^{2+} channels have been identified in TC, nRT and cortical neurones. LVA T-type Ca^{2+} current (I_T) is particularly relevant to this thesis, given the importance of this current in the firing dynamics of nRT and TC neurones. As such it will be discussed in some detail. Both HVA and LVA voltage-gated calcium channels (VGCCs) respond to alterations in membrane potential by permitting rapid Ca^{2+} influx, increasing intracellular concentrations from the nanomolar to the micromolar range. This both contributes to a variety of signalling events (including the initiation of synaptic transmission) and depolarises the plasma membrane (Perez-Reyes, 2003; Nilius et al., 2006).

VGCCs consist of an α1 pore-forming subunit as well as β, α2δ, and sometimes γ subunits (the latter varying between subtypes). The structure of the α1 subunit determines the precise activation kinetics of the channel, generating the variation between subtypes in activation, inactivation, and deactivation rates (Perez-Reyes, 1999; Cain and Snutch, 2010; Catterall, 2011).

1.2.5.5.1 HVA Ca^{2+} currents

HVA currents were the first recorded Ca^{2+} current, requiring significant membrane depolarisation in order to activate and possessing both large per-channel conductance and slow voltage-dependent inactivation. This first current was designated L-type, based on its long-lasting inactivation. Since then several further variants of HVA Ca^{2+} currents have been discovered: N, P/Q, and R, all of which are present in thalamic neurones (Zhang et al., 2002; van de Bovenkamp-Janssen et al., 2004; Llinás et al., 2007; Rankovic et al., 2011). They vary in kinetics and pharmacology.

1.2.5.5.2 LVA Ca^{2+} currents

A Ca^{2+} current activated at more negative membrane potentials was first discovered in starfish eggs (Hagiwara et al., 1975) and characterised in dorsal root ganglion, inferior olive, and thalamic neurones (Llinás and Yarom, 1981; Llinás and Jahnsen, 1982; Carbone and Lux, 1984; Jahnsen and Llinás, 1984a, 1984b). It was termed T-type, due to the transient opening dictated by its high rate of inactivation. The activation of the current was dependent on preceding de-inactivation of a sufficient proportion of T-type channels by hyperpolarisation. Its kinetics result in a depolarising potential (LTCP) both slower and more prolonged than that mediated by Na^+ [Fig. 1.5] (Crunelli et al., 1989). Cloning of the channel revealed a subfamily of three α1 Ca^{2+} subunits distinct from the existing HVA subfamily. These were designated α1G, α1H, and α1I (now termed $Ca_V3.1$, $Ca_V3.2$ and $Ca_V3.3$ after renaming of the family according to sequence similarity).

There are significant similarities between the pore-forming subunit structures of T-type Ca^{2+} channels and the K^+, Na^+, and HVA Ca^{2+} voltage-gated ion channels. Amino acid homology suggests that Ca_V3 channels are as closely related to Na^+ as to HVA Ca^{2+} channels. These channels are all large proteins (>200 kDa) containing four homologous domains, each with 6 transmembrane segments (S1 to S6). Critical elements within each domain include a voltage-sensing component (S4), a filter for ion selectivity (P loop between S5 and S6), and an inner channel wall (S6). Both N and C terminals are intracellular, as are linking segments connecting

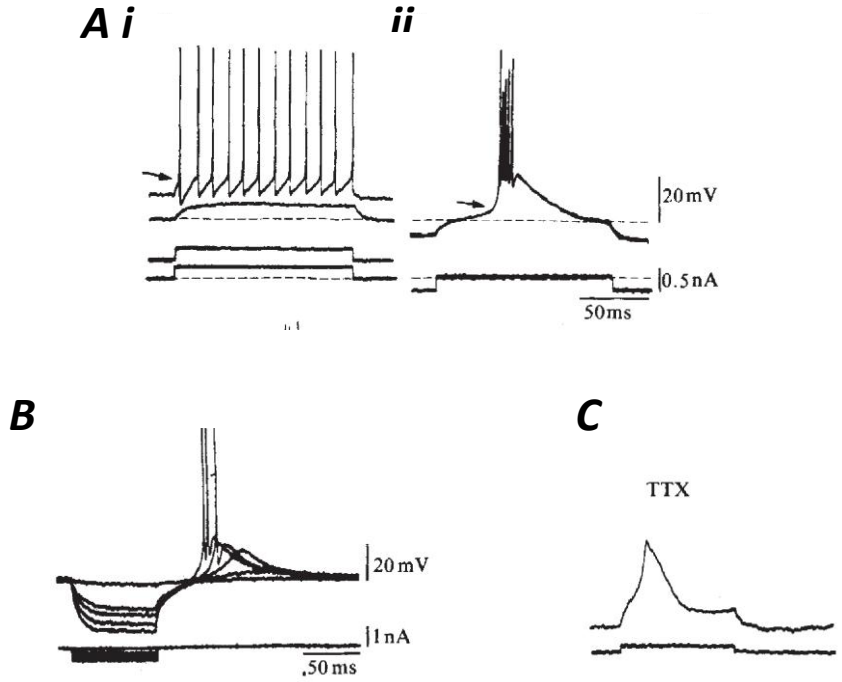

Figure 1.5 LTCPs and high-threshold bursts

Ai shows tonic firing induced by sustained depolarisation of a thalamic neurone. ***Aii*** by contrast shows the effect of the same sustained depolarisation after a D.C. hyperpolarising pulse has deinactivated T-type calcium channels. The slow, prolonged depolarisation is a low-threshold calcium potential (LTCP) due to I_T and the high-frequency burst crowning it is composed of Na^+-dependent action potentials. ***B*** shows the effect of varying degrees of hyperpolarisation on the shape of the LTCP. ***C*** demonstrates that the burst is Na^+-dependent (i.e. blocked by 1 µg/mL tetrodotoxin (TTX)) while the LTCP is not. Figures adapted from Llinas & Jahnsen, 1982.

the four homologous domains (Perez-Reyes, 2006; Talavera and Nilius, 2006). There is currently no evidence for the association of auxiliary subunits with endogenous T-type Ca^{2+} channels [Fig. 1.6].

T-type Ca^{2+} channels are selective for Ca^{2+} over other cations through high affinity rather than pore diameter, and achieve high throughput by electrostatic repulsion. Single channel conductance is estimated at 1 pS. Channel gating states are either open or closed and either activated or inactivated (Perez-Reyes, 2003). Variations in gating properties between isoforms are detailed in Table 1.2.

The three subtypes of T-type Ca^{2+} channels are expressed in the thalamus in varying locations and to varying degrees. There are high levels of α1G mRNA expression in TC neurones, and of both α1H and α1I mRNA in nRT neurones (Craig et al., 1999; Talley et al., 1999). Immunolabelling suggested some expression of all protein subunits in both TC and nRT (McKay et al., 2006). Significantly for this thesis, layer V pyramidal cortical neurones express both strong LVA Ca^{2+} currents (Sayer et al., 1990; Markram and Sakmann, 1994; de la Peña and Geijo-Barrientos, 1996; Larkum and Zhu, 2002; Goldberg et al., 2004) and $Ca_V3.1$/α1G protein and mRNA (Craig et al., 1999; Ernst et al., 2009).

Subcellular localisation of T-type Ca^{2+} channel subtypes suggests both somatic and dendritic expression (extending to distal dendrites to varying extents depending on cell type and Ca_V isoform) in TC and nRT neurones (McKay et al., 2006). LVA Ca^{2+} currents in both TC and nRT neurones have also been localised, suggesting a significant role for both proximal (Tarasenko et al., 1997; Zhou et al., 1997; Zhuravleva et al., 2001), and latterly also distal (Crandall et al., 2010; Errington et al., 2010, 2012), dendritic T-type Ca^{2+} channels.

Toxins such as ω-conotoxin and agatoxin do not block the T-type Ca^{2+} current as they do HVA currents. Di- and tri-valent cations including Ni^{2+} and Cd^{2+} act as unspecific antagonists of all cation pores, and can in some conditions favour T-type channels to a limited extent (Fox et al., 1987). A variety of other pharmacological agents including antihypertensive and antiepileptic drugs also act as non-specific modulators (Heady et al., 2001; Perez-Reyes, 2003). ETX was once considered to exert some or all of its therapeutic effects via inhibition of T-type Ca^{2+} channels in thalamic neurones (Coulter et al., 1989a, 1990; Huguenard and Prince, 1994; Gomora et al., 2001). However recent evidence suggests it may have little effect on I_T at relevant concentrations, and rather may have other absence-relevant thalamic and cortical

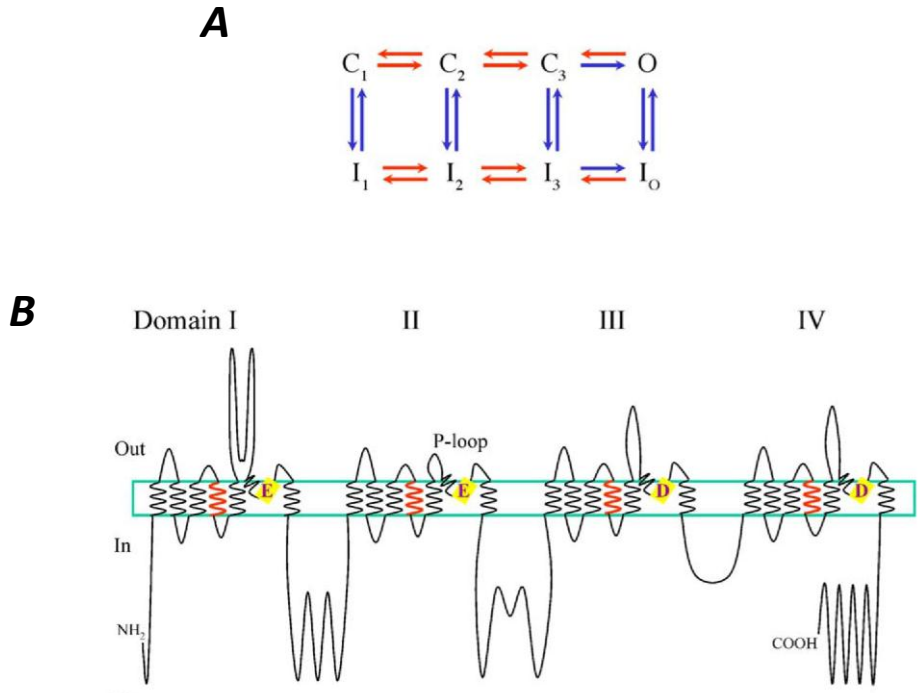

Figure 1.6 Gating model and structure of the T-type Ca^{2+} channel

A Representation of one of the gating models for the T-type Ca^{2+} channel. Red and blue arrows represent voltage dependent and voltage independent transitions respectively. C: closed, I: inactivated, O: open. States C_1 and I_1 are the most probable at resting membrane potential. Membrane depolarisation shifts the model to the right along either the upper or the lower tier, while shifting between tiers is voltage-independent.

B Topological model of the T-type Ca^{2+} channel. Each of the four domains (I to IV) is formed of 6 TM segments, the 6^{th} of which forms the intracellular portion of the pore (yellow rectangles) and the 4^{th} of which forms the voltage sensor (red chain). Image taken from Talavera & Nilius, 2006.

	$Ca_V3.1$	$Ca_V3.2$	$Ca_V3.3$
Pore-forming subunit	α1G	α1H	α1I
Activation constant (ms)	0.8 ± 0.1	1.34 ± 0.1	7.2 ± 0.8
Inactivation constant (ms)	18.8 ± 1.6	23.4 ± 0.3	122 ± 5
Deactivation constant (ms)	2.6 ± 0.2	3.6 ± 0.4	1.12 ± 0.1
Recovery constant (ms)	137 ± 5	448 ± 36	260 ± 30
Functional differences	Fastest current attenuation at high frequencies, rate of recovery is dependent on duration of depolarisation	Faster repolarisation causes increased current attenuation	Facilitates over first few APs at high frequency, slowest high-frequency current attenuation
Physiological consequences	Expressed in TC neurones, bursts are shorter and faster	Longer bursts, possibly modulates nRT activity over multiple-burst series	Accelerates at the start of a burst that lasts longer, matches the properties of nRT neurones

Table 1.2 Voltage-gated calcium channel subtypes

Adapted from Cain & Snutch, 2010. Comparison of the compositions, critical kinetic values and resulting activity of the different T-type Ca^{2+} channel subunits.

effects including inhibition of the non-inactivating Na^+ current and the Ca^{2+} activated K^+ current (Pfrieger et al., 1992; Leresche et al., 1998; Crunelli and Leresche, 2002b; Richards et al., 2003).

It wasn't until 2008 that 3,5-dichloro-N-[1-(2,2-dimethyl-tetrahydro-pyran-4-ylmethyl)-4-fluoro-piperidin-4-ylmethyl]-benzamide (TTA-P2), the first potent and specific antagonist of all isoforms of T-type Ca^{2+} channels, was synthesised (Shipe et al., 2008; Yang et al., 2008). It is capable of blocking LTCPs in multiple neuronal types (Boehme et al., 2011). The IC_{50} for I_T inhibition by bath application to thalamic neurones was 22 nM, but 1 μM was required to block synaptically-evoked LTCPs under certain conditions, suggesting a robust redundancy of T-type Ca^{2+} channels in LTCP generation (Dreyfus et al., 2010). Two further specific channel blockers have since been detected (Tringham et al., 2012). Notably, all of these T-type Ca^{2+} channel antagonists have been shown to suppress absence seizures in rat genetic models when administered systemically. TTA-P2 has also been used to confirm the existence of a "window" component of I_T that is permanently active around resting membrane potential (Dreyfus et al., 2010). This current had been predicted to exist from analysis of the overlap of steady-state activation and inactivation curves of I_T, and is a significant factor in determining TC and nRT membrane potential, as discussed in the following section (Hughes et al., 2002; Crunelli et al., 2005).

1.2.6 Electrophysiology of thalamic neurones

TC and nRT neurones share many aspects of their electrophysiology. Neuronal electrophysiology can be thought of as the combination of synaptic and electrical input with intrinsic currents to generate membrane dynamics and consequent neuronal output. The particular combination of these factors in thalamic neurones results in their having two general firing patterns: sustained, regular 'tonic' firing of APs and high-frequency 'bursts' of APs (Jahnsen and Llinás, 1984a). The input-dependent balance between the two (McCormick, 1992), and the capability of the latter to support intrinsic oscillations, has been suggested as being crucial to distinctions between behavioural states related to consciousness, sleep, and arousal (Steriade et al., 1993; Steriade and Contreras, 1995; Sherman, 2001).

1.2.6.1 Tonic firing of thalamic neurones

Tonic firing is the archetypal activity of neurones: responding to depolarising input that crosses the Na^+ channel activation threshold by generation of a single AP. This initial Na^+ spike is inevitably followed by a repolarisation that continues into an afterhyperpolarisation,

generated by the combination of Na^+ channel deactivation and K^+ channel activation (Jahnsen and Llinás, 1984a, 1984b). It is commonly suggested that, when TC neurones are at a resting membrane potential (above approx. -50 mV) conducive to firing in this mode, they are capable of relaying incoming sensory information to the neocortex with high fidelity (Sherman, 2001; Groenewegen and Witter, 2004).

This is because TC neurones in tonic firing mode are relatively responsive to single inputs, and tend to treat all such inputs relatively equally regardless of their timing. Variation in response to a given post-synaptic input arises from variation in the other input with which it is contemporaneous, and not from cell-intrinsic variations in membrane state. Such tonic firing is typically observed during waking and REM sleep. Neurones of the nRT also display tonic firing during the awake state, reaching much higher frequencies than that of TC neurones (Steriade et al., 1986). Their membrane potential during such periods tends to be slightly higher than that of TC neurones, being at or above approx. -45 mV (Bal and McCormick, 1993).

1.2.6.2 Burst firing of thalamic neurones

Burst firing of thalamic neurones is a property owing primarily to their expression of low-voltage activated T-type Ca^{2+} channels. If the preceding membrane potential is sufficiently negative to permit large-scale de-inactivation of T-type channels, then a depolarisation will trigger regenerative activation of the channels and an influx of Ca^{2+} ions, resulting in a prolonged depolarisation (relative to that mediated by Na^+ channels) (Llinás and Yarom, 1981; Jahnsen and Llinás, 1984a; Crunelli et al., 1989). This is known as an LTCP, and can reach the threshold potential for Na^+ channel activation. If this occurs, the LTCP will be crested with a high-frequency (200-400 Hz) burst of APs [Fig. 1.7]. A varying number of APs can be generated depending on the duration of the LTCP (Zhan et al., 1999, 2000). This mechanism explains how a hyperpolarisation of thalamic neurones can generate an excitatory response (Andersen et al., 1964).

Properties of LTCP-evoked bursts differ in TC and nRT neurones [Fig. 1.7]. An nRT LTCP requires a larger depolarisation in order to be triggered, but is inactivated more slowly and so expresses a longer depolarisation, lasting approximately 50 ms (Huguenard and Prince, 1992). This results in a longer train of APs with an accelerating-decelerating intra-spike interval pattern, as opposed to the constant deceleration observed in TC neurones (Domich et al., 1986). This is as a result of the differing T-type Ca^{2+} channel subunit expression in nRT and TC (Perez-Reyes, 2003; Cain and Snutch, 2010).

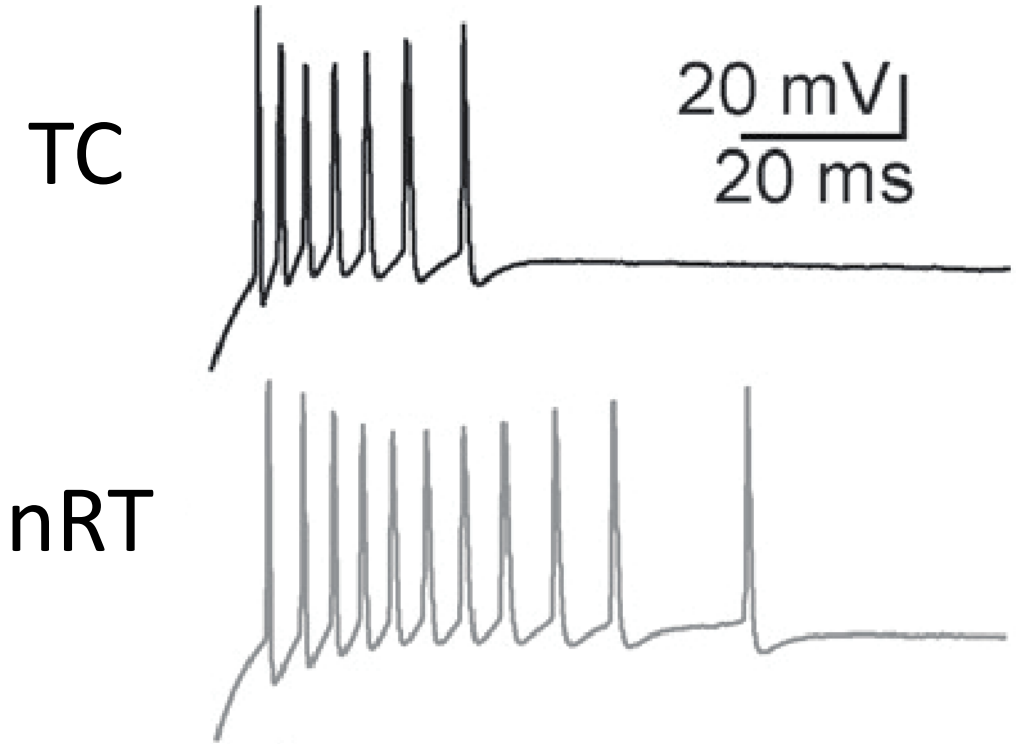

Figure 1.7 TC and nRT LTCP-mediated bursts

Illustration of the different inter-spike interval (ISI) patterns observed in TC and nRT neurones – the latter clearly shows an acceleration (decrease in ISI) followed by a deceleration, while the former shows a straight deceleration. The higher spikes per burst ratio of nRT neurones is also apparent (reproduced from Tscherter et al., 2011).

A neurone in burst firing mode is dominated by the dynamic interplay of intrinsic currents. As a result, the treatment of incoming sensory input is very much dependent on its timing (Groenewegen and Witter, 2004). This is part of the association of rhythmic burst firing with sleep states, when decreased input from ascending brainstem afferents hyperpolarises the membrane into a range at which I_T is de-inactivated and bursts are inducible (McCormick and Prince, 1987). In this condition the unreliable transmission of information results in an effective separation of the cortex from sensory input. The various oscillations observed within the TC network during such states (slow < 1 Hz, δ, and spindles) arise from rhythmic activity on the cellular level in TC, nRT and cortex. In the thalamus such rhythmic activity involves intrinsic pace-making dependent on the interaction of LTCPs with other membrane currents (McCormick and Pape, 1990a; Leresche et al., 1991; Steriade et al., 1991, 1993).

1.2.6.3 δ oscillation in TC neurones

The δ oscillation is a form of rhythmic burst firing of TC neurones generated by the interaction of I_T and I_h, and as such exists at hyperpolarised membrane potentials within the activation ranges of these currents (Leresche et al., 1990; McCormick and Pape, 1990a). This hyperpolarisation is achieved during slow-wave sleep when the thalamic δ oscillation is part of an EEG rhythm of similar frequency, 0.5 to 4 Hz (Steriade et al., 1991).

The progression of membrane current events generating the δ oscillation is as follows: hyperpolarisation of TC neurones, possibly by cortical activation of group III mGluRs, de-inactivates I_T and activates I_h, which slowly depolarises membrane potential to the point of LTCP generation by I_T [Fig. 1.8A]. During the depolarising peak of the LTCP I_h becomes deactivated and I_T inactivated, resulting in a hyperpolarisation. This reactivates I_h and the cycle is perpetuated (McCormick and Pape, 1990a; Soltesz et al., 1991). Variation of membrane potential within the δ oscillation range determines its precise frequency and the amplitude of its LTCPs via I_T and I_h modulation (Leresche et al., 1991).

1.2.6.4 "Window" current in thalamic neurones

The "window" current resulting from the overlap of I_T activation and inactivation curves (Coulter et al., 1989c; Crunelli et al., 1989; Hernández-Cruz and Pape, 1989) was first suggested to contribute to TC neuronal activity by input signal amplification (Williams et al., 1997a). This phenomenon, being Ca^{2+} dependent and occurring within a voltage range matching that of I_T activation and inactivation overlap (-60 to -65 mV), transduces a small physiological current input into a large and long-lasting non-linear response. This was present

only at appropriate ratios of leak K^+ conductance (g_{leak}) and maximal I_T conductance, when the *I*/*V* plot of I_{leak} intersected with that of $I_{Twindow}$ at three distinct points of zero net current [Fig. 1.8B].

TC neurones expressing this input signal amplification also exhibited an intrinsic, low frequency oscillatory activity. At more hyperpolarised starting potentials this was a δ oscillation as described above, but more depolarised starting points resulted in an I_{CAN}-generated plateau depolarisation succeeding some or all LTCPs (Tóth et al., 1998; Hughes et al., 1999, 2002; Crunelli et al., 2005). This plateau, inducible by the activation of postsynaptic mGluRs associated with cortical input (Hughes et al., 2002), reduced the frequency of the rhythm to that of the EEG slow (< 1 Hz) oscillation. Neurones of the nRT are also capable of exhibiting an intrinsic slow oscillation upon mGluR activation (or alternative methods of I_{Leak} reduction). In this case the oscillation is shaped by the Ca^{2+}-activated K^+ current $I_{K(Ca)}$, which shortens the length of both up (depolarised) and down (hyperpolarised) states, while $I_{Twindow}$ and I_h were again essential for its generation (Blethyn et al., 2006).

The existence of such bistability suggests that $I_{Twindow}$ contributes to resting membrane potential, and this has since been confirmed in TC neurones (Dreyfus et al., 2010). Upon application of 1 μM TTA-P2 (a concentration that blocks 96% of I_T and effectively abolishes LTCPs) to rat TC neurones held at -70 mV there is observed a hyperpolarisation of approx. 3 mV [Fig. 1.8C]. This was conclusively attributed to $I_{Twindow}$ and provides a potential avenue by which $I_{Twindow}$ can influence neuronal excitability in all behavioural states.

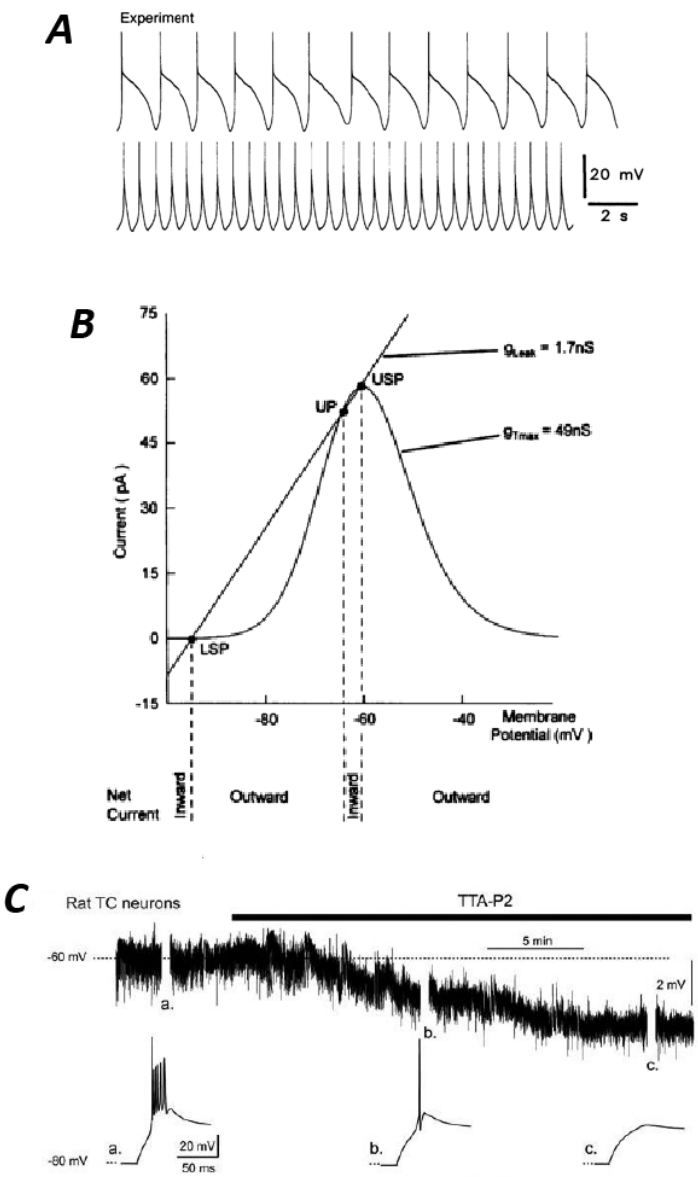

Figure 1.8 ***$I_{Twindow}$ contribution to thalamic neurone physiology***

A shows an intrinsic, low-frequency oscillation in TC neurones. The upper and lower traces show the upper and lower membrane potentials at which the oscillation can be observed (from Williams et al., 1997b). ***B*** shows the generation of bistability and input signal amplification by the intersection of I_T and I_{Leak} current/potential plots. USP and LSP denote upper and lower stable potentials at which the net current is 0 (from Williams et al., 1997b). ***C*** shows the contribution of $I_{Twindow}$ to membrane potential in a rat TC neurone as revealed by application of TTA-P2 (from Dreyfus et al., 2010).

1.3 Experimental Models of Absence Seizures

The utility of any model of a disease rests on its similarity to the human condition and its tractability to investigation. The former is more complex, and opinion is divided on how best to assess this similarity. By definition, a useful model must have predictive validity: information gleaned from its study must be applicable to the human disease. Initially, however, models must be judged on their face validity and/or partial mechanistic validity: similarity of symptoms and/or of known causal mechanisms (Willner, 1984; van der Staay et al., 2009). In the field of absence epilepsy models are judged on the former via their similarity to the clinical characteristics of stereotypical ASs, as follows:

- Bilaterally synchronous SWDs and behavioural arrest
- SWDs measurable in the thalamocortical loop, and not in the hippocampus
- Defined pharmacology
    - Seizures blocked by ETX, valproic acid and lamotrigine
    - Seizures aggravated by carbamazepine and phenytoin
    - Seizures aggravated by GABA agonists (progabide, vigabatrin, tiagabine, baclofen)
    - Seizure blocked by $GABA_B$ antagonists

As is the case with any disease, models of AE must also exhibit symptoms (in this case seizures) that are reproducible, quantifiable and, for practicality of study, somewhat predictable. The GABAergic component of experimental ASs (aggravation by GABA agonists and blocking by $GABA_B$ antagonists) is sometimes held to be an important consideration in determining their quality as a model because of the association of the GABAergic system with ASs (Snead et al., 1999; Depaulis and van Luijtelaar, 2006a; Noebels, 2006). However, this association is based in large part on other models (Snead, 1990, 1992a, 1996) and anecdotal clinical evidence (Parker et al., 1998), and mechanistic validity cannot be assumed. This GABAergic pharmacology should therefore be a lesser consideration than the criteria listed above.

O. Carter Snead (Snead, 1992a) has proposed a set of criteria that have to be fulfilled in order for a condition to be a model of ASs. However, no such list can be definitive and so the strengths and weaknesses of any proposed model should be assessed individually, to determine their impact on the interpretation of data collected from the model and their relevance to clinical ASs. This is particularly true given the variation within clinical ASs, and

their relationship to other IGEs. It is my opinion that the failure to carry out such assessments, and the wholesale acceptance or rejection of a model on the basis of a small number of over-weighted criteria, are greatly to the detriment of the field.

Models of ASs can be divided into genetic and pharmacological, also referred to as spontaneous and induced. Genetic models are further divided into monogenic and polygenic, with the former being mice with mutations of specific genes (Noebels, 2006) and the latter being rats with ASs of unknown genetic provenance that are selectively inbred to maximise and stabilise expression (Depaulis and van Luijtelaar, 2006a). Pharmacological models are divided into acute and chronic (Cortez and Snead, 2006), but the latter category features atypical ASs and is not relevant here. This thesis will concentrate somewhat on select pharmacological and monogenic models, but primarily on the Genetic Absence Epilepsy Rat from Strasbourg (GAERS), an example of a polygenic model of ASs. Relevant characteristics of the primary models discussed are arranged in Tables 1.3, 1.4, and 1.5.

1.3.1 Pharmacological models

Pharmacological, also known as inducible, models of ASs are those generated by systemic administration of a pharmacological compound (Cortez and Snead, 2006). They have something of a benefit in predictability over genetic seizures given the ease of standardising drug doses. However what they gain in predictability between animals they lose (for most purposes) in stability/reproducibility of seizure events in the same animal. It can be to varying degrees both/either beneficial and detrimental to have seizures generated by known pharmacological pathways, which depends on how closely the induced event resembles a clinical seizure and on the (unknowable) likelihood that such a resemblance is generated by entirely unrelated mechanisms. In short, we often have fewer indicators of mechanistic validity in pharmacological compared to genetic models. The logistics of experimental protocols and the undeniable advantage of including multiple types (i.e. pharmacological as well as genetic) of model in an investigation preserve an important place for drug-induced seizures in the arsenal of an absence epilepsy researcher. Selected well-established pharmacological models are compared in Table 1.3.

All of the pharmacological models listed here modulate GABAergic neurotransmission. The γ-hydroxybutyrate (GHB) model acts (at least partly) via $GABA_BRs$ while 4,5,6,7-tetrahydroisoxazolo[5,4-c]pyridin-3-ol (THIP) increases tonic $GABA_A$ current via extrasynaptic δ subunit-containing receptors . The fact that feline penicillin generalised epilepsy (FPGE) and

pentylenetetrazol (PTZ) models both involve weak $GABA_AR$ antagonists is worthy of note; all $GABA_AR$ antagonists can in fact induce SWDs at appropriately low doses. As is detailed in section 1.3.1.1 there is evidence from the FPGE model that these doses are unlikely to fully inhibit $GABA_AR$ IPSPs, as these Cl^- dependent potentials are a central component of cortical neuronal activity during FPGE SWDs (Giaretta et al., 1987).

1.3.1.1 Feline penicillin generalised epilepsy

The first animal model of ASs to receive extensive study was FPGE (Prince and Farrell, 1969). The model is induced by injection of large doses of penicillin intramuscularly (i.m.) to cats. After approx. 1 hr., bilaterally synchronous SWDs at 3-5 Hz (similar to SWD frequency in humans) develop with accompanying dramatically impaired responsiveness to presented stimuli and facial muscle automatisms. Behavioural responsiveness is normal between SWDs, but generalized tonic clonic seizures (GTCs) are also observed sporadically (Prince and Farrell, 1969; Gloor and Testa, 1974; Kostopoulos et al., 1981b; Taylor-Courval and Gloor, 1984; Avoli, 1995). Intraventricular (i.v.) injection of penicillin induces a similar response in cats but with a different time course and greater prevalence of GTCs (Avoli, 1995).

There has been significant analysis of the differential contributions of thalamic and cortical regions to FPGE and of the relationship of the induced SWDs to sleep spindles (Kostopoulos et al., 1981b; Avoli and Gloor, 1982; Avoli et al., 1983; McLachlan et al., 1984). Both cortex and thalamus are necessary for SWDs in FPGE, with the cortex appearing to lead the thalamus both in initiation of a discharge and in each oscillation within it, and with SWDs able to evolve from sleep spindles. Intracellular recordings suggest increased firing in both cortex and thalamus during the spike component of a cycle and general suppression of firing by intracortical IPSPs during the wave component (Giaretta et al., 1987, reviewed by Avoli, 1995). Interestingly, these IPSPs were Cl^- dependent, indicating that the penicillin concentration used achieved only an incomplete block of $GABA_ARs$. FPGE has a similar pharmacological profile to clinical absence, responding to both ETX and sodium valproate (Guberman et al., 1975; Pellegrini et al., 1978).

Rats do not respond to penicillin (injected i.m. or intraperitoneally (i.p.)) in the same way as cats, developing instead different and varied epileptiform activity that does not resemble clinical SWDs (Avoli, 1980; Snead, 1992a). The expense and impracticalities of cat work, particularly when there is no intrinsic advantage, thus limit the usefulness of the FPGE model of ASs as does variation due to inconsistent penetration of the blood-brain barrier by penicillin

(Cortez and Snead, 2006). There are also no developmental data which, given the significance of such factors in CAE, is another major drawback of the model.

1.3.1.2 The γ-hydroxybutyrate model

γ-hydroxybutyric acid (GHB) is a metabolite of GABA that occurs endogenously at micromolar concentrations in multiple brain regions (Bessman and Fishbein, 1963; Roth and Giarman, 1969; Maitre, 1997). When administered to multiple species of animal it induces a sequence of EEG and behavioural events that bear a significant resemblance to clinical ASs (Marcus et al., 1967; Godschalk et al., 1976, 1977; Bearden et al., 1980). The pro-drug of GHB, γ-butyrolactone (GBL), is now commonly used in place of GHB due to greater consistency and rapidity of onset (Bearden et al., 1980; Snead, 1992a).

The EEG and behavioural effects of GHB administration have significant similarities with, and differences from, clinical ASs. The SWDs induced by GHB, cortically and thalamically (Vergnes et al., 1987), have a less regular waveform than that of human SWDs or of many genetic models (see section 1.3.3). The frequency of GHB SWDs in rats and mice has been reported as everything from 3-4 Hz (similar to clinical absence) to 7-9 Hz (similar to polygenic rat models), varying significantly both between and within species (Godschalk et al., 1977; Snead, 1988, 1991, 1992b; Depaulis et al., 1989). It is possible that SWDs in rodents intrinsically differ in frequency to those of humans. The behavioural component of GHB seizures is often underplayed, with quantification resting solely on SWDs (Snead, 1992a; Kim et al., 2001; Zaman et al., 2011). On top of this, parameters investigated and methods of quantification vary between studies, from cumulative duration per time bin to overall power within a given frequency range and everything in between.

The behavioural and EEG components in the GHB model are as follows. After drug administration there is 5 – 15 minutes latency before SWDs of 1-5s duration begin to appear on the EEG, accompanied by behavioural arrest. These events continue for 15 – 20 minutes, with individual SWD duration gradually increasing. After this stage, SWD becomes continuous. No behavioural arrest can be ascertained from this point onwards for two reasons: there are no inter-ictal periods with which to contrast ictal behaviour, and the confounding sedative effect of GHB begins to take full effect. This has been acknowledged since the earliest characterisations of the model (Godschalk et al., 1977). This later stage cannot therefore be classified as a model of ASs.

Thalamic involvement in GHB-induced SWDs has been demonstrated both by local electrical recording (Vergnes et al., 1987; Banerjee et al., 1993), lesion studies (Vergnes and Marescaux, 1992; Banerjee et al., 1994) and direct thalamic administration (the latter is capable of both inducing (Snead, 1991) and exacerbating (Liu et al., 1991) SWDs). In fact, some studies have investigated subregional cortical and thalamic involvement in GHB-induced SWDs by both EEG mapping and lesion studies (Banerjee et al., 1993, 1994). Interestingly, the particular subregions involvement did not appear to exactly match those thought to be significant in spontaneous AS models (see sections 1.3.2 and 1.3.3), with bilateral lesions of somatosensory thalamus (VPL) and reticular thalamus (nRT) failing to abolish seizures where intralaminar thalamic nuclei lesions succeeded (it must be noted that the precision of electrolytic lesions is notoriously limited). Further, no SWDs were present in deep cortical layers V and VI.

The pharmacological profile of GHB-induced SWDs is close to the ideal for a model of clinical ASs. ETX has been universally described as significantly suppressing GHB-induced SWDs (Godschalk et al., 1976; Ishige et al., 1996). Evidence regarding the effect of sodium valproate is mixed however, with at least one study indicating a lack of effect (Ishige et al., 1996) but others showing a suppression similar to that caused by ETX (Snead, 1992a; Kumaresan et al., 2000). The GHB model of ASs has often been employed to contrast seizure characteristics in transgenic and wild-type mice (Snead et al., 2000; Kim et al., 2001; Cheong et al., 2009; Zaman et al., 2011). Pharmacologically induced seizures are the only immediate option for such an experiment.

The consequences of the difficulties in behavioural quantification of the GHB model are apparent when the model is used to test the effects of pharmacological or genetic interventions on ASs. When the behavioural component cannot be analysed due to the limitations of continuous SWDs and sedation, changes to seizures are judged solely on SWDs that are generated by unknown mechanisms and imperfectly resemble the clinical phenomenon. Short of complete reversion to a non-synchronous EEG, the significance of changes in SWD waveform (e.g. loss of power at certain frequencies (Kim et al., 2001; Song et al., 2004; Zaman et al., 2011)) can only be guessed at.

Characterisation of the model is also far from complete. While there have been some pharmacological and electrophysiological investigations, (Snead, 1991; Zhang et al., 1991; Banerjee and Snead, 1995; Ishige et al., 1996; Aizawa et al., 1997a, 1997b; Gervasi et al., 2003) other facets (e.g. effects of circadian rhythms, subtleties of behaviour) of the model have not been investigated to the extent seen for polygenic rat models of ASs (see section 1.3.3).

1.3.1.3 The THIP and PTZ Models

The other two acute pharmacological models of typical ASs are those of THIP and PTZ. Neither is employed in this thesis, nor have they been regularly used in significant studies in the field. However, they are worthy of discussion due to the inferences that can be drawn from them regarding the mechanisms of other models and of the disease itself.

THIP is a $GABA_AR$ agonist that is selective for extrasynaptic receptors ($eGABA_ARs$) incorporating the ð subunit. These receptors elicit a persistently active (tonic) current in rat and mouse TC neurones *in vitro* when activated (Belelli et al., 2005; Jia et al., 2005; Cope et al., 2009) (see section 1.2.4). Systemic or thalamic administration of THIP to adult rats induces electrographic and behavioural abnormalities, including SWDs with behavioural arrest, at appropriate doses (approximately 10 mg/kg systemic, 70µM to 100µM thalamic microdialysis) (Fariello and Golden, 1987; Cope et al., 2009).

The THIP model is summarised and compared to other experimental models of ASs by Cortez and Carter Snead (Cortez and Snead, 2006). Its full pharmacological profile has not been investigated. Due to the more established nature of the GHB and PTZ models, use of THIP to induce experimental absence seizures tends to be as a supplementary model.

Systemic administration of pentylenetetrazol (PTZ) is another established acute pharmacological model of ASs. Like penicillin, PTZ is a weak antagonist of $GABA_ARs$. As mentioned above, all $GABA_AR$ antagonists can induce absence-like seizures at appropriate (low) doses, but PTZ is the most comprehensively characterised of these (Snead et al., 2000).

Although PTZ meets the pharmacological criteria commonly demanded of models of ASs, it differs from other pharmacological models in that the drug employed can also induce clonic and tonic/clonic seizures at higher doses. The dose at which absence-like seizures are induced in 100% of mice is 30mg/kg, whereas clonic seizures begin to be induced above 35 mg/kg and tonic seizures above 60mg/kg. The ability of $GABA_AR$ antagonists to induce both ASs and convulsive seizures is another indicator of the complex alterations of inhibitory neurotransmission implicated in absence epileptogenesis.

1.3.2 Monogenic mouse models

Mouse strains with a spontaneous mutation of a single gene can exhibit ASs, often among other pathologies. Such strains include stargazer, lethargic and tottering mice, which have

provided some insight into potential contribution of single genes to ASs and also help to highlight the relative benefits and drawbacks of polygenic rat models such as GAERS and WAG/Rij. All three of these mouse strains were identified and isolated first by general phenotypical abnormalities, later by their particular SWD and AS properties (all feature SWDs with frequencies between 5 and 7 Hz), and only more recently by the identification of the spontaneous single gene mutation responsible for these phenotypes (Fletcher et al., 1996; Burgess et al., 1997; Letts et al., 1998). Features of these three models are detailed in Table 1.4.

By contrast with polygenic rat models, there are other neurological abnormalities comorbid with ASs in monogenic mouse models. Stargazer, lethargic and tottering mice all have different varieties of ataxia, while tottering also display spontaneous motor seizures with clonic and tonic-clonic components and lethargic mice are hypoactive and have developmental immunological defects (Dung and Swigart, 1971; Dung et al., 1977; Noebels and Sidman, 1979; Noebels et al., 1990; Khan and Jinnah, 2002). Due to these abnormalities, such strains are also often used as models of ataxia and have limitations as models of CAE. However, with proper contextualisation useful information may still be gleaned regarding specific gene- or protein-dependent pro-absence effects (Crunelli and Leresche, 2002a).

1.3.3 Polygenic rat models

There are two regularly used and comprehensively characterised models of absence seizures: GAERS and WAG/Rij. Both have had the various behavioural, developmental and electroencephalographic features of their AS studied to a far greater degree than any pharmacological or monogenic mouse models, and are free of neuropathological abnormalities (Danober et al., 1998; Renier and Coenen, 2000). As can be seen from Table 1.3 compared to 1.4 and 1.5 the only major drawbacks associated with these two rat strains are the developmental contrast with CAE, i.e. that the rats develop seizures in adolescence which strengthen and persist into old age, and the SWD frequency. There is some recent evidence that, in at least one colony of GAERS, SWDs with behavioural arrest can be observed as early as post-natal day 23 (Girod et al., 2012).

It is worthy of note that, in every other rat strain in which it has been investigated, individuals expressing ASs of variable duration and EEG clarity have been discovered (Chocholová, 1983; Buzsáki et al., 1990; Inoue et al., 1990), although there is some debate regarding the distinction between rodent ASs/high-voltage spindles and a mu oscillation associated with

Model	EEG	Ontogeny	Genesis	Phenotype	SWD Pharmacology	References
FPGE	Prolonged bursts of bilateral, symmetrical, generalised SWDs at 4-5 Hz	Adult cats only used	Weak $GABA_AR$ antagonism, apparent incomplete block of IPSPs	Impaired responsiveness to stimuli, facial automatisms, some tonic-clonic seizures	Suppressed by ETX & sodium valproate; prolongs GHB-induced SWDs	Prince & Farrell, 1989 Taylor-Courval & Gloor, 1984 Avoli, 1995
GHB	Brief bursts of bilateral, generalised SWDs between 2 and 10 Hz	Fully developed at P28	$GABA_BR$ agonism, possible $GABA_AR$ and/or GHBR agonism	Abolition of responsiveness and directed movement	Suppressed by ETX, TMD, valproate, exacerbated by CBZ, phenytoin, pro-GABA drugs	Godschalk et al., 1976 Snead et al., 1991 Kumaresan et al., 2000
THIP	Bursts of bilateral, symmetrical, generalised SWDs at 6-8 Hz	Adult rats only used	δ-containing $eGABA_AR$ antagonism	Abolition of responsiveness and directed movement	Suppressed by ETX, diazepam, valproate; prolongs & slows GAERS SWDs	Fariello & Golden, 1987 Cope et al., 2009
PTZ	Bursts of bilateral, symmetrical, generalised SWDs at 6-8 Hz	Adult rats only used	Weak $GABA_AR$ antagonism	Abolition of responsiveness and directed movements, tonic-clonic seizures at higher doses	Suppressed by ETX & valproate, exacerbated by CBZ & phenytoin	Snead et al., 2000 Cortez & Snead, 2006

Table 1.3 Pharmacological models of absence seizures

Model	EEG	Ontogeny	Genotype	Phenotype	SWD Pharmacology	References
Stargazer (stg)	Prolonged bursts of bilateral, symmetrical, apparently generalised SWDs at 6-7Hz	Phenotype displayed by PND14; by 1 month mean SWD duration is 6s & occurrence ~2/min.	Autosomal recessive inheritance. Mutation of Ca^{2+} channel γ_2 subunit gene which encodes stargazing, AMPAR trafficking protein.	SWDs with immobility, reduced size, ataxia, spontaneous head tossing, males impotent, impaired conditioned eyeblink reflex.	ETX, NMDA antagonist & $GABA_B$ antagonist suppress.	Noebels, 2006
Tottering (tg)	Bursts of bilateral, symmetrical, generalised SWDs at 6Hz	Phenotype developed by PND28; SWDs last 1-10s & occur every ~every 2 min.	Autosomal recessive inheritance. Mutation of Ca^{2+} channel α_1 subunit.	SWDs with immobility & vibrissal twitching, splayed stance & ataxia, reduced size.	ETX & diazepam suppress, phenytoin ineffective.	Noebels, 2006
Lethargic (lh)	Bursts of bilateral, symmetrical, generalised SWDs at 5-6Hz	Phenotype displayed by PND15, SWDs by 18; mean duration 1.5sec & occurrence ~2/min.	Autosomal recessive; mutation of Ca^{2+} channel β_4 subunit gene.	SWDs with immobility, reduced size, immunological deficits, decreased fertility, high mortality to 2 months	ETX, clonazepam, trimethadone suppress; baclofen & tiagabine exacerbate.	Noebels, 2006

Table 1.4 Monogenic mouse models of absence seizures

Model	EEG	Ontogeny	Genotype	Behaviour	Pharmacology	References
GAERS	Burst of bilateral, symmetrical SWDs at 7-11Hz; 2-6 times background voltage amplitude[1]; restricted to cortex & lateral thalamus[2,3]	Seizures begin past 1 month, fully expressed at 4; number & duration gradually increase to 1/min and 17±10 sec at 6 & 18 months respectively[4]	Dominant inheritance, variability suggests multiple genetic loci. Homozygous missense mutation of $Ca_V2.2$ identified[6]	Immobility, rhythmic movements of vibrissae & orofacial region[1], loss of responsiveness to mild stimuli[7].	Suppressed by ETX and valproate[2]; exacerbated by anticonvulsants & GABAmimetics/boosters[2,5]; unaffected by $GABA_AR$ antagonists; exacerbated/suppressed by $GABA_B$ agonists & antatonists respectively[8]	[1]Vergnes et al., 1982 [2]Marescaux et al., 1984 [3]Vergnes et al., 1990 [4]Vergnes et al., 1986 [5]Marescaux et al., 1992a [6]Powell et al., 2009 [7]Lannes et al., 1988 [8]Marescaux et al., 1992b
WAG/Rij	Burst of bilateral, symmetrical SWDs at 7-11Hz[2,3]; less common type 2 SWDs differ from typical[1,2,3]	Seizures begin past 2.5 months; fully expressed at 6; max number & duration 16-20/hr & 5±2 sec respectively[4]	Mendelian inheritance of one dominant gene and multiple modulators[5]; abnormal $GABA_AR$ α_3 subunit protein in nRT[6]	Identical to GAERS[3]	Suppressed by ETX & valproate[7]; exacerbated by anticonvulsants & GABAmimetics[7,8]; exacerbated/suppressed by GABA agonists[9] & $GABA_B$ antagonists[10] respectively	[1]Drinkenburg et al., 1993 [2]Meeren et al., 2002 [3]van Luijtelaar and Coenen, 1986 [4]Coenen and Van Luijtelaar, 1987 [5]Peeters et al., 1992 [6]Liu et al., 2007 [7]Peeters et al., 1992a [8]Coenen et al., 1995 [9]Kamiński et al., 2001 [10]Peeters et al., 1989

Table 1.5 Polygenic rat models of absence seizures

resting wakefulness (Wiest and Nicolelis, 2003; Shaw, 2004)[1]. GAERS were developed from such a discovery by selective breeding for the AS phenotype (from Wistars) leading to longer and more stable seizures with more constant EEG correlates. WAG/Rij are an even more striking example of this phenomenon as they were already fully inbred when they were discovered to invariably display SWDs. Also significant is that 100% of normal Wistar rats past 84 weeks of age display SWDs indistinguishable from those of GAERS and WAG/Rij (van Luijtelaar et al., 1995).

This report will concentrate on GAERS, as they are the model used in the following experiments, but will also mention significant aspects of the WAG/Rij strain. The two models are similar in many fundamental aspects of their pathophysiology but do differ in some others (Akman et al., 2010). It should be noted that there are no structural lesions or gross morphological abnormalities in either strain, as is the case for CAE.

1.3.3.1 Genetic Absence Epilepsy Rats from Strasbourg (GAERS)

This rat strain was developed in the laboratory of Christian Marescaux in the early 1980s (Vergnes et al., 1982; Marescaux et al., 1984a, 1984b) by selective breeding from the 30% of Wistar rats in their facility that already displayed short and irregular spontaneous SWDs. A control strain of SWD-free Wistars (non-epileptic controls, NECs) was also introduced by this group.

1.3.3.1.1 Primary characteristics of absence seizures in GAERS

A comprehensive review of the early characterisation of the GAERS model can be found in Marescaux et al. (1992a), and an even more thorough and recent treatment of the model and some of the information regarding clinical ASs thus fair gained from its study in Danober et al. (1998). GAERS and WAG/Rij as models of ASs are also both reviewed and summarised by Depaulis and van Luijtelaar (2006b). The key features of the models are behaviour and the EEG correlate, with pharmacology a significant secondary feature. To summarise, GAERS display behavioural arrest with concomitant bilaterally synchronous SWDs in EEG. The behavioural arrest specifically features cessation of all gross movement, but frequently involves rhythmic twitching of the vibrissae and facial muscles. This particular feature is of interest in light of

[1] It is plausible, given the possibility of sensory processing during AS mentioned in section 1.1.1.1, that resting wakefulness-related oscillations and SWDs are closely related phenomena (Drinkenburg et al., 2003; Kelly, 2004; Chipaux et al., 2013).

discoveries regarding the specific cortical site of origin of AS-related electrophysiological activity (see section 1.4.2).

During seizure, the animals are unresponsive to sensory stimulation unless it is sufficiently strong and novel. There is evidence that cortical sensory processing (in the form of event-related potentials and vibrissal pyramidal neurone firing) can take place during SWDs in fentanyl-anaesthetised GAERS (Chipaux et al., 2013). Although this is far from a conclusive demonstration of consciousness, when considered in context with results of a similar bent in clinical (Berman et al., 2010, reviewed by Blumenfeld, 2005) and experimental (Drinkenburg et al., 2003) ASs, as well as the uncertain distinction between experimental ASs and resting wakefulness-associated oscillations (Wiest and Nicolelis, 2003; Shaw, 2004), it is worthy of further study.

SWDs are reported as arising from normal background EEG (but see Pinault et al. (2001) for an alternative hypothesis). The likelihood of seizure varies depending on level of wakefulness, with the considerable majority occurring during restful wakefulness, followed by during transitions from wakefulness to early stages of sleep or vice versa. Very few seizures are generally observed in GAERS during slow-wave sleep or active behaviour (Lannes et al., 1988). Probably as a consequence of this arousal-dependence, tendency to seize in GAERS varies according to time of day relative to their circadian rhythm (Faradji et al., 2000).

SWDs in GAERS have a frequency of 7-11Hz and last on average between 10 and 30 seconds, with frequency decreasing towards the end of an event. Depending on the location of the recording electrodes, voltage amplitude of an SWD varies around the hundred μV range. Variation in apparent cortical site of origin of SWDs in GAERS has been observed since the earliest studies of the model (Danober et al., 1998), but wasn't investigated at high temporal and spatial resolution until the 2000s (Polack et al., 2007). Depth EEG/LFP has recorded SWDs from all layers of the cortex and from the thalamus. No SWDs are present in cerebellum or in the structures of the limbic system: hippocampus, septum, amygdala, cingulate and piriform cortices (Vergnes et al., 1987).

The developmental profile of ASs in GAERS differs drastically from that of those in CAE. SWDs (of variable frequency and waveform, but constant amplitude) with accompanying behavioural arrest first begin to appear in the EEG after 1 month of age (but see Girod et al., 2012 as mentioned above), and are invariably expressed by the 4-month point. SWDs reach their highest frequency (both of occurrence and internal) and duration by 6 months of age. GAERS

display SWDs from this point throughout their lives, as might be expected based on the development of similar events in aged Wistar rats (Vergnes et al., 1986).

1.3.3.1.2 Pharmacology of absence seizures in GAERS

Pharmacology of ASs in GAERS conforms to that expected of a model of clinical ASs. Historically, reports were of >90% suppression by ETX and sodium valproate, as well as trimethadione and benzodiazepines, while lamotrigine was ineffective (van Luijtelaar et al., 2002). Vigabatrin, tiagabine, and gabapentin, which aggravate clinical ASs, do likewise in GAERS (Marescaux et al., 1992a, 1992b) while some more novel antiepileptics are effective in their suppression (Gower et al., 1995; Rigoulot et al., 2003). However, unpublished observations in this lab suggest an efficacy of ETX below that initially reported: approximately 70% suppression of seizures, which is more in line with that achieved by chronic oral administration in a recent study (Dezsi et al., 2013). It also cannot be ignored that the 100 to 150mg/kg doses of ETX which are generally administered to GAERS are 2 to 3 times the maximum dose given to CAE sufferers (Glauser et al., 2010). This may be due to general inter-species metabolism-related differences, but is not certain: studies have suggested that brain tissue concentrations achieved by 100mg/kg i.p. in GAERS (~ 1000 µM) are not completely dissimilar to those achieved within the standard dosing range in humans (~ 500 µM) (Patel et al., 1977; Coulter et al., 1989a; Glauser et al., 2010).

As suggested by the exacerbation by vigabatrin, GAERS seizures demonstrate sensitivity to many drugs interfering with GABAergic neurotransmission. There appears to be a complex relationship between GAERS SWDs and GABA. Agonists and antagonists of $GABA_B$ exacerbate and suppress seizures respectively (Marescaux et al., 1992a, 1992b) while antagonists specific to $GABA_AR$ have varying effects (Marescaux et al., 1992b; Vergnes et al., 2000, 2001). Furthermore, the ability of muscimol and THIP, $GABA_AR$ agonists (the latter selective for extrasynaptic, δ subunit-containing receptors), to exacerbate seizures combined with the alteration of tonic $GABA_A$ current in GAERS, among other models of ASs, would support this idea of a complex relationship (see sections 1.2.3.1.5 and 1.3.5.6).

1.3.3.1.3 Genetic components of absence seizures in GAERS

Surprisingly, given that transmission of ASs is inherited in GAERS in an apparently autosomal dominant fashion (Marescaux et al., 1992a), primarily quantitative trait loci (stretches of DNA) and very few specific genes have been associated with the inheritance of seizures. The sole gene that has been associated and is also obviously phenotypically relevant is that of $Ca_V3.2$, a

subtype of the T-type Ca^{2+} channel (see section 1.4), which was found to have undergone a point mutation in GAERS with effects on seizure expression depending on whether it was expressed in a splice variant containing or omitting exon 25 of the gene (Powell et al., 2009). This is notable as the human gene encoding $Ca_v3.2$ is associated with ASs, and this association has been hypothesised to be dependent on splice variation also (section 1.1.1.3, Zhong et al., 2006).

1.3.3.1.4 Neurotransmitter alterations in GAERS

Neurotransmitter-related investigations in GAERS have thus far centred on GABA, and multiple abnormalities have been discovered. Extracellular concentration of GABA in thalamic relay nuclei is increased in GAERS relative to the NECs (Richards et al., 1995), an effect which has been attributed to a dysfunction in GABA transporter-1 (GAT-1) in the thalamus (Cope et al., 2009), given the importance of this transporter in thalamocortical neurones and the decrease in uptake measured in GAERS (Sutch et al., 1999). Any substances that increase GABA concentrations also exacerbate SWDs in GAERS (Danober et al., 1998). There is no observed change in GABAergic neurones or in relative proportion, affinity and expression of $GABA_A$ receptor subtypes in TC and nRT neurones of GAERS (Knight and Bowery, 1992; Snead, 1992b; Spreafico et al., 1993). However, there is a reduction in binding of antibodies specific to the β_2-β_3 subunits of the $GABA_AR$ in the cortex (Spreafico et al., 1993) and miniature $GABA_A$ IPSCs were larger and more resistant to baclofen, while paired-pulse depression was less effective, in GAERS than in NEC nRT, but not in VB or cortical layers II/III (Bessaïh et al., 2006).

$GABA_BRs$ feature centrally in many hypotheses of AS generation, due to the ability of a slow $GABA_B$-mediated IPSP to deinactivate T-type Ca^{2+} channels and thus promote burst firing in cells of the thalamocortical network (Crunelli and Leresche, 1991) as well as the $GABA_BR$ and extrasynaptic $GABA_AR$-mediated increase in thalamic tonic current necessary for the expression of ASs in multiple models (Cope et al., 2009). Systemic pharmacological modulation of $GABA_B$ neurotransmission can enhance and suppress SWDs in GAERS (Richards et al., 1995; Vergnes et al., 1997; Danober et al., 1998). Further, administration of the $GABA_B$ agonist baclofen to either thalamocortical relay nuclei or to the nRT increases, where the antagonist CGP-35348 suppresses, GAERS SWDs (Liu et al., 1992). Despite this, molecular biology assays have showed opposing variations in $GABA_{B1}$ and $GABA_{B2}$ mRNA and protein (Princivalle et al., 2003), with no changes in $GABA_B$ receptor binding, density and affinity of receptors. There have been no studies that would suggest a causative role of $GABA_B$ alterations in the development of GAERS SWDs.

As well as GABAergic transmission, glutamatergic neurotransmission may be involved in GAERS pathogenesis. Pharmacological manipulation (both activation and inhibition) of the NMDA receptor, globally or thalamically, can suppress ASs (Koerner et al., 1996). Glutamatergic synapses are also more directly implicated via an enhanced cortical NMDA response in GAERS compared to NEC rats (Pumain et al., 1992) as well as a decrease in cortical glutamate uptake along with an increase in VGlut2 and synaptophysin expression (Touret et al., 2007). An observed increase (relative to NEC) in cortical expression of the AMPA regulatory protein stargazin (Powell et al., 2008) in adult but not in pre-seizure juvenile GAERS (Kennard et al., 2011) may have a significant role in increasing AMPAR expression and, consequently, cortical excitability.

1.3.3.2 WAG/Rij

Most WAG/Rij SWDs are very similar to those of GAERS, with identical frequency and waveform. The average incidence and duration, however, are both decreased in WAG/Rij to 5 seconds and 15-20 per hour respectively (Akman et al., 2010). There is also a second, rare type of SWD observed in WAG/Rij that increases in occurrence with age: a local event restricted to the occipital and parietal cortices. Its intra-ictal frequency is marginally lower (6-7 Hz) and its spikes are reversed in polarity relative to type 1 WAG/Rij and GAERS SWDs (Depaulis and van Luijtelaar, 2006a).

The existence of two forms of SWDs in WAG/Rij, both concomitant with behavioural symptoms of ASs (and with variation in sensory processing during seizure as described by Drinkenburg et al., 2003), is a useful demonstration of the potential variety in EEG signature of events with the same behavioural effects. With this variety in mind, one must be cautious in attributing any real significance to changes in properties of SWDs in these or any other models of SWDs unless there is also a quantifiable change in behaviour. Any oscillatory EEG signature within the established frequency range may be as valid as any other, particularly given the fundamental differences between clinical SWDs and those of all established models.

1.3.4 Spontaneous absence seizures in other rodents

High-voltage rhythmic EEG activities with behavioural disturbances have been identified in Fisher 344 (Jandó et al., 1995) and Long-Evans rats. The fact that the latter is a commonly used laboratory strain renders extremely interesting a study demonstrating that their absence-like events are similar behaviourally, electrographically and pharmacologically to those of GAERS and WAG/Rij (Shaw, 2004). A contradictory study, showing that sensory perception during

such events is not inhibited relative to that during anaesthesia (Wiest and Nicolelis, 2003), does not preclude these events from being considered a form of experimental ASs given the potential variation in consciousness during clinical and other experimental ASs . Interestingly, the activity of cortical and TC neurones during high-voltage rhythmic spindles (HVRS) in Long-Evans is remarkably similar to that during SWDs in GAERS (Polack and Charpier, 2006).

There have been multiple strains of mice proposed as models of ASs because of activity resembling SWDs, with varying degrees of apparent behavioural arrest. These have generally been used for a single study or series of studies, and have very little characterisation as models. Examples include mice with dysfunctional mGluR7 (Bertaso et al., 2008), GluA4 knockout mice (Beyer et al., 2008; Paz et al., 2011), phospholipase C beta4 knockout mice (Cheong et al., 2009), and $GABA_B$ knockout mice (Schuler et al., 2001).

1.3.5 Summary of experimental absence seizures

Of the various models of absence seizures, none perfectly replicate the human clinical condition. The most tractable for genetic studies are monogenic mice and pharmacological models, while the strongest (by assessment of face and mechanistic validity) are the polygenic rat models. There are no *in vitro* models of absence seizures, but slice preparations can be useful for studying putative oscillatory mechanisms at the subcellular level.

1.4 Pathophysiological mechanisms of absence seizures

Uncovering the neuronal mechanisms by which ASs are generated within the TC network is one of the primary research goals in the field. Human AS studies have been primarily concerned with localisation of SWDs and relative temporal activation of brain regions (Salek-Haddadi et al., 2003; Labate et al., 2005; Betting et al., 2006; Craiu et al., 2006; Hamandi et al., 2006; Laufs et al., 2006; Moeller et al., 2008; Bai et al., 2010; Berman et al., 2010; Tenney et al., 2013; Foley et al., 2013; Liao et al., 2013), as the only invasive electrophysiological study occurred prior to the availability of electrodes with single neurone resolution (Williams, 1953). Consequently, pathophysiological mechanisms of ASs on the neuronal level have been investigated in experimental models.

1.4.1 Cortical mechanisms

Cortical neuronal activity during ASs was first investigated in the FGPE model. Extracellular recordings showed that all cortical neurones (pyramidal and non-pyramidal) displayed a clear

firing preference for the spike of the SWC, and had almost no activity during the wave (Kostopoulos et al., 1981a; Avoli and Kostopoulos, 1982; Avoli et al., 1983). Intracellular recordings indicated that the spike-associated APs of deep cortical neurones were preceded by depolarisations while the wave-associated silences involved Cl^- mediated hyperpolarisations (Fisher and Prince, 1977; Giaretta et al., 1987). Abolition of SWDs by cortical post-ictal depression suggested that cortical hyper-excitability was a requirement for SWD expression (Avoli et al., 1981).

Further *in vivo* experiments involving SWDs in anaesthetised cats (Steriade and Contreras, 1995) as well as HVS in rats (Kandel and Buzsáki, 1997) confirmed this spike-associated high density cortical output. In the latter of these experiments, the observation of SWC peak-associated high-frequency field oscillations and active current sources was attributed to large-scale interneuronal activation. This represents a rare investigation of a cell type-specific hypothesis of cortical involvement in AS. It was shown in anaesthetised animals (Steriade and Contreras, 1998), computational models (Destexhe, 1998), and thalamic slices (Blumenfeld and McCormick, 2000) that increases in cortical excitability could induce cortical and/or thalamic oscillations resembling SWDs. The pharmacological increase in cortical excitability was induced by the $GABA_AR$ antagonist bicuculline, and $GABA_BR$-induced K^+ currents generated the wave observed in the computational model, but the observation of Cl^- mediated IPSPs in FGPE suggests that $GABA_AR$ contribution to cortical generation of SWDs cannot be ruled out.

Intracellular recordings both in anaesthetised cats (Steriade and Contreras, 1995) and rats under neuroleptanalgesia (Charpier et al., 1999; Pinault, 2003; Chipaux et al., 2013) confirmed the presence of rhythmic, synaptically driven depolarisations and firing [Fig. 1.9]. Given the consensus surrounding the nature of cortical activity during ASs, attention turned to its precise timing relative to EEG events and thalamic activity. Although multi-unit recordings suggested that VB and VL thalamic neurones discharged before those of cortical layers IV/V (Seidenbecher et al., 1998), more precise single cell timings indicate cortical activity approx. 20 ms prior to the SWC peak negativity, compared to approx. 12 ms for both TC and nRT (Pinault, 2003).

The most recent advancement in cortical pathophysiology of ASs involves the identification of an SWD initiation site in both WAG/Rij and GAERS models [Fig. 1.10]. The peri-oral region of WAG/Rij somatosensory cortex was found, by nonlinear association analysis of LFPs, to consistently lead all other cortical and thalamic signals within the first 200ms of an SWD

(Meeren et al., 2002). GAERS SWDs were detectable in LFPs of facial somatosensory cortex before those of other cortical and thalamic regions, while layer V/VI neurones of this region were more depolarised and more active during seizure than those of both other layers of the same region and layer V/VI of other regions (Polack et al., 2007). Interestingly, these deep layer neurones of the cortical focus alone exhibited brief (< 1 s) epochs of oscillatory activity, similar to that displayed during seizure, inter-ictally and pre-ictally.

The idea of a cortical initiation site in WAG/Rij and GAERS has been supported by studies showing greater sensitivity of this region to pharmacological disruption of seizures (Manning, 2004; Sitnikova and van Luijtelaar, 2004; Polack et al., 2007; van Raay et al., 2012), while the hypothesis of an increase in GAERS cortical excitability as a causal change in AS-prone animals has been supported by the identification of an increase in stargazin and AMPAR proteins GluA1 and GluA2 in GAERS somatosensory cortex (Powell et al., 2008; Kennard et al., 2011). This increase appeared to be developmentally associated with the onset of seizures, but it should be noted that thalamic expression of these proteins was not measured and that the change was not mirrored in WAG/Rij. A primarily cortical source of the excitatory drive propagating ASs had also been suggested by the observation of multiple current sinks and sources throughout cortical layers during HVS (Kandel and Buzsáki, 1997).

In summary, all available evidence from both *in vivo* and *in vitro* studies has reached a consensus regarding hyperactivity of cortical pyramidal neurones during experimental AS. Recent evidence also supports the hypothesis of a cortical initiation site leading other activity during, and sometimes before, seizure. There is a lack of information regarding the role of different types of cortical neurones in seizure initiation and propagation, with most studies so far concentrating on pyramidal neurones and some limited evidence suggesting a significant level of interneuronal activity.

1.4.2 Thalamic mechanisms

Neuronal activity of the thalamus during ASs was also first investigated in the FGPE model. It was found that dorsal thalamic neurones of the cat fired rhythmically during SWDs but were less uniformly synchronous with specific SWC features than were cortical units – they separated into two groups with firing peaks approx. 45 ms before and after the SWC peak (Avoli et al., 1983). Subsequent experiments in multiple *in vivo* models of AS and *in vitro* models of SWDs have confirmed the presence of rhythmic firing (Banerjee et al., 1993; Inoue et al., 1993; von Krosigk et al., 1993; Seidenbecher et al., 1998; Blumenfeld and McCormick,

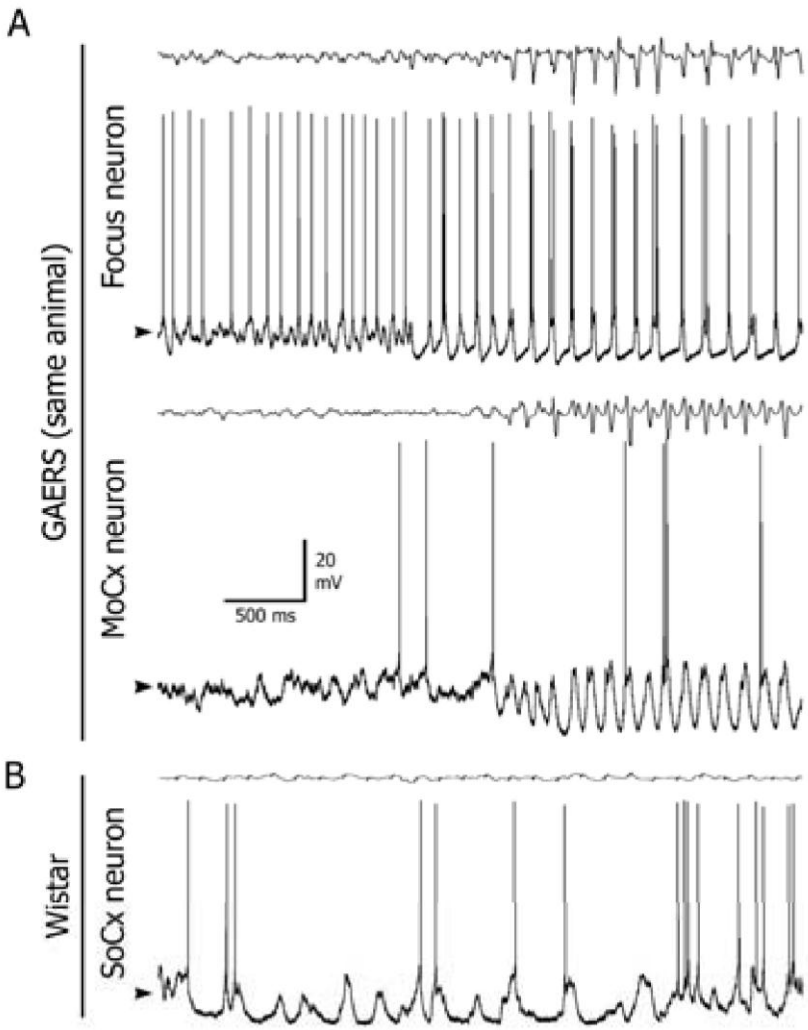

Figure 1.9 Intracellular activity of cortical neurones during SWD in GAERS

Intracellular recordings of neurones from layer V neurones of different cortical areas: S1po (initiation site of ASs) in GAERS, motor cortex (MoCx) in GAERS and S1po in Wistar. ***A*** Note the hyperactivity including regular action potential firing and some high-frequency bursts in the GAERS S1po neurone only, starting before the SWD is detectable on the EEG. The GAERS MoCx neurone membrane potential begins to oscillate in phase with each cycle of the SWD but displays a much lower firing rate and relatively hyperpolarised membrane potential. ***B*** The Wistar neurone demonstrates normal activity for an S1po cell layer V cell. Taken from Polack et al., 2007.

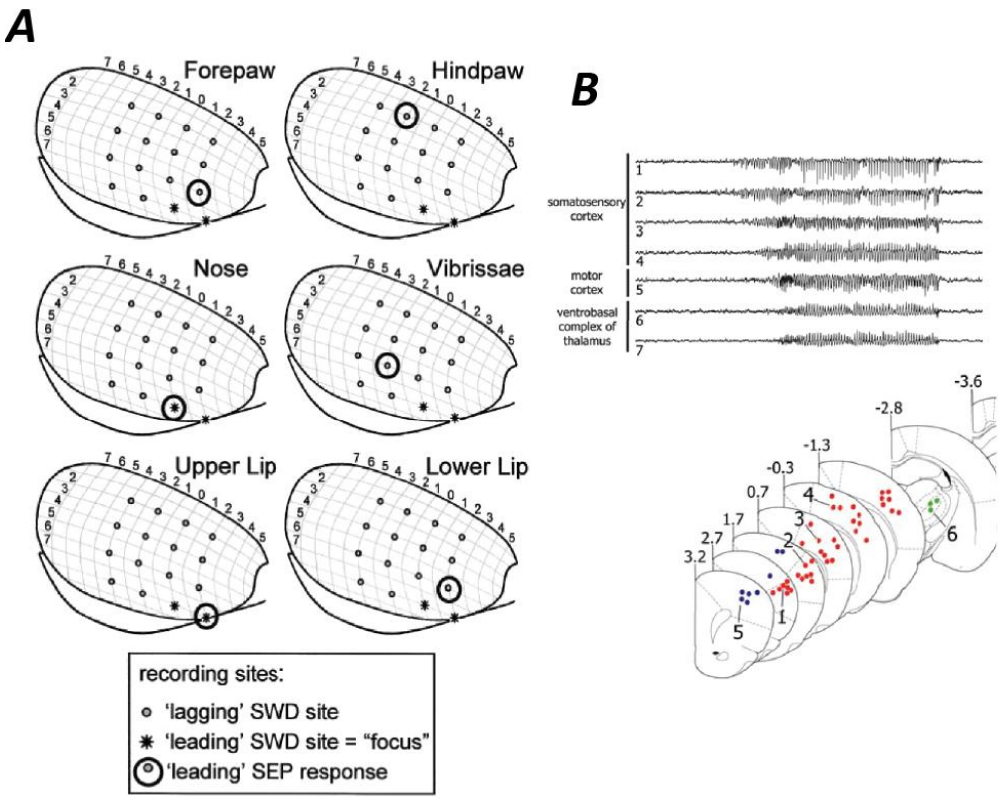

Figure 1.10 An S1po cortical initiation site of absence seizures in WAG/Rij and GAERS

Representations of the cortical focus of absence seizures in ***A*** WAG/Rij and ***B*** GAERS. ***A*** In the former case, the figure shows in which subregions of S1 cortex SWDs tended to lead according to nonlinear association analysis. ***B*** In the latter case recording of local LFPs compared only somatosensory cortex with motor cortex and thalamus, showing that ~99% of SWDs were detectable first in the former. Figures taken from Meeren et al., 2002, and Polack et al., 2007.

2000; Biagini et al., 2001; Meeren et al., 2002), but its nature at the level of single thalamic neurones is the subject of polarised debate.

Activity of TC neurones during SWD-like oscillations in $GABA_AR$ antagonist (bicuculline)-treated thalamic slices (von Krosigk et al., 1993) involves repetitive LTCP-mediated bursts interspersed with $GABA_B$ IPSPs (Bal et al., 1995a). Recording of peri-geniculate nucleus (PGN, an analogue of the nRT for the lateral geniculate nucleus) neurones in the same conditions revealed EPSP-induced LTCP-mediated rhythmic bursts. This prompted the hypothesis that ASs involve rhythmic burst firing of all TC neurones that excites those of the nRT, causing them to burst in turn and thus reciprocally inhibit TC neurones via a $GABA_B$ IPSP, which triggers a rebound burst upon its decay to complete the cycle [Fig. 1.11]. Although the oscillation was called absence-like, no behaviour is observable in slice preparations and the similarity of the slice LFP observed to thalamic LFP during absence is not definitive on its own. The effect of ETX on the oscillation was not tested.

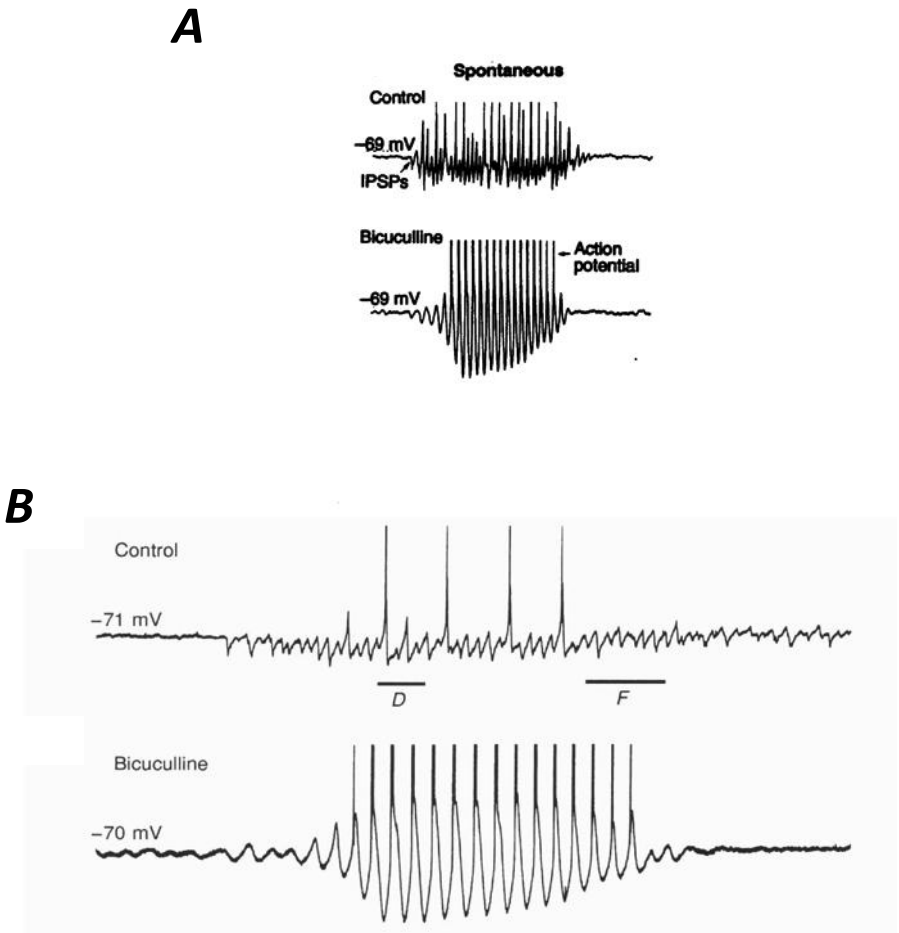

Figure 1.11 Paroxysmal activity in thalamocortical slices induced by $GABA_AR$ block

Intracellular recordings of TC neurones in thalamocortical slices from von Krosigk et al., 1993 and Bal et al., 1995. The cellular activity in the upper traces resembles that observed during spindle waves *in vivo*. The activity in the lower traces is the result of application of 25 µM bicucculine ($GABA_AR$ antagonist) to the same slice. This oscillation, being at a lower frequency than the spindle activity, featured thalamic bursts at every cycle.

TC-triggered cortico-thalamic bursts, in a non-bicuculline-treated slice, could shift oscillation frequency from spindle-like to (human) AS-like with a concomitant significant increase in nRT bursting (Blumenfeld and McCormick, 2000). This extended the hypothesis network wide, to suggest how TC $GABA_A$ vs $GABA_B$ inhibitory balance might determine the form of oscillation expressed and placing considerable emphasis on the driving role of the thalamus in AS propagation.

Some support for the hypothesis of TC LTCPs being both present and (to some degree) causal during ASs comes from studies showing that upregulation of $Ca_V3.1$ T-type Ca^{2+} channels induces an AS phenotype in mice (Ernst et al., 2009), while knockout of the same gene abolished TC burst firing and prevented induction of AS by GHB (Kim et al., 2001). Furthermore, an increase in I_T induced by $Ca_V2.1$ loss of function also appears to generate AS (Zhang et al., 2002, 2004; Song et al., 2004). Such support comes with two caveats: none of these experiments showed that specifically thalamic $Ca_v3.1$ was responsible for the AS-related phenotypes, and removal of I_T is likely to have consequences beyond a simple abolition of the ability to fire bursts. The putative I_T-blocking effect of ETX on ASs showed in these studies may be seen to support the *in vitro* hypothesis (Coulter et al., 1989b, 1990; Huguenard and Prince, 1994), but this also suffers from a lack of region specificity as well as evidence suggesting ETX acts primarily via other channels (Pfrieger et al., 1992; Leresche et al., 1998; Crunelli and Leresche, 2002b).

Very much in opposition to this hypothesis are results of multiple intracellular recording studies in anaesthetised, SWD-expressing animals. Cats that express SWDs under urethane or ketamine/xylazine were found to have predominantly ictally silent TC neurones (60% of cells), with the remainder expressing rhythmic bursts in synchrony with the SWD. It was suggested that the summation of nRT-originating IPSPs were responsible for the inhibition of the former group, while the firing of the latter group (and that of the nRT) was ascribed to cortical excitation (Steriade and Contreras, 1995).

Under an anaesthetic regime of fentanyl and haloperidol GAERS continue to express SWDs, during which most TC neurones expressed similar, but not identical, activity to that observed in the anaesthetised cats. Intracellular recordings showed that 26 of 28 cells fired only sparsely during seizure (at a range of holding potentials) and underwent a sequence of one EPSP and multiple IPSPs over each SWC, all mounted on a tonic hyperpolarisation [Fig.1.12]. The IPSPs were sometimes followed by one or more APs (near the spike of an SWC) that could be mounted on an LTCP, depending on the membrane potential. Notably, the IPSPs appeared to

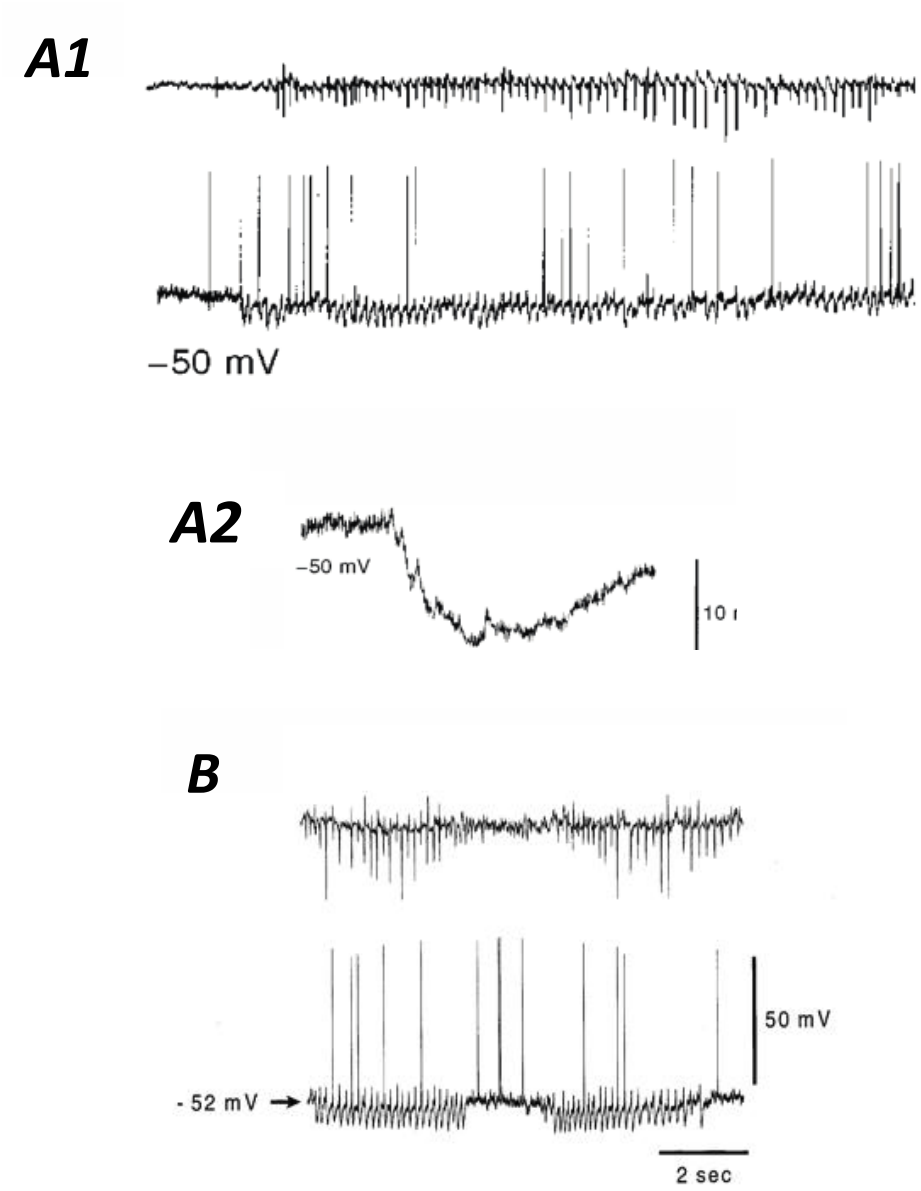

Figure 1.12 Intracellular activity of TC neurones during SWD in GAERS

A,B Intracellular recordings of TC neurones showing a tonic hyperpolarisation and sparse firing (lower traces) associated with SWDs (upper traces). ***A2*** shows an expanded trace demonstrating the sequence of EPSPs and multiple IPSPs at each cycle of an SWD. Note the lack of LTCPs and burst firing during the SWD. Modified from Pinault et al., 1998 and Charpier et al., 1999.

be $GABA_A$R-mediated while the tonic hyperpolarisation displayed no clear reversal potential (Pinault et al., 1998). Further investigation, in the same conditions, of TC neuronal behaviour during GAERS SWDs confirmed the absence of rhythmically alternating $GABA_B$ IPSPs and LTCPs, but suggested that the long-lasting hyperpolarisation may represent the summation of multiple extremely prolonged $GABA_B$ IPSPs (Charpier et al., 1999). Simultaneous recordings of cortical and TC/nRT neurones also suggested that the depolarising waves observed at each cycle, which sometimes triggered single APs or bursts, were composed of EPSPs of cortical origin in both thalamic cell types (Pinault, 2003). It was also demonstrated that HVS in Long-Evans under fentanyl anaesthesia featured almost identical TC and CT membrane activity to GAERS SWDs (Polack and Charpier, 2006). Intracellular activity of nRT neurones during SWDs [Fig. 1.13] showed rhythmic hyperpolarisations followed by LTCPs and high-frequency bursts accompanying the spike of each SWC (Slaght et al., 2002).

It is apparent that *in vitro* and *in vivo* evidence suggests two very different pictures of TC and nRT activity during AS. In the former, stimulation of cortical afferents by TC bursts promotes nRT activity that in turn generates TC $GABA_B$ IPSPs, and rebound bursts. In the latter, prolonged TC inhibition (mixed with some EPSPs) and nRT activation suggests a driving role for cortical input. Although the latter hypothesis appears more consistent with the discovery of the cortical initiation site in GAERS and WAG/Rij, neither can be considered definitive given their limitations.

TC slice oscillations *in vitro* can only be judged on their similarity to true SWDs on the LFP level, and will never reproduce the complexity of the intact animal. It is noteworthy that application of K^+ channel and excitatory amino acid antagonists to cortico-thalamic slices also generates SWD-like oscillations, but featuring depressed rather than elevated TC activity (Biagini et al., 2001). Evidence from *in vivo* preparations suffers from the same caveat, to a lesser degree: SWDs under anaesthesia can not be presumed to be equivalent to those accompanying ASs due to the lack of a behavioural correlate. Finally, the lack of ensemble recordings of single units in either situation means that we have no demonstration of the firing dynamics of individual cortical, TC or nRT neurones with physiological membrane conditions during ASs.

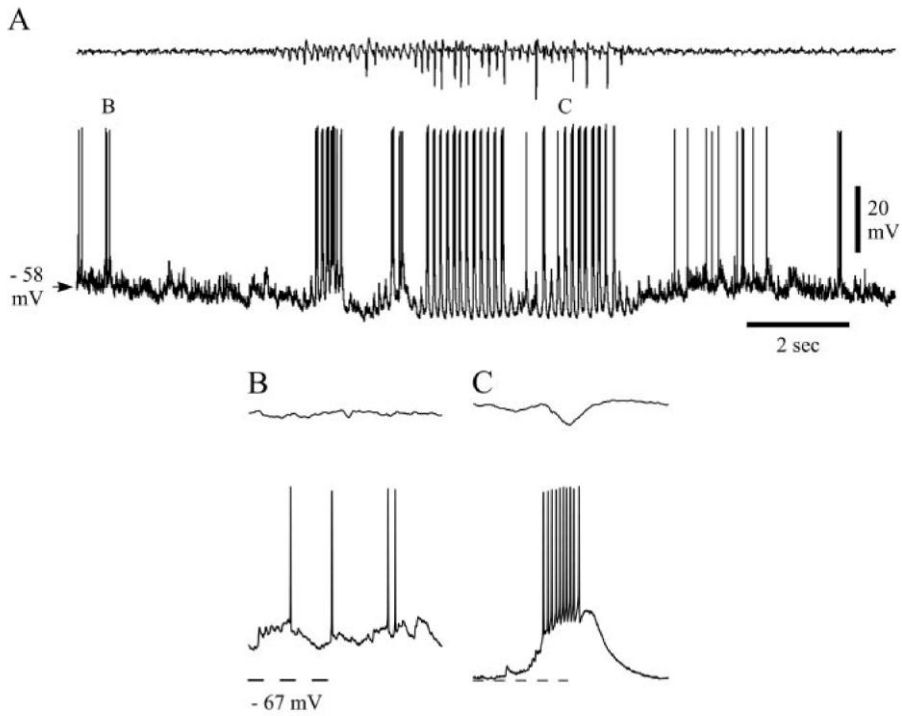

Figure 1.13 Intracellular activity of nRT neurones during SWD in GAERS

A Intracellular recordings show that background activity of nRT neurones changed from either occasional tonic firing or mixed lower frequency bursts to high-frequency burst activity phase-locked to each cycle of the SWD. The tonic hyperpolarization observed here was seen for the majority of SWDs. ***B*** and ***C*** show expanded traces from the pre-ictal and ictal periods respectively. The latter shows an LTCP crowned with a high-frequency burst of APs. High-frequency EPSPs can also be seen on the rising phase of the LTCP. Taken from Slaght et al., 2002.

1.5 Thesis Aims

The primary aims of this thesis are 1) to determine the firing dynamics of TC neuronal activity during ASs and 2) to investigate the contribution of T-type $Ca2^{+}$ channel-mediated activity in these neurones to the initiation and the propagation of ASs. Both of these aims are in service to the greater goal of understanding the neuronal mechanisms by which ASs are generated, spread throughout the TC network, and exert their behavioural effects. The nature of TC and nRT neuronal activity was investigated by extracellular recording of multiple isolated neurones of that type, while their significance was investigated by measuring the effect on AS of blocking T-type $Ca2^{+}$ channels in those regions.

Chapter 2 – Methods

2.1 Animal experiments and ethical statement

GAERS were bred in-house in an established colony at the School of Biosciences, Cardiff University (UK). All rats had access to food and water *ad libitum*. The housing room was maintained on a 12:12 hour light:dark cycle with light on at 08:00 and off at 20:00. Ambient temperature was maintained at 19-21°C with 45-65% relative humidity. Male rats of 4 to 7 months of age (300 – 350g) were used for the following experiments. All animal experiments were approved by the Home Office and carried out in accordance with local ethical guidelines.

2.2 *In vivo* reverse microdialysis and EEG recordings in GAERS.

2.2.1 Anaesthesia and analgesia

Anaesthesia was induced by isoflurane inhalation, delivered to an induction box at 5% concentration in 2L/minute oxygen. After transfer of the animal to a stereotaxic frame, anaesthetic delivery (via mask) was gradually reduced to a maintenance level of 1.5% to 2.5% isoflurane in 1L/minute oxygen. Appropriate surgical level of anaesthesia was maintained, with absence of hind leg withdrawal reflex and tail pinch reflex (Flecknell, 2009) and steady breathing rate as primary criteria. Rectal temperature was also monitored, as measured by the probe of a homeothermic heat blanket (#507220F, Harvard Apparatus, Kent, UK), and maintained at 37 °C.

General analgesia was provided by subcutaneous administration of 2mg/kg meloxicam (Metacam, Boehringer Ingelheim, Berkshire, UK) during surgery, when maintenance level of anaesthesia was reached. After the 48-hour period for which this injection provided general analgesia, animals were monitored for persistent signs of pain or infection and culled if necessary.

2.2.2 Surgical procedures

2.2.2.1 Implantation of EEG electrodes

The rat was positioned on a stereotaxic frame, stabilising the head via a horizontal mouthpiece bar behind the upper incisors, non-traumatic ear bars in both auditory canals, and a further horizontal bar clamped over the snout. The snout was partially enclosed in a custom-made

mask guiding vaporised anaesthetic across the nostrils and being cleaned by a scavenging system installed beneath.

Hair was removed from the top of the head, from eye-level to the nape of the neck. The skin was cleaned and sterilised with iodine-impregnated medi-wipes before application of lidocaine for local analgesia. Paraffin-based eye lubricant (Lacrilube, Allergan Inc, California, USA) was applied to both eyes before shielding from surgical lighting with a homemade single-use mask. A scalpel (blade 10/10a/11) was used to make a single midline incision from between the eyes to the back of the skull. Hemostatic forceps and Dieffenbach/bulldog clamps (WPI, Florida, USA) were used to retract skin and connective tissue anteriorly and posteriorly, opening up the skull area.

The skull surface thus exposed (revealing both lambda and bregma as well as all of frontal, parietal and occipital bones not occluded by muscle) was cleared of connective tissue using light abrasion with a jeweller's forceps (WPI, Florida, USA), and any blood vessels in the surrounding area were constricted by application of chilled sterile saline or, if necessary, cauterised (Bovie cauteriser, Bovie Medical Corp, USA).

Six gold-plated screws (1cm, Svenska Dentorama AB, UK) were used to record fronto-parietal EEG with cerebellar ground and reference from each animal. Each screw post was soldered to the exposed end of an ~3cm length of insulated copper wire prior to surgery. A dental drill was used to make six holes in the skull: bilaterally over the frontal cortex, parietal cortex and cerebellum [Fig. 2.1]. The dura mater was left intact where possible. The posts were screwed into the skull, sufficient for stabilisation but not to impinge upon the dura, and fixed permanently with methylacrylic cement. Each copper wire was then soldered to an individual channel of a 6-pin straight solder tail PCB socket connector (Preci-Dip, Switzerland). Additional cement was applied to completely cover the wires and keep the connector in place above the skull midline, creating a smooth-sided single-piece cap. Care was taken to ensure wires from different screws had no points of contact.

2.2.2.2 Implantation of microdialysis probes in the rat

After implantation of the EEG screw electrodes, two guide cannulae for CMA 12 microdialysis probes [Fig. 2.2] (Linton Instruments, UK) were lowered into the brain terminating at an appropriate adjacency to the area of interest. Craniotomies were opened above the target location using a dental drill and the bent tip of a 26-gauge needle (BD Microlance 3, Becton

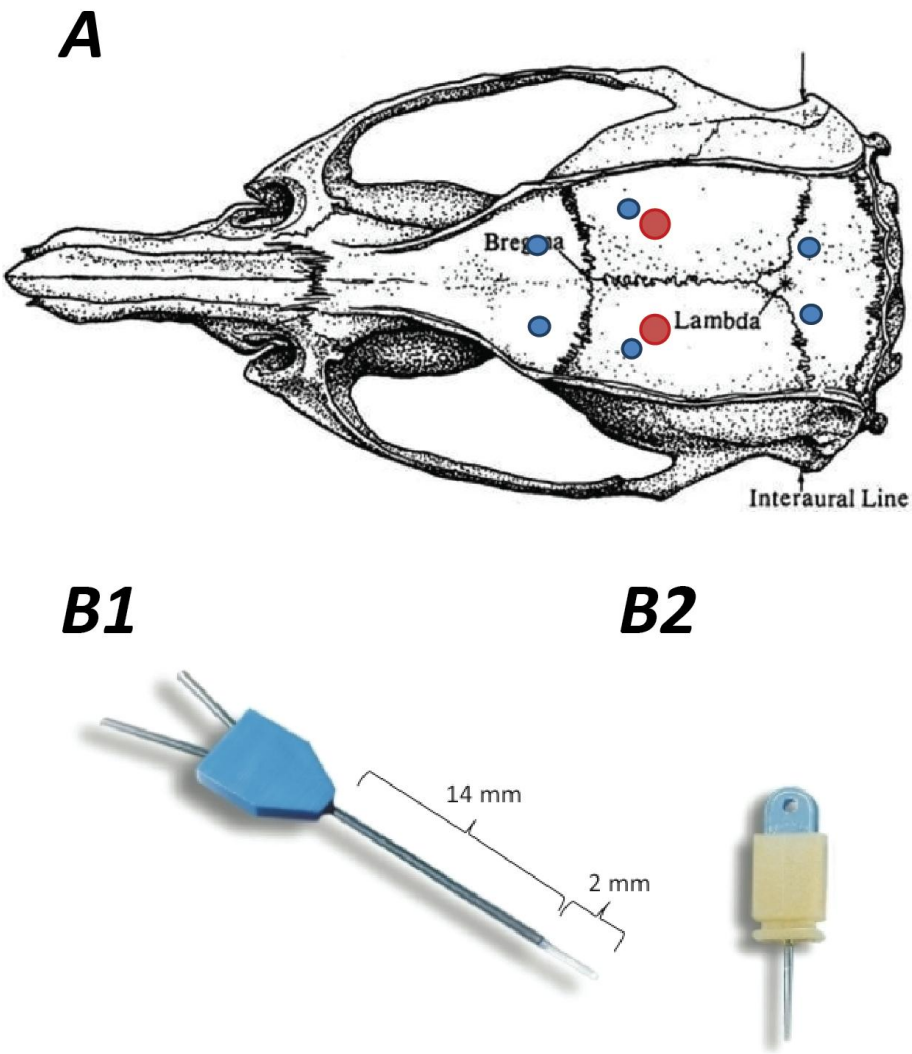

Figure 2.1 Frontoparietal EEG and thalamic microdialysis probe locations

A Overhead view of the rat skull showing the approximate locations of EEG screw post electrodes (blue) and microdialysis probes (red). ***B1*** Microdialysis probe, consisting of an inlet and an outlet, a plastic body and stainless steel 14 mm shaft that fits tightly within the guide cannula, and a 2 mm x 0.5 mm microdialysis membrane that extends beyond the silicon-coated cannula. ***B2*** The guide cannula includes a dummy probe to seal the cannula while the probe is not inserted, preventing any contaminants from entering the tissue. Figures in (B) taken and modified from www.microdialysis.se (CMA website).

Dickinson & Co, Ire.) to remove bone and dura mater. Bovine collagen coagulant (Lysostypt, B Braun Melsungen, Germany) was applied to staunch any bleeding from minor blood vessels within the craniotomies. The guide cannulae were lowered using a CMA 11/12 probe clip stereotaxic attachment (Linton Instruments, UK).

For the VB, stereotaxic positioning was at its dorsal extremity, above the exact midpoint in the transverse plane. The co-ordinates of the lower extremity of the microdialysis guide cannula relative to bregma were AP: -3.35mm, ML: ±2.8mm, DV: -4.4mm (Paxinos and Watson, 2008). For the nRT, stereotaxic positioning was again at the dorsal extremity of the VB but more lateral and medial than the transverse midpoint, to achieve probe positioning adjacent to but not within the bulk of the nRT. The co-ordinates relative to bregma were AP: -3.2mm, ML: ±3.55mm, DV -4.2mm [Fig. 2.2].

Once in position, any further bleeding was stopped before affixing cannulae to screw posts and to the skull with methylacrylic cement. The final cap structure incorporated all electrode wires and microdialysis guide cannulae. Skin rostral and caudal to the cap was sutured (16mm braided black silk sutures with X-8 needle, Cole Parmer, London, UK). As the cement was setting, the region around the implant was cleaned with sterile saline and antiseptic wound powder was applied around the margins of the incision and cap. Once the cement had set, the animal was removed from the stereotaxic frame and allowed to recover on the homeothermic blanket while being monitored.

2.2.3 Experimental protocols

All animals were returned to their home cage and allowed to recover from surgery for a minimum of 5 days prior to experiments. On the day of the experiment, for the duration of the recording and microdialysis protocol each animal was placed in an individual purpose-built plexiglass box housed within a Faraday cage to reduce extrinsic electrical interference with EEG signal. Each experiment consisted of a four-hour protocol. The first hour allowed habituation of the animal to the recording environment and stabilisation of seizure level (see behavioural observations under section 2.2.4.6 below). The second hour consisted of EEG recording during reverse microdialysis administration of artificial cerebrospinal fluid (aCSF). Hours three and four consisted of EEG recording during reverse microdialysis administration of either aCSF or test solution (TTA-P2 in aCSF at 300µM and 1mM concentrations) at a flow rate of 1 µL/min.

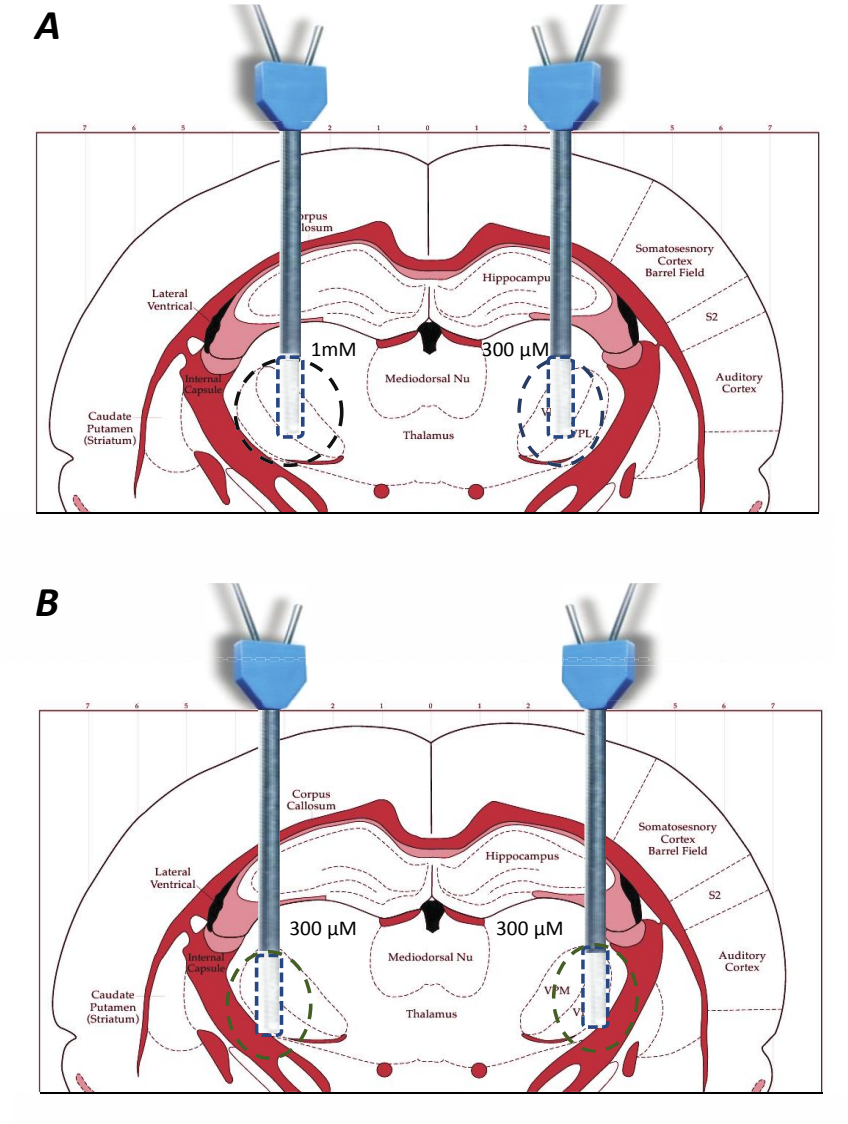

Figure 2.2 Microdialysis co-ordinates for VB and nRT

Coronal section of the rat brain showing locations targeted with microdialysis probes. ***A*** shows central VB position and ***B*** shows more lateral nRT-targetting position. Coloured circles correspond to estimated spread of TTA-P2 at 1hr time point at each location (blue: VB, green: nRT), with the former showing both 1mm and 300 µM concentrations.

A delay of 6 to 7 days between experiments was observed to allow animals to fully eliminate drugs and return to baseline conditions. Each animal was recorded from twice, once with aCSF and once with TTA-P2. Further recordings were not attempted due to the risk of significant damage to brain tissue carried by repeated insertions of a microdialysis probe.

2.2.3.1 EEG recording

As the animal was placed in the recording cage, the PCB connector on their implant cap was connected via a pre-amplifier and multi-strand insulated copper wire cable to an analogue EEG amplifier (4-channel SBA4-v6 BioAmp, SuperTech Inc., Hungary). A counterweighted swivel arm positioned above the recording chamber allowed free movement of the animal while connected. The pre-amplifier applied a high-pass filter to the received signal at 0.08 Hz, while the amplifier applied a gain of 1000 and a low-pass filter at 500 Hz. Impedance of the pre-amplifier was 10 MOhm. The signal was converted into digital form at a sampling rate of 1k Hz by a Cambridge Electronic Design (CED) Micro3 D.130 digitiser and CED Spike2 7.3. Signal was recorded, for all four hours of the protocol, as amplified differential EEG between frontal and parietal screw electrodes, with cerebellar reference, and recordings were stored on external hard drives.

2.2.3.2 Reverse microdialysis

The dummy probes within microdialysis probe guide cannulae were replaced with CMA 12 probes (Linton Instruments, UK) 18 hours prior to recording. This time delay was in order to allow brain tissue to recover from the trauma of insertion before recording began. The delay was introduced after pilot experiments suggested suppression of ASs in animals immediately after probe insertion. Animals were restrained in a towel during manual probe insertion to minimise anxiety and allow smooth insertion.

Immediately following connection of the EEG recording cable, FEP tubing (0.18 µL/cm internal volume) and tubing adaptors (Linton Instruments, UK) were used to connect the inlet of each probe via an adapted catheter (B Braun Melsungen, Germany) to 1mL syringes containing aCSF. The 1 mL syringes were secured in a 4-channel microdialysis pump (CMA 400, Linton Instruments, UK). Four cm of FEP tubing was connected to the outlet of each probe to direct exiting fluid away from the EEG connection. The tubing from syringe to probe consisted of two parts, with the 10 cm closest to the probe connected with the rest of the tubing via an adaptor. This facilitated switching of syringes with minimal disturbance of the animal. The

function of each microdialysis probe was checked by pushing a minimal amount of liquid at a flow rate of 10 µL/minute. The pump was then switched off for the 1 hr habituation period.

The microdialysis pump was switched on at a flow rate of 1 µL/min throughout the second hour of the protocol (pre-drug control). After this period the syringes were exchanged with a set containing TTA-P2 in aCSF at the desired concentration (0 µM to 1 mM), which was supplied at the same flow rate for 2 hours. At the end of the recording session probes were removed and, if undamaged, washed with and stored in deionised water for re-use. Dummy probes were replaced in the guide cannulae after cleaning with deionised water and 80% ethanol sequentially.

2.2.3.3 Behavioural observations and manipulation

Behaviour of all animals was monitored throughout the experiments, both in order to time interventions appropriately and to correlate with recorded EEG. A video camera recorded activity simultaneously to EEG recording, using Spike 2 video software (CED, Cambridge, UK) to precisely time-match EEG and video.

Due to dependency on the sleep/wake cycle of ASs in GAERS it was desirable to maintain a stable level of arousal in the animals throughout the reverse microdialysis and recording period. This was reinforced by pilot experiments demonstrating that increasing time in sleep over the four-hour period, as animals became used to their environment and progressed further into the dormant portion of their sleep/wake cycle, corresponded to decreasing time in AS during aCSF microdialysis. Infrequent stimulation, involving gentle handling of the animal, proved most effective at maintaining a stable baseline while minimising confounding effects of irregular experimenter intervention. A constant starting time was also observed, with all recordings commencing at 8 am, the start of the sleep portion of the GAERS sleep/wake cycle.

2.2.3.4 Histological processing

After the second recording session, animals were sacrificed by administration of a terminal dose of 200 mg/kg sodium pentobarbital (Euthatal, Merial Animal Health Ltd, Essex, UK) and intra-cardiac perfusion after breathing and all peripheral reflexes had ceased. While the euthatal took effect, 1 µL of thionine dye was applied within the base of both guide cannulae using a 10 µL Hamilton syringe in order to highlight the probe's tracks. Phosphate-buffered saline (PBS, 0.9% NaCl) was perfused to flush the vasculature of blood before chilled 4%

paraformaldehyde (PFA, buffered in 0.9% NaCl PBS) was administered as the fixative. The descending artery from the heart was clamped with hemostatic forceps to speed PFA delivery to the brain. Upon cessation of all muscle convulsive responses to PFA the brain was removed and immerse fixed in 4% PFA for a further 4 hours.

Brains were then kept refrigerated in 0.9% NaCl PBS until slicing and imaging. Brains were sliced around the region of interest at a thickness of 100µm on a Leica VT 1000S vibratome while immersed in chilled 0.9% NaCl PBS. Slices were mounted on microscope slides and photographed using a Nikon D90 camera (Nikon Imaging, UK). Images were then inspected and rated on proximity of probe track to desired location, damage to target region, and any other abnormal damage and/or bleeding. Any animals with probe tracks damaging target region or with abnormal damage to other regions were excluded from analysis, as were animals in which tracks significantly deviated from desired path. Five of 30 animals were excluded in this fashion, leaving a total of 25 animals among 3 groups.

2.2.4 Data analysis

Spike 2 software (v2.708, Cambridge Electronic Design Ltd., UK) was used for offline filtering and SWD identification, while Matlab (R2011b, The Mathworks Inc., USA) was used for SWD quantification and inspection of intra-SWD parameters (on unfiltered waveforms). SWD identification was performed blind (i.e. without knowledge of the drug with which the animal in question had been treated).

2.2.4.1 Absence seizure identification

SWDs were isolated from the rest of the EEG signal using the SeizureDetect script (kindly provided by Steven Clifford of CED) designed for sleep spindle and AS detection). The process of detection involves multiple steps. First, baseline EEG (desynchronised, active or resting wakefulness) is identified manually and a voltage amplitude threshold set at 5-7 times standard deviation of the mean, depending on signal-to-noise ratio of the signal. Secondly, parameters for initial seizure detection are applied to all points that cross this threshold (henceforth referred to as crossings, while SWDs are henceforth referred to as events). The parameters are as follows:

- Maximum time between initial two crossings of 0.2 s
- Maximum time between any two crossings within an event of 0.35 s
- Minimum 5 crossings per event

- Minimum time of 0.5 s between any two events for them to count as separate (otherwise overriding 0.35 s limit and merging events)
- Minimum event duration of 1 s.

The final component of the SeizureDetect script gated detected events by dominant frequency band (calculated by time intervals between crossings rather than by spectrographic analysis). If >25% of crossing intervals were outside the 5-12 Hz range then events were excluded from the final analysis. This included high-frequency artifacts as well as lower-frequency, high-amplitude sleep-related events. Designated SWDs were then visually inspected to ensure parameters were appropriate and signal-to-noise ratio was sufficient for effective isolation. Video recordings were inspected for each session to ensure SWDs featured concurrent behavioural arrest. Figure 2.3 shows a sample SWD.

2.2.4.2 Absence seizure quantification

Three parameters of ASs were calculated for all experimental groups in 20-minute epochs: total AS duration, average AS duration, and total number of ASs. As is discussed below (section 2.4), a 1-hour epoch from 40 to 100 minutes post drug was calculated to be the optimal period for quantifying drug effect during microdialysis. A script was designed in Matlab to calculate these values based on input of the start and end time of each seizure in a recording. Values were expressed as raw values (seconds per hour, seconds, and seizure number respectively) and as a percentage of the corresponding value across the hour of pre-drug control (normalised values). The normalised values were used for inferential statistics due to the extremely high variability in time spent in seizure between recording sessions and the low variability between pre- and post-drug portions of a single recording session.

2.2.5 Principles of reverse microdialysis

The technique of local drug administration by reverse microdialysis merits an in-depth investigation of its advantages and limitations over other methods of drug delivery.

Dialysis refers to the passage of a molecule across a permeable membrane from a compartment of higher concentration to one of lower concentration of that particular molecule. Microdialysis is a technique originally designed to monitor levels of particular molecules, either endogenous species or drugs, in organic tissue (Galvan et al., 2003). This involves passing of a control liquid along the inside of a microdialysis membrane within the tissue and sampling the concentration of the molecules of interest picked up by that liquid as

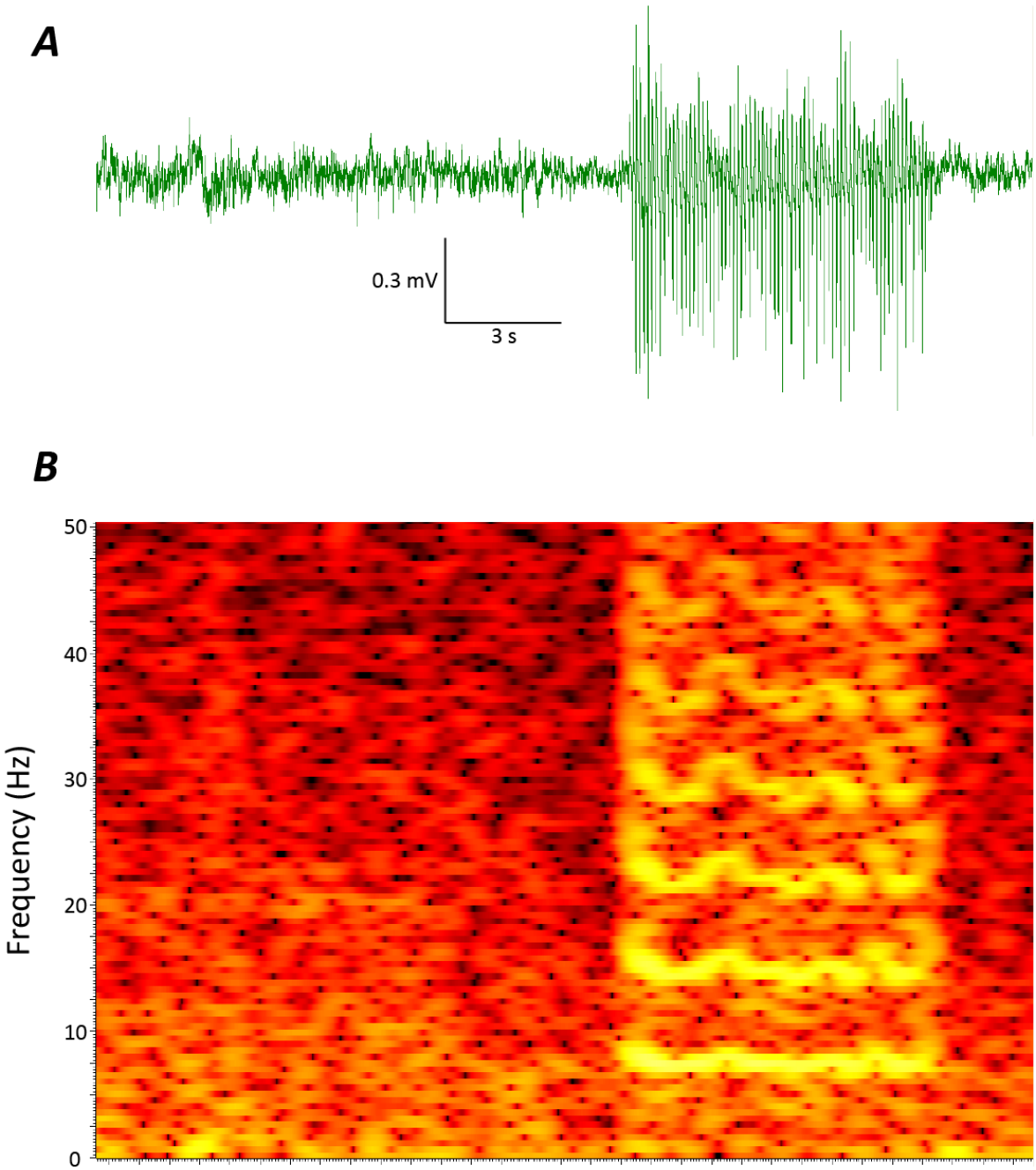

Figure 2.3 GAERS frontoparietal SWD

A A sample SWD recorded from frontoparietal subdural electrodes in GAERS. EEG before and after SWD shows low-voltage desynchronised waveform typical of wakeful states, with no post-ictal depression. ***B*** Sonogram of the same ictal and inter-ictal periods shows peak power of SWD entirely within the 6 – 8 Hz band, with harmonics recurring around multiples of 7 Hz.

it exits the microdialysis probe. It can be used *in vivo* or *in vitro*, and allows frequent or even continuous sampling of tissue without the trauma of excising parts of the tissue for analysis.

The principle can be reversed, dissolving a higher concentration of a molecule of interest in the input liquid to introduce it to the extracellular space of the target tissue across the dialysis membrane (Höcht et al., 2007). The input solution maintains a bidirectional exchange of molecules (down their concentration gradients) with interstitial fluid. This concentration-driven diffusion across a membrane has been shown to be the sole significant driver of molecular exchange/transport during microdialysis, with effects of osmosis and hydrostatic pressure being minimal (Bungay et al., 1990).

In order to prevent alteration of the composition of this fluid, microdialysis input solutions should mimic the interstitial fluid for all species except those that are being measured or supplied. In the case of the experiments detailed in Chapter 4, TTA-P2 was dissolved in artificial cerebrospinal fluid (aCSF, Tocris Bioscience, Bristol UK), which closely resembles CSF of the rat brain (Davson et al., 1987).

Administration of a drug by reverse microdialysis can be divided into two stages: diffusion of the drug across the membrane, and further transport of the drug through the tissue. The primary factors determining rate of membrane diffusion are membrane size (Plock and Kloft, 2005) and permeability. The former must be balanced with considerations for minimising trauma to the brain and risk of diffusion beyond the target region. Probe dimensions appropriate to VB targeting were taken from Richards et al. (2003), who used a cylindrical probe of 2 mm length by 1 mm diameter. The same probe design was used for nRT targeting.

Membrane permeability must be matched to the molecular weight and hydrophobicity of the species in question, and CMA 12 microdialysis probes (Linton Instrumentation, UK), with a cut-off of 20 kDa, allowed the passage of TTA-P2. This permeability level has been shown to block the passage of larger molecules, including bacteria (Shippenberg and Thompson, 2001).

Once diffusion of the drug across the microdialysis probe membrane has occurred, the concentration of the drug that spreads throughout the target area is dependent on its transportation through the tissue in that area. In the brain this occurs primarily by diffusion through extracellular space. The spatial arrangement of extracellular space, neurones, and glia results in a spread of drug that is both complex and dependent on intrinsic properties of the molecule in question (Boehnke and Rasmusson, 2001). *In vitro* experiments suggested that

concentration of drug in dialysis membrane-adjacent tissue reached ~10% of input concentration (Juhász et al., 1990; Portas et al., 1996), but the experiments in this thesis required knowledge of concentration throughout the target region and beyond, not just in the immediate vicinity of the probe.

With this in mind, concentration selection and targeting in these experiments was based on work done by Dr François David and Mr Joscha Schmiedt in the Crunelli lab (David et al., 2013). These experiments measured the percentage block of LTCP-mediated burst firing (under ketamine anaesthesia) of Wistar rat TC and nRT neurones after 1 hour of microdialysis at varying input concentrations and distance from the probe membrane, as well as the distance at which a 50% block of burst firing was achieved over time for 300 µM TTA-P2. The results [Fig. 2.4] show that an input concentration of 300 µM achieves a full block of LTCP-mediated bursts up to 600µm from the probe membrane. When considered in conjunction with the dimensions of the CMA 12 probe, this would result in a concentration of TTA-P2 appropriate for blocking of LTCPs existing throughout the VB. By contrast, 1 mM TTA-P2 achieved a block up to 750 µm from the membrane, which when administered to the centre of the VB would also reach a considerable proportion of the nRT.

The distance/time relationship of half-block by 300µM TTA-P2 showed that distance blocked began to plateau after 40 mins. For this reason the hour from 40 minutes to 100 minutes post-drug was calculated to be the period during which 300 µM TTA-P2 would be affecting the target area (entirety of VB or majority of nRT plus majority of VB, depending on probe position) while minimising potential blocking of T-type Ca^{2+} channels beyond the target area. This hour was therefore chosen as the period in which drug effect on ASs and SWDs would be measured. When 1mM TTA-P2 was being administered the possible spread of drug beyond the target region was of less significance, so the decision was taken to calculate drug effect based on the same post-drug hour as for 300 µM.

The advantages and disadvantages of local drug administration by reverse microdialysis are listed here.

Advantages:

- Flow rate can be adjusted to achieve desired delivery with minimal depletion of endogenous compounds; in this case 1µL/min proved appropriate (Shippenberg and Thompson, 2001).

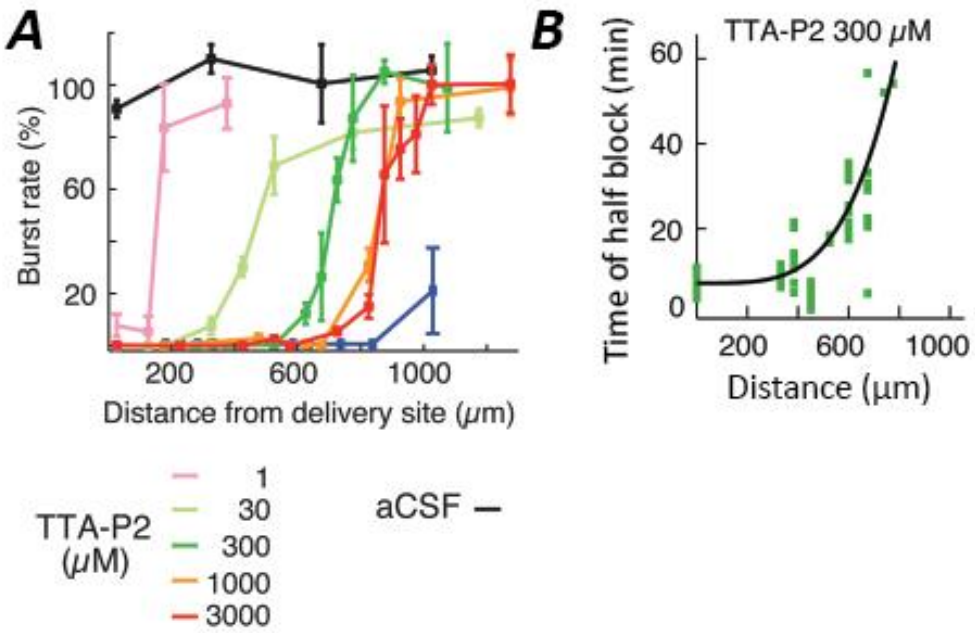

Figure 2.4 Dose and distance dependence of TTA-P2 block of LTCP-mediated high frequency bursts

A Graph of percentage of bursts remaining at 1hr versus distance from the microdialysis membrane for a range of concentrations of TTA-P2. 300 µM achieves 100% block up to 600 µm from microdialysis membrane, while 1 mM achieves 100% block up to 700 µm. ***B*** Time at which 50% block of burst firing was achieved at various distances from microdialysis membrane for 300 µM TTA-P2. Curve begins to plateau at approx. 40 minutes.

- Drug delivery can be maintained at a constant rate for a sustained period of time (Höcht et al., 2007).
- No introduction of fluid prevents tissue trauma from turbulence or pressure (Shippenberg and Thompson, 2001).
- Probe function can be monitored throughout the experiment by assessing the output (Höcht et al., 2007).
- Can be achieved in freely moving animals allowing for behavioural assessment.

Disadvantages:

- Initial probe introduction is more traumatic than that of a microinjection needle due to larger area/volume of membrane than of needle tip.
- The membrane can be easily damaged and can become blocked if introduced continuously for very long periods (days).

The disadvantages were dealt with in these experiments as follows: introduction of the probe approximately 18 hours before each recording session allowed time for the tissue to recover from the initial insult before experiments took place, and careful monitoring of probe integrity and function before and during insertion minimised the proportion of blocked or damaged membranes.

2.3 *In vivo* ensemble unit recordings in GAERS

2.3.1 Electrode and microdrive preparation

Four shank, linear, 32-site silicon probes (Buzsaki32) were purchased from NeuroNexus (Michigan, USA). The probe design was originally developed by the Buzsaki lab for inter-laminar cortical recordings. An alternate probe with varying recording site sizes/impedances was also custom made by NeuroNexus according to a design by Dr François David and Prof Vincenzo Crunelli aiming to detect signal from a single neurone per site. The layout of both probes is shown in Figure 2.5. An Omnetics (Minneapolis, USA) HST/32V-G20 headstage/preamplifier was attached by a 2cm-long flexible ribbon. The 34-pin headstage interfaced with a HSC-32V Omnetics/Plexon cable. Recording sites of all shanks were cleaned before implantation by immersion in detergent at 60°C for four hours, before rinsing with deionised water.

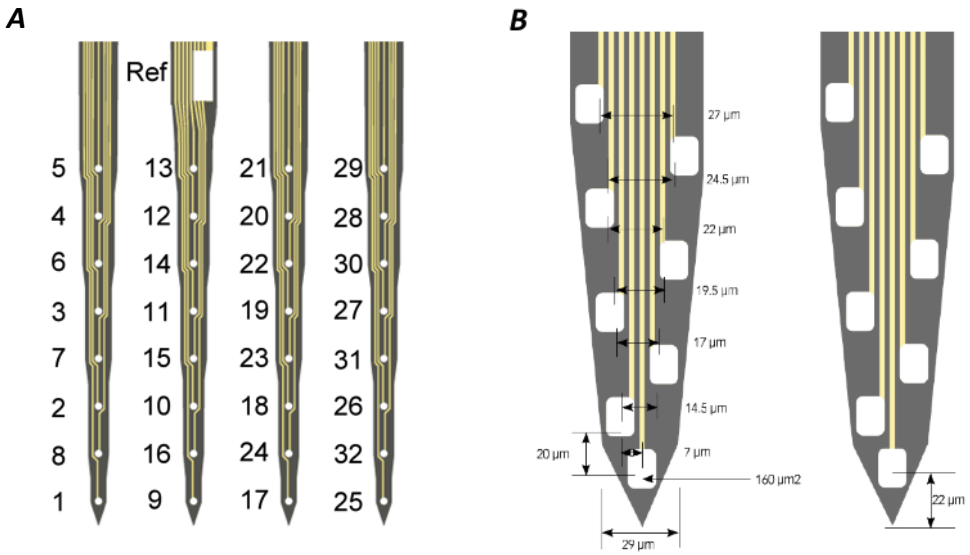

Figure 2.5 Multi-shank silicon electrode site maps

A Representation of the 32 channel, 4 shank custom recording electrode. Recording site areas are, from top to bottom: 100 μm^2, 75 μm^2, 50 μm^2, 25 μm^2, 25 μm^2, 25 μm^2, 50 μm^2, 75 μm^2. ***B*** Expanded view of Buzsaki32 probe recording sites on 2 (of 4) shanks, site areas are all 160 μm^2.

The silicon probe was mounted on a microdrive similar to that described by Vandecasteele et al., (2012). The microdrive consists of a plastic stage, on which the probe is mounted by grip cement, movable between two fixed brass platforms by the turn of a screw. It allows approximately 8mm total movement in the dorso-ventral plane and has dimensions of 1.2cm x 0.9cm x 0.4cm.

2.3.2 Anaesthesia and analgesia

The same anaesthetic regimen detailed in section 2.2.1 was employed for the implantation of the microdrive-mounted silicon electrode in GAERS.

2.3.3 Surgical procedures

2.3.3.1 Implantation of ground, reference and fronto-parietal EEG screws

Initial arrangement and preparation of the rat was carried out in the same fashion as detailed in section 2.1.3.1 above, up to the point of skull surface cleaning and preparation. Due to the importance of maintaining a secure implantation for a prolonged period (> 1 month), H_20_2 was carefully applied to the skull surface, avoiding any other tissue, in order to facilitate the removal of organic debris that could later destabilise the cement cap. Once the skull surface was prepared, stereotaxic co-ordinates for the silicon probe implantation were calculated before any insertion of screws or cementing.

Holes for ground and reference screw posts (00-90, 1/8" stainless steel screws with soldered copper wires) were drilled through the skull above the cerebellum as described in section 2.1.3.1 above. Holes for EEG gold-plated screw posts were also drilled in similar positions above the frontal and left parietal cortex only. The right parietal cortex was avoided to facilitate later implantation of the silicon electrode. The muscle lateral to the right parietal cortex was resected with minimal damage to allow the drilling of two further anchor screw postholes and the insertion of the screw posts (compare Figure 2.6 showing screws and probe positioning with Figure 2.1).

All screw posts were cemented to the skull surface and each other using Metabond dental cement (Parkell Inc, NY, USA). The parietal skull surface was kept free of cement for later opening of the silicon probe craniotomy.

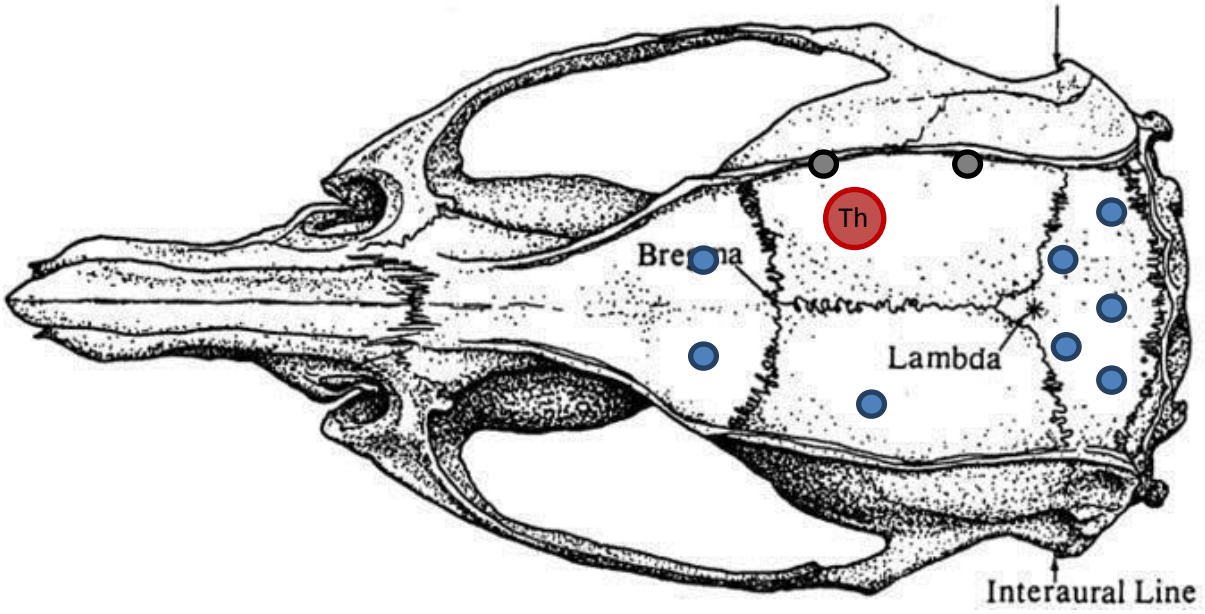

Figure 2.6 Cerebellar reference screws and silicon electrode locations

Overhead view of the rat skull showing approximate locations of anchor screws (black), EEG, ground and reference epidural screws (blue), and craniotomy for implantation of four-shank silicon electrode (red) into VB.

2.3.3.2 Implantation of microdrive-mounted silicon probe

Two sets of co-ordinates were used for the silicon probes. The first, for initial experiments, had the shanks of the probe parallel to the rostro-caudal axis to maximise area of the VB sampled. The second was employed in later experiments and featured a probe orientation parallel to the medio-lateral axis to sample both VB and nRT simultaneously. Rostro-caudal probes were centred at AP: - 3.35 mm, ML: ± 2.8 mm while medio-lateral probes were centred at AP - 3.2 mm, ML ± 3 mm (Paxinos and Watson, 2008). A cross was marked by scraping with a scalpel blade at this location on the skull surface. After screw insertion and securing with cement, a round-head drill bit was used to drill in a circle around the implantation site, carefully thinning the skull without penetrating until a circle of bone could be lifted away using a bent 26-gauge needle. The dura was pierced with a curved insect needle and no. 10 scalpel blade. Any minor bleeding was staunched by irrigation with sterile, chilled 0.9% NaCl.

When the dura was retracted, the silicon probe and microdrive were positioned in a stereotaxic arm above the target region. Position was readjusted as necessary to avoid major vasculature on the brain surface, and then smoothly lowered into the brain (observing initial entry to ensure shanks did not bend) until dorsoventral co-ordinates were reached (approximately 4mm dorsal from the brain surface, i.e. the top of the thalamus). The microdrive was secured with grip cement, while the same product was used to create a mini-Faraday cage and protective structure of copper mesh. The craniotomy was sealed with liquid paraffin wax.

2.3.4 Experimental protocols

Recording commenced immediately after surgery in order to monitor neuronal activity during recovery from anaesthesia, and likewise was continued daily during the animal's full recovery. Data for analysis, however, was collected only after the animal had recovered for 2 days. The recording protocol involved connecting the animal, in its home cage (which was nested within a Faraday cage for the duration of the recordings), 1 hour into the sleep portion of its sleep/wake cycle (9am). Upon connection the presence or absence (on any channels) of thalamic neurones suitable for recording was assessed based on the shape and amplitude of any visible spikes. If no such neurones were present, the silicon probe was moved dorsally within the brain on its microdrive by turning its screw either ⅛, ¼, ½, or 1 full turn. Each full turn corresponds to an approximately 270 µm movement.

Each recording lasted 1 to 5 hours, depending on the quality and stability of neurones recorded and the behaviour of the animal during the session. Each session included multiple sleep sessions, for characterisation of the high frequency LTCP-mediated burst signature of recorded neurones, and multiple ASs. Gentle and infrequent manual stimulation was provided if necessary.

The head-mounted HST/32V-G20 VLSI-based preamplifier has a 20x gain on the 32 high-impedance channels, as well as on 2 low-impedance reference channels, and unity gain on two buffered ground channels. This was connected to a Plexon data acquisition system consisting of the Recorder/64 amplifier and processing software. Gain was set to either 12,500x or 15,000x (maintained throughout a session) and the processing software was set to sample at 20 kHz with a 50 Hz notch filter. Online filtering could be used to visualise the raw, recorded signal as either LFP (low-pass filtering at 300 Hz) or as spiking/unit activity (high-pass filtering at 1000 Hz).

2.3.5 Data analysis

Analysis of the recordings used the NDManager, Neuroscope, and Klusters suite of software designed by the Buzsaki lab for the processing and visualising of the activity of multiple simultaneously-recorded spikes and LFP (Hazan et al., 2006).

2.3.5.1 Spike sorting

Spikes were extracted and then assigned to neurones by measuring the similarity of their principal components. Extraction of spikes first necessitated high-pass filtering of the obtained signal by subtraction median filtering (subtracting the output waveform of a median filter from the original waveform) using the “hipass” script of the Ndmanager program. Spikes were then identified using the “extractspikes” script of the same program, which recorded the time of occurrence and 32-sample peak-centred waveform of each spike exceeding 2 standard deviations of the mean (filtered) waveform. These extracted waveforms were submitted to principal component analysis, recording the first four principal components of each spike on each channel (8 channels per group for the Buzsaki32 probe, 1 for the custom design) as features.

Clustering involved two stages. The first used the unsupervised KlustaKwik program (Kadir et al., 2013) to group spikes with similar features into clusters based on a Classification Expectation Maximisation (CEM) algorithm (Celeux and Govaert, 1992; Harris et al., 2000;

Pouzat et al., 2002, Schmitzer-Torbert et al., 2005). Briefly, this method groups Gaussian distributions of spikes in a cluster [Fig. 2.7A] based on the assumption that each spike should be identical apart from the addition of stationary Gaussian background noise. The limitations of this assumption necessitate the second stage of clustering: supervised grouping of existing clusters that have been separated by CEM due to variation in spike shape but are deemed to originate from the same neurone. This variation can be caused by electrode drift, intra-burst variation, non-stationary noise (including multi-unit activity), and spike misalignment (Pedreira et al., 2012).

The second stage also involved supervised refinement of appropriate clusters and elimination of unsuitable clusters. Refinement consists of excluding any parts of automatically created clusters that are deemed to arise from noise, and clusters were deemed unsuitable if their spike waveforms were not distinct from background noise during all behavioural states, including ASs. Frequently, spike waveform would be constant and distinct during sleep and wakefulness but would be insufficiently large, relative to the high-frequency multi-unit noise observed at each SWC cycle, to sort during ASs. In this case the entire cluster was eliminated.

2.3.5.2 Behavioural state identification

The recordings were divided into one of three behavioural states: sleep, wake, and AS. Isolation of SWDs and confirmation of behavioural arrest were carried out as detailed in section 2.2.4.1 above. Detection of sleep periods, from the non-seizure parts of the recording, was achieved by plotting cumulative power over the 0.5 to 4 Hz frequency range, and setting a threshold at 2.5 standard deviations above the baseline value during a visually identified period of wakefulness. The remaining time (neither seizure nor sleep) was classified as wakefulness.

2.3.5.3 Neuronal classification

Neurones were classified as TC, nRT or unknown non-thalamic based on 1) recording site position during the relevant session (any neurones recorded while the sites were outside the VB/nRT region were excluded), 2) burst signature during sleep, and 3) spike half-width. The probe position during a given session was calculated retrospectively from its final position and recorded microdrive movements. Burst signature refers to the progression of inter-spike intervals over the course of an LTCP-mediated burst. These bursts were defined as three or more spikes with inter-spike intervals of ≤ 7 ms preceded by an interval of ≥100 ms. Spike width was calculated as half the interval between the positive shoulders preceding

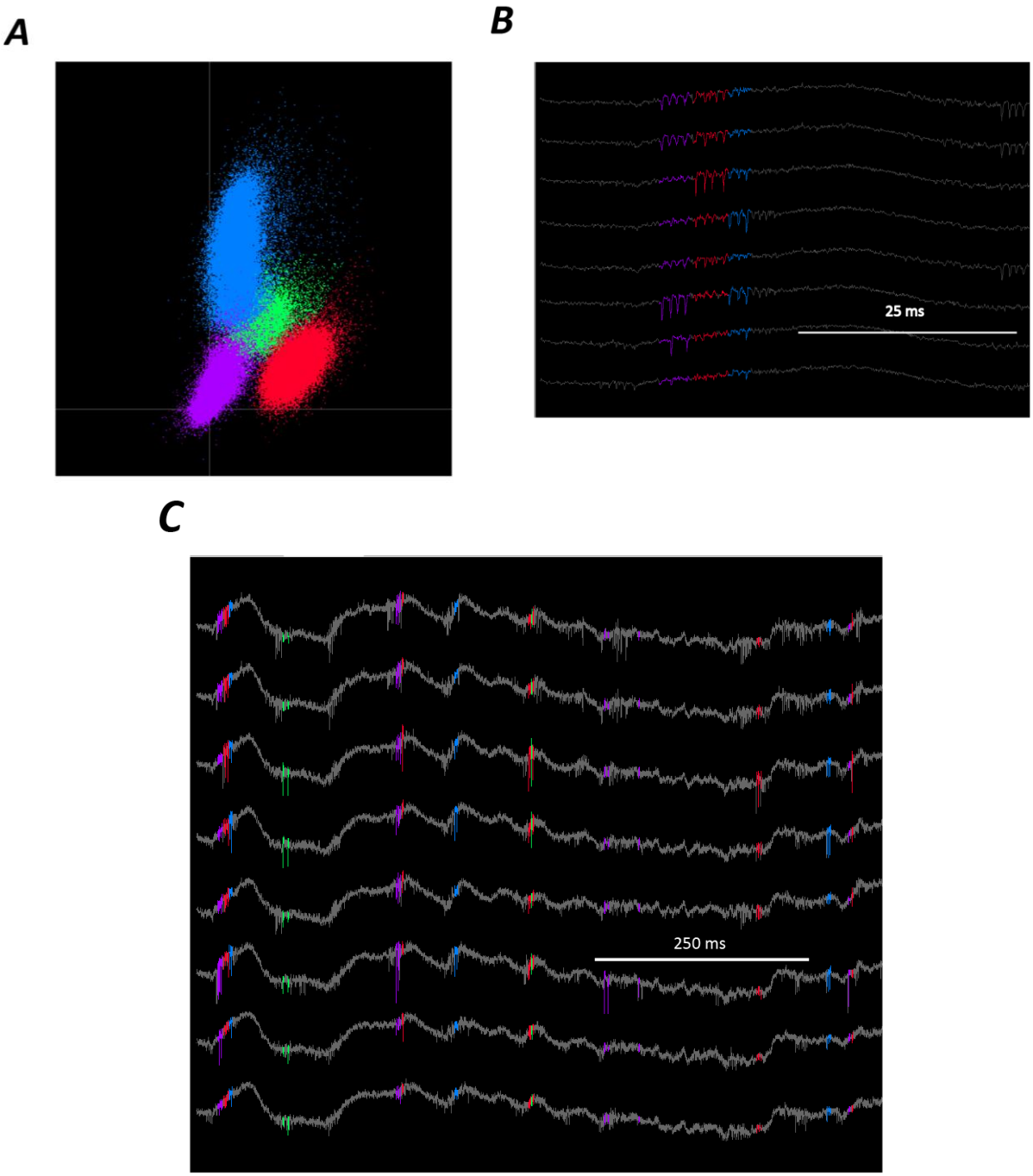

Figure 2.7 Neurone clustering

A Sample of 2-dimensional cluster parameter plot (of 25 total parameters used for Buzsaki probe recordings, 5 total parameters for custom probe recordings) showing 4 distinct neuronal waveforms. ***B*** Representation of 3 of these waveforms (purple, red, blue) across 8 grouped channels showing high-frequency bursts during sleep. ***C*** Trace display at lower magnification showing spike pattern of all four groups across a period of transition out of sleep.

and following the negative trough of a spike.

Any neurones recorded while the relevant recording site was definitely not within the VB were labelled unknown, as were any neurones that did not burst during periods of sleep. nRT neurones were defined as those with a mean number of spikes per burst greater than 3, a ratio of first to shortest ISIs greater than 1.3, a minimum ISI duration greater than 2 ms, and a spike half-width less than 0.25 ms, while TC neurones had those values less than 4, less than 1.4, less than 3 ms, and greater than 0.275 ms respectively [Fig. 2.8]. These are in agreement with previously noted trends for an accelerando-decelerando pattern in nRT bursts, which also tend to include more spikes than bursts of TC and have longer inter-spike intervals (Domich et al., 1986; Steriade et al., 1986; Huguenard and Prince, 1992) [see Fig. 1.7]. Recent evidence also suggests that nRT spikes in the VB are considerably narrower than those of TC neurones (Bartho and Acsády, unpublished data).

2.3.5.4 Neurone firing classification

Neuronal output was divided into single spikes, bursts, and doublets. The former included all spikes separated by > 7 ms, bursts were defined as above, and doublets were defined as any 2 consecutive spikes separated by ≤ 7 ms and preceded by an ISI of ≥ 100 ms (Llinás and Jahnsen, 1982; Huguenard and Prince, 1992).

2.3.5.5 Intra- and inter-neuronal associations

The relationships between spike trains of simultaneously recorded neurones were investigated by calculating auto- and cross-correlograms during each behavioural state (sleep, wake and seizure) using the Matlab script xcorr. 5 s epochs, divided into millisecond bins, were used for correlogram calculation.

2.3.5.6 Neurone-behaviour association

Single spike, doublet, burst, and total firing rates in each of the three behavioural conditions, as well as during transitions between conditions, were calculated across entire recording sessions, not by averaging the rates in individual behavioural epochs.

Transitions from wakefulness to seizure and vice versa were investigated by plotting mean activity rates (+/- standard error of the mean) 15 s before and after seizure start and end times. Only seizures of ≥ 15 s duration with preceding/following (as appropriate) wake periods also ≥ 15 s were selected. This allowed presentation of prolonged ictal and inter-ictal periods.

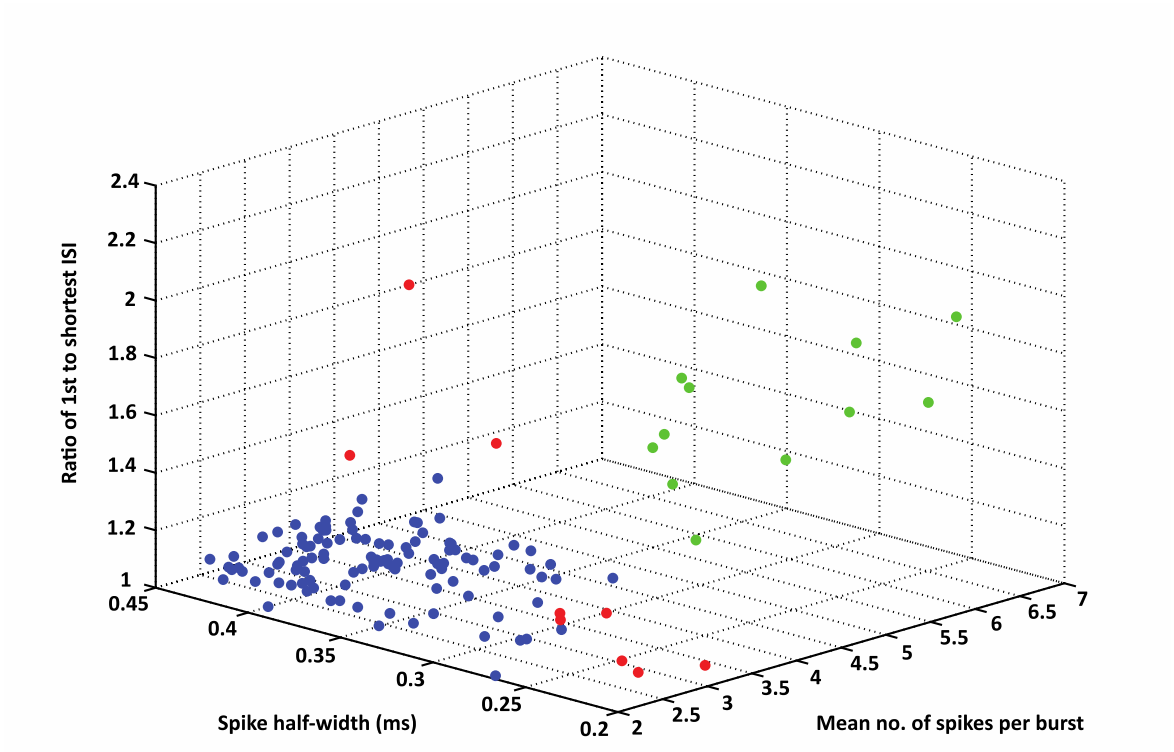

Figure 2.8 Neuronal classification

Parameters used to distinguish TC (blue, n = 104), nRT (green, n = 12) and unknown (red, n = 9) neurones were ratio of 1st to shortest ISI, spike half-width, and mean number of spikes per burst. Note the distinct clusters of TC and nRT neurones achieved by plotting these parameters.

Variation in neuronal activity between seizures was investigated by calculating correlation coefficients of firing and bursting rate for each seizure with seizure length, ictal EEG and LFP power at 6-8 Hz, arousal level before and after seizure, proximity of other seizures before and after seizure, and firing/bursting rates before and after seizure. Where differences between median correlation coefficients and zero were detected, coefficients of determination were also calculated.

2.3.5.7 Neurone-EEG association

Spike-triggered average EEG, SWC spike-triggered average neuronal firing, and proportion of SWCs exhibiting single spikes, bursts and silence were calculated. Mean EEG values surrounding ictal spikes and bursts (burst time taken as time of first spike) were calculated across entire recording sessions, and then averaged across all neurones of the same type (TC or nRT). Due to possible variation in SWD feature timing between animals with varying EEG electrode positions, all such analysis was carried out separately for each animal.

Peaks of SWC spikes were detected by finding all local maxima more than 3 standard deviations above the mean DC-removed EEG amplitude and refining to maintain only the ultimate maximum within each SWC. Spike and burst rates were averaged in 1 ms bins for 200 ms either side of each of these peaks. Heights of the central peaks of these distributions were calculated relative to the minima of the 150 ms (approximately SWC frequency) flanking them. Widths of the central peaks were calculated at 10% and 50% of their total relative heights.

SWC epochs were extrapolated from spike peak detections by selecting periods between adjacent peaks with intervals less than 200 ms. These epochs were used to calculate per-SWC firing, bursting, single spike, and doublet rates across entire recording sessions.

2.4 Drugs

The concentrations of drugs used in each experiment are stated in the relevant chapter results section, i.e. sections 3.3 and 4.3.

2.4.1 Sources of drugs

aCSF was purchased from Tocris Biosciences (Bristol, UK).

3,5-dichloro-N-[1-(2,2-dimethyl-tetrahydro-pyran-4-ylmethyl)-4-fluoro-piperidin-4-ylmethyl]-benzamide (TTA-P2) was a kind gift from Merck Inc., USA.

2.4.2 Formulation of solutions

TTA-P2 was dissolved in DMSO (2% of final solution) before addition to aCSF. An identical concentration of DMSO was added to the aCSF solutions. The pH of both solutions was 7 ± 0.4.

2.5 Statistical analysis

2.5.1 Microdialysis experiments

Paired Gosset's t-test was used for analysis of the effect of TTA-P2 on GAERS ASs. This decision was made due to the pre-experiment designation of a particular post-drug period (40 minutes to 100 minutes, see section 2.2.1) as that during which TTA-P2 would be affecting the target area without significantly spreading to other areas. This allowed the calculation of a single biologically relevant value per parameter per recording, suggesting a t-test to compare aCSF and TTA-P2 treatments. The fact that each animal received both aCSF and TTA-P2 on different recording days meant that a paired test was appropriate.

To confirm the observed effect using a more conservative statistical method, avoiding any need for normalising post-drug values as a percentage of pre-drug, 2 way repeated measures ANOVA was carried out using time (pre vs post drug) and treatment (aCSF vs TTA-P2) as factors. If an interaction could be detected between the factors, Bonferroni post-hoc tests were used to investigate each treatment individually.

2.5.2 Unit recording experiments

Medians and 5^{th} to 95^{th} percentile ranges were used to describe the distributions of each rate in each behavioural state, and Wilcoxon's matched pairs tests were used to compare rates of the same activity in different behavioural states. Wilcoxon's signed rank tests were used to investigate whether medians of distributions of correlation coefficients between activity rates and other ictal parameters differed from zero. In both cases signed rank tests were chosen due to the non-normal nature of the distributions studied.

The same descriptors of centre and spread were used for distributions of per-SWC rate, of percentages of SWCs accompanied by various types of firing, of rate standard deviations, and of firing rate – parameter R^2 values.

Chapter 3 – Activity of TC and nRT neurones during absence seizures in freely moving GAERS

3.1 Introduction

The best existing indications of thalamic activity during ASs come from intracellular and multi-unit recordings in anaesthetised animals (*in vivo*) and in thalamic and thalamocortical slices (*in vitro*). The two methods have suggested completely different activities: predominant silence, mediated by EPSP and $GABA_A$ IPSP barrages, in anaesthetised *in vivo* (Steriade and Contreras, 1995; Pinault et al., 1998) and burst firing on each cycle of an SWD, mediated by $GABA_B$ IPSPs and LTCPS, in slice *in vitro* (von Krosigk et al., 1993; Bal et al., 1995a, 1995b; Blumenfeld and McCormick, 2000) experiments. Neither situation features the behavioural correlate necessary to constitute true ASs, and consequently the true activity of TC and nRT neurones during ASs remains uncertain.

The experiments detailed here contain the first thalamic neuronal ensemble recordings in an experimental model of ASs. Both TC and nRT neurones were recorded and the results gained provide an understanding of the nature and the timing of output of the these neurones during GAERS ASs.

3.2 Methods

The methods used for this set of experiments are detailed in section 2.2.

3.3 Results

This section will discuss, in turn, results pertaining to the firing dynamics of TC neurones, to those of nRT neurones, and to the relationship between the two during ASs recorded in freely moving GAERS. To investigate the electrical activity of thalamic neurones during ASs, extracellular single unit, LFP and EEG recordings were obtained from 5 freely moving GAERS rats over multiple 1.5 to 3 hour sessions. Data were obtained from 134 neurones over 46 recording sessions, and 3420 ASs (mean 74.35 seizures per session, 55.45 seizures per neurone). Of these neurones 104 were classified as TC and 12 as nRT based on their spike waveform and burst signature during sleep (see section 2.3.5.3). The remaining 18 were unclassifiable due to these distinguishing factors (waveform and burst) fitting into neither category (9 neurones), to the burst firing rate during sleep being less than that during waking, indicating that these were not thalamic neurones (8), or to there being fewer than 10 seizures

during the recording period of the neurone (1). These group sizes were used throughout the following analyses except when otherwise indicated.

All recording sessions were divided into mutually exclusive seizure, sleep, and wake segments based on EEG parameters and behavioural observation (see section 2.2.4.1 and 2.3.5.2). Seizures lasted between 2 and 200 s, with a mean duration of 11.47 ± 4.42 s. AS peak frequency was invariably 7 ± 0.5 Hz, with the only elevated power outside the 6 to 8 Hz band being harmonics at 14 and 21 Hz [see Fig. 2.3]. SWC amplitude varied from 0.5 to 2 mV in the waxing and waning pattern common to frontoparietal EEG. All of these features are comparable to those previously reported for GAERS (Marescaux et al., 1992a).

3.3.1 Firing dynamics of TC neurones during absence seizures

3.3.1.1 Firing rate of TC neurones decreases during seizure

An initial overview of TC neurone activity during ASs was obtained by viewing raster plots of TC spike times and simultaneous EEG, allowing the comparison of activity during multiple ictal and inter-ictal periods [Fig. 3.1A]. It also demonstrated, on the millisecond timescale, the temporal association of TC spikes and SWCs. This immediately suggested that TC neuronal activity significantly decreases during seizure, and that TC neurones fire mostly in synchrony with SWCs. The mean auto-correlogram of TC neurones during absence seizures revealed peaks recurring at the frequency of SWDs (6 to 8 Hz) that were absent from auto-correlograms of sleep and wake states [Fig. 3.1B].

For a quantitative investigation of the relative level of TC activity during ASs, descriptive statistics of firing rates during each behavioural state were calculated for all ASs in all TC neurones. Throughout this chapter, descriptive statistics are chosen to provide the most accurate overview possible of each distribution. The median was chosen as a measure of centre and 5^{th} to 95^{th} percentile range as a measure of spread due to their robustness to outliers and ability to summarise non-normal distributions, in contrast with the mean and standard deviation or standard error. Thus, in this chapter all descriptors of distribution will be in the form of a median followed by a 5^{th} to 95^{th} percentile range unless otherwise stated.

The firing rate during seizure (median = 6.23 Hz, 5^{th} to 95^{th} percentile range = 2 to 13.45Hz) was lower than that during wakefulness (11.01 Hz, 2.81 − 22.33 Hz) by signed rank test ($P < 0.0001$) but slightly higher than that during sleep (5.53 Hz, 1.68 − 11.51 Hz, $P = 0.0002$).

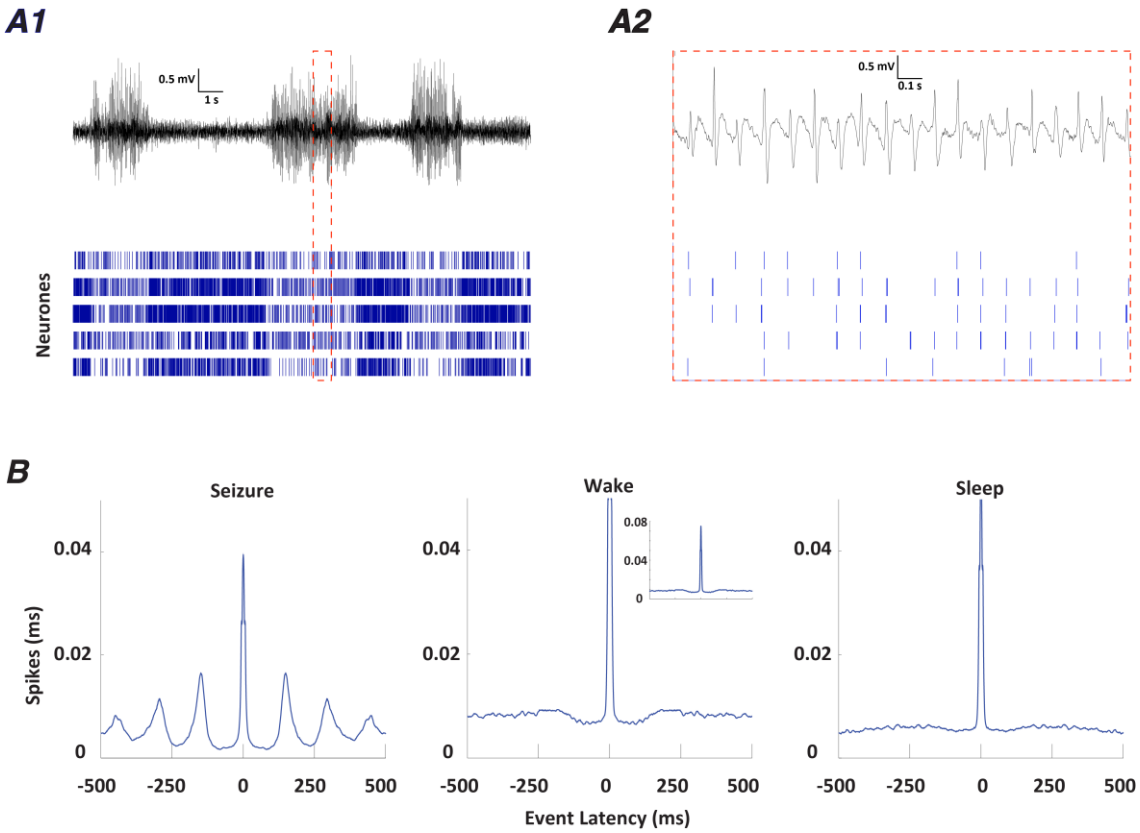

Figure 3.1 TC activity is decreased and periodic during seizure

A1 Simultaneous EEG trace (top) and spike rasters of 5 TC neurones demonstrate the decrease in firing rate associated with ASs. ***A2*** An expanded section of A1 shows the synchrony of neuronal firing to SWCs, as well as providing a rough impression of the relative prevalence of ictal silence, single spikes and multi-spike events for these neurones. ***B*** Mean auto-correlograms during each behavioural state confirm the periodic nature of TC activity during seizure, n = 104. Peak of wake autocorrelogram is shown as an inset to maintain consistent scaling between behavioural states.

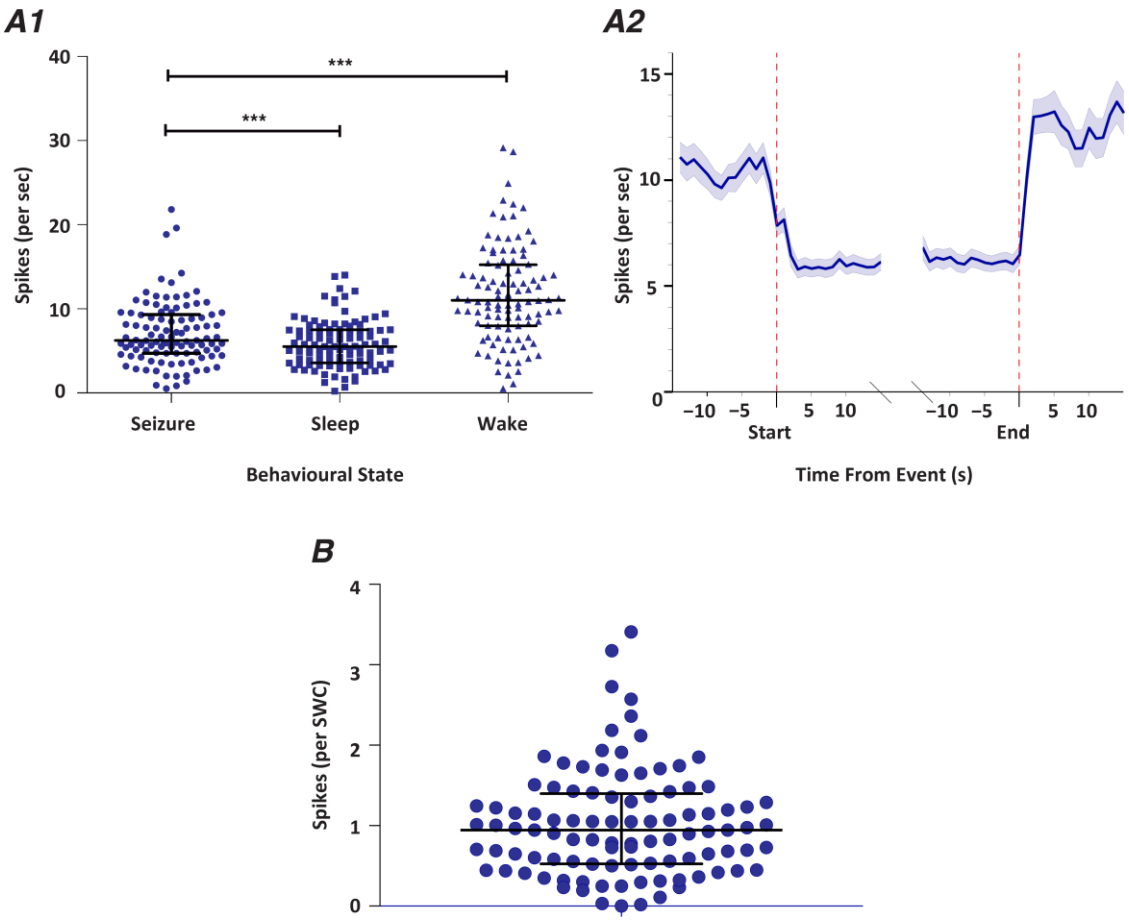

Figure 3.2 TC firing rate during seizure is lower than during wakefulness

A1 Firing rate during ASs with a centre (line indicates median, bars indicate interquartile (IQ) range) and distribution more similar to that of sleep than of wake. ***A2*** The evolution of firing at the start and end of seizures above 15s duration shows how firing rate changes at transitions between wakefulness and seizure. Note that the rates in A2 should not be considered as absolutes, given the selection of 15s+ seizures only (see section 2.3.5.6). In this (and similar plots in following figures) vertical dashed lines indicate the start and end of the SWD as detected in the EEG. ***B*** Distribution of mean firing rates per SWC. For this and all subsequent figures *** = P < 0.001, ** = P < 0.01, * = P < 0.05.

Plotting mean per-second firing rates over periods of transition from wakefulness to seizure [Fig. 3.2A] provided a visual summary of the relative rates and an indication of any transient rate changes around seizure start or end points. The observed ictal (~6 Hz) and inter-ictal (~12 Hz) rates are similar to the total median rates in the equivalent states. Mean rates appear stable throughout seizures, and there are no obvious fluctuations pre- or post-seizure.

Whereas per-second firing rates are useful for comparison of ictal and non-ictal activity, per-SWC firing rate is a more relevant seizure-specific descriptor of activity levels [Fig. 3.2B], since each SWC comprises a single, distinct opportunity for interaction between cortical and thalamic populations. The median rate was 0.94 spikes per SWC (0.2 − 2.35 spikes/SWC).

These data indicate that TC ictal firing rate is lower than that of waking periods. Neurones are approximately as active ictally as they are during sleep, representing a significant decrease in activity from waking levels. Approximately one spike per SWC is fired on average, indicating that a hypothesis of ictal TC hyperactivity, through high-frequency burst firing or otherwise, isn't supported by the data. Overall, it appears that seizure initiation from a state of wakefulness is accompanied by an increase in homogeneity and decrease in intensity of TC activity levels, as well as the establishment of a periodic firing pattern.

3.3.1.2 TC neurones are mostly silent during seizure, with single spikes observed during the greater portion of active SWCs

3.3.1.2.1 85% of SWDs are accompanied by neuronal silence or single spikes

To investigate the relative prevalence of LTCP-dependent bursts, single spikes, and doublets, the proportion of all events (an event being any one of those three forms of output) belonging to each firing mode during seizure was calculated [Fig. 3.3A]. The median burst percentage of events was 5.05% (0.59 − 23.10%), single spike percentage was 81.28% (45.29 − 94.93%), and doublet percentage was 19.71% (3.44 − 31.81%). Repeating the same measures for percentages of all spikes, rather than by percentage of all unique events, yielded a median burst spike percentage of 19.07% (4.92 − 45.53%), a single spike percentage of 60.96% (24.81 − 84.80%), and a doublet spike percentage of 19.36% (5.18 − 40.31%).

A more SWD-specific measure of the contribution of each output type involved calculating the percentage of SWCs during which TC neurones exhibited each of four types of activity (silence, single spikes, doublets, and bursts). It was found that (based on median values) TC neurones were silent during 48.19% of SWCs (10.46 − 90.72%), fired bursts during 2.26% (0.1 − 13.10%),

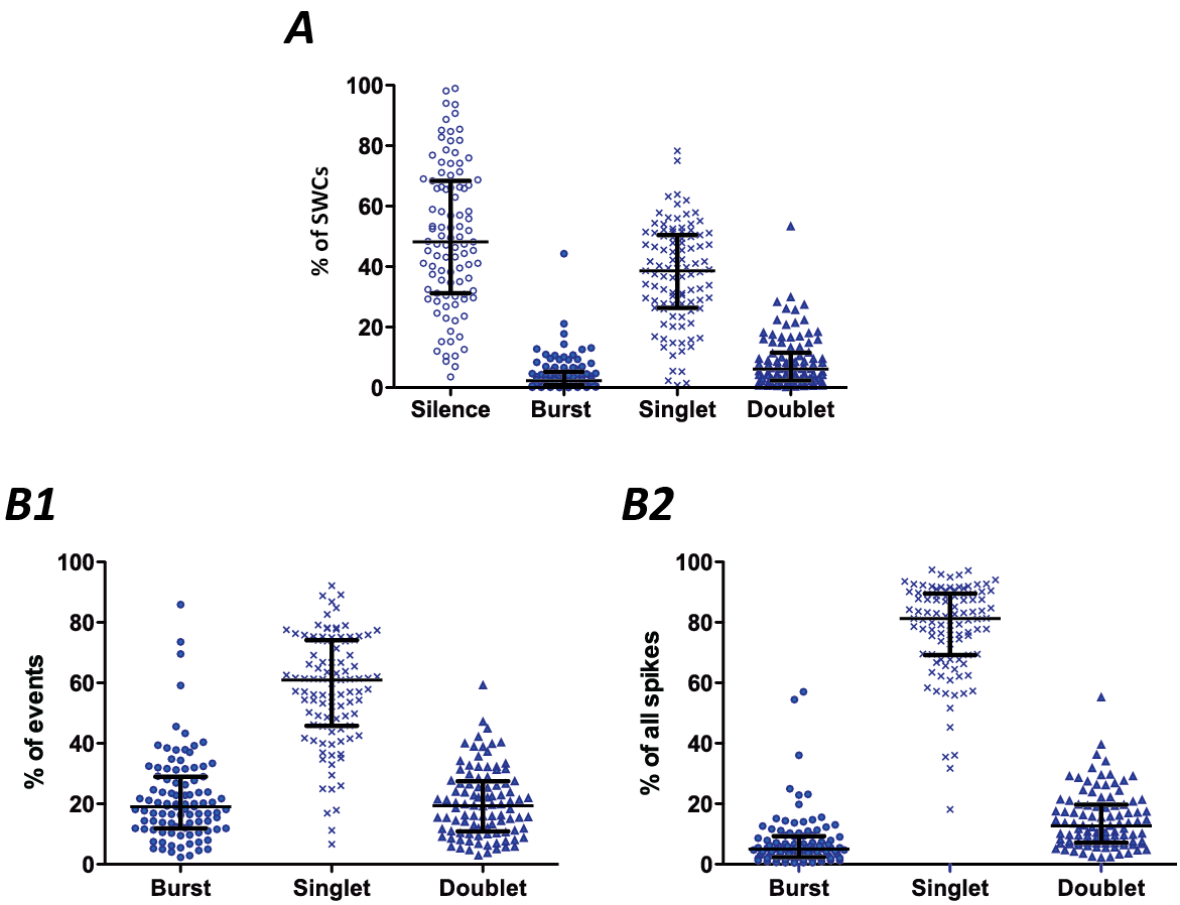

Figure 3.3 Analysis of TC activity with respect to SWCs

A More SWCs are accompanied by neuronal silence (48%) than by any form of output. ***B1*** Of those SWCs that are accompanied by output more than 80% have single spikes while less than 10% have doublets and less than 5% have bursts. ***B2*** Single spikes correspond to more than 60% of all ictal spikes, and bursts and doublets to less than 20% each.

single spikes only during 38.65% (5.47 − 61.99%), and doublets during 6.1% (0.528 − 26.07%) [Fig. 3.3B].

These results indicate that nearly half of SWCs are unaccompanied by TC output. Output accompanying the remaining half of SWCs is predominantly comprised of single spikes, while all other activity is present during less than 10%.

3.3.1.2.2 Bursts occur in TC neurones during a small minority of SWCs

Given the differences in TC input, output, contributing membrane currents, and overall state of the thalamocortical network associated with LTCP-mediated burst firing and tonic AP firing, the relative and absolute quantification of these two firing modes during seizure was the next priority.

Burst rate of TC neurones during seizure (0.43 events/second (e/s), 0.14 − 1.53 e/s) was found to be higher than that during wakefulness (0.17 e/s, 0.03 − 0.78 e/s, $P < 0.0001$) and lower than that during sleep (0.57 e/s, 0.1 − 1.11 e/s, $P = 0.0355$) by matched pairs test [Fig. 3.4A]. The distribution of seizure bursting rate is noticeably different to that of sleep. The former appears to be lognormal, given that the natural log of the distribution passed Kolmogorov-Smirnov, D'Agostino & Pearson, and Shapiro-Wilk normality tests (all $P > 0.1$), while the latter appears to be normal (again passes all normality tests at $P > 0.1$).

Transition period burst rate plots showed waking (~0.15 e/s) and ictal (~0.35 e/s) rates approximately matching the observed total waking and ictal rates. They also demonstrated a dramatic transient increase in burst rate for the second immediately post seizure initiation, exceeding 0.65 e/s [Fig. 3.4A]. When this was further investigated it transpired that firing rates over the first 200 ms (0.9 e/s, time bin chosen to include the first SWC) and over the first 1 s (0.74 e/s) were higher than the overall median firing rate (signed-rank test, $P < 0.0001$ in both cases). Apart from this peak, ictal and inter-ictal rates appeared stable.

Neuronal output attributable to burst firing was also investigated by calculating the rates of spikes that were part of bursts during each behavioural state. The median burst spike rate during seizure was 1.67 Hz (0.50 to 7.28 Hz). During sleep the equivalent rate was 2.58 Hz (0.44 − 6.66 Hz) and during wakefulness it was 2.14 Hz (0.23 − 9.14 Hz). When the ictal median was compared to those of sleep and waking states by matched pairs tests, it was found to be smaller than both ($P = 0.001$ for sleep and $P = 0.036$ for wakefulness) [Fig. 3.4B].

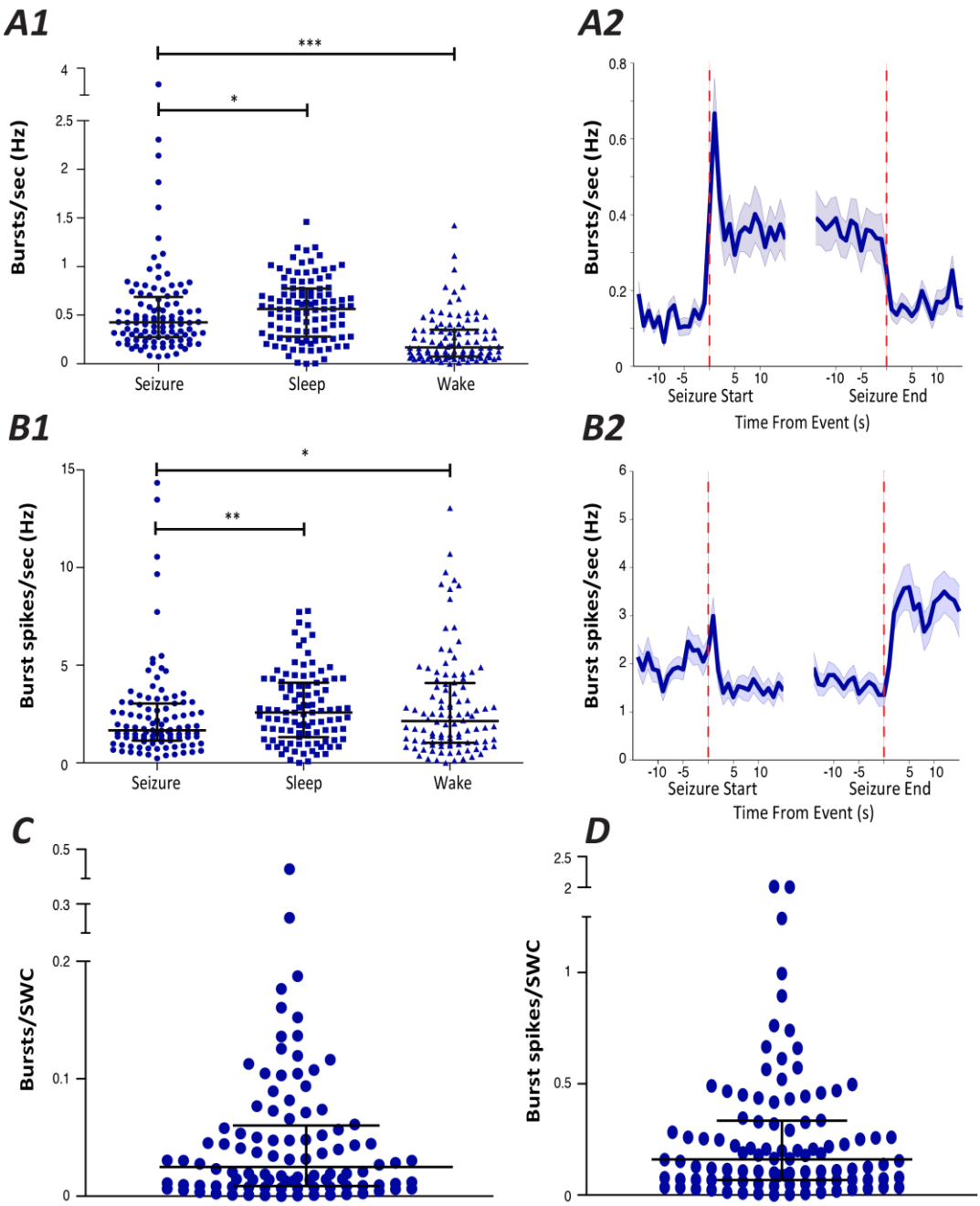

Figure 3.4 ***TC neurones fire LTCP-mediated bursts during 3% of SWCs***

A1 TC neurones seizure burst rate distribution is elevated relative to that of wakefulness and lower than that of sleep (lines indicate median, bars indicate IQ range). ***A2*** Evolution of bursting at the start and end of seizures above 15s duration shows how burst rate changes at transitions between wakefulness and seizure. ***B*** These representations are repeated for burst-attributable spike rates. ***C*** Bursts per SWC show that the median bursts/SWC corresponds to one burst every 33 SWCs. ***D*** Burst component spikes per SWC indicate a median level of LTCP-mediated output of 0.16 spikes per SWC.

Transition period burst spike rate plots showed waking (~2 Hz) and ictal (~1.5 Hz) rates roughly comparable to the corresponding absolute median rates (compare figures A2 and B2 with seizure and waking values in A1 and B1). Ictal burst spike rates appeared stable while pre- and post-ictal waking burst spike rates did not. The latter two rates were generally variable rather than demonstrating any discrete peaks and troughs.

As with firing rate, burst and burst spike rate was also calculated per SWC. The median burst rate per SWC was 0.03 e/SWC (0.001 − 0.16 e/SWC), corresponding to one burst every 33 SWCs. The median burst spike rate per SWC was 0.16 spikes/SWC (0.01 − 0.89 s/SWC) [Fig. 3.4C]. This suggests that the vast majority of ictal cycles are not accompanied by LTCP-mediated bursts in TC neurones.

3.3.1.2.3 Single spikes occur in TC neurones during less than half of SWCs

Single spike rate of TC neurones during seizure (3.49 Hz, 1.29 − 7.39 Hz) was lower than that during wakefulness (8.11 Hz, 2.11 − 14.79 Hz, $P < 0.0001$), and higher than that during sleep (2.07 Hz, 0.58 − 5.26 Hz, $P < 0.0001$) [Fig. 3.5A1].

Single spike rates over periods of wake to seizure transition and vice versa [Fig. 3.5A2] showed mean wake (~8.5 e/s) and ictal (~3.5 e/s) rates roughly approximating the medians of the entirety of the corresponding states. The rates appeared stable both ictally and peri-ictally with no obvious peaks or troughs. The median rate of single spikes per SWC was 0.35 spikes/SWC (0.03 − 0.54 spikes/SWC), corresponding to one single spike every 2.85 SWCs [Fig. 3.5A3].

3.3.1.2.4 Doublets occur in TC neurones during less than 10% of SWCs

Doublet rate of TC neurones during seizure (0.57 doublets/sec (d/s), 0.24 − 2.07 d/s) was elevated relative to that during sleep (0.31 d/s, 0.14 to 0.57 d/s, $P < 0.0001$) and relative to that during wakefulness (0.16 d/s, 0.06 to 0.36 d/s, $P < 0.0001$) [Fig. 3.5B1).

Plotting doublet rates during wake to seizure transition periods and vice versa [Fig. 3.5B2] showed mean wake (~0.2 d/s) and ictal (~0.6 d/s) rates roughly approximating the medians of the entirety of the corresponding states. Doublet rates appeared mostly stable in both seizure and wake states with the exception of a transient increase over the first second of seizure. This is similar to the peak observed in burst rates at the start of ASs. Doublet rates over the first 200 ms (0.95 d/s) and first 1 s (0.86 d/s) were both higher than across all ASs (signed rank

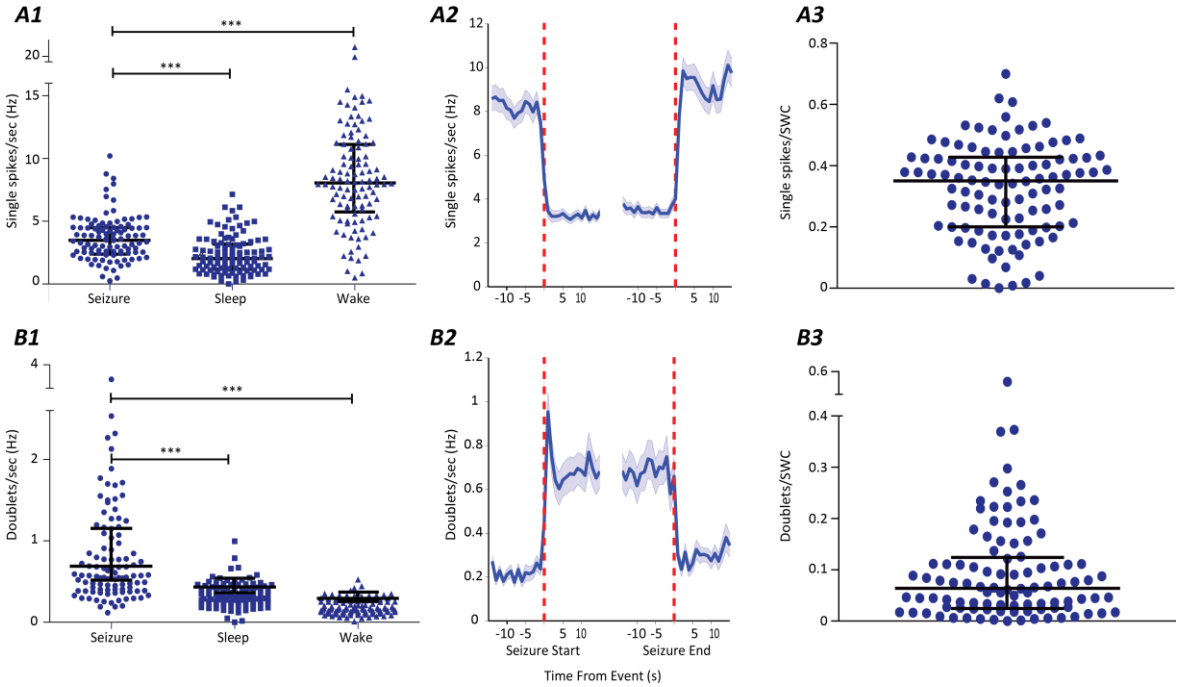

Figure 3.5 TC neurones fire single spikes during 35% of SWCs and doublets during 6.5%

A1 Single spikes per second are elevated during seizure relative to during sleep, but significantly decreased from waking states. ***A2*** Evolution of single spike rates at seizure start and end, again representing only seizures of 15s+ during wakefulness. ***A3*** The median incidence of single spikes per SWC shows that TC neurones fire a single spike every 2.85 SWCs. ***B1*** Doublets per second are elevated during seizure compared to both sleep and wake states, and (similarly to bursts) are log-normally distributed where sleep and wake rates or not. ***B2*** Evolution of doublet rates at seizure start and end, with the same provisos as (A2). ***B3*** Doublets per SWC suggest a median incidence of one doublet every 15.4 SWCs. In (1) and (3) central lines indicate median and bars indicate IQ range.

A		**Median**	**5th Percentile**	**95th Percentile**	**Mean ± SEM**
Seizure	All spikes	6.23	13.45	2	7.06 ± 0.37
	Bursts	0.42	1.53	0.14	0.55 ± 0.05
	Single spikes	3.49	7.39	1.29	3.64 ± 0.17
	Doublets	0.57	2.07	0.24	0.80 ± 0.06
	Burst spikes	1.67	7.28	0.50	2.43 ± 0.23
Sleep	All spikes	5.53	11.51	1.68	5.84 ± 0.28
	Bursts	0.57	1.11	0.1	0.57 ± 0.03
	Single spikes	2.07	5.26	0.58	2.35 ± 0.15
	Doublets	0.31	0.57	0.14	0.33 ± 0.02
	Burst spikes	2.58	6.66	0.44	2.81 ± 0.18
Wake	All spikes	11.01	22.33	2.81	11.70 ± 0.57
	Bursts	0.17	0.78	0.03	0.25 ± 0.02
	Single spikes	8.11	14.79	2.11	8.40 ± 0.38
	Doublets	0.16	0.36	0.06	0.19 ± 0.01
	Burst spikes	2.14	9.14	0.23	2.90 ± 0.26

B	**Median**	**5th Percentile**	**95th Percentile**	**Mean ± SEM**
All spikes	0.94	0.2	2.35	1.02 ± 0.07
Bursts	0.02	0.001	0.16	0.05 ± 0.01
Single spikes	0.35	0.03	0.54	0.32 ± 0.02
Doublets	0.07	0.0004	0.27	0.09 ± 0.01
Burst spikes	0.16	0.01	0.89	0.27 ± 0.03

Table 3.1 TC neurone activity in different behavioural states

A Behavioural state statistics (all values in Hz). ***B*** Seizure-specific statistics (all values per-SWC).

test, P < 0.0001 in both cases). The median rate of doublets per SWC was 0.07 e/SWC (0.004 – 0.27 e/SWC), corresponding to one doublet every 15.4 SWCs [Fig. 3.5B3].

3.3.1.3 TC neurone activity doesn't vary predictably within or between seizures

3.3.1.3.1 TC neurone output does not change qualitatively from seizure to seizure

In order to estimate variation in neuronal firing activity from one seizure to another, the distribution of mean firing and burst rates across all seizures was calculated for each TC neurone and the corrected sample standard deviation of each of these distributions plotted [Fig. 3.6A]. The medians of these standard deviations were 2.63 Hz and 0.32 Hz for firing rates and burst rates respectively [Table 3.2]. Variations of these magnitudes are minor relative to median firing and burst rates of 6.23 Hz and 0.43 Hz respectively.

Visual inspection of the individual firing rate and burst rate distributions (Fig 3.6B) suggests that, for the majority of neurones, activity during seizure is distributed around its mean value in a normal, or other unimodal, fashion (allowing for varying number of seizures between neurones). While some neurones have rates spread considerably from the mean, none have the bimodal distribution of mean seizure rates that would suggest a qualitative switch between firing modes from seizure to seizure.

Firing Rate	**Standard Deviation**	**Mean**
Mean	3.14 Hz	7. 06 Hz
Median	2.63 Hz	6.23 Hz
5th to 95th percentiles	1.06 to 6.33 Hz	2 to 13.45 Hz
Burst Rate		
Mean	0.37 Hz	0.55 Hz
Median	0.32 Hz	0.43 Hz
5th to 95th percentiles	0.1 to 0.9 Hz	0.14 to 1.53 Hz

Table 3.2 TC neurone inter-seizure variation

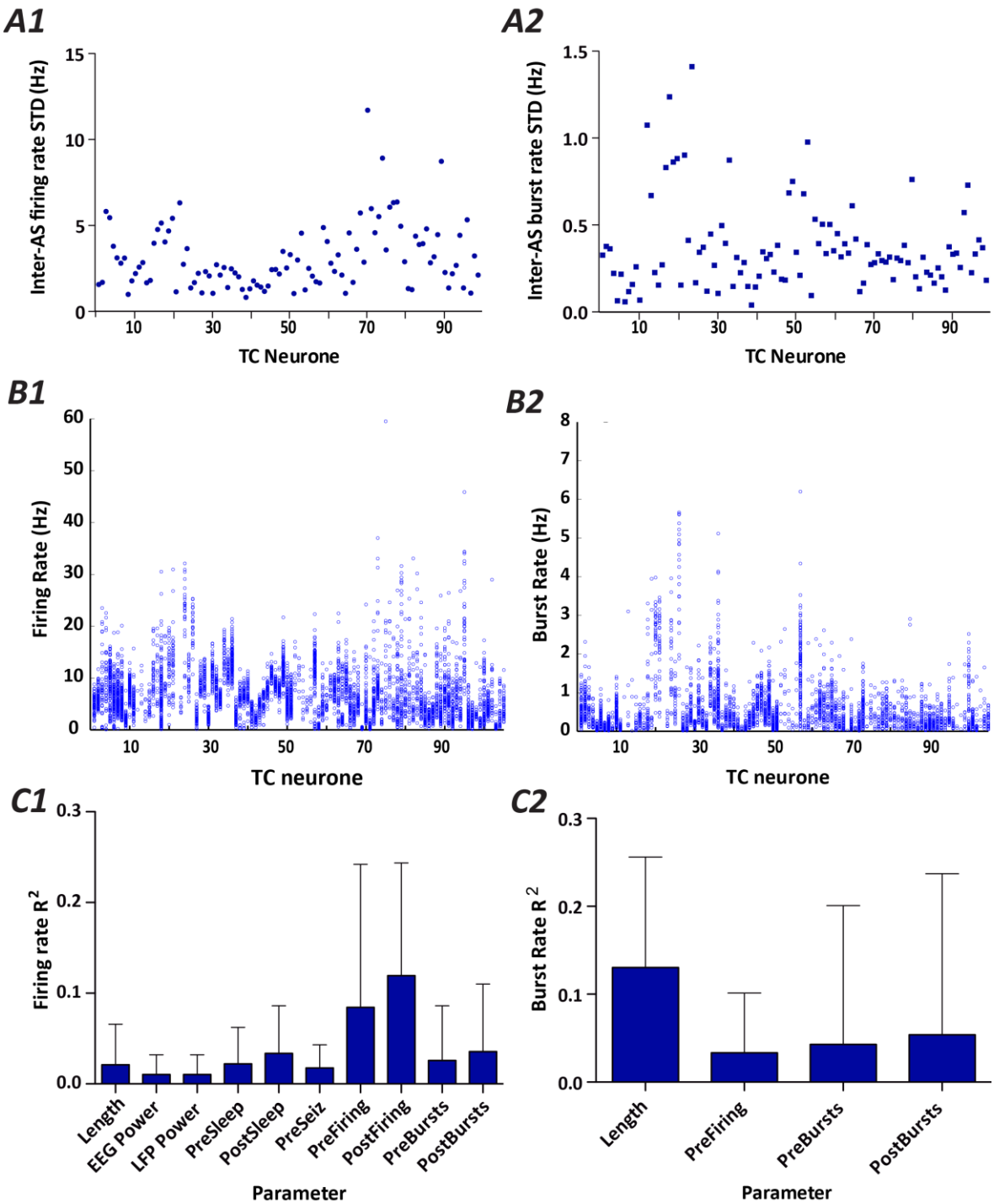

Figure 3.6 TC neurones have minor inter-seizure variations in firing activity

A Standard deviations of mean seizure firing (A1) and burst (A2) rates of TC neurones. ***B*** Firing rate (B1) and burst rate (B2) for each seizure plotted individually. ***C*** Coefficients quantifying influence of sources of variation of ictal firing and burst rate, plotted as median plus IQ range.

3.3.1.3.2 Inter-seizure variation in TC ictal activity is partially explained by variations in seizure length and peri-ictal activity

To investigate the source of inter-seizure variation in neuronal activity, the mean correlation coefficients (r values) between mean seizure activity (represented as firing rate and as burst rate) and a variety of seizure parameters were calculated. These were: seizure length, EEG power at peak seizure frequency, LFP power at peak frequency, sleep/wake balance before and after seizure, prevalence of other seizures before and after seizure, and neuronal activity before and after seizure. Correlation coefficient distributions were tested for significant differences from zero (by signed-rank tests). In any case in which a difference was detected, an R^2 value (coefficient of determination) was calculated to estimate the proportion of the variation in seizure activity that can be explained by variation in the tested parameter [Table 3.3].

Of the parameters tested, 2 shared more than 5% variation with mean ictal firing rate: the firing rate in the 5 second sections immediately pre- (8.4%) and post- (11.9%) seizure. Both parameters were positively correlated with ictal firing rate. All other parameters (except the proportion of the post-ictal 5 seconds spent in seizure) had a median correlation coefficient significantly differing from zero, but all had R^2 values suggesting that the shared variation was very small. Only two parameters, seizure length and post-seizure burst rate, shared more than 5% of variation with ictal burst rate (13% and 5.4% respectively) while pre-seizure firing rate and bursting rate were also correlated [Fig. 3.6C].

It is notable that there is a large degree of variation in coefficients of determination between neurones. The results suggest that though peri-ictal activity and seizure length (in the case of bursts) sometimes increase and decrease, respectively, with ictal activity, they are not reliable predictors of it.

3.3.1.4 TC neurone ictal output is periodic and EEG-synchronous

3.3.1.4.1 The temporal relationship between activity of simultaneously recorded TC neurones displays SWC-associated periodicity

Cross-correlograms were composed during each behavioural state, as shown in the example in Figure 3.7. Inter-ictal (wake state) cross-correlograms sometimes display a central peak, indicating neurones that tend to be contemporaneously active, but never demonstrate

	All Spikes		Bursts	
	r value sign & significance	R-squared median	r value sign & significance	R-squared median
Seizure length	P < 0.0001 (–)	0.02	P < 0.0001 (–)	0.13
EEG 6 to 8 power	P = 0.014 (+)	0.01	n.s.	–
LFP 6 to 8 power	P = 0.014 (+)	0.02	n.s.	–
Pre-seizure sleep	P = 0.001 (–)	0.02	n.s.	–
Post-seizure sleep	P = 0.0003 (–)	0.03	n.s.	–
Pre-seizure ictal	P = 0.003 (–)	0.02	n.s.	–
Post-seizure ictal	n.s.	–	n.s.	–
Pre-seizure spikes	P < 0.0001 (+)	0.08	P = 0.0003 (+)	0.03
Post-seizure spikes	P < 0.0001 (+)	0.12	n.s.	–
Pre-seizure bursts	P = 0.0002 (+)	0.03	P < 0.0001 (+)	0.04
Post-seizure bursts	P < 0.0001 (+)	0.04	P < 0.0001 (+)	0.05

Table 3.3 Sources of variation in TC ictal activity

Significance and direction (+ indicates positive correlation) of detected differences between correlation coefficient distributions and zero for various seizure parameters, and median coefficients of variation for those parameters in which difference was detected. Highlighted values indicate greater than 5% shared variation. Signs indicate direction of correlation. Pre- and post-seizure parameters were all calculated over 5 second epochs.

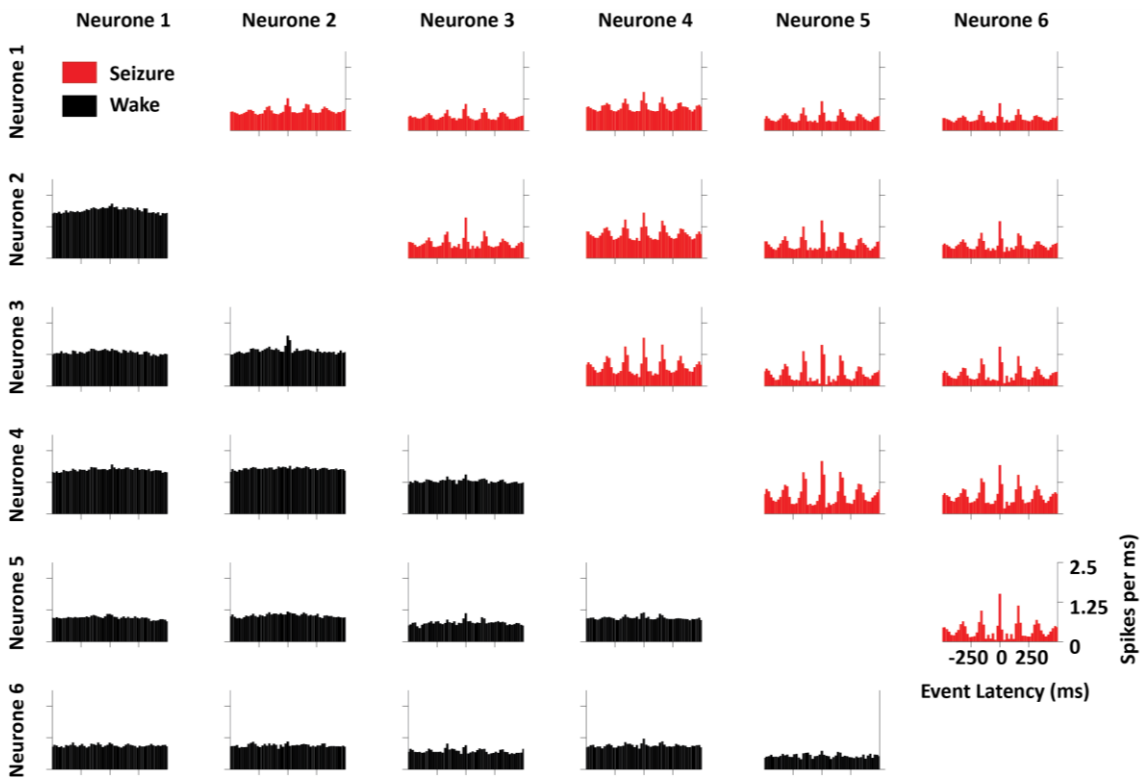

Figure 3.7 TC neurone firing synchrony during ASs

Ictal cross-correlograms of 6 simultaneously recorded TC neurones show peaks repeating at SWD frequency as well as a larger and narrower central peak. These are invariably and often, respectively, absent in inter-ictal cross-correlograms.

flanking peaks distinct from background noise. Ictal cross-correlograms for simultaneously recorded TC neurones show peaks at SWD frequency (~7 Hz, inter-peak latency of ~140 ms), with larger and narrower central peaks representing synchronous spikes.

3.3.1.4.2 TC neuronal firing shows a clear phase preference during SWDs

The synchrony between TC neuronal activity and SWCs evident in the raster-EEG plots previously discussed [Fig. 3.1A] was investigated in greater detail by calculating SWC spike peak-triggered neuronal activity and ictal neuronal spike-triggered EEG averages. Two animals did not have frontoparietal EEG and so were excluded from these analyses, leaving 3 GAERS with 79 neurones.

Averaging the spike rates (in millisecond bins) surrounding the peak of the spike of each SWC revealed a strong temporal association between ictal EEG and neuronal activity [Fig. 3.8A1]. There was a local maximum 4 ms prior to the SWC spike, reaching approx. 7 times the adjacent local minimum (0.07 spikes/ms compared to 0.01 spikes/ms). The width of the peak surrounding this maximum was 43 ms at its base (calculated as 10% of its total height relative to the adjacent minimum), from −28 to +15 ms (relative to SWC peak). At 50% of the total height, a point at which the peak was clearly unimodal, the width was 11 ms (−11 to 0 ms). Flanking maxima were also apparent 141 ms either side of the SWC peak-associated maximum (142 ms before and 141 ms after), matching the inverse of the peak frequency of SWDs (7 Hz).

Mean SWC peak-triggered burst rate followed a similar pattern, with the central maximum slightly earlier (6 ms prior to SWC peak) than that of firing rate [Fig. 3.8B1]. This maximum reached 0.004 burst/ms, starting from adjacent minima of 0 burst/ms, and had a width at 10% height of 31 ms (−25 to +6 ms) and a width at 50% height of 12 ms (−16 to −4 ms). Flanking maxima were again apparent (149 ms prior to and 138 ms after the primary peak).

The distribution of SWC peak-triggered single spikes featured a central maximum at 4 ms prior to the peak, with a height of 0.021 single spikes/ms starting from adjacent minima of 0.003 single spikes/ms (a 7-fold increase) [Fig. 3.8C1]. The width of this peak at 10% height was 28 ms (−23 to +5 ms) and at 50% height it was 5 ms (−7 to −2 ms). Flanking maxima were set 143 ms prior to and 142 ms after the primary peak.

All distributions display clear SWC-associated preference, indicating that TC ictal firing is synchronous with SWDs. The degree of synchrony varies from case to case: spiking is elevated from the inter-peak baselines for approximately 30% of a SWC (43/142 ms) in the case of the

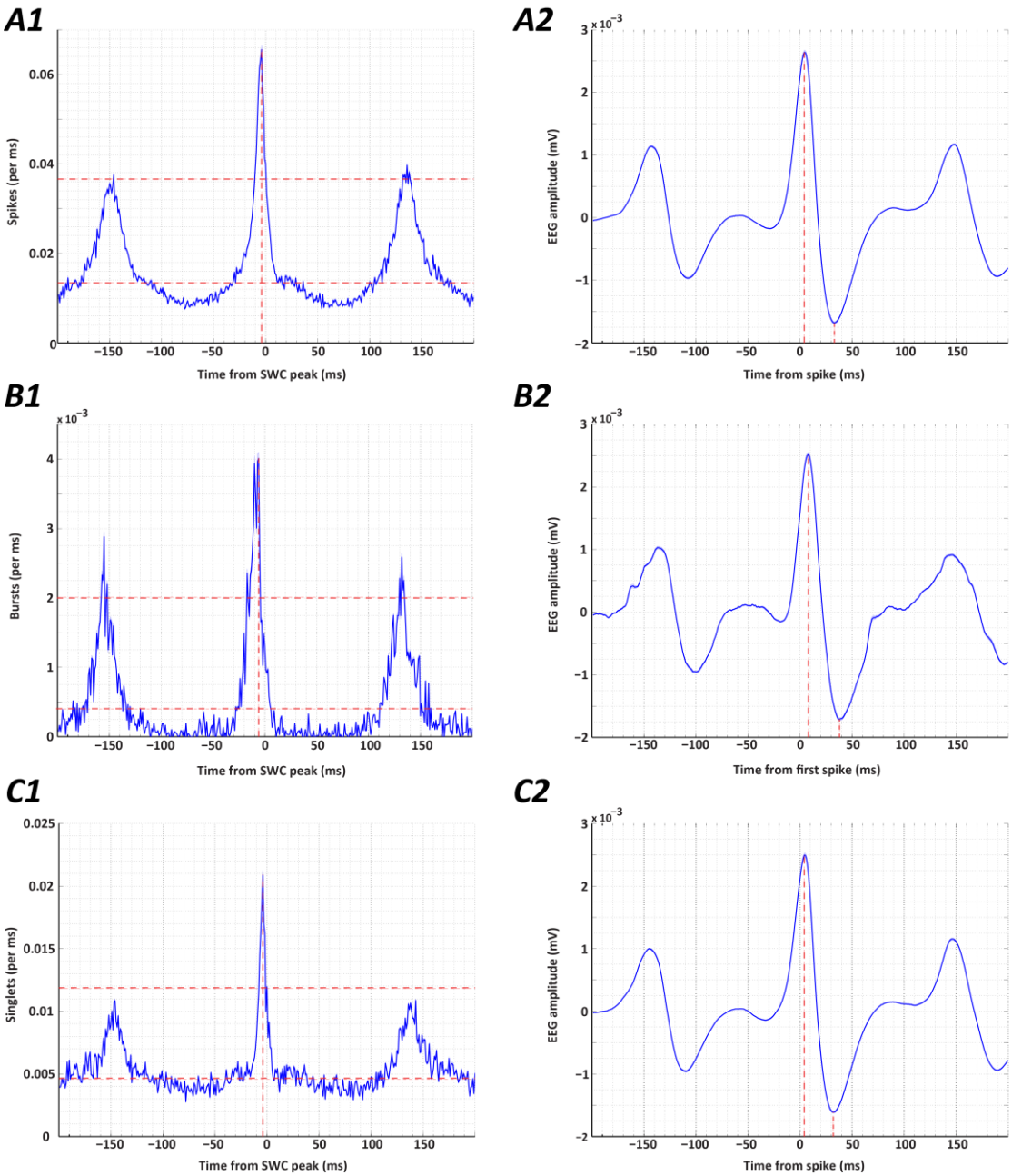

Figure 3.8 ***TC neurones fire preferentially immediately prior to SWC peaks***

A TC ictal firing (A1) is concentrated 4 ms prior to SWC peak while the maximum of neuronal spike-triggered average EEG (A2) is located 4 ms after the spike. ***B*** The peak of burst firing (B1) occurs 6ms prior to SWC maximum, while burst-triggered EEG (B2) peaks 9 ms after the burst centre. ***C*** The peak of single spike firing (C1) occurs 4 ms prior to SWC maximum, and single spike-triggered EEG (C2) peaks 4 ms after the single spike centre. Shaded area denotes SEM (largely invisible due to large group size and low variance). Red vertical dashed lines mark maxima while red horizontal dashed lines mark 10% and 50% of total height.

firing distribution, 22% (31/142) in the case of the bursting distribution, and 20% (28/142) in the case of the single spike distribution. The widths of the distribution at 50% height (relative to baseline) provide a measure of the time during which activity is significantly elevated, and correspond to 7.7%, 8.5%, and 3.5% of each SWC for firing, bursts and single spikes respectively.

Calculation of the mean EEG values (after removal of DC components) surrounding ictal TC peaks confirmed the temporal association between neurones and EEG evident from SWC-triggered neuronal firing distributions [Fig. 4.7A2, B2, C2]. In spike-, burst-, and single spike-triggered EEG the distinctive spike-and-wave shape associated with ictal EEG was visible. The peak of the EEG waveform was 4 ms delayed relative to neuronal spikes, 8 ms delayed relative to bursts, and 4 ms delayed relative to single spikes. The minor discrepancy between the offsets of the averaged SWC peak and burst firing centre, and the actual SWC peaks and burst firing maximum, can be explained by uneven distribution of spikes either side of the point of maximum firing density. The positive-going (downward) peak of the EEG is in all cases delayed by >30 ms relative to neuronal activity. Without precise knowledge of the significance of the EEG peak, or its relationship to the firing of other populations, the exact relative timing of firing maxima is not significant and thus is better used as an approximate guide to TC (and later nRT) firing preferences.

3.3.2 nRT neurone behaviour during absence seizures

3.3.2.1 Firing rate of nRT neurones varies during seizure

The 12 neurones classified as nRT based on spike waveform and burst characteristics were used to form a preliminary impression of the level and the nature of nRT activity during ASs. Viewing raster plots of nRT spike times and simultaneous EEG, allowing the comparison of activity during multiple ictal and inter-ictal periods [Fig. 3.9A, B]. It also demonstrated the temporal association of nRT spikes and SWCs, which was confirmed by the ictal auto-correlogram of nRT neurones showing peaks repeating at approximately 7 Hz, corresponding to the peak frequency of SWDs [Fig. 3.9C]. The EEG/spike raster plots also suggested that nRT neurones have varying output during seizure.

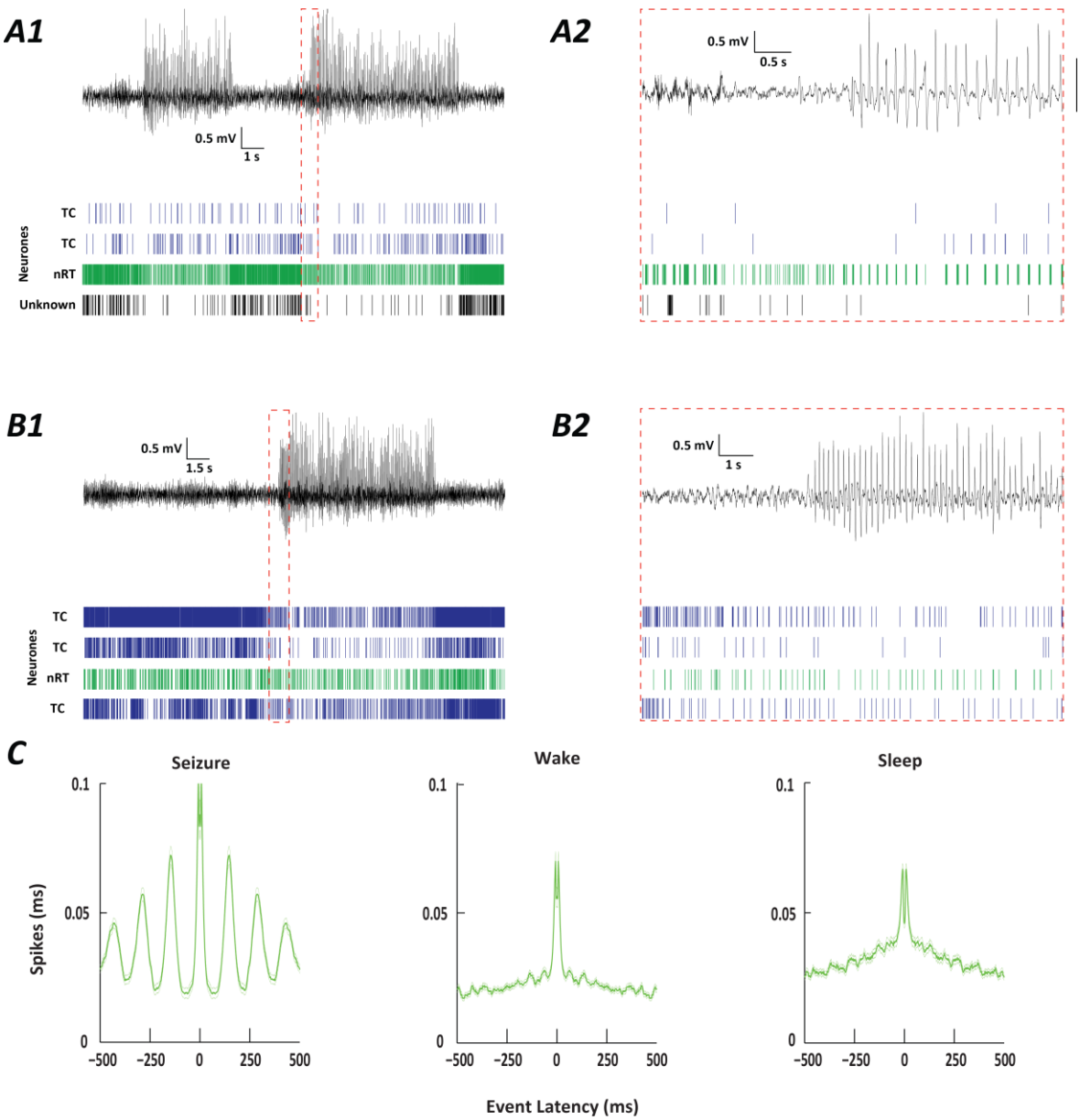

Figure 3.9 nRT activity is variable during seizure

A1, B1 Simultaneous EEG trace (top) and spike rasters of 2 separate nRT neurones (one each in A and B) demonstrating the diversity in their firing rates changes associated with ASs: A1 shows a decrease (from a highly active baseline) during AS while B2 maintains a constant, less active level. Simultaneously recorded TC and unclassified neurones are also included for comparison. ***A2, B2*** Expanded sections of EEG and rasters showing the contrast between regularly bursting (A2) and regularly tonic firing (B2) nRT neurones. ***C*** Mean auto-correlogram during each behavioural state confirms the periodic nature of nRT activity during seizure (n = 12 neurones).

Firing rate of nRT neurones was higher during seizure (56.95 Hz, 8.92 Hz − 65.77 Hz)[2] than during sleep (18.97 Hz, 9.96 − 30.26 Hz, P = 0.0010). No difference could be detected between seizure and wake firing rate (45.24, 9.52 − 58.65 Hz, P > 0.05) [Fig. 3.10A].

Plotting per-second firing rates at transition periods from wakefulness to seizure and vice-versa [Fig. 3.10A] showed mean rate was largely unchanged between the two states, and had a high degree of variance commensurate with the diversity of nRT activity. Mean waking and seizure rates of approximately 40 Hz were comparable to the medians rates of all combined seizure and wake states. A brief (approx. 2 s) decrease in firing rate was apparent both immediately prior to seizure initiation and following seizure termination [Fig. 3.10A2].

The median ictal firing rate per SWC was 7.74 spikes/SWC (0.80 − 13.29 spikes/SWC) [Fig. 3.10B]. This and all other analyses involving individual SWC identification have n = 11, due to EEG quality during the recording of 1 nRT neurone being insufficient for SWC peak detection.

The most striking facet of nRT firing rates is their non-normal distribution, with very large spread, during seizure and waking states. Of the 12 neurones, 7 have mean ictal firing rates above 50 Hz while 3 have mean ictal firing rates below 30 Hz. It is immediately apparent that nRT ictal firing rate distribution is not concentrated around a centre, with a small proportion of outliers (as is TC ictal firing rate distribution). Instead it is spread, unevenly but definitely, over a large range (~ 9 Hz to ~ 66 Hz). As such, single-value descriptors will not be very useful when describing this population.

3.3.2.2 A subset of nRT neurones fire frequent bursts during AS

3.3.2.2.1 nRT neurones can express any of silence, single spikes, or bursts as a prominent activity during seizure

Between 0.46% and 74.76% of SWCs were accompanied by neuronal silence, while between 0.2% and 40.35% were accompanied by bursts, between 13.83% and 98.96% by single spikes, and between 0.14% and 7.30% by doublets. 4 neurones have ≥ 40% of SWCs accompanied by silence, while 6 have < 10% [Fig. 3.11A].

Bursts accompanied between 0.2% and 74.01% of active cycles, single spikes accompanied between 25.36% and 99.48%, and doublets accompanied between 0.3% and 11.94%. In this

[2] With sample sizes less than 20, the 5th to 95th percentile interval is equal to the entire range of the distribution.

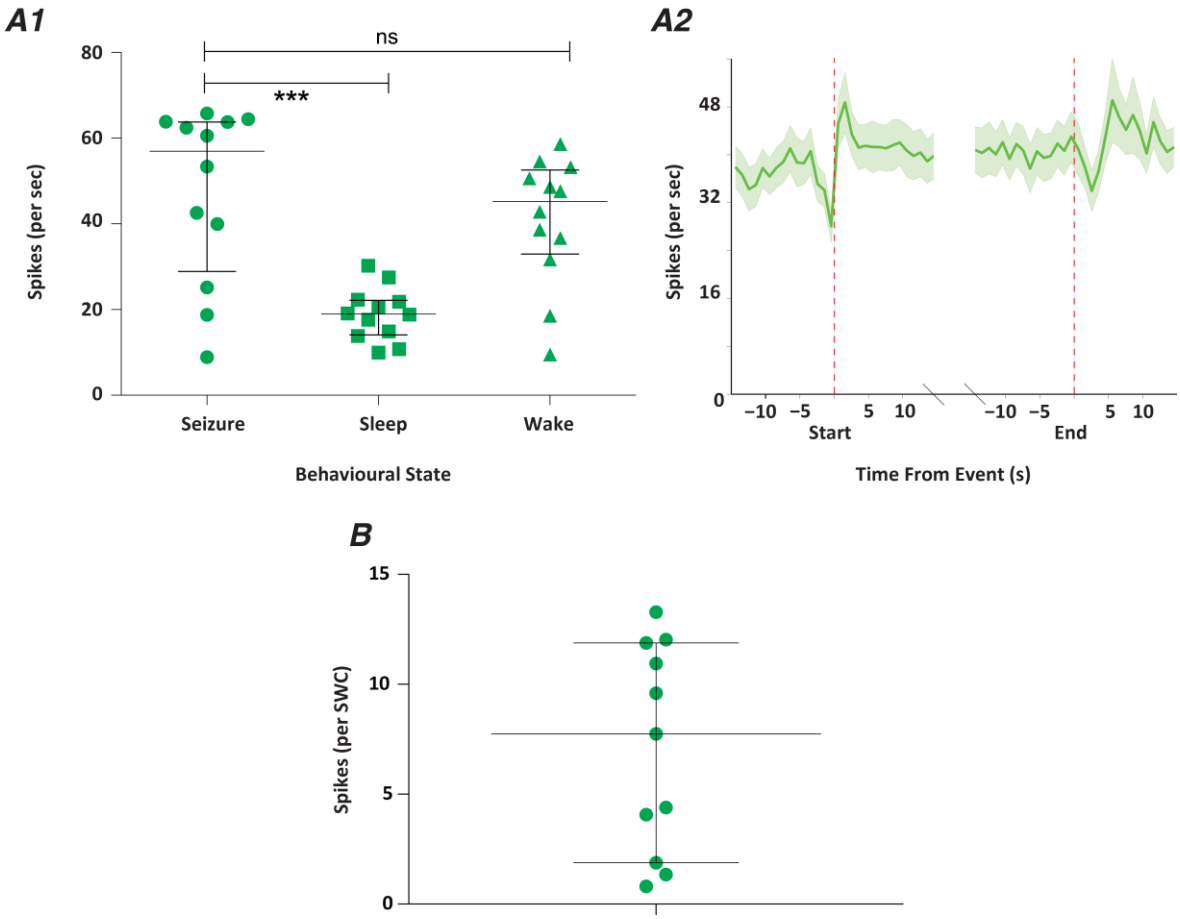

Figure 3.10 nRT firing rate during seizure is highly variable between neurones

A1 nRT ictal firing rate is elevated relative to that of sleep and has a completely different distribution. This distribution, and its median, is similar to that of waking firing rates (P = 0.1099). There is no obvious centre of the distribution. ***A2*** The evolution of firing at transitions from wakefulness to seizure (≥ 15 s duration) and vice versa suggest that, while overall rate stays relatively constant, there are changes around the start and end of seizures. ***B*** Firing rate per SWC confirms the diversity of nRT ictal activity levels.

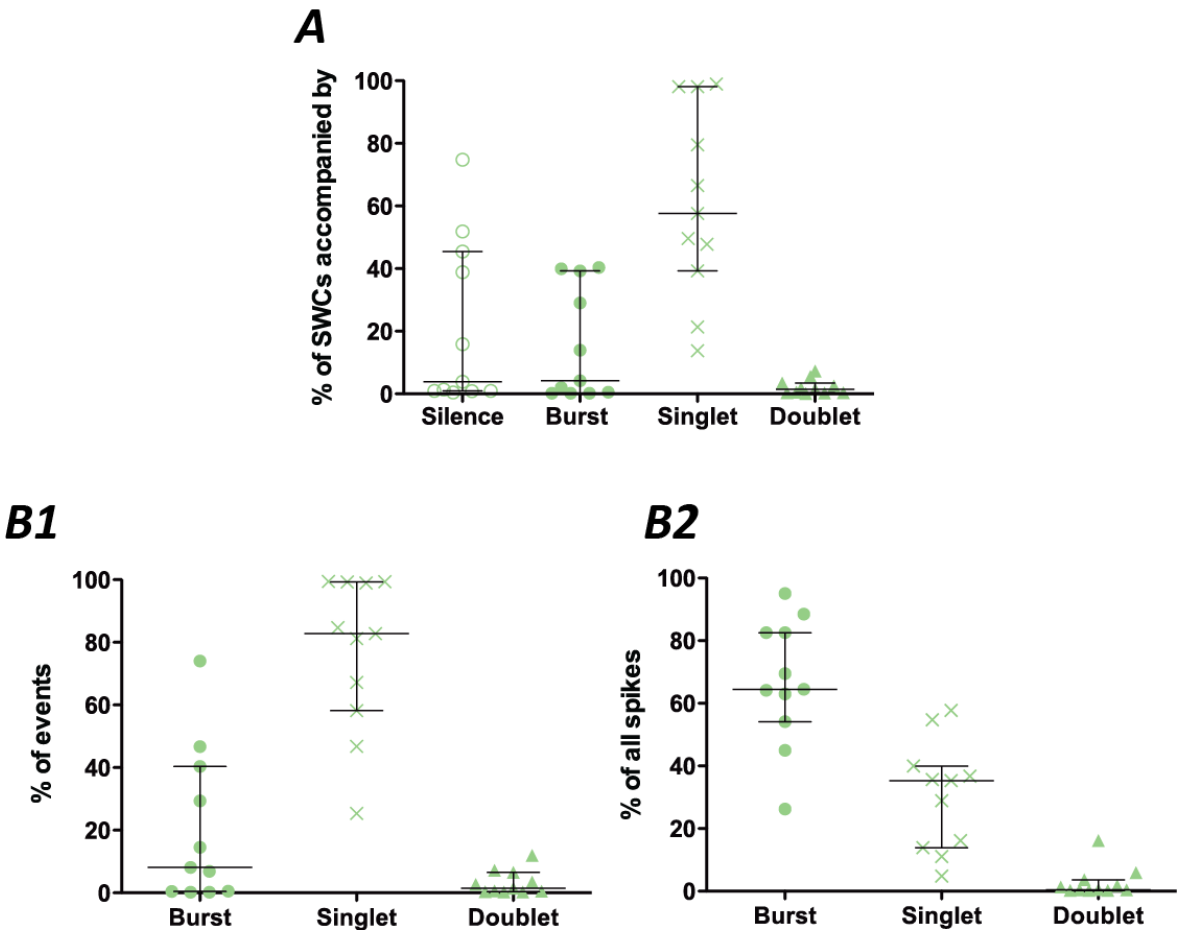

Figure 3.11 Bursts accompany varying percentages of SWCs across nRT neurones

A Bursts occur on up to 40% of cycles, less than single spikes and silence for most neurones. ***B1*** Bursts events of nRT neurones are generally less prevalent than single spikes during absence ASs. ***B2*** Spikes in bursts constitute the majority of all neuronal output. In all cases there is a great degree of diversity between neurones, without any apparent trends in the relative prevalence of different activities.

case, as so often for these nRT statistics, the measure of centre was not informative: both burst and single spike percentages have ranges of greater than 70%, with 3 of 12 neurones having bursts as more than 40% of events [Fig. 3.11B1]. Bursts contributed between 26.20% and 95.04% of all spikes, single spikes contributed between 4.77% and 57.68%, while doublets contributed between 0.19% and 16.12% [Fig. 3.11B2].

These results suggest that nRT neurones express a diverse range and combination of activity during ASs. The sample size employed is insufficient to lend weight to any precise predictions of nRT contribution to SWDs, but some limited conclusions can be drawn: nRT neurones can frequently express bursts, single spikes, or silence during ASs. Half of all neurones studied (6/12) are active during more than 90% of SWCs.

3.3.2.2.2 Bursts occur in nRT neurones during between 0.3% and 50% of SWCs

To gain an insight into of the nature of nRT neurone activity during absence seizures, the prevalence of high-frequency bursts was measured in each behavioural state. Due to the diversity of ictal burst firing rates between nRT neurones, the following paragraphs will attempt to describe the distributions as a whole rather than in terms of single-value summaries.

Burst rate of nRT neurones during ASs (1.56 e/s, 0.19 − 5.62 e/s) was greater than that during sleep (0.31 e/s, 0.11 − 1.52 e/s, P = 0.0005) and that during wakefulness (0.09 e/s, 0.03 − 0.36 e/s P = 0.0005, signed rank test in both cases) [Fig. 3.12A]. The distribution during AS could be described as roughly bimodal, with concentrations of 5 points between 0 and 1 e/s and 4 points between 3 and 4 e/s. An assumption of bimodality cannot be gainfully tested with such a small sample size, but it is clear that for ictal bursting rate, as for ictal firing rate, nRT neurones do not centre on any one frequency.

The burst spike rate during ASs (40.38 Hz, 3.56 − 60.10 Hz) was larger than that during both sleep (8.04 Hz, 3.58 − 20.25 Hz, P = 0.001) and wakefulness (21.06 Hz, 2.36 − 31.65 Hz, P = 0.0005, signed rank test in both cases) [Fig. 3.12B1].

In the cases of both burst rate and burst-attributable spike rate, plotting the rates during transitions from wake to seizure and vice versa [Fig 3.12A2,B2] suggested mean waking (0.4 e/s, 20 Hz) and seizure (2 e/s, 30 Hz) rates comparable to the corresponding total medians. No transient increases (ictally or inter-ictally) were obvious in either case (bearing in mind the considerably high degrees of variance).

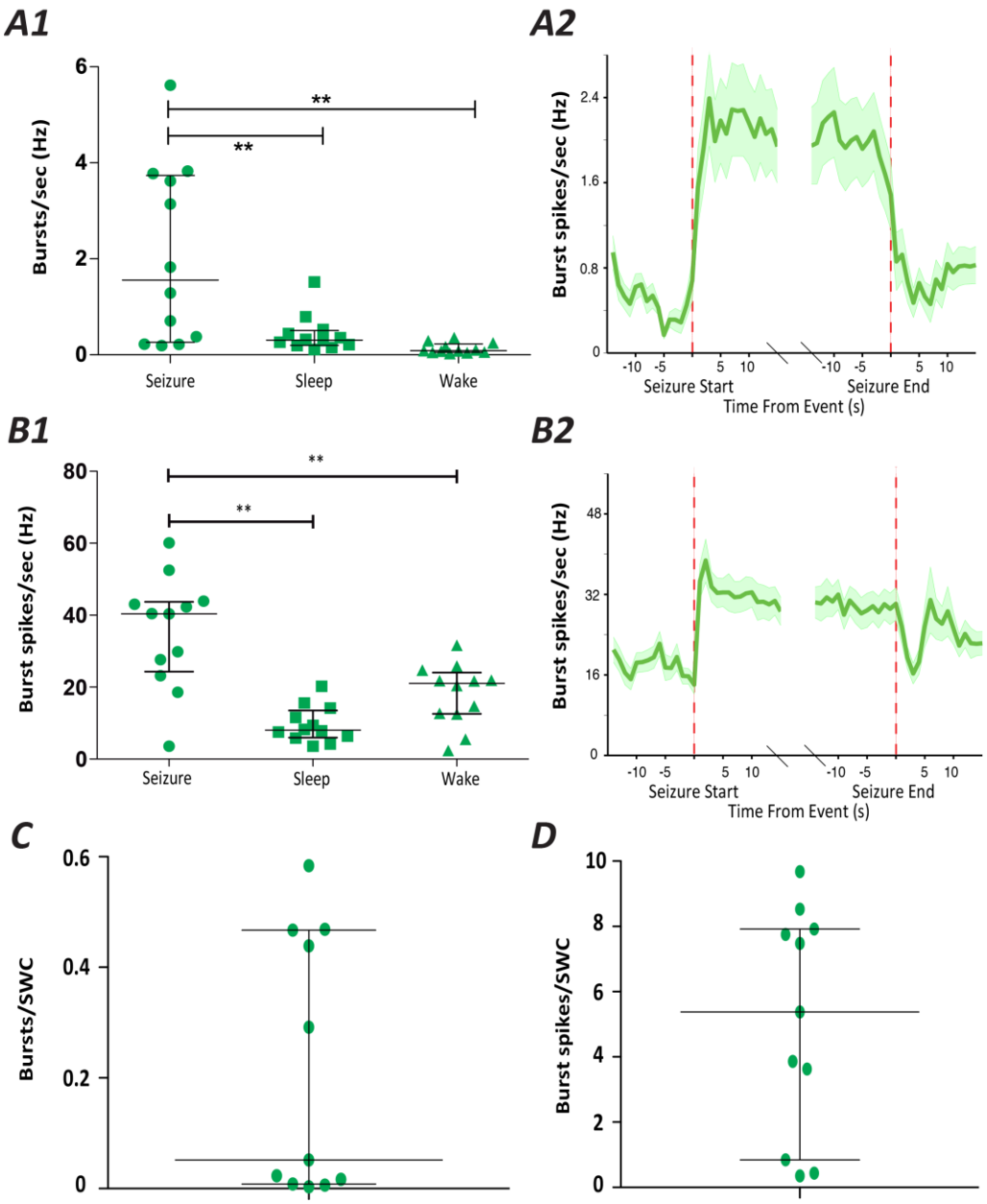

Figure 3.12 nRT bursting rate during seizures

A1 Ictal burst rate of nRT neurones is elevated relative to both sleep and wake rates, but also has a markedly different and non-normal distribution. ***A2*** The evolution of mean burst rates at transitions to and from wakefulness and seizures of ≥ 15s duration shows that bursting increases at the start of seizure, but that variance increases considerably also. ***B1, B2*** Burst-attributable spike rates are similarly distributed to burst rates. ***C*** Between 0.3% and 5.3% of SWCs can be accompanied by bursts, depending on the neurone. ***D*** Burst-attributable spikes/SWC are again similarly distributed to bursts/SWC.

The median rate of bursts per SWC was 0.05 e/SWC (0.003 − 0.58 e/SWC) [Fig. 3.12C]. Visual inspection of the distribution indicates that measures of centre are particularly inappropriate for this parameter, given the massive discrepancy between the sampled values. Again the spread suggests bimodality, with one mode centred below 0.1 e/SWC and one centred above 0.4 e/SWC.

Burst-attributable spikes per SWC were more evenly distributed, with a median of 5.38 s/SWC and a range from 0.35 − 9.68 s/SWC [Fig. 3.12D]. Although five neurones have rates considerably higher than the median (>7.5 s/SWC), the remainder are more evenly spread over the range, suggesting uniformity more than bimodality. These values suggest that some nRT neurones fire LTCP-dependent high-threshold bursts during a significant minority of SWCs (over 40%) while for others the vast majority of SWCs go unaccompanied by bursts.

3.3.2.2.3 Single spikes occur in nRT neurones during between 10% and 100% of SWCs

Single spike rate during AS (8.25 Hz, 1.89 − 32.13 Hz) was lower than that during wakefulness (23.30 Hz, 6.71 − 32.73 Hz, P = 0.012), but no difference could be detected between AS and sleep (8.91 Hz, 6.21 − 12.32 Hz, P > 0.05, signed rank test in both cases) despite the obviously different distributions [Fig. 3.13A1]. Once again there was considerable diversity in rates during AS.

Mean single spike rates during transition periods from wake to seizure and vice versa showed wake (~20 Hz) and ictal (~10 Hz) rates comparable to the median rates calculated over the entirety of the corresponding behavioural state [Fig. 3.13A2]. No transient increases or decreases in single spike rate were apparent in these plots.

The distribution of single spikes per SWC had a median of 0.54 Hz (0.11 − 0.96 Hz) [Fig. 3.13A3]. The range over which these rates were spread was considerable (from approx. 1 spike per 10 SWCs to approx. 1 spike per SWC) and the distribution was more even than that of the per-second rates, appearing more uniform than uni- or bimodal.

3.3.2.2.4 Doublets occur in nRT neurones during a small minority of SWCs

The doublet rate in nRT neurones during ASs (0.34 e/s, 0.15 − 0.96 e/s) was higher than that during sleep (0.09 e/s, 0.05 − 0.23 e/s, P = 0.0005) and that during wakefulness (0.08 e/s, 0.05

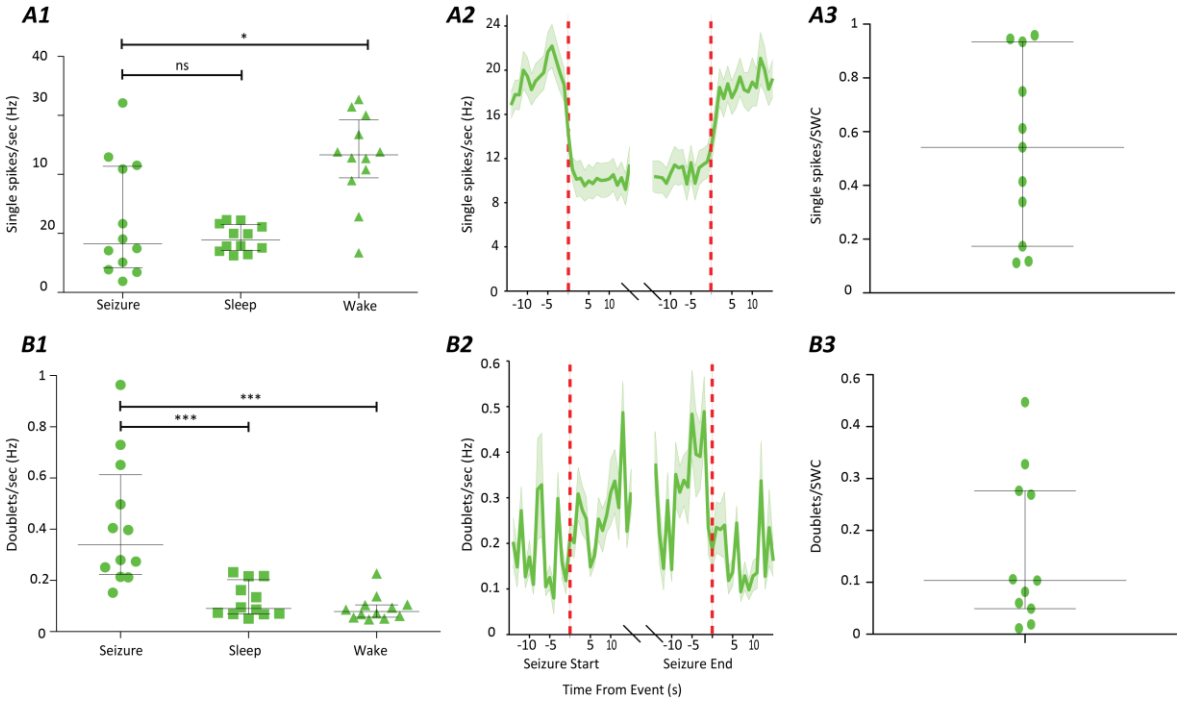

Figure 3.13 nRT neurones fire single spikes and doublets at variable rates during seizure

A1 Single spike rates are lower during seizure than during wakefulness. This does not apply to all neurones due to the high variance of the distributions. ***A2*** Single spike activity over periods of transition into and out of seizures of 15s+ duration shows the overall decrease as well as the high variance during both seizure and wakefulness. ***A3*** These values correspond to anywhere between 0.1 and 1 spike per SWC. ***B1*** Doublet rates are higher during seizure than during either sleep or wakefulness. ***B2*** Their activity during transition periods shows the low incidence and high variance of doublets in both waking and seizure. ***B3*** This is reflected in an incidence of less than 1 doublet every 10 SWCs in the most frequent case.

− 0.23 e/s, P = 0.0005, signed rank test in both cases). The range of ictal values was wider than those of non-ictal states, but the distribution gave no hint of bimodality [Fig. 3.13B1].

Mean doublet rates during transition periods from wake (~0.1 e/s) to seizure (~0.3 e/s) and vice versa were very roughly comparable to the median rates calculated over the entirety of the corresponding behavioural state [Fig. 3.13B2]. Rates were extremely variable pre-ictally, ictally, and post-ictally. When expressing doublet rates as per-SWC, the median was 0.02 e/SWC (range = 0.002 − 0.09 e/SWC) [Fig. 3.13B3]. This corresponds to less than 1 doublet in 10 SWCs even in the most extremely elevated case.

Firing dynamics of nRT neurones in all behavioural states are summarised in Table 3.4.

3.3.2.3 Inter-seizure activity variance differs hugely between nRT neurones

3.3.2.3.1 Burst rate and firing rate vary greatly in distinct subgroups of nRT neurones

In addition to the variation in seizure-related activity between nRT neurones, inter-seizure variation within a single neurone was also investigated. This was estimated quantitatively by calculating the corrected sample standard deviation of ictal firing rates and burst rates (across all seizures) for each nRT neurone [Fig. 3.14A]. The means of these distributions were 18.74 Hz and 0.72 Hz for firing and bursting respectively, while their medians were 14.29 Hz and 0.66 Hz [Table 3.5].

Visual inspection of the mean rate per seizure for each nRT neurone [Fig. 3.14B] suggests that both firing rate and burst rate have diverse and unrelated levels of inter-seizure variation among nRT neurones. Neurones number 4, 6 and 7 have seizure firing rates distributed between 10 and 120 Hz with no apparent centre of concentration. Neurone 12 has a lesser, but still considerable spread of firing rates (this neurone has only 12 associated seizures) while neurone 11 appears bimodally distributed. The remaining neurones each have single centres of concentration of firing rate distributions.

When it comes to burst rates, the seizure-by-seizure plot suggests an overall lower degree of variation with all but 2 neurones having clear centres of burst rate distribution [Fig. 3.14B2]. Of interest among the remaining neurones is the confirmation that burst rates can completely differ from neurone to neurone not just in mean values, but also in entire distributions across seizure.

		Median	Minimum	Maximum	Mean ± SEM
Seizure	All spikes	6.23	2	7.06 ± 0.37	13.45
	Bursts	0.43	0.14	0.55 ± 0.05	1.53
	Single spikes	3.49	1.29	3.64 ± 0.17	7.39
	Doublets	0.57	0.24	0.8 ± 0.06	2.07
Sleep	All spikes	5.53	1.68	5.84 ± 0.28	11.51
	Bursts	0.57	0.1	0.57 ± 0.03	1.11
	Single spikes	2.07	0.58	2.35 ± 0.15	5.26
	Doublets	0.31	0.14	0.33 ± 0.02	0.57
Wake	All spikes	11.01	2.81	11.70 ± 0.57	22.33
	Bursts	0.17	0.03	0.25 ± 0.02	0.78
	Single spikes	8.11	2.11	8.40 ± 0.38	14.79
	Doublets	0.16	0.06	0.19 ± 0.01	0.36

	Median	5th Percentile	95th Percentile	Mean ± SEM
All spikes	7.74	0.80	13.29	7.09 ± 1.43
Bursts	0.05	0.003	0.58	0.21 ± 0.07
Single spikes	0.54	0.11	0.96	0.54 ± 0.01
Doublets	0.02	0.002	0.09	0.03 ± 0.01
Burst spikes	5.38	0.35	9.68	5.08 ± 1.04

Table 3.4 nRT neurone activity in different behavioural states

A Behavioural state statistics (all values in Hz). ***B*** Seizure-specific statistics (all values in per-SWC).

Firing Rate	**Standard Deviation**	**Mean**
Mean	18.74 Hz	47.46 Hz
Median	14.29 Hz	56.95Hz
5th to 95th percentiles	3.80 to 42.35 Hz	8.92 to 65.77 Hz
Bursting Rate		
Mean	0.72 Hz	2.07 Hz
Median	0.66 Hz	1.56 Hz
5th to 95th percentiles	0.15 to 2.12 Hz	0.19 to 5.62 Hz

Table 3.5 Descriptive statistics of inter-seizure variation in nRT neurones

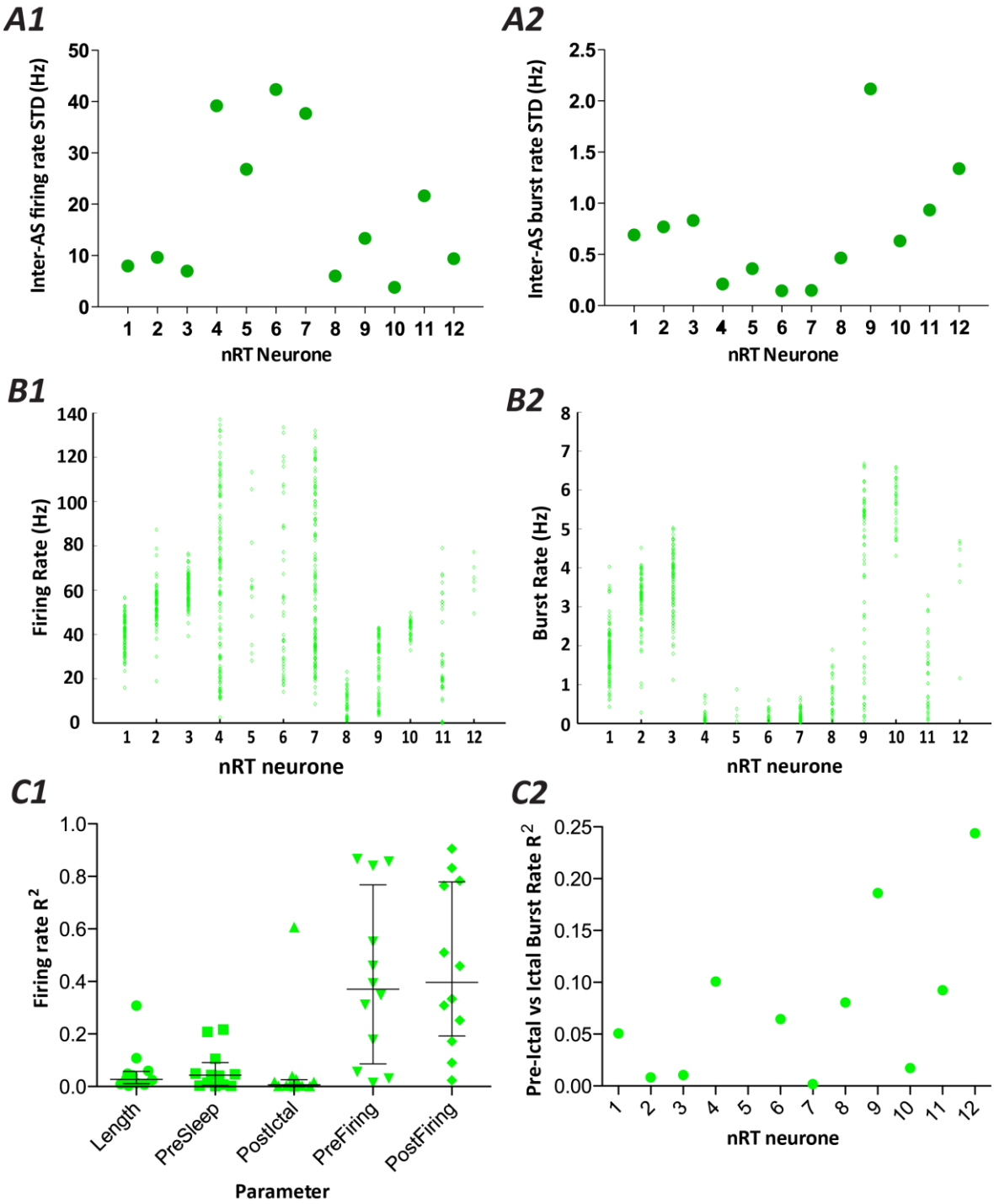

Figure 3.14 Inter-seizure variation in firing and bursting rates

A Standard deviations of mean seizure firing (A1) and burst (A2) rates of nRT neurones. ***B*** Firing rate (B1) and burst rate (B2) for each seizure are plotted for each neurone. ***C*** Coefficients showing sources of variation in AS firing (C1) and burst (C2) rates. The two parameters with largest median coefficients of variation, pre- and post-ictal firing rate, also have very large inter-neuronal diversity in those coefficients. Note that apparent clusters in ***A*** and ***B*** are not divided by animal or by recording position.

3.3.2.3.2 Variation in ictal activity of nRT neurones is strongly related to variation in peri-ictal activity of those neurones

Mean correlation coefficients (r values) between mean seizure activity (for all spikes and for bursts only) and the same AS parameters described in section 3.3.1.3.2 were calculated in order to quantitatively investigate the source(s) of inter-seizure variation in nRT neuronal activity. The results are arranged in Table 3.6.

Seizure length, pre-seizure arousal state and post-seizure ictal activity were all correlated with ictal firing rate, but r-squared values suggested that they shared less than 5% variation (median R-squared = 0.027, 0.043, and 0.001 respectively). Pre-ictal and post-ictal firing rate, on the other hand, were strongly correlated with ictal firing rate – in both cases explaining more than 35% of variation (median R-squared = 0.371 and 0.396 respectively) [Table 3.6, Fig. 3.14C1]. Ictal burst rate was regularly correlated with only one of the parameters investigated, pre-ictal burst rate, and that with a shared variation of only 6.5% (median R-squared = 0.065 [Fig. 3.14C2].

These results suggest that nRT ictal firing rate is positively correlated with firing rate (of the same neurone) before and after seizure. Shared variation isn't absolute, suggesting that other neuronal, network, and/or behavioural factors may also be related to ictal firing rate. It also varies hugely between neurones, confirming the nRT diversity suggested by previous analyses. No assumptions of causality should be made based on this data. Ictal burst firing rate, by contrast, has no strongly correlated parameters among those studied.

3.3.2.4 nRT ictal output is periodic and EEG-synchronous

3.3.2.4.1 Multiple nRT neurones were not recorded simultaneously

At no point during the experiments were multiple nRT neurones recorded simultaneously, therefore ictal inter-neuronal relationships could not be investigated for this population. This was due to the scarcity of nRT neurones.

3.3.2.4.2 nRT neurones show a clear phase preference during SWDs

The synchrony between nRT neuronal activity and SWCs suggested by the raster-EEG plots shown in Figs. 3.9 and 3.15 was investigated in greater detail by calculating SWC peak-triggered neuronal firing averages and neuronal spike-triggered EEG averages. As with TC

	All Spikes		Bursts	
	r value sign & significance	r-squared median	r value sign & significance	r-squared median
Seizure length	P = 0.021 (–)	0.03	n.s.	–
EEG 6 to 8 power	n.s.	–	n.s.	–
LFP 6 to 8 power	n.s.	–	n.s.	–
Pre-seizure sleep	P = 0.034 (–)	0.04	n.s.	–
Post-seizure sleep	n.s.	–	n.s.	–
Pre-seizure ictal	n.s.	–	n.s.	–
Post-seizure ictal	P = 0.021 (+)	0.001	n.s.	–
Pre-seizure spikes	P = 0.001 (+)	0.37	n.s.	–
Post-seizure spikes	P = 0.009 (+)	0.4	n.s.	–
Pre-seizure bursts	n.s.	–	P = 0.0244 (+)	0.07
Post-seizure bursts	n.s.	–	n.s.	–

Table 3.6 Sources of variation in nRT ictal activity

Mean correlation coefficient distributions are significantly different from zero in the cases of seizure length, pre-seizure sleep, pre-seizure firing rate and post-seizure firing rate vs. ictal firing rate. R-squared values in the latter two cases are significantly larger than the former two (highlighted cells). Signs indicate direction of correlation.

neurones, necessary variation in EEG electrode position meant that 2 animals were excluded from these analyses, leaving a sample size of 8 neurones from 3 rats.

There was an immediately apparent synchrony between SWCs and nRT activity, with a maximum exactly contemporaneous with the SWC spike [Fig. 3.15A1]. The maximum reached approximately 7 times the preceding local minimum (0.07 spikes/ms compared to 0.01 spikes/ms). The peak surrounding the central maximum was 76 ms wide at 10% of its maximum height (−39 to +37 ms relative to SWC peak) and 14 ms (−8 to +6 ms) at half its total height. Flanking maxima were also apparent ~140 ms either side of the SWC peak-associated maximum (147 ms before and 132 ms after), which latency corresponds approximately to the inverse of the peak frequency of SWDs (7 Hz).

SWC peak-triggered burst times [Fig. 3.15B1] were similarly distributed (taken as the time of the first spike of a burst), but centred 6 ms prior to the SWC spike at a maximum of 0.005 bursts/ms (compared to adjacent minima of 0). The width at 10% height was 21 ms (−14 to +7 ms), and at 50% height was 7 ms (−7 to 0 ms). Flanking maxima were again apparent, at latencies of −147 and +132 ms relative to the primary maximum.

The distribution of single spikes [Fig. 3.15C1] was also centred at the same time as the SWC peak, reaching 0.017 single spikes/ms in a 10-fold increase from a minimum of 0.004 single spikes/ms. Unlike other parameters, single spike distribution featured a secondary maximum 22ms delayed relative to the first, reaching 0.012 single spikes/ms. Its 10% width was 62 ms (−10 to +52 ms) due partly to this secondary maximum, and its 50% width was 11 ms (−6 to +5 ms). Flanking maxima were apparent approximately 140 ms before and after the primary maximum.

All forms of nRT output occur preferentially around the peak of the SWC. The degree of synchrony can be estimated by reference to the percentage of an SWC during which firing is elevated (using 10% of maximum height as a threshold). These worked out as approx. 53.5%, 14.8%, and 44% of the SWC for all spikes, bursts, and single spikes respectively. An alternative measure, estimating only the proportion of the SWC during which activity is significantly elevated (50% max. height threshold), worked out at 9.9%, 4.9% and 7.7% for all spikes, bursts and single spikes respectively.

The synchronicity of nRT neuronal firing and EEG was confirmed by the calculation of mean EEG values surrounding ictal spikes, bursts, and single spikes (again using first spikes of bursts

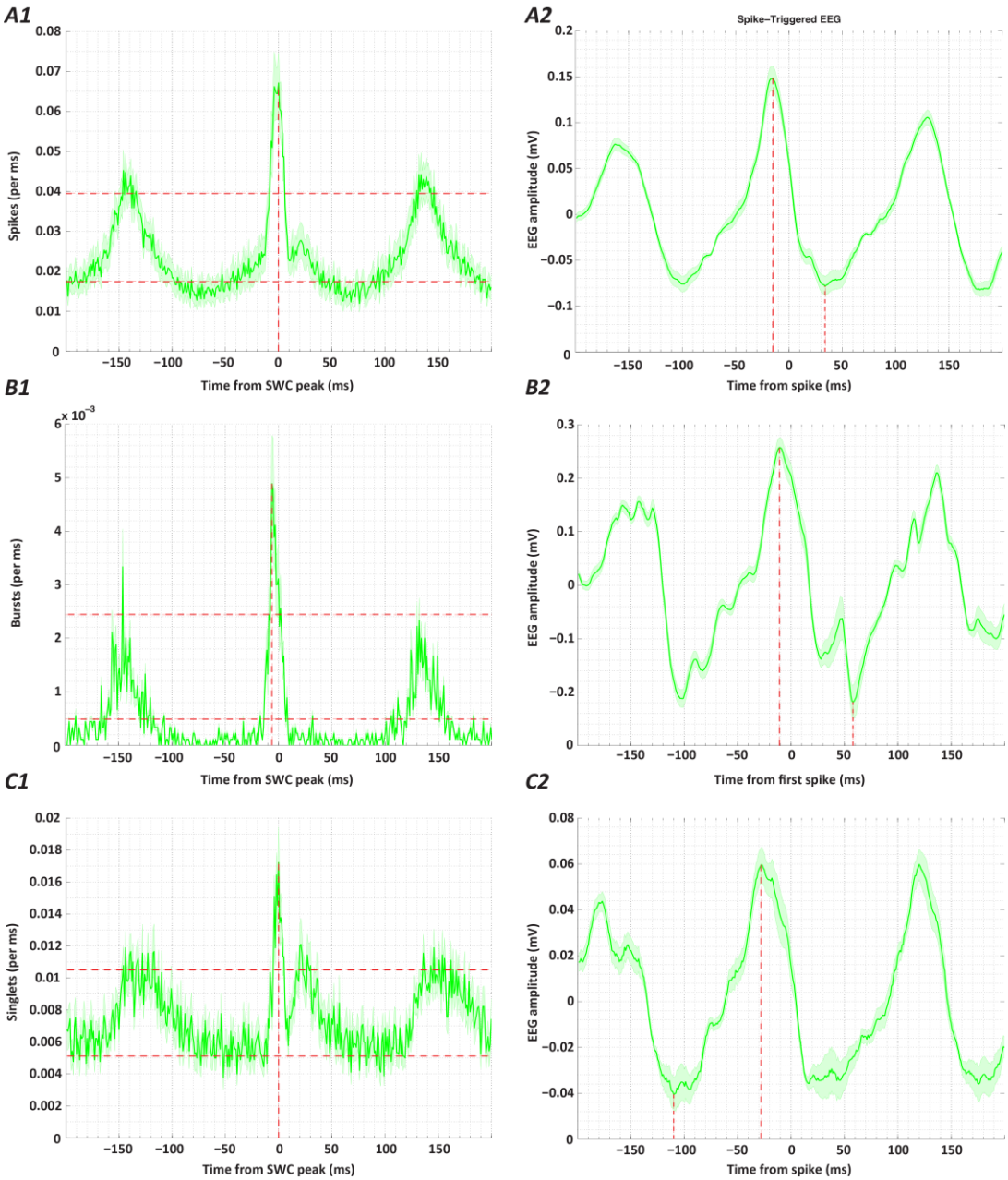

Figure 3.15 SWC and nRT neuronal synchrony

A nRT ictal firing (1) is concentrated at the time of the SWC peak while the maximum of neuronal spike-triggered average EEG (2) is located 15 ms prior to the spike. ***B*** Burst firing (1) is concentrated 6ms prior to SWC maximum, while burst-triggered EEG (2) peaks 7 ms prior to the burst centre. ***C*** Single spikes (1) are concentrated at the time of the SWC peak, and single spike-triggered EEG (2) peaks 17 ms prior to the single spike centre. Shaded area denotes SEM. Red vertical dashed lines mark maxima while red horizontal dashed lines mark 10% and 50% of total height.

only) [Fig. 3.15A2,B2,C2]. In all cases, the resulting EEG waveform roughly resembled a spike-and-wave. The peak of the averaged waveforms was 15 ms prior to ictal spikes, 11 ms prior to bursts, and 28 ms prior to single spikes. These do not correspond to the inverses of the SWC-triggered neuronal peaks due to the uneven distribution of spikes either side of these points of maximum neuronal firing. The positive-going (downward) peak of the EEG is delayed by >25 ms relative to all forms of nRT neuronal output.

3.3.3 Relationships between TC and nRT neuronal firing during absence seizures

The temporal relationship of TC and nRT neuronal firing during ASs is of interest due to their mutual monosynaptic connections and their shared excitatory input from the neocortex. Combined EEG/ raster plots of the spike times of simultaneously recorded TC and nRT neurones [Fig. 3.9A] demonstrated that nRT neurones had a higher output during seizure than their TC contemporaries. Cross-correlograms of all simultaneously active TC and nRT neurones [Fig. 3.16] showed no consistent trend in TC firing leading nRT or vice versa. TC firing led in 6/12 pairs while nRT firing led in 1/12, the remaining pairs either being apparently synchronous or having nRT peaks both before and after those of TC. Latencies between the peaks of TC and nRT firing were between 0 and 25 ms.

3.3.4 Discussion

3.3.4.1 Summary

3.3.4.1.1 Overview of TC and nRT neurone output during absence seizures

Recordings of single-unit activity from thalamic neurones suggest that VB TC neurones either are silent or fire a single spike 4 ms prior to the EEG spike of the overwhelming majority of SWCs. LTCP-dependent bursts are present during less than 5% of SWCs, and occur about 6 ms prior to the EEG spike. Doublets are present during less than 10% of SWCs. Neurones of the nRT meanwhile express diverse activity during ASs: some (4/11) fire bursts about 6 ms ms prior to the spike of 40% of SWCs, others (4/11) fire single action potentials in synchrony with the spike of more than 80% of SWCs, while still others (3/11) fire single spikes or are silent during SWCs in similar proportions to the majority of TC cells.

3.3.4.2 Methodological considerations for AS single unit recordings

The difficulties in isolating the activities of single neurones during ASs must be considered when interpreting these results. The consequence of synchronous TC and nRT activity during

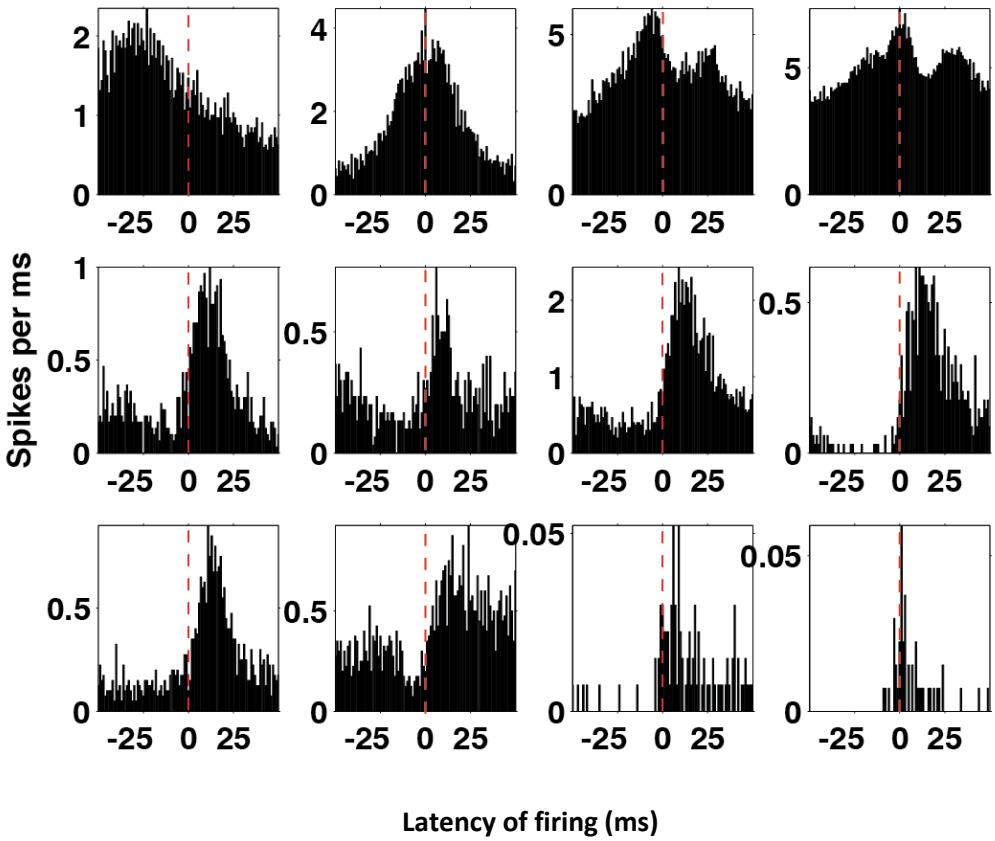

Figure 3.16 TC and nRT neurones have periodic temporal relationships

Ictal cross-correlograms of all simultaneously-active TC vs. nRT neurones (plots show distribution of nRT firing around TC spikes) show some cases of TC leading (subfigures 5 to 12), one of nRT leading (1) and some case of apparent synchrony or bimodality (2, 3, 4).

AS was that the waveforms of any neurones detectable on a given channel tended to overlap temporally.

In addition, during seizures a high-frequency oscillation of no particular waveform was visible on most channels, potentially attributable to the summation of simultaneous voltage deflections of otherwise undetectable neurones. As mentioned in section 2.2, neurones were only analysed if their waveforms had a high signal to noise ratio and were distinguishable from all other neurones, even during seizure, as well as from this high-frequency noise.

A few selection biases may arise from this stringency. Neurones that are asynchronous with the SWD and with other neurones during seizure are more likely to be isolable: this is not considered to be a problematic bias because few such neurones were recorded. Neurones that generate a larger voltage deflection, as detected by the recording electrode, will also be favoured. This may result in a bias towards neurones of certain morphologies, positions and/or orientations, but the homogeneous organisation of the VB thalamus (see section 1.3) doesn't suggest any reason why such a bias would compromise my results.

3.3.4.3 Nature of thalamic activity during absence seizures

A discussion of TC and nRT activity during ASs in freely moving GAERS should be contextualised with prior results obtained both in GAERS and in other models of experimental absence seizures and/or SWDs under different experimental conditions. The observation that TC neurones are mostly silent and fire very few high-frequency bursts during ASs is a significant clarification of the existing uncertainty stemming from contradictory results in *in vivo* and *in vitro* models of SWDs. The diverse mix of bursts, single spikes, and silence observed in nRT neurones during ASs also represents a significant expansion and refinement of current knowledge in the field.

3.3.4.3.1 Compatibility with existing knowledge of thalamic AS activity

Single unit intracellular recordings in anaesthetised GAERS are among the previous best approximation of thalamic electrical behaviour during ASs. For TC neurones, these experiments suggest predominant silence during SWDs with occasional single spikes or bursts, due to incoming sequences of EPSPs and $GABA_A$ IPSPS (Pinault et al., 1998; Charpier et al., 1999; Pinault, 2003). An experiment in the same condition employing multi-unit extracellular VB and nRT recordings (Seidenbecher et al., 1998) suggested that the former cell type express bursts at each SWC, while single unit extracellular recordings suggested firing at each SWC

composed of an approximately equal mix of single spikes and bursts (Pinault et al., 1998). Discrepancies between these results and those observed in this thesis can be explained by the contribution of multiple neurones to multi-unit bursts and to the difference between anaesthetised SWDs and absence seizures (see below). It is evident that, if each TC neurone fires a single spike on ~50% of SWCs, then the simultaneously recorded firing of 6 or more TC neurones would appear as a burst in multi-unit recordings such as those of Seidenbecher et al. (1998) in GAERS, or indeed those of Williams (1953) in humans.

In nRT neurones, the same regime with intracellular recordings revealed high-frequency burst firing at every cycle of an SWD, mediated by a large tonic hyperpolarisation and rhythmic barrages of EPSPs (Slaght et al., 2002). Multi-unit recordings in the same conditions also showed regular bursts but again couldn't identify the individual neuronal contributions to these (Seidenbecher et al., 1998). The fact that only some of the nRT neurones recorded here exhibited regular bursting might be explained by differences between fentanyl/haloperidol-facilitated SWDs and ASs (Inoue et al., 1994) – an anaesthetic regime could be reasonably expected to homogenise behaviour within a neuronal population.

Aside from that discovered in GAERS, electrophysiological evidence regarding the activity of thalamic neurones during ASs stems from neuronal recordings in anaesthetised *in vivo* or *in vitro* models of SWDs. In the former case, isolated unit information comes from two sets of experiments, neither in well-established models of ASs. The first involved extracellular and intracellular TC neurone recordings during paroxysmal oscillations that developed from sleep-resembling oscillations in (a minority of) urethane and ketamine/xylazine anaesthetised cats (Steriade and Contreras, 1995). The observation of silence in TC neurones during 60% of SWCs and SWC-locked high-frequency bursts during the remaining 40% is compatible with the results presented here. Silence is the predominant activity in both experiments, and both ketamine/xylazine and urethane anaesthetic regimes increase the probability of TC neurone burst firing (Crunelli et al., 2012; David et al., 2013; Huh and Cho, 2013). Interestingly, these experiments (Steriade and Contreras, 1995) also demonstrated variation in nRT activity during SWDs, with most nRT neurones bursting regularly and a subset failing to exhibit any alterations in discharge pattern during the event. The second experiment involved recordings from TC neurones in Long-Evans rats and high-voltage rhythmic spikes under fentanyl anaesthesia (Kandel and Buzsaki, 1997). It showed a pattern of predominant silence based on a tonic hyperpolarisation similar to that observed in GAERS and, as such, entirely compatible with the results presented in this thesis.

Multi-unit recordings from fentanyl-fluanisone anaesthetised WAG/Rij rats showed activity in specific thalamic nuclei (VPL, VPM and VL) as well as in nRT being elevated and phase-locked in relation to SWCs (Inoue et al., 1993). The authors of this paper did not make any claims regarding the extent or nature of individual neuronal output. No multi- or single-unit recordings have been attempted in pharmacological models of ASs. Current knowledge regarding thalamic involvement in GHB-induced ASs is limited to recordings showing VB, medial, and reticular thalamic nuclei LFPs roughly synchronous with cortical SWC spikes (Banerjee et al., 1993). In summary, therefore, the findings of all these experiments are entirely consistent with the results presented in this thesis in terms of general VB and nRT activity during AS.

By contrast, the TC neurone firing dynamics observed here cannot be reconciled with the *in vitro* hypothesis of rhythmic LTCPs generating high-frequency bursts at each cycle of an SWD (von Krosigk et al., 1993; Bal et al., 1995a, 1995b). This can be explained by the potential for different neuronal activities underlying two superficially similar oscillations, in particular when the *in vitro* SWDs occurred in a TC network deprived of the cortex and of course did not and couldn't have any behavioural correlate (Buzsáki et al., 2012). The nRT neurone behaviour observed here is in broad agreement with the observation of regular bursts in many neurones during experimental AS, but involves considerable inter-neuronal variation in both the nature and the timing of output.

3.3.4.2.2 TC activity at absence seizure initiation

The results provide some entirely novel information regarding the activity of TC neurones during the first 200 ms of an AS. The rates of both burst and doublet firing are elevated during this period relative to their rates throughout the entirety of a seizure, both exceeding 0.9 events per second. This indicates that bursts and doublets are much more likely to occur during the first SWC of an ASs, suggesting that initiation of a seizure may initially promote some TC excitation before strongly inhibiting that population. This is compatible with the ability of a hyperpolarisation to either induce LTCP-mediated bursting or silence TC neurones depending on its amplitude and duration.

A second, indirect consequence of this observation is an increased likelihood that TC bursts and doublets are generated by the same underlying mechanisms. They share similar rate distributions during ASs and alter similarly upon seizure initiation. Furthermore, the low number of spikes per burst observed in TC relative to nRT neurones, both historically (Domich

et al., 1986; Tscherter et al., 2011) and in this study (see section 2.3.5.3) as well as the greater prevalence of doublets in TC neurones (in all behavioural states) makes it plausible that these two forms of output are mechanistically similar.

3.3.4.2.3 Variation in TC and nRT neuronal activity during AS

Neurones of both populations express somewhat varied activity within seizures, demonstrating that the connectivity of the TC network permits diversity in thalamic activity even in the ictal state. The wide variety of nRT behaviour suggests that component populations of the TC network may express multiple forms of activity during ASs. This in turn suggests that *in vitro* or anaesthetised models of SWDs that feature more stereotyped, constant behaviour across this neuronal population do not reproduce the complexity of TC network dynamics during ASs.

Within a neurone, inter-seizure variation is low for TC, with firing and bursting rates tending to be distributed pseudo-normally around a single mode and varying, on average, by less than 3 Hz and 0.5 Hz respectively. These variations would suggest that TC output tends to stay the same from seizure to seizure. Variation is considerable for some nRT neurones – 3 of 11 cells have firing rates ranging from 10 Hz in one seizure to 100 Hz in another, while 1 further neurone varies in bursting rate from 0.1 e/s in one seizure to 7 Hz in another. Such variation implies that some nRT neurones are capable of significantly varying their behaviour (e.g. from an average of more than 10 spikes per SWC to less than 1, or from an average of nearly 1 burst per SWC to less than 1 burst per 10) depending on their own state and/or that of the thalamocortical network, at the point of seizure initiation. It is noteworthy that firing rate during an AS tends to vary in proportion to the firing rate immediately before and after that seizure, supporting the hypothesis that (in some cases at least) activity of an nRT neurone during seizure may be dependent on its activity immediately prior.

3.3.4.3 Synchrony of thalamic activity during AS in GAERS

As well as the content of ictal TC and nRT output, the temporal relationship of such output with that of other neurones and with the EEG features known to delineate a single cycle of network activity (i.e. the SWC) are of interest. These experiments provide the first opportunity to relate the output of single isolated thalamic units to fronto-parietal EEG in freely moving GAERS. All forms of output of both populations studied were heavily biased towards an epoch (of varying duration depending on cell and output type) centred on the peak of an SWC spike. In the case of TC neurones both LTCP-dependent bursts and –independent spikes were

concentrated <10 ms prior to this spike, while nRT neurone output was concentrated more precisely in synchrony with the spike.

The existing literature provides evidence regarding the temporal relationship of thalamic output and fronto-parietal cortical SWDs garnered from *in vivo* studies employing LFP and multi-unit recordings. In GAERS, the single unit extracellular and intracellular recordings under fentanyl/haloperidol anaesthesia again provide the most relevant results (Pinault et al., 1998; Slaght et al., 2002; Pinault, 2003). In these experiments TC neurone firing was centred 10 to 12 ms prior to the negative-going peak of the SWC spike, corresponding closely to the 4 ms lag observed here. As with the nature of nRT activity, so is there a disparity in the timing of nRT activity between these experiments and the results detailed here. The fentanyl-haloperidol SWC peak tended to be 7 ms after the centre of nRT firing and 19 ms after the centre of nRT bursting, compared to 0 ms and 6 ms respectively for the SWC peak in freely moving animals.

Both multi-unit and LFP recordings from all experimental models of SWDs and ASs concur that VB and nRT activity are concentrated around the peak of the cortical SWC (Banerjee et al., 1993; Inoue et al., 1993; Steriade and Contreras, 1995; Danober et al., 1998). There is no particular dispute on this subject in the literature, and the demonstration that this relationship holds for ASs in freely moving GAERS confirms and refines our existing knowledge regarding the temporal relationship between cortex and thalamus in ASs.

In summary, both TC and nRT firing tends to occur in close proximity to the peak of the SWC. TC neuronal firing is concentrated 4 ms prior to that peak, but the preponderance of bursts in many nRT neurones results in a centre of firing more in synchrony with it. The first nRT spike of an SWC tends to be located less than 5 ms prior to the peak, favouring the possibility that both TC and nRT populations may be excited by the same input, consistent with the observations by Pinault et al. (1998) and Slaght et al. (2002) of small depolarisations (i.e. EPSPs) in both cell types preceding any firing. The lack of a consistent latency between TC and nRT firing observed in these experiments argues against the alternative of direct TC excitation of nRT.

3.3.4.4 Implications for thalamocortical network generation and propagation of AS

Both the form and the timing of TC and nRT activity during ASs have implications for the set of potential roles these populations could play in the initiation and propagation of ASs. The relatively low, albeit synchronous, output from TC neurones (when considered as a proportion

of SWCs) could be taken together with the identification of a layer V peri-oral somatosensory cortex initiation site for SWDs (Meeren et al., 2002; Polack et al., 2007, 2009) and the observation that corticothalamic neurones tend to fire before thalamic neurones within an SWC (Pinault, 2003; Polack et al., 2007) to propose that, of the two populations of projection neurones involved in the thalamocortical network, it is that of deep layer cortical neurones that provide the primary driving source behind absence seizure propagation.

The contribution of cortical neurones of particular layers and types (excitatory and inhibitory) to each cycle of an AS, in terms of output and synchrony, must be established by recording of multiple isolated units in order to usefully test any hypotheses regarding the interplay of the component neurones of the network. Thus far, layer-specific cortical recordings have either included been multi-unit or LFP (Kandel and Buzsáki, 1997) or taken place in fentanyl-anaesthetised rats (Pinault, 2003; Polack et al., 2007).

3.3.4.5 Mechanisms underlying TC and nRT firing during absence seizures

In isolation, the results of this chapter do not permit any conclusions to be drawn regarding the membrane potential dynamics of TC and nRT neurones during ASs. The paucity of high-frequency bursts observed in the former population does, however, suggest that LTCPs in these neurones may not be as critical to AS generation and propagation as thought from their prevalence in *in vitro* SWD models (Bal et al., 1995a). It would, rather, seem to lend credence to the hypothesis that TC and nRT membrane activity during AS may be similar to those observed in neurolept-anaesthetised GAERS (Pinault et al., 1998, 2006; Slaght et al., 2002): a small tonic hyperpolarisation with rhythmic EPSP/IPSP sequences in TC neurones, and a large tonic hyperpolarisation with sequences of small depolarising potentials regularly leading to burst-crested LTCPs.

Information regarding the currents involved in TC and nRT neurones during AS and the membrane potentials that their interplay generates must come from intracellular recordings or from interventional experiments manipulating one or more of these currents pharmacologically. The results of such an experiment, involving the application of a T-type Ca^{2+} channel blocker to the VB and to the nRT and the monitoring of its effect on GAERS ASs, are discussed in the following chapter.

In summary, the results of this chapter suggest that the overwhelming majority of GAERS VB neurones are mostly silent during AS, and when they do fire it's almost always in the form of a

single AP within 10 ms of the spike of an SWC. For illustration, Figure 3.18 shows the output of 50 simulated VB neurones during an AS, with firing probabilities at each SWC calculated from the median sample percentages. It demonstrates that, although the firing probability of a given VB neurone during a given SWC is about 50%, there is output from the nucleus at every cycle. Neurones of the GAERS nRT, on the other hand, exhibit extremely diverse activity during AS – differing both between neurones and (in some cases) between seizures, ranging from predominant silence to regular bursts via single spikes, but all output also being synchronous with the SWC peak negativity.

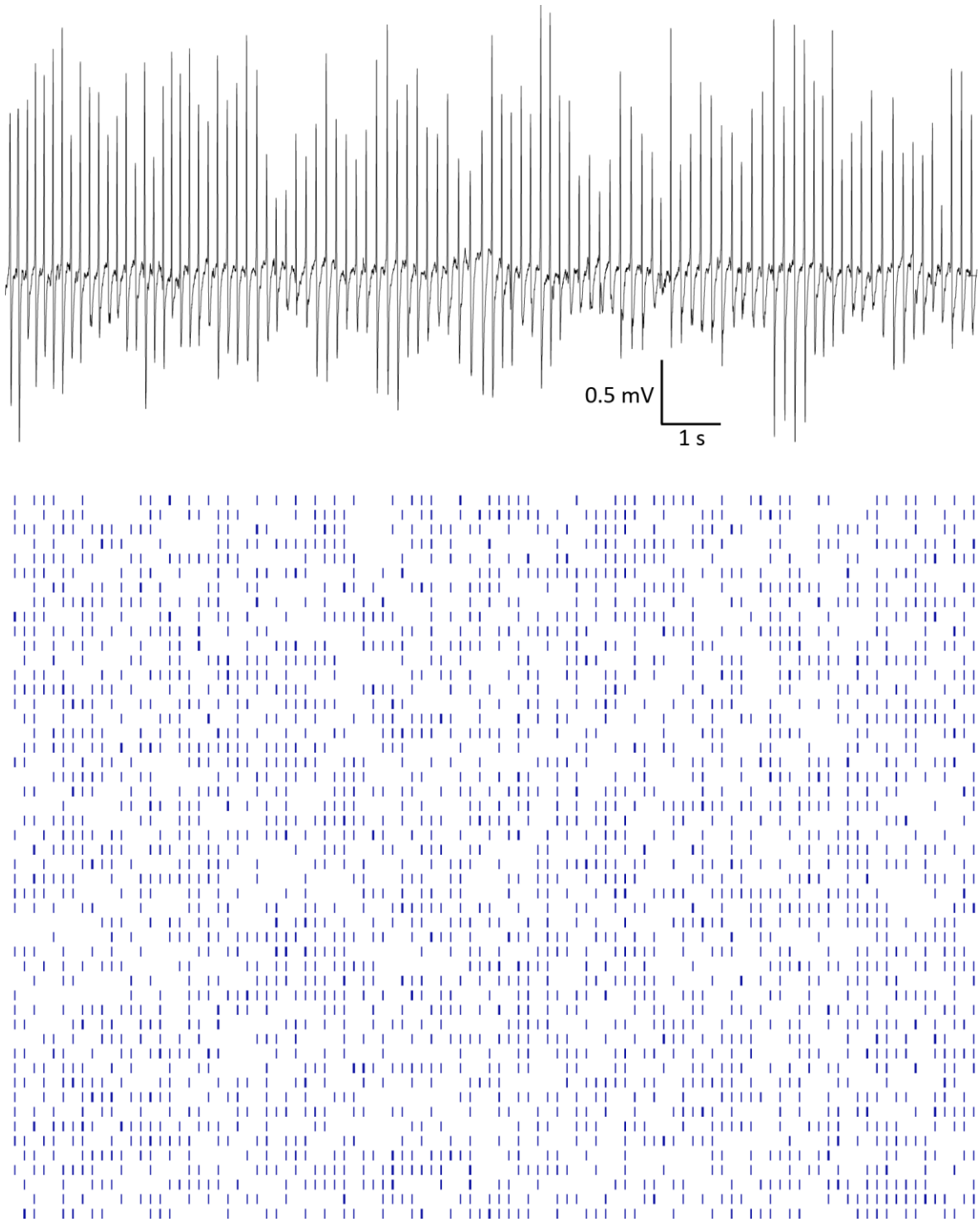

Figure 3.18 Activity of 50 simulated TC neurones during an AS

Firing, burst, doublet and silence probability at each SWC corresponds to the median values observed for the sample of recorded VB neurones. All bursts include 4 spikes.

Chapter 4 – T-type calcium channel activity in nRT, but not in VB, is necessary for normal expression of absence seizures in GAERS

4.1 Introduction

As described in section 1.2.5.5, in TC and nRT neurones T-type calcium channels are responsible for LTCPs and associated burst firing, as well as for a persistently active 'window' inward current, and for increases in intracellular Ca^{2+} concentrations that either activate or modulate other channels (i.e. I_{CAN}, $I_{K(Ca)}$, I_h). Microdialysis of the potent and selective T-type Ca^{2+} channel blocker TTA-P2 is capable of inhibiting high-frequency bursts throughout the VB and in the nRT (David et al., 2013), with the robust redundancy in thalamic T-type Ca^{2+} channels for LTCP generation (Dreyfus et al., 2010) suggesting that such an inhibition signifies a near-complete block of T-type Ca^{2+} channels.

The results detailed in the previous chapter suggest that TC burst firing is rare during ASs, while a proportion of nRT neurones burst frequently. The rationale behind this chapter's experiments is twofold. Firstly, if pharmacological inactivation of T-type Ca^{2+} channels in either TC or nRT neurones has an effect on the expression of ASs in a polygenic model, then activity mediated by those channels was playing a significant role in these seizures. High-frequency bursts are invariably such an activity. It must be noted, however, that non-LTCP-mediated firing can also be dependent on these channels (Deleuze et al., 2012). Secondly, the contribution of T-type Ca^{2+} channels in TC and nRT neurones to ASs is of interest in its own right, independently of specific forms of output, in the context of the potential roles of T-type Ca^{2+} channel related genetic alterations in both human and experimental ASs (Kim et al., 2001; Chen et al., 2003a, 2003b; Heron et al., 2004; Khosravani et al., 2004, 2005; Song et al., 2004; Singh et al., 2007; Ernst et al., 2009).

In this chapter, therefore, I describe the effects of microdialysis application of TTA-P2 in the thalamus on AS expression in freely moving GAERS.

4.2 Methods

The methods employed for this batch of experiments are detailed in section 2.2.

4.3 Results

4.3.1 Block of VB T-type Ca^{2+} channels does not affect GAERS absence seizures

To determine whether activation of T-type Ca^{2+} channels of TC neurones is necessary for the normal expression of ASs in GAERS, epidural EEG and behavioural monitoring were used to record seizure occurrence and SWD parameters while a 300µM concentration of the specific T-type Ca^{2+} channel antagonist TTA-P2 was administered to the centre of the VB by microdialysis (see section 2.2 for targeting and concentration calculations, including Figure 2.2 for area of effect).

For a group of 8 animals, no significant difference could be detected in the total time spent in seizure (as a percentage of pre-drug control hour) between 300µM TTA-P2 treated and aCSF treated sessions (P = 0.769, 95% CI = −39.46 to 30.43) [Fig. 4.1A]. Likewise, no significant difference could be detected in average length of seizure (P = 0.5, −11.49 to 21.38) [Fig. 4.1B] or in number of seizures (P = 0.644, −22.22 to 14.48) [Fig. 4.1C]. Finally, there was no significant difference detectable in power at the peak frequency of SWDs (6-8Hz) between 300µM TTA-P2 and aCSF (P = 0.453, −0.22 to 0.43) [Fig. 4.1D]. Two way repeated measures ANOVA, using time (pre- vs. post-drug[3]) and treatment (aCSF vs. TTA-P2) as factors, did not suggest treatment or interaction of factors as sources of the variation in total time spent in seizure, average seizure length, number of seizures, or power at peak seizure frequency.

These results suggested that a block of T-type Ca^{2+} channels throughout the VB does not affect GAERS ASs.

3.3.2 Block of nRT T-type Ca^{2+} channels inhibits the expression of GAERS ASs

The first strategy employed to block T-type Ca^{2+} channels in the nRT involved increasing the concentration of TTA-P2 administered by microdialysis to the centre of the VB from 300µM to 1mM. This increased the distance from the microdialysis membrane at which a 90% block of burst firing was achieved at 1 hour post-drug from 600µm to 750µm. This change resulted in the theoretical volume of effective channel block at 1 hour including the majority of the nRT as well as the VB (see Fig. 2.5).

[3] Post-drug is used in this chapter, for the sake of brevity, to refer to the hour during which dialysis was affecting the target area.

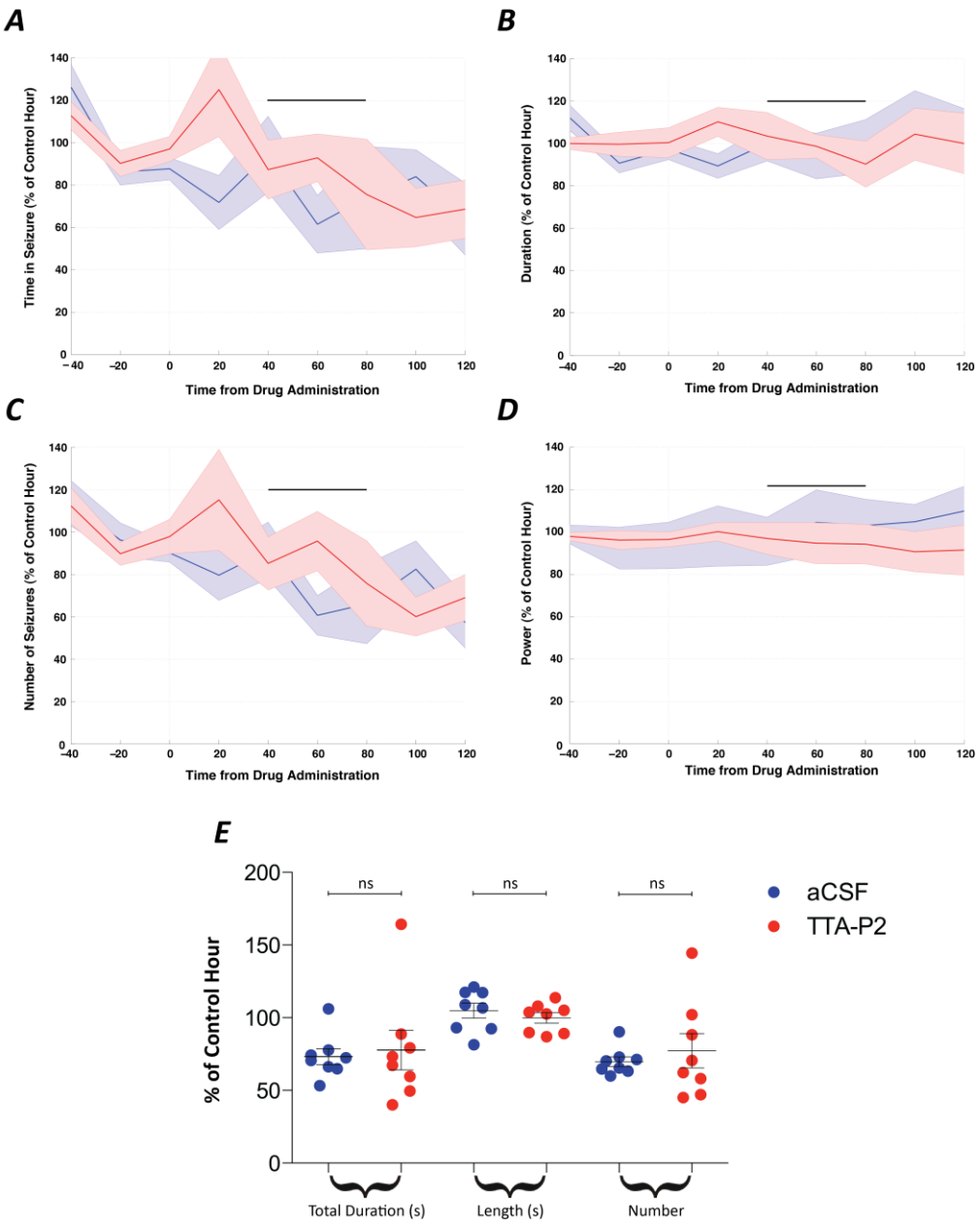

Figure 4.1 300µM TTA-P2 in the central VB doesn't suppress absence seizures

A Total time spent in seizure, ***B*** mean seizure duration, ***C*** number of seizures and ***D*** ictal powear at 6-8 Hz were unchanged by microdialysis of 300 µM TTA-P2 (red) relative to during microdialysis of aCSF (blue). In this and Figures 4.2 & 4.3, parameters are plotted in 20-min bins during pre-drug control and 2 hours of drug administration. At time zero dialysis solution was changed from aCSF to test solution (either aCSF or 300 µM TTA-P2). Black horizontal bars indicate the hour used for effect quantification. ***E*** All the parameters of interest during the target hour only, for both TTA-P2 and aCSF.

In 11 animals the administration of 1mM TTA-P2 throughout the VB and nRT resulted in a significant decrease (by 56.16% of pre-drug control[4]) in time spent in seizure (as a percentage of the pre-drug control hour) compared to aCSF control (P = 0.0063, 19.82 to 92.51) [Fig. 4.2A]. This decrease involved both shorter (by 31.1%) seizures (P = 0.0129, 8.17 to 54.03) [Fig. 4.2B], and a lower (by 33.52%) incidence of seizure (P = 0.0258, 4.97 to 62.06) [Fig. 4.2C]. Despite this decrease in time spent in seizure there was no detectable change in ictal power at 6-8Hz (0.695, −0.18 to 0.26) [Fig. 4.2D].

Two way repeated measures ANOVA using time (pre vs post drug) and treatment (aCSF vs TTA-P2) found that interaction between factors was a significant source of variation of time spent in seizure (P = 0.0013) and of number of seizures (P = 0.0068). Bonferroni post-hoc tests showed that 1mM TTA-P2 treatment involved a significant difference between pre- and post-drug time spent in seizure (P < 0.001) and number of seizures (P < 0.001) while aCSF treatment did not in either case (P > 0.05). Time/treatment interaction was not found to be a significant source of variation of average seizure duration or power at peak seizure frequency. Treatment was not a significant source of variation of any parameter.

These results suggest that blocking T-type Ca^{2+} channels throughout the VB and nRT decreases the time spent in ASs by GAERS. This effect could be attributed either to a cumulative effect of VB and nRT T-type Ca^{2+} channel inhibition, an nRT-only effect (given the lack of change when the VB only was reached), or even an effect that required T-type Ca^{2+} channels throughout the entirety of the VB to be blocked before emerging, i.e. the 600µm block distance achieved by 300µM TTA-P2 (see Fig. 2.5) may not have been sufficient for this. In order to clarify this situation, a complementary strategy to differentiate nRT and VB effects was employed.

Moving the microdialysis probe positioning laterally and reverting to a 300µM TTA-P2 concentration (see Fig. 2.2) was estimated to achieve a 90% (or higher) block of bursts throughout a similar or greater proportion of the nRT than the central VB 1mM protocol, while simultaneously achieving a block throughout a significantly reduced proportion of the VB.

This method resulted in a significant decrease (46.74%) in time spent in seizure (as a percentage of the control hour) for 300µM TTA-P2- compared to aCSF-treated animals (n = 6,

[4] Differences between groups are given in percentages (of pre-drug control) as both are measured in those units, these do not refer to a ratio of the TTA-P2 and aCSF groups.

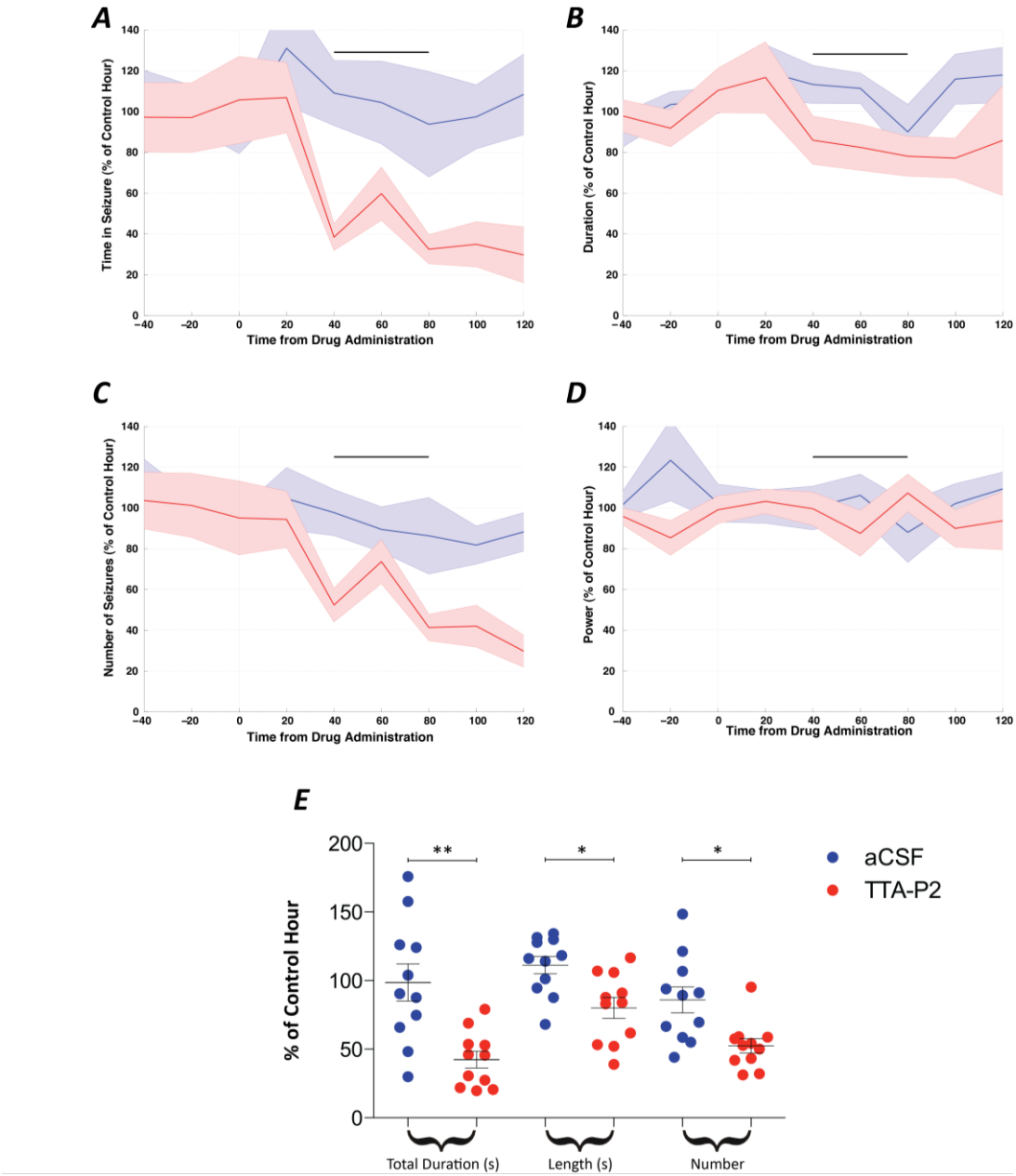

Figure 4.2 1mM TTA-P2 in the VB and nRT suppresses absence seizures

A Total time spent in seizure was decreased by 56% during microdialysis of 1mM TTA-P2 relative to during microdialysis of aCSF control. ***B*** There was a 31% reduction in mean duration of seizure and (***C***) a 34% reduction in number of seizures. ***D*** There was no detectable change in ictal power at 6-8Hz. At time zero dialysis solution was changed from aCSF to test solution (either aCSF or 1 mM TTA-P2). Black horizontal bars indicate the hour used for effect quantification. ***E*** All the parameters of interest during the target hour only, for both TTA-P2 and aCSF.

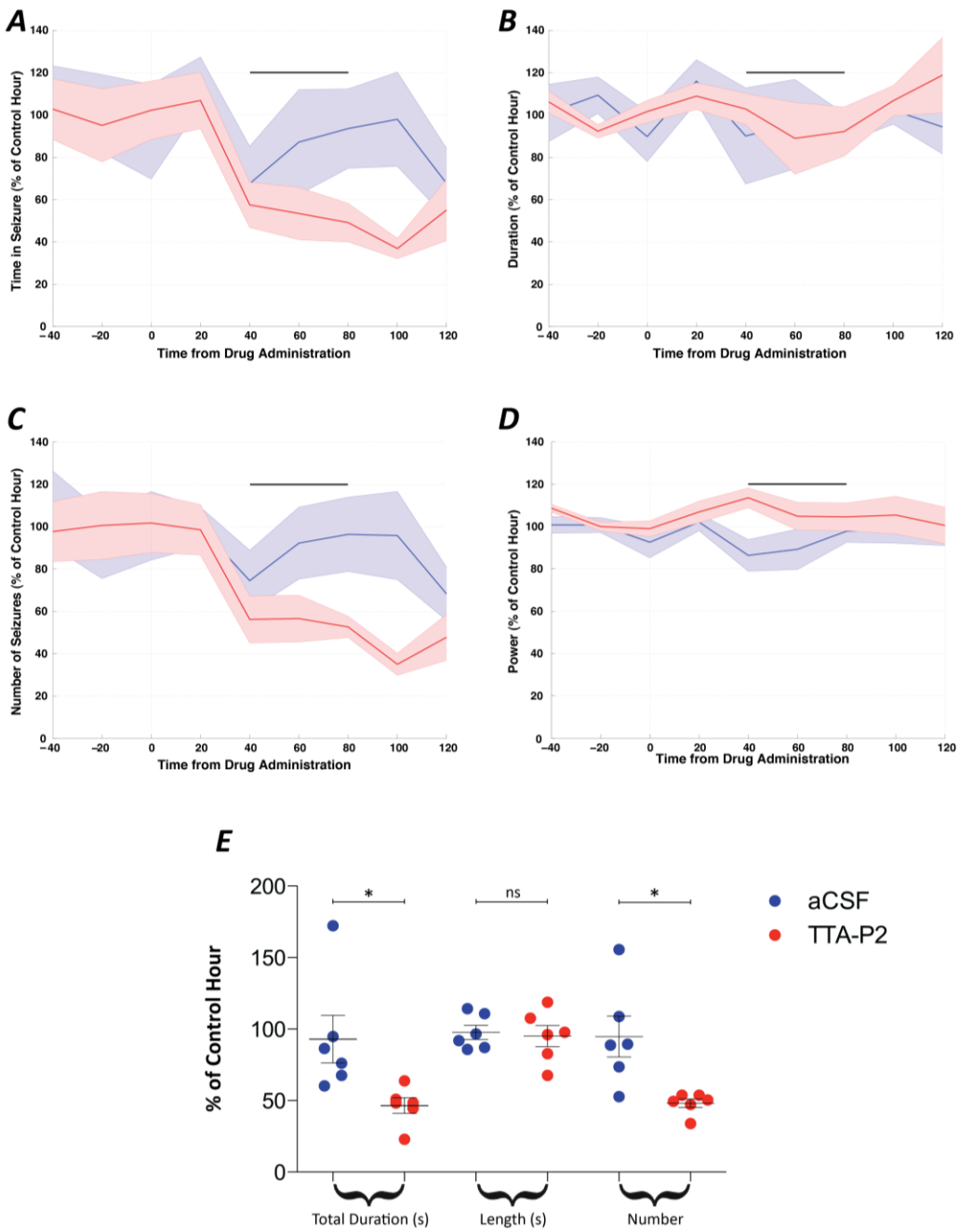

Figure 4.3 300µM TTA-P2 adjacent to the nRT suppresses absence seizures

A Total time spent in seizure was decreased by 46% during microdialysis of 300µM TTA-P2, compared to during microdialysis of aCSF control. ***B*** The decrease was not accompanied by a detectable change in mean length of seizure but rather (***C***) solely by a 47% decrease in number of seizures. ***D*** Ictal power at 6-8Hz was not detectably changed. At time zero dialysis solution was changed from aCSF to test solution (either aCSF or 300 µM TTA-P2). Black horizontal bars indicate the hour used for effect quantification. ***E*** All the parameters of interest during the target hour only, for both TTA-P2 and aCSF.

P = 0.0326, 95% CI = 5.68 to 87.15) [Fig. 4.3A]. This decrease was of a similar order to that observed in the 1mM VB group, but unlike that group the decreased time spent in seizure did not involve shorter seizures (P = 0.832, 95% CI = −27.26 to 32.44) [Fig. 4.3B]. Rather, there was a mean 46.74% decrease in number of seizures (P = 0.0148, 95% CI = 13.8 to 79.68) [Fig. 4.3C]. Again, power at 6-8Hz showed no detectable difference between groups (P = 0.275, 95% CI = −0.31 to 0.11) [Fig. 4.3D].

Again the result was confirmed by 2 way repeated measures ANOVA using time (pre vs. post drug) and treatment (aCSF vs. TTA-P2) as factors. Interaction between the factors was found to be a significant source of variation in time spent in seizure (P = 0.0265) and in number of seizures (P = 0.0118). Bonferroni post-hoc tests showed that 300µM TTA-P2 treatment involved a significant difference between pre- and post-drug time spent in seizure (P < 0.01) and number of seizures (P < 0.01) while aCSF treatment did not in either case (P > 0.05). Time/treatment interaction was not found to be a significant source of variation of average seizure duration or power at peak seizure frequency. Treatment was not a significant source of variation of any parameter.

The observation of a similar level of seizure suppression when nRT T-type Ca^{2+} channel inhibition was maintained and VB T-type Ca^{2+} channel inhibition was decreased suggested that seizure suppression could be attributed to nRT, rather than TC or combined TC and nRT, block of these channels.

4.4 Discussion

4.4.1 Summary of results

These results suggest that activity of T-type calcium channels in the nRT, but not the VB, are necessary for full expression of ASs in GAERS.

4.4.2 Methodological considerations

The advantages and limitations of microdialysis administration should be born in mind when discussing these results (see section 3.2). The ideal local administration of a drug would involve an identical, calculated concentration being delivered to every neurone within the target area and no drug reaching neurones extrinsic to that area. The drug concentrations applied and the microdialysis protocols followed here were designed to approach this ideal condition as closely as possible.

The administration of 300µM from a membrane placed in the centre of the VB was judged the most likely to block T-type Ca^{2+} channels throughout this entire structure without spreading to the nRT [Fig. 2.5]. Spread to other nuclei of the thalamus could not be ruled out, but was estimated to be minor due to the dimensions of the VB. Furthermore, lesion studies in GAERS (Vergnes and Marescaux, 1992; Meeren et al., 2009) showing the persistence of ASs after the ablation of the anterior, posterior and midline thalamic nuclei suggest that these regions are of minor importance in AS pathophysiology compared to the VB and nRT.

Selective drug administration to the entirety of the nRT with the exclusion of the VB is not currently possible due to the size and shape of the former nucleus and its spatial relationship with the latter. Due to this limitation, the effect of TTA-P2 on the nRT had to be calculated primarily by differential comparison with the effect on the VB. This involved dialysis of a larger concentration (1mM) from the same position in the central VB, as its effective spread was calculated to include the majority of both structures at the 1 hour mark. However, this strategy could not rule out the possibility that any effect observed was due to either a) reaching the *entire* VB, assuming 300µM fell short of this, or b) the combined effect of VB and nRT block, where neither alone would be sufficient.

To mitigate these possibilities, a further strategy of nRT administration was attempted. The microdialysis probes were re-positioned in a manner designed to combine maximum proximity to the bulk of the nRT, spread to the entire nRT, and restriction from as much of the VB as possible. The latter two aims are mutually exclusive given that the nRT extends in part around 3 sides of the VB. The compromise position and concentration (300 µM) sacrificed a block of the most medial extremities of the nRT in order to avoid spreading throughout the entire VB. These results excluded possibility a) above, that blocking T-type Ca^{2+} channels of the entire VB was responsible from the block at 1mM. This, together with the considerably higher output of the nRT than the VB observed in Chapter 3, and in particular its greater prevalence of LTCP-dependent bursts, suggests that the nRT block mediated the majority or all of the observed effect on seizures.

4.4.3 Implications for TC neurone contribution to AS

The finding that T-type Ca^{2+} channel-dependent activity of TC neurones of the VB is not required for expression of absence seizures is compatible with their electrical behaviour as detailed in Chapter 3 and with existing anaesthetised *in vivo* results, both suggesting that definitively T-channel-dependent activity (i.e. high frequency bursts) is rare in TC neurones

during seizure (Steriade and Contreras, 1995; Pinault et al., 1998; Charpier et al., 1999; Pinault, 2003). It is less, however, compatible with the *in vitro* hypothesis of SWDs that involves high frequency bursting of TC neurones at each SWC (von Krosigk et al., 1993; Bal et al., 1995a). In order to reconcile these two results one would have to posit that TC neurones burst regularly during ASs, but that this bursting is not at all necessary for the perpetuation of the seizure.

The major findings of these experiments also suggests that the observed ability of α1G T-type Ca^{2+} channel upregulation to induce ASs (Ernst et al., 2009), and of α1G knockout to suppress pharmacologically induced ASs (Kim et al., 2001), is not attributable to T-type Ca^{2+} channel-dependent activity of TC neurones. These observations may alternatively be explained by the actions of cortical α1G channels, by developmental mechanisms that compensate for the genetic deficit, or (in the case of the knockout) by differences in T-channel-dependent thalamic activity between the GAERS and the GHB models of AS (Song et al., 2004).

It may be relevant that repeated measures ANOVA with Bonferroni post-hoc tests did not suggest a TTA-P2-induced change in average seizure duration in any of the groups studied, and paired t-tests suggested such a change for the combined VB and nRT group only. This indicates that inhibition of T-type Ca^{2+} channels in the nRT is more likely to prevent seizures from being initiated than curtail the perpetuation of a seizure. This may mean that T-type Ca^{2+}-dependent activity in nRT neurones is necessary to start but not to perpetuate a seizure, or else that a larger proportion of nRT neurones must express such activity for initiation than for continuation.

Only the combined VB and nRT block appeared to attenuate ASs that were already in process (even this result was not conclusive, as it was detectable only when mean seizure duration was considered as a proportion of pre-drug control). This suggests a number of possibilities. Either the extra volume affected in the VB (relative to the 300 µM VB group) mediated this attenuation, or the combined VB and nRT block, or the (smaller) medial areas of the nRT unaffected by the 300 µM nRT group, or some combination of these three. All of these possibilities imply that some availability of T-type Ca^{2+} channels throughout the entirety of the VB is necessary for an AS to continue, and that a block of a sufficient proportion of channels increases the probability for a seizure to end after a given SWC.

Finally, it is noteworthy that none of the locations and concentrations of TTA-P2 employed changed the power of SWDs at 6-8Hz in a detectable fashion. The lack of change during thalamic administration, given the previously noted ability of similarly spatially restricted

thalamic intervention to alter seizure properties (Richards et al., 2003) might suggest that SWD frequency is determined primarily by the cortex rather than the thalamus. This is plausible, particularly in GAERS, given the relative timing of cortical and thalamic discharges, the observation of EPSPs of presumed cortical origin immediately prior to AP firing of both TC and nRT neurones in SWDs of fentantyl-anaesthetised GAERS (Pinault et al., 1998; Charpier et al., 1999; Slaght et al., 2002; Pinault, 2003), and the low density of TC output as shown in Chapter 3.

In summary, the results of this chapter provide convincing evidence that T-type Ca^{2+} channel activity of TC neurones of the VB is not necessary for the expression of ASs in GAERS, while that of nRT neurones is. In terms of neuronal output, these channels are most commonly associated with LTCP-mediated burst firing and their block can be assumed to prevent any expression of such bursts (David et al., 2013). However, T-type Ca^{2+} channel activation can also facilitate non-LTCP-mediated firing via the tonically depolarising effect of $I_{TWindow}$ on membrane potential (Deleuze et al., 2012). Given that $I_{TWindow}$ requires a greater degree of channel availability than do LTCPs (Dreyfus et al., 2010), administration of TTA-P2 will also have decreased the probability of all AP firing. No conclusions can be drawn from this, however, until the actual contribution of T-type Ca^{2+} channels to the tonic firing of thalamic neurones in different behavioural states including ASs (i.e. such firing as observed in Chapter 3) is measured.

Although these data do not preclude the possibility of T-type Ca^{2+} channels being necessary in other thalamocortical nuclei, the VB contains a significant proportion of primary TC neurones (Groenewegen and Witter, 2004) and is reciprocally connected with the somatosensory cortex, known to be the initiation site of ASs in both GAERS and WAG/Rij (Meeren et al., 2002; Gurbanova et al., 2006; Polack et al., 2007). As such, it is a worthy subject of investigation in its own right.

When the results of this chapter are considered together with those of Chapter 3, it can be stated that the rare high-frequency bursts observed in VB neurones of GAERS during ASs are not necessary for the initiation or for the propagation of these seizures. Some T-type Ca^{2+} channel-mediated activity of the nRT is necessary for AS initiation, but whether this activity is limited to the high-frequency bursts that are often observed in a subset of nRT neurones or also includes other nRT output cannot yet be determined.

Chapter 5 – General discussion

5.1 Major findings

The data presented and described in Chapters 3 and 4 of this thesis significantly expand our current understanding of the activity of thalamic neurones during AS and the significance of this activity to seizure initiation and perpetuation. They represent the first selective manipulation of TC T-type Ca^{2+} channels, and the first recording of isolated thalamic unit activity from a freely moving model of ASs. In Chapter 3 the observation of a mix of silence and SWC phase-locked single spikes with a very low incidence of burst firing in TC neurones, and of regular SWC phase-locked burst firing in some nRT neurones, is a major step towards resolving the controversy between *in vitro* and *in vivo* hypotheses of thalamic activity in ASs. Chapter 4 describes the lack of effect on GAERS AS of a block of T-type Ca^{2+} channels throughout the somatosensory thalamus, by contrast with the suppression of ASs achieved by reticular thalamic T-type Ca^{2+} channel antagonism.

Another important finding of this thesis involves the temporal relationship between thalamic activity and SWD features of GAERS ASs investigated in Chapter 3. The results confirm and refine the nature of the relationship previously observed in other experimental ASs and SWDs. Both TC and nRT neuronal firing peaked in close temporal proximity (<10 ms latency) to the maximum negativity of SWCs, and while both displayed clear and considerable unimodal phase preference, synchrony was not absolute. These firing distributions suggest that TC and nRT neurones tend to be excited by a common, phasic input during GAERS ASs just as during anaesthetised SWDs.

Although the conclusions of Chapter 3 as they relate to nRT neurones are limited, the massive variation in degree, nature, and synchrony of activity of those neurones during ASs is another significant finding of this thesis. In contrast to the homogeneity of the recorded TC neurones, nRT cells could frequently express one or more of the following during seizure: single spikes, high frequency bursts, and silence. Further, multiple nRT neurones expressed firing apparently temporally unrelated to EEG features during AS.

5.2 Thalamic neuronal output during absence seizures

The spiking activity of VB neurones observed during AS is consistent with that suggested by the *in vivo* hypothesis presented in section 1.4.2: predominant thalamic silence, occasional spikes and rare bursts. This activity was observed during SWDs in ketamine/xylazine and

urethane anaesthetised cats (Steriade and Contreras, 1995) as well as GAERS and Long-Evans under fentanyl/haloperidol anaesthesia (Pinault et al., 1998; Charpier et al., 1999; Polack and Charpier, 2006). The fact that individual VB neurones tend not to fire during about 50% of SWCs suggests that these neurones are unlikely candidates as initiators of seizure. The majority of conclusions to be drawn from this result, however, require its contextualisation with extant knowledge regarding intracellular activity and spike timing throughout the TC network.

It has been suggested by *in vivo* anaesthetised cortical and thalamic recordings that TC neurones receive repeating rhythmic EPSP and $GABA_A$ IPSP sequences during seizure, superimposed on a tonic hyperpolarisation. The timing of these synaptic potentials confines any output that does occur to a period centred approx. 10 ms prior to the peak negativity of an SWC. This output is sometimes generated by an LTCP and sometimes arises directly as a result of synaptically generated depolarising potentials. The IPSPs, and possibly the tonic hyperpolarisation, can be attributed to nRT inhibition on a scale higher than that seen in other behavioural states. The EPSPs, particularly those that occur immediately before the period of potential output, can be attributed to corticothalamic excitation (Steriade and Contreras, 1995; Pinault et al., 1998; Charpier et al., 1999; Pinault, 2003).

The level of VB activity recorded in Chapter 3 is entirely consistent with this hypothesis, the occasional single spikes and rarer multi-spike events representing instances when incoming EPSPs (and possibly an intrinsic LTCP) were sufficient to overcome the phasic and tonic hyperpolarisations to reach AP threshold. Recorded nRT activity could also be explained within this framework, allowing for considerable variation in either the patterns of cortical and TC excitation and intra-nRT inhibition received by nRT neurones or variation in the intrinsic properties of these neurones. This work requires significant expansion before it can be ascertained whether the proportions of each firing type recorded here is representative of a true division in the nRT between neurones that burst frequently, those that fire tonically, and those that remain predominantly silent.

The timings of VB and nRT activity observed here also supports this hypothesis, both being centred less than 10 ms prior to the peak negativity of the SWC. Estimations of corticothalamic projection neurone spike timing obtained from fentanyl SWDs suggest a peak approx. 20 ms prior to the SWC negativity (Pinault, 2003; Polack et al., 2007). This is compatible with cortical excitation of both TC and nRT neurones. The observed peak in VB bursts during the first 200 ms of ASs would also be entirely consistent with this idea, suggesting that monosynaptic

cortico-TC excitation initially outweighs disynaptic cortico-nRT-TC inhibition but that the emerging tonic hyperpolarisation quickly reduces the probability of a TC neurone evoking an LTCP and associated high-frequency burst. The leading role of hyper-excitable layer V/VI neurones of the somatosensory cortex in SWDs again supports this hypothesis (Polack et al., 2007, 2009).

An acceptance of this hypothesis of TC network activity during ASs suggests a causal role for the cortex in seizure initiation and propagation. This is also supported by the results of the microdialysis experiments in Chapter 4. The ability of GAERS to express ASs as normal when T-type Ca^{2+} channels were largely blocked throughout the VB confirms that the cortex did not require excitement by VB bursts in order to start or to maintain a seizure. Although the results of Chapter 3 clearly show that the VB as a whole does provide synchronous output to the cortex at each cycle, the lack of an effect of VB T-channel block also raises the distinct possibility that this output is not actually necessary for AS expression. This is because the block of $I_{Twindow}$, and the resulting membrane hyperpolarisation, would lower the probability of reaching an AP activation threshold independently of LTCPs. Although the actual activity of each population during T-channel inhibition remains to be determined, it is inarguable that it will involve considerably decreased firing probability.

The lower frequency of seizure initiation when nRT T-type Ca^{2+} channels were blocked, on the other hand, suggests that in the absence of output from this population the TC network is less able to enter a pathological oscillatory state. The mixed activity observed in nRT neurones may partially explain the failure of nRT T-channel inhibition to completely abolish ASs or, indeed, to have any effect on individual seizure duration. High levels of seizure-associated tonic activity suggests that the nRT can maintain a high output, and hence a strong inhibition of TC, without the involvement of LTCPs. Again, building concrete hypotheses regarding the nRT is premature due to the low number of neurones from this nucleus recorded.

5.3 The role of thalamic I_T in absence seizures

The experiments detailed in Chapter 4 also have consequences for hypotheses of thalamic T-type Ca^{2+} channel alterations having a causal role in the development of an AS phenotype. It is still a possibility that an increase in T-channels in TC neurones is capable of directly causing and/or facilitating ASs (Zhang et al., 2002; Song et al., 2004; Ernst et al., 2009), and that a complete abolition of it suppresses the possibility of inducing AS. However, these results suggest that TC neurone T-channel-mediated activity is not a necessary part of AS initiation or

maintenance in all models. Further, when these results are considered together with the limitations of the genetic manipulation studies listed above in terms of region specificity, potential indirect causation, and relative strength of the models used, they also suggest that TC neurone T-type Ca^{2+} channels are an unlikely candidate as a common root cause of experimental and clinical AS.

5.4 Suggested future work

5.4.1 Consolidation of nRT activity during ASs

The first priority following from the results of this thesis is to increase the number of nRT neurones recorded during ASs and other behavioural states. As mentioned previously, the true relative prevalence of each type of activity observed cannot currently be estimated due to the possibility that particular nRT regions may have been unevenly sampled. Mapping of the position of each nRT neurone recorded may also reveal whether the heterogeneity of output is due to distinct populations, perhaps with connectivity to distinct dorsal thalamic nuclei, or that these diverse neurones are spread throughout the nucleus. In the process of this consolidation greater consistency in EEG electrode position can also be achieved, permitting confirmation of the TC and nRT synchrony observed so far.

5.4.2 Cortical activity during ASs

Another priority involves recording of cortical neurones of all layers and in multiple regions using the same techniques employed in Chapter 3. Comparisons can again be made with existing studies of cortical AS pathophysiological mechanisms (Kandel and Buzsáki, 1997; Charpier et al., 1999), and the aim will be to observe the activity and synchrony of intra-cortical excitatory and inhibitory neurones as well as of CT projection neurones. This will allow the comparison of TC and nRT spike times with those of CT neurones of different areas, testing the hypothesis of cortico-thalamic excitation in the freely moving GAERS.

5.4.3 Activity of other thalamic nuclei during ASs

This project investigated neurones of the VB due to its status as the largest first order thalamic nucleus, the simplicity of the neuronal composition of the rat VB, and not least the precedent for investigations of AS pathophysiological in the somatosensory system (including the initiation site's location in facial somatosensory cortex). However, the contribution of other thalamic nuclei, both first- and higher-order, may be of relevance. In particular the more

diffuse pattern of cortical innervation of higher-order nuclei (Jones, 2002) suggests a potential role in propagation of seizures to new cortical regions.

There may also be wider value in studying the relative timing of different reciprocally connected cortical and thalamic populations during ASs. The relatively homogeneous nature of AS activity (in TC and CT neurones, at least according to current information) may enable the acquisition of useful insights into the spread of signals within subnetworks of shared modality and throughout the TC network as a whole.

5.4.4 Genetically targeted manipulation of TC network populations during ASs

In order to investigate the precise functional contribution of an activity in a particular neuronal population during ASs it would be necessary to selectively alter or remove that activity only. Opto- and/or pharmacogenetic techniques would have advantages in this endeavour over the local reverse microdialysis used in this thesis due to their potential specificity to particular cell types (allowing, for example, selective modulation of the irregularly-shaped nRT) and the potential variety of modulation offered by the former (relative to channel-specific pharmacological agents). Either technique would have to be paired with isolated unit recordings in order to monitor effects on cellular activity, and could reveal what forms of TC, nRT and cortical firing are compatible with normal AS expression and what forms of firing affect seizure initiation, propagation, or quality.

5.4.5 Precise role of thalamic I_T in ASs

A secondary continuation of this project might involve a more in-depth investigation of thalamic T-type Ca^{2+} channels in GAERS ASs. Although used primarily as a tool to manipulate neuronal activity and output for the purpose of this thesis, investigating the role of the T-type Ca^{2+} channel in its own right, as implicated in genetic studies, is a worthy objective. This would involve measurement of VB and nRT activity during an AS while VB and/or nRT T-channels are inhibited by TTA-P2 microdialysis, to see whether this inhibition prevents the expression of bursts or of all spikes and whether it affects the synchrony of any remaining output. Such an experiment would also reveal what both types of thalamic neurones are doing while seizures are altered (or unaltered) as seen in Chapter 4. A potential variation would involve measurement of activity while T-channels are inhibited in the region of the recorded cells only, to see how a neurone without that current behaves during an otherwise normal AS.

5.4.6 Composition of cellular activity during ASs

Investigating the contribution of other intrinsic and synaptic currents to TC and nRT activity could be achieved in multiple consecutive steps. First, intracellular thalamic and cortical recordings in head-restrained GAERS would enable the comparison of AS-related membrane potential events in un-anaesthetised GAERS vs. GAERS under the influence of fentanyl/haloperidol. Second, application of potential antagonists of those intrinsic and synaptic currents (e.g. I_h) implicated by intracellular recordings could be applied in a highly localised fashion to confirm the channels and/or ions involved. Finally, simultaneous microdialysis and isolated unit recordings could be used to investigate the global role of those currents observed in TC and nRT neurones, in a similar fashion to that recommended for TTA-P2 and T-type Ca^{2+} channel-mediated currents.

References

Aizawa M, Ito Y, Fukuda H (1997a) Pharmacological profiles of generalized absence seizures in lethargic, stargazer and gamma-hydroxybutyrate-treated model mice. Neurosci Res 29:17–25

Aizawa M, Ito Y, Fukuda H (1997b) Roles of gamma-aminobutyric acidB (GABA B) and gamma-hydroxybutyric acid receptors in hippocampal long-term potentiation and pathogenesis of absence seizures. Biol Pharm Bull 20:1066–1070

Akman O, Demiralp T, Ates N, Onat FY (2010) Electroencephalographic differences between WAG/Rij and GAERS rat models of absence epilepsy. Epilepsy Res 89:185–193

Amaral D (2000) The Functional Organisation of Perception and Movement. In: Principles of Neural Science, 4th ed. (Kandel E, Schwartz J, Jessell T, eds). McGraw-Hill.

Andersen P, Eccles JC, Sears TA (1964) The ventro-basal complex of the thalamus: types of cells, their responses and their functional organisation. J Physiol 174:370–399

Avoli M (1980) Electroencephalographic and pathophysiologic features of rat parenteral penicillin epilepsy. Exp Neurol 69:373–382

Avoli M (1995) Feline generalized penicillin epilepsy. Ital J Neurol Sci 16:79–82

Avoli M, Gloor P (1982) Interaction of cortex and thalamus in spike and wave discharges of feline generalized penicillin epilepsy. Exp Neurol 76:196–217

Avoli M, Gloor P, Kostopoulos GK, Gotman J (1983) An analysis of penicillin-induced generalized spike and wave discharges using simultaneous recordings of cortical and thalamic single neurons. J Neurophysiol 50:819–837

Avoli M, Kostopoulos G (1982) Participation of corticothalamic cells in penicillin-induced generalized spike and wave discharges. Brain Res 247:159–163

Avoli M, Siatitsas I, Kostopoulos G, Gloor P (1981) Effects of post-ictal depression on experimental spike and wave discharges. Electroencephalogr Clin Neurophysiol 52:372–374

Bai X, Vestal M, Berman R, Negishi M, Spann M, Vega C, DeSalvo MN, Novotny EJ, Constable RT, Blumenfeld H (2010) Dynamic time course of typical childhood absence seizures: EEG, behavior, and functional magnetic resonance imaging. J Neurosci 30:5884–5893

Bal T, McCormick DA (1993) Mechanisms of oscillatory activity in guinea-pig nucleus reticularis thalami in vitro: a mammalian pacemaker. J Physiol 468:669–691

Bal T, von Krosigk M, McCormick DA (1995a) Synaptic and membrane mechanisms underlying synchronized oscillations in the ferret lateral geniculate nucleus in vitro. J Physiol 483 (Pt 3:641–663

Bal T, von Krosigk M, McCormick DA (1995b) Role of the ferret perigeniculate nucleus in the generation of synchronized oscillations in vitro. J Physiol 483 (Pt 3:665–685

Baldy-Moulinier M (1992) Sleep architecture and childhood absence epilepsy. Epilepsy Res Suppl 6:195–198

Banerjee P, Hirsch E, Snead OC (1993) gamma-Hydroxybutyric acid induced spike and wave discharges in rats: relation to high-affinity [3H]gamma-hydroxybutyric acid binding sites in the thalamus and cortex. Neuroscience 56:11–21

Banerjee P, Snead OC (1995) Presynaptic Gamma-hydroxybutyric Acid (GHB) and Gamma-aminobutyric AcidB (GABAB) release of GABA and glutamate (GLU) in rat thalamic ventrobasal nucleus (VB): a possible mechanism for the generation of absence-like seizures induced by GHB. J Pharmacol Exp Ther

Banerjee P, Snead OC, Iii S (1994) Thalamic mediodorsal and intralaminar nuclear lesions disrupt the generation of experimentally induced generalized absence-like seizures in rats. Epilepsy Res 17:193–205

Bearden LJ, Snead OC, Healey CT, Pegram G V (1980) Antagonism of gamma-hydroxybutyric acid-induced frequency shifts in the cortical EEG of rats by dipropylacetate. Electroencephalogr Clin Neurophysiol 49:181–183

Beenhakker MP, Huguenard JR (2009) Neurons that fire together also conspire together: is normal sleep circuitry hijacked to generate epilepsy? Neuron 62:612–632

Belelli D, Peden DR, Rosahl TW, Wafford K a, Lambert JJ (2005) Extrasynaptic GABAA receptors of thalamocortical neurons: a molecular target for hypnotics. J Neurosci 25:11513–11520

Berg AT, Berkovic SF, Brodie MJ, Buchhalter J, Cross JH, van Emde Boas W, Engel J, French J, Glauser TA, Mathern GW, Moshé SL, Nordli D, Plouin P, Scheffer IE (2010) Revised terminology and concepts for organization of seizures and epilepsies: report of the ILAE Commission on Classification and Terminology, 2005-2009. Epilepsia 51:676–685

Berkovic SF (1997) Genetics of epilepsy syndromes. In: Epilepsy: a Comprehensive Textbook (Engel J, Pedley TA, eds), pp 217–224. Philadelphia: Lippincott-Raven.

Berkovic SF, Howell RA, Hay DA, Hopper JL (1998) Epilepsies in twins: genetics of the major epilepsy syndromes. Ann Neurol 43:435–445

Berman R, Negishi M, Vestal M, Spann M, Chung MH, Bai X, Purcaro M, Motelow JE, Danielson N, Dix-Cooper L, Enev M, Novotny EJ, Constable RT, Blumenfeld H (2010) Simultaneous EEG, fMRI, and behavior in typical childhood absence seizures. Epilepsia 51:2011–2022

Bertaso F, Zhang C, Scheschonka A, de Bock F, Fontanaud P, Marin P, Huganir RL, Betz H, Bockaert J, Fagni L, Lerner-Natoli M (2008) PICK1 uncoupling from mGluR7a causes absence-like seizures. Nat Neurosci 11:940–948

Bessaïh T, Bourgeais L, Badiu CI, Carter D a, Toth TI, Ruano D, Lambolez B, Crunelli V, Leresche N (2006) Nucleus-specific abnormalities of GABAergic synaptic transmission in a genetic model of absence seizures. J Neurophysiol 96:3074–3081

Bessman SP, Fishbein WN (1963) Gamma-Hydroxybutyrate, a Normal Brain Metabolite. Nature 200:1207–1208

Betting LE, Mory SB, Lopes-Cendes I, Li LM, Guerreiro MM, Guerreiro CAM, Cendes F (2006) MRI volumetry shows increased anterior thalamic volumes in patients with absence seizures. Epilepsy Behav 8:575–580

Beyer B, Deleuze C, Letts V a, Mahaffey CL, Boumil RM, Lew T a, Huguenard JR, Frankel WN (2008) Absence seizures in C3H/HeJ and knockout mice caused by mutation of the AMPA receptor subunit Gria4. Hum Mol Genet 17:1738–1749

Biagini G, D'Antuono M, Tancredi V, Motalli R, Louvel J, D'Arcangelo G, Pumain R, Warren RA, Avoli M (2001) Thalamocortical connectivity in a rat brain slice preparation: participation of the ventrobasal complex to synchronous activities. Thalamus Relat Syst 1:169–179

Bianchi A, Italian LAE Collaborative Group (1995) Study of concordance of symptoms in families with absence epilepsies. In: Typical Absences and Related Epileptic Syndromes (Duncan JS, Panayiotopoulos CP, eds), pp 328–337. London: Churchill Livingstone.

Blethyn KL, Hughes SW, Tóth TI, Cope DW, Crunelli V (2006) Neuronal basis of the slow (<1 Hz) oscillation in neurons of the nucleus reticularis thalami in vitro. J Neurosci 26:2474–2486

Blume W, Lüders HO, Mizrahi E, Tassinari C, van Emde Boas W, Engel J (2001) Glossary of descriptive terminology for ictal semiology: report of the ILAE task force on classification and terminology. Epilepsia 42:1212–1218

Blumenfeld H (2002) The thalamus and seizures. Arch Neurol 59:135–137

Blumenfeld H (2005) Consciousness and epilepsy: why are patients with absence seizures absent? Prog Brain Res 150:271–286

Blumenfeld H, McCormick DA (2000) Corticothalamic inputs control the pattern of activity generated in thalamocortical networks. J Neurosci 20:5153–5162

Boehme R, Uebele VN, Renger JJ, Pedroarena C (2011) Rebound excitation triggered by synaptic inhibition in cerebellar nuclear neurons is suppressed by selective T-type calcium channel block. J Neurophysiol 106:2653–2661

Boehnke SE, Rasmusson DD (2001) Time course and effective spread of lidocaine and tetrodotoxin delivered via microdialysis: an electrophysiological study in cerebral cortex. J Neurosci Methods 105:133–141

Bouma PA, Westendorp RG, van Dijk JG, Peters AC, Brouwer OF (1996) The outcome of absence epilepsy: a meta-analysis. Neurology 47:802–808

Browne TR, Penry JK, Proter RJ, Dreifuss FE (1974) Responsiveness before, during, and after spike-wave paroxysms. Neurology 24:659–665

Budde T, Mager R, Pape H-C (1992) Different Types of Potassium Outward Current in Relay Neurons Acutely Isolated from the Rat Lateral Geniculate Nucleus. Eur J Neurosci 4:708–722

Bungay PM, Morrison PF, Dedrick RL (1990) Steady-state theory for quantitative microdialysis of solutes and water in vivo and in vitro. Life Sci 46:105–119

Burgess DL, Jones JM, Meisler MH, Noebels JL (1997) Mutation of the Ca2+ channel beta subunit gene Cchb4 is associated with ataxia and seizures in the lethargic (lh) mouse. Cell 88:385–392

Buzsáki G, Anastassiou CA, Koch C (2012) The origin of extracellular fields and currents--EEG, ECoG, LFP and spikes. Nat Rev Neurosci 13:407-420

Buzsáki G, Smith A, Berger S, Fisher LJ, Gage FH (1990) Petit mal epilepsy and parkinsonian tremor: hypothesis of a common pacemaker. Neuroscience 36:1–14

Cain SM, Snutch TP (2010) Contributions of T-type calcium channel isoforms to neuronal firing. Channels (Austin) 4:475–482

Callenbach PMC, Bouma PAD, Geerts AT, Arts WFM, Stroink H, Peeters EAJ, van Donselaar C a, Peters a CB, Brouwer OF (2009) Long-term outcome of childhood absence epilepsy: Dutch Study of Epilepsy in Childhood. Epilepsy Res 83:249–256

Carbone E, Lux H (1984) A low voltage-activated, fully inactivating Ca channel in vertebrate sensory neurones. Nature 310:501–502

Catterall W a (2011) Voltage-gated calcium channels. Cold Spring Harb Perspect Biol 3:a003947

Cechetto DF, Saper CB (1987) Evidence for a viscerotopic sensory representation in the cortex and thalamus in the rat. J Comp Neurol 262:27–45

Celeux G, Govaert G (1992) A classification EM algorithm for clustering and two stochastic versions. Comput Stat Data Anal 14:315–332

Charpier S, Leresche N, Deniau J-M, Mahon S, Hughes SW, Crunelli V (1999) On the putative contribution of GABA(B) receptors to the electrical events occurring during spontaneous spike and wave discharges. Neuropharmacology 38:1699–1706

Chen Y, Lu J, Pan H, Zhang Y, Wu H, Xu K, Liu X, Jiang Y, Bao X, Yao Z, Ding K, Lo WHY, Qiang B, Chan P, Shen Y, Wu X (2003a) Association between genetic variation of CACNA1H and childhood absence epilepsy. Ann Neurol 54:239–243

Chen Y, Lu J, Zhang Y, Pan H, Wu H, Xu K, Liu X, Jiang Y, Bao X, Zhou J, Liu W, Shi G, Shen Y, Wu X (2003b) T-type calcium channel gene alpha (1G) is not associated with childhood absence epilepsy in the Chinese Han population. Neurosci Lett 341:29–32

Cheong E, Zheng Y, Lee K, Lee J, Kim S, Sanati M, Lee S, Kim Y-S, Shin H-S (2009) Deletion of phospholipase C beta4 in thalamocortical relay nucleus leads to absence seizures. Proc Natl Acad Sci U S A 106:21912–21917

Chioza B et al. (2006) Evaluation of CACNA1H in European patients with childhood absence epilepsy. Epilepsy Res 69:177–181

Chipaux M, Vercueil L, Kaminska A, Mahon S, Charpier S (2013) Persistence of Cortical Sensory Processing during Absence Seizures in Human and an Animal Model: Evidence from EEG and Intracellular Recordings. PLoS One 8:e58180

Chocholová L (1983) Incidence and development of rhythmic episodic activity in the electroencephalogram of a large rat population under chronic conditions. Physiol Bohemoslov 32:10–18

Coenen AM, Blezer EH, van Luijtelaar EL (1995) Effects of the GABA-uptake inhibitor tiagabine on electroencephalogram, spike-wave discharges and behaviour of rats. Epilepsy Res 21:89–94

Coenen AM, Van Luijtelaar EL (1987) The WAG/Rij rat model for absence epilepsy: age and sex factors. Epilepsy Res 1:297–301

Constantinople CM, Bruno RM (2011) Effects and mechanisms of wakefulness on local cortical networks. Neuron 69:1061–1068

Constantinople CM, Bruno RM (2013) Deep Cortical Layers Are Activated Directly by Thalamus. Science (80-) 340:1591–1594

Cope DW, Di Giovanni G, Fyson SJ, Orbán G, Errington AC, Lorincz ML, Gould TM, Carter D a, Crunelli V (2009) Enhanced tonic GABAA inhibition in typical absence epilepsy. Nat Med 15:1392–1398

Cope DW, Hughes SW, Crunelli V (2005) GABAA receptor-mediated tonic inhibition in thalamic neurons. J Neurosci 25:11553–11563

Cortez M a, Snead OC (2006) Pharmacologic Models of Generalized Absence Seizures in Rodents. In: Models of Seizure and Epilepsy (Pitkanen A, Schwartzkroin PA, Moshe S, eds), pp 111–126. Elsevier Academic Press.

Coulter D, Huguenard JR, Prince D a (1989a) Characterization of ethosuximide reduction of low-threshold calcium current in thalamic neurons. Ann Neurol 25:582–593

Coulter D, Huguenard JR, Prince D a (1989b) Specific petit mal anticonvulsants reduce calcium currents in thalamic neurons. Neurosci Lett 98:74–78

Coulter D, Huguenard JR, Prince D a (1990) Differential effects of petit mal anticonvulsants and convulsants on thalamic neurones: GABA current blockade. Br J Pharmacol 100:807–813

Coulter D, Huguenard JR, Prince DA (1989c) Calcium currents in rat thalamocortical relay neurones: kinetic properties of the transient, low-threshold current. J Physiol:587–604

Cox CL, Sherman SM (1999) Glutamate inhibits thalamic reticular neurons. J Neurosci 19:6694–6699 Available at: http://www.ncbi.nlm.nih.gov/pubmed/10414998 [Accessed January 23, 2014].

Crabtree JW, Collingridge GL, Isaac JT (1998) A new intrathalamic pathway linking modality-related nuclei in the dorsal thalamus. Nat Neurosci 1:389–394

Craig PJ, Beattie RE, Folly E a, Banerjee MD, Reeves MB, Priestley J V, Carney SL, Sher E, Perez-Reyes E, Volsen SG (1999) Distribution of the voltage-dependent calcium channel alpha1G subunit mRNA and protein throughout the mature rat brain. Eur J Neurosci 11:2949–2964

Craiu D, Magureanu S, van Emde Boas W (2006) Are absences truly generalized seizures or partial seizures originating from or predominantly involving the pre-motor areas? Some clinical and theoretical observations and their implications for seizure classification. Epilepsy Res 70 Suppl 1:S141–55

Crandall SR, Govindaiah G, Cox CL (2010) Low-threshold Ca2+ current amplifies distal dendritic signaling in thalamic reticular neurons. J Neurosci 30:15419–15429

Crunelli V, Hughes SW (2010) The slow (<1 Hz) rhythm of non-REM sleep: a dialogue between three cardinal oscillators. Nat Neurosci 13:9–17

Crunelli V, Leresche N (1991) A role for GABAB receptors in excitation and inhibition of thalamocortical cells. Trends Neurosci 14:16–21

Crunelli V, Leresche N (2002a) Childhood absence epilepsy: genes, channels, neurons and networks. Nat Rev Neurosci 3:371–382

Crunelli V, Leresche N (2002b) Block of Thalamic T-Type Ca2+ Channels by Ethosuximide Is Not the Whole Story. Epilepsy Curr 2:53–56

Crunelli V, Lightowler S, Pollard CE (1989) A T-type Ca2+ current underlies low-threshold Ca2+ potentials in cells of the cat and rat lateral geniculate nucleus. J Physiol:543–561

Crunelli V, Lörincz ML, Errington AC, Hughes SW (2012) Activity of cortical and thalamic neurons during the slow (<1 Hz) rhythm in the mouse in vivo. Pflugers Arch 463:73–88

Crunelli V, Tóth TI, Cope DW, Blethyn KL, Hughes SW (2005) The "window" T-type calcium current in brain dynamics of different behavioural states. J Physiol 562:121–129

Danober L, Deransart C, Depaulis A, Vergnes M, Marescaux C (1998) Pathophysiological mechanisms of genetic absence epilepsy in the rat. Prog Neurobiol 55:27–57

David F, Schmiedt JT, Taylor HL, Orban G, Di Giovanni G, Uebele VN, Renger JJ, Lambert RC, Leresche N, Crunelli V (2013) Essential thalamic contribution to slow waves of natural sleep. J Neurosci 33:19599–19610

Davson H, Welch K, Segal M (1987) Physiology and Pathophysiology of the Cerebrospinal Fluid. Churchill Livingstone.

De la Peña E, Geijo-Barrientos E (1996) Laminar localization, morphology, and physiological properties of pyramidal neurons that have the low-threshold calcium current in the guinea-pig medial frontal cortex. J Neurosci 16:5301–5311

Deleuze C, David F, Béhuret S, Sadoc G, Shin H-S, Uebele VN, Renger JJ, Lambert RC, Leresche N, Bal T (2012) T-type calcium channels consolidate tonic action potential output of thalamic neurons to neocortex. J Neurosci 32:12228–12236

DeLorey TM, Handforth A, Anagnostaras SG, Homanics GE, Minassian BA, Asatourian A, Fanselow MS, Ellison GD, Olsen RW, Delgado-Escueta A (1998) Mice lacking the beta3 subunit of the GABAA receptor have the epilepsy phenotype and many of the behavioral characteristics of Angelman syndrome. J Neurosci 18:8505–8514

Depaulis A, Snead OC, Marescaux C, Vergnes M (1989) Suppressive effects of intranigral injection of muscimol in three models of generalized non-convulsive epilepsy induced by chemical agents. Brain Res 498:64–72

Depaulis A, van Luijtelaar G (2006a) Genetic Models of Absence Epilepsy in the Rat. In: Models of Seizure and Epilepsy (Pitkanen A, Schwartzkroin PA, Moshé SL, eds), pp 233–248. International: Elsevier Academic Press.

Depaulis A, van Luijtelaar G (2006b) Characteristics of Genetic Absence Seizures in the Rat. In: Models of Seizure and Epilepsy, 1st ed. (Pitkanen A, Schwartzkroin PA, Moshe S, eds), pp 233–248. International: Elsevier Academic Press.

Deschênes M, Paradis M, Roy JP, Steriade M (1984) Electrophysiology of neurons of lateral thalamic nuclei in cat: resting properties and burst discharges. J Neurophysiol 51:1196–1219

Deschênes M, Veinante P, Zhang ZW (1998) The organization of corticothalamic projections: reciprocity versus parity. Brain Res Brain Res Rev 28:286–308

Desguerre I, Chiron C, Loiseau J, Dartigues JF, Dulac O, Loiseau P (1994) Epidemiology of idiopathic generalized epilepsies. In: Idiopathic Generalized Epilepsies: Clinical, Experimental and Genetic Aspects (Malafosse A, Genton P, Hirsch E, Marescaux C, Broglin D, Bernasconi R, eds), pp 19–26. London: John Libbey.

Desîlets-Roy B, Varga C, Lavallée P, Deschênes M (2002) Substrate for cross-talk inhibition between thalamic barreloids. J Neurosci 22:RC218

Destexhe A (1998) Spike-and-wave oscillations based on the properties of GABAB receptors. J Neurosci 18:9099–9111

Destexhe A, Sejnowski J, Huguenard JR, Contreras D, Steriade M, Sejnowski TJ (1996) In vivo, in vitro, and computational analysis of dendritic calcium currents in thalamic reticular neurons. J Neurosci 16:169–185

Dezsi G, Ozturk E, Stanic D, Powell KL, Blumenfeld H, O'Brien TJ, Jones NC (2013) Ethosuximide reduces epileptogenesis and behavioral comorbidity in the GAERS model of genetic generalized epilepsy. Epilepsia

Domich L, Oakson G, Steriade M (1986) Thalamic burst patterns in the naturally sleeping cat: a comparison between cortically projecting and reticularis neurones. J Physiol 379:429–449

Doyle J, Ren X, Lennon G, Stubbs L (1997) Mutations in the Cacnl1a4 calcium channel gene are associated with seizures, cerebellar degeneration, and ataxia in tottering and leaner mutant mice. Mamm Genome 8:113–120

Dreifuss F (1990) The syndromes of generalized epilepsy. In: Generalized Epilepsy Neurobiological Approaches (Avoli M, Gloor P, Kostopoulos GK, Naquet R, eds). Boston: Birkhauser.

Dreyfus F, Tscherter A, Errington AC, Renger JJ, Shin H-S, Uebele VN, Crunelli V, Lambert RC, Leresche N (2010) Selective T-type calcium channel block in thalamic neurons reveals channel redundancy and physiological impact of ITwindow. J Neurosci 30:99–109

Drinkenburg WH, van Luijtelaar EL, van Schaijk WJ, Coenen AM (1993) Aberrant transients in the EEG of epileptic rats: a spectral analytical approach. Physiol Behav 54:779–783

Drinkenburg WHIM, Schuurmans MLEJ, Coenen AML, Vossen JMH, van Luijtelaar ELJM (2003) Ictal stimulus processing during spike-wave discharges in genetic epileptic rats. Behav Brain Res 143:141–146

Duncan JS (1997) Idiopathic generalized epilepsies with typical absences. J Neurol 244:403–411

Dung HC, Lawson RL, Stevens M (1977) A study of the increased serum level of IgG1 in “lethargic” mice combined with a depressed thymus-dependent lymphoid system. J Immunogenet 4:287–293

Dung HC, Swigart RH (1971) Experimental studies of “lethargic” mutant mice. Tex Rep Biol Med 29:273–288

Engel J (2001) A proposed diagnostic scheme for people with epileptic seizures and with epilepsy: report of the ILAE Task Force on Classification and Terminology. Epilepsia 42:796–803

Engel J (2006a) Report of the ILAE classification core group. Epilepsia 47:1558–1568

Engel J (2006b) ILAE classification of epilepsy syndromes. Epilepsy Res 70 Suppl 1:S5–10

Ernst WL, Zhang Y, Yoo JW, Ernst SJ, Noebels JL (2009) Genetic enhancement of thalamocortical network activity by elevating alpha 1g-mediated low-voltage-activated calcium current induces pure absence epilepsy. J Neurosci 29:1615–1625

Errington AC, Hughes SW, Crunelli V (2012) Rhythmic dendritic Ca 2 + oscillations in thalamocortical neurons during slow non-REM sleep-related activity in vitro . J Physiol 4975.

Errington AC, Renger JJ, Uebele VN, Crunelli V (2010) State-dependent firing determines intrinsic dendritic Ca2+ signaling in thalamocortical neurons. J Neurosci 30:14843–14853

Ettinger AB, Bernal OG, Andriola MR, Bagchi S, Flores P, Just C, Pitocco C, Rooney T, Tuominen J, Devinsky O (1999) Two cases of nonconvulsive status epilepticus in association with tiagabine therapy. Epilepsia 40:1159–1162

Faradji H, Rousset C, Debilly G, Vergnes M, Cespuglio R (2000) Sleep and epilepsy: A key role for nitric oxide? Epilepsia 41:794–801

Fariello RG, Golden GT (1987) The THIP-induced model of bilateral synchronous spike and wave in rodents. Neuropharmacology 26:161–165

Farrant M, Nusser Z (2005) Variations on an inhibitory theme: phasic and tonic activation of GABA(A) receptors. Nat Rev Neurosci 6:215–229

Feucht M, Fuchs K, Pichlbauer E, Hornik K, Scharfetter J, Goessler R, Füreder T, Cvetkovic N, Sieghart W, Kasper S, Aschauer H (1999) Possible association between childhood absence epilepsy and the gene encoding GABRB3. Biol Psychiatry 46:997–1002

Feucht M, Möller U, Witte H, Schmidt K, Arnold M, Benninger F, Steinberger K, Friedrich MH (1998) Nonlinear dynamics of 3 Hz spike-and-wave discharges recorded during typical absence seizures in children. Cereb Cortex 8:524–533

Fisher RS, Prince DA (1977) Spike-wave rhythms in cat cortex induced by parenteral penicillin. II. Cellular features. Electroencephalogr Clin Neurophysiol 42:625–639

Flecknell P (2009) Laboratory Animal Anaesthesia. Academic Press.

Fletcher CF, Frankel WN (1999) Ataxic mouse mutants and molecular mechanisms of absence epilepsy. Hum Mol Genet 8:1907–1912

Fletcher CF, Lutz CM, O'Sullivan TN, Shaughnessy JD, Hawkes R, Frankel WN, Copeland NG, Jenkins N a (1996) Absence epilepsy in tottering mutant mice is associated with calcium channel defects. Cell 87:607–617

Foley E, Cerquiglini A, Cavanna A, Nakubulwa MA, Furlong PL, Witton C, Seri S (2013) Magnetoencephalography in the study of epilepsy and consciousness. Epilepsy Behav

Fox AP, Nowycky MC, Tsien RW (1987) Kinetic and pharmacological properties distinguishing three types of calcium currents in chick sensory neurones. J Physiol 394:149–172

French JA, Pedley TA (2008) Clinical practice. Initial management of epilepsy. N Engl J Med 359:166–176

Fuentealba P, Steriade M (2005) The reticular nucleus revisited: intrinsic and network properties of a thalamic pacemaker. Prog Neurobiol 75:125–141

Galvan A, Smith Y, Wichmann T (2003) Continuous monitoring of intracerebral glutamate levels in awake monkeys using microdialysis and enzyme fluorometric detection. J Neurosci Methods 126:175–185

Gervasi N, Monnier Z, Vincent P, Paupardin-Tritsch D, Hughes SW, Crunelli V, Leresche N (2003) Pathway-specific action of gamma-hydroxybutyric acid in sensory thalamus and its relevance to absence seizures. J Neurosci 23:11469–11478

Giaretta D, Avoli M, Gloor P (1987) Intracellular recordings in pericruciate neurons during spike and wave discharges of feline generalized penicillin epilepsy. Brain Res 405:68–79

Girod S, Chabrol T, Benoit P, Depaulis A, Guillemain I (2012) Early development of seizures in the somatosensory cortex in a genetic model of absence epilepsy in the rat: Ontogenesis revisited. In: Society for Neuroscience Annual Meeting. New Orleans.

Glauser T, Cnaan A, Shinnar S, Hirtz DG, Dlugos D, Masur D, Clark PO, Capparelli E V, Adamson PC (2010) Ethosuximide, valproic acid, and lamotrigine in childhood absence epilepsy. N Engl J Med 362:790–799

Glauser TA, Cnaan A, Shinnar S, Hirtz DG, Dlugos D, Masur D, Clark PO, Adamson PC (2012) Ethosuximide, valproic acid, and lamotrigine in childhood absence epilepsy: Initial monotherapy outcomes at 12 months. Epilepsia

Gloor P, Testa G (1974) Generalized penicillin epilepsy in the cat: effects of intracarotid and intravertebral pentylenetetrazol and amobarbital injections. Electroencephalogr Clin Neurophysiol 36:499–515

Glykys J, Mody I (2007) Activation of GABAA receptors: views from outside the synaptic cleft. Neuron 56:763–770

Godschalk M, Dzoljic MR, Bonta IL (1976) Antagonism of gamma-hydroxybutyrate-induced hypersynchronization in the ECoG of the rat by anti-petit mal drugs. Neurosci Lett 3:145–150

Godschalk M, Dzoljic MR, Bonta IL (1977) Slow wave sleep and a state resembling absence epilepsy induced in the rat by gamma-hydroxybutyrate. Eur J Pharmacol 44:105–111

Goldberg JH, Lacefield CO, Yuste R (2004) Global dendritic calcium spikes in mouse layer 5 low threshold spiking interneurones: implications for control of pyramidal cell bursting. J Physiol 558:465–478

Goldie L, Green JM (1961) Spike and wave discharges and alterations of conscious awareness. Nature 191:200–201

Gomora JC, Daud a N, Weiergräber M, Perez-Reyes E (2001) Block of cloned human T-type calcium channels by succinimide antiepileptic drugs. Mol Pharmacol 60:1121–1132

Gotman J, Grova C, Bagshaw A, Kobayashi E, Aghakhani Y, Dubeau F (2005) Generalized epileptic discharges show thalamocortical activation and suspension of the default state of the brain. Proc Natl Acad Sci U S A 102:15236–15240

Gower AJ, Hirsch E, Boehrer A, Noyer M, Marescaux C (1995) Effects of levetiracetam, a novel antiepileptic drug, on convulsant activity in two genetic rat models of epilepsy. Epilepsy Res 22:207–213].

Groenewegen H, Witter M (2004) Thalamus. In: The Rat Nervous System, 3rd ed. (Paxinos G, ed), pp 407–445. International: Elsevier Academic Press.

Guberman A, Gloor P, Sherwin AL (1975) Response of generalized penicillin epilepsy in the cat to ethosuximide and diphenylhydantoin. Neurology 25:785–64

Guillery RW (1995) Anatomical evidence concerning the role of the thalamus in corticocortical communication: a brief review. J Anat 187 (Pt 3:583–592

Gurbanova A a, Aker R, Berkman K, Onat FY, van Rijn CM, van Luijtelaar G (2006) Effect of systemic and intracortical administration of phenytoin in two genetic models of absence epilepsy. Br J Pharmacol 148:1076–1082

Haas JS, Landisman CE (2011) State-dependent modulation of gap junction signaling by the persistent sodium current. Front Cell Neurosci 5:31

Haas JS, Zavala B, Landisman CE (2011) Activity-dependent long-term depression of electrical synapses. Science 334:389–393

Hagiwara S, Ozawa S, Sand O (1975) Voltage clamp analysis of two inward current mechanisms in the egg cell membrane of a starfish. J Gen Physiol 65:617–644

Halász P, Terzano MG, Parrino L (2002) Spike-wave discharge and the microstructure of sleep-wake continuum in idiopathic generalised epilepsy. Neurophysiol Clin 32:38–53

Hamandi K, Salek-Haddadi A, Laufs H, Liston A, Friston KJ, Fish DR, Duncan JS, Lemieux L (2006) EEG-fMRI of idiopathic and secondarily generalized epilepsies. Neuroimage 31:1700–1710

Harris K, Henze D, Csicsvari J (2000) Accuracy of tetrode spike separation as determined by simultaneous intracellular and extracellular measurements. J:401–414

Harris RM, Hendrickson AE (1987) Local circuit neurons in the rat ventrobasal thalamus--a GABA immunocytochemical study. Neuroscience 21:229–236

Hasuo H, Phelan KD, Twery MJ, Gallagher JP (1990) A calcium-dependent slow afterdepolarization recorded in rat dorsolateral septal nucleus neurons in vitro. J Neurophysiol 64:1838–1846

Hazan L, Zugaro M, Buzsáki G (2006) Klusters, NeuroScope, NDManager: a free software suite for neurophysiological data processing and visualization. J Neurosci Methods 155:207–216

Heady TN, Gomora JC, Macdonald TL, Perez-Reyes E (2001) Molecular pharmacology of T-type Ca2+ channels. Jpn J Pharmacol 85:339–350

Hempelmann A, Cobilanschi J, Heils A, Muhle H, Stephani U, Weber Y, Lerche H, Sander T (2007) Lack of evidence of an allelic association of a functional GABRB3 exon 1a promoter polymorphism with idiopathic generalized epilepsy. Epilepsy Res 74:28–32

Hernández-Cruz a, Pape H-CC (1989) Identification of two calcium currents in acutely dissociated neurons from the rat lateral geniculate nucleus. J Neurophysiol 61:1270–1283

Heron SE, Phillips H a, Mulley JC, Mazarib A, Neufeld MY, Berkovic SF, Scheffer IE (2004) Genetic variation of CACNA1H in idiopathic generalized epilepsy. Ann Neurol 55:595–596

Hirata A, Castro-Alamancos MA (2010) Neocortex network activation and deactivation states controlled by the thalamus. J Neurophysiol 103:1147–1157

Höcht C, Opezzo JAW, Taira CA (2007) Applicability of reverse microdialysis in pharmacological and toxicological studies. J Pharmacol Toxicol Methods 55:3–15

Holmes MD, Brown M, Tucker DM (2004) Are “generalized” seizures truly generalized? Evidence of localized mesial frontal and frontopolar discharges in absence. Epilepsia 45:1568–1579

Horita H (2001) Epileptic seizures and sleep-wake rhythm. Psychiatry Clin Neurosci 55:171–172

Horita H, Uchida E, Maekawa K (1991) Circadian rhythm of regular spike-wave discharges in childhood absence epilepsy. Brain Dev 13:200–202

Hughes SW, Cope DW, Blethyn KL, Crunelli V (2002) Cellular mechanisms of the slow (<1 Hz) oscillation in thalamocortical neurons in vitro. Neuron 33:947–958

Hughes SW, Cope DW, Tóth TI, Williams SR, Crunelli V (1999) All thalamocortical neurones possess a T-type Ca2+ “window” current that enables the expression of bistability-mediated activities. J Physiol 517 (Pt 3:805–815

Huguenard JR, Coulter DA, Prince DA (1991) A fast transient potassium current in thalamic relay neurons: kinetics of activation and inactivation. J Neurophysiol 66:1304–1315

Huguenard JR, Prince D a (1992) A novel T-type current underlies prolonged Ca(2+)-dependent burst firing in GABAergic neurons of rat thalamic reticular nucleus. J Neurosci 12:3804–3817

Huguenard JR, Prince D a (1994) Intrathalamic rhythmicity studied in vitro: nominal T-current modulation causes robust antioscillatory effects. J Neurosci 14:5485–5502

Huh Y, Cho J (2013) Urethane anesthesia depresses activities of thalamocortical neurons and alters its response to nociception in terms of dual firing modes. Front Behav Neurosci 7:141

Hwang H, Kim H, Kim SH, Kim SH, Lim BC, Chae J-H, Choi JE, Kim KJ, Hwang YS (2012) Long-term effectiveness of ethosuximide, valproic acid, and lamotrigine in childhood absence epilepsy. Brain Dev 34:344–348

Iannetti P, Spalice A, De Luca PF, Boemi S, Festa A, Maini CL (2001) Ictal single photon emission computed tomography in absence seizures: apparent implication of different neuronal mechanisms. J Child Neurol 16:339–344

ILAE (1981) Proposal for Revised Clinical and Electroencephalographic Classification of Epileptic Seizures. Epilepsia 22:489–501

ILAE (1989) Proposal for Revised Classification of Epilepsies and Epileptic Syndromes. Epilepsia 30:389–399

Imbrici P, Jaffe SL, Eunson LH, Davies NP, Herd C, Robertson R, Kullmann DM, Hanna MG (2004) Dysfunction of the brain calcium channel CaV2.1 in absence epilepsy and episodic ataxia. Brain 127:2682–2692

Inoue M, Ates N, Vossen JM, Coenen a M (1994) Effects of the neuroleptanalgesic fentanyl-fluanisone (Hypnorm) on spike-wave discharges in epileptic rats. Pharmacol Biochem Behav 48:547–551

Inoue M, Duysens J, Vossen JM, Coenen a M (1993) Thalamic multiple-unit activity underlying spike-wave discharges in anesthetized rats. Brain Res 612:35–40

Inoue M, Peeters BW, van Luijtelaar EL, Vossen JM, Coenen AM (1990) Spontaneous occurrence of spike-wave discharges in five inbred strains of rats. Physiol Behav 48:199–201

Ishige K, Aizawa M, Ito Y, Fukuda H (1996) gamma-Butyrolactone-induced absence-like seizures increase nuclear CRE- and AP-1 DNA-binding activities in mouse brain. Neuropharmacology 35:45–55

Ito M, Ohmori I, Nakahori T, Ouchida M, Ohtsuka Y (2005) Mutation screen of GABRA1, GABRB2 and GABRG2 genes in Japanese patients with absence seizures. Neurosci Lett 383:220–224

Jahnsen H, Llinás RR (1984a) Electrophysiological properties of guinea-pig thalamic neurones: 205–226.

Jahnsen H, Llinás RR (1984b) IONIC BASIS FOR THE ELECTRORESPONSIVENESS. :227–247.

Jandó G, Carpi D, Kandel A, Urioste R, Horvath Z, Pierre E, Vadi D, Vadasz C, Buzsáki G (1995) Spike-and-wave epilepsy in rats: sex differences and inheritance of physiological traits. Neuroscience 64:301–317

Janz D (1997) The idiopathic generalized epilepsies of adolescence with childhood and juvenile age of onset. Epilepsia 38:4–11

Jia F, Pignataro L, Schofield CM, Yue M, Harrison NL, Goldstein P a (2005) An extrasynaptic GABAA receptor mediates tonic inhibition in thalamic VB neurons. J Neurophysiol 94:4491–4501

Jones EG (1985) The Thalamus, 1st ed. New York: Plenum.

Jones EG (2002) Thalamic circuitry and thalamocortical synchrony. Philos Trans R Soc Lond B Biol Sci 357:1659–1673

Jones EG, Powell TPS (1969) An Electron Microscopic Study of the Mode of Termination of Cortico-Thalamic Fibres within the Sensory Relay Nuclei of the Thalamus. Proc R Soc B Biol Sci 172:173–185

Jouvenceau A, Eunson LH, Spauschus A, Ramesh V, Zuberi SM, Kullmann DM, Hanna MG (2001) Human epilepsy associated with dysfunction of the brain P/Q-type calcium channel. Lancet 358:801–807

Juhász G, Kékesi K, Emri Z, Soltesz I, Crunelli V (1990) Sleep-promoting action of excitatory amino acid antagonists: a different role for thalamic NMDA and non-NMDA receptors. Neurosci Lett 114:333–338

Kadir SN, Goodman DFM, Harris KD (2013) High-dimensional cluster analysis with the Masked EM Algorithm. :10

Kagan R, Kainz V, Burstein R, Noseda R (2013) Hypothalamic and basal ganglia projections to the posterior thalamus: Possible role in modulation of migraine headache and photophobia. Neuroscience 248C:359–368

Kamiński RM, Van Rijn CM, Turski WA, Czuczwar SJ, Van Luijtelaar G (2001) AMPA and GABA(B) receptor antagonists and their interaction in rats with a genetic form of absence epilepsy. Eur J Pharmacol 430:251–259

Kananura C, Haug K, Sander T, Runge U, Gu W, Hallmann K, Rebstock J, Heils A, Steinlein OK (2002) A splice-site mutation in GABRG2 associated with childhood absence epilepsy and febrile convulsions. Arch Neurol 59:1137–1141

Kandel A, Buzsáki G (1997) Cellular-synaptic generation of sleep spindles, spike-and-wave discharges, and evoked thalamocortical responses in the neocortex of the rat. J Neurosci 17:6783–6797

Kang J-QJ, Macdonald RL (2004) The GABAA receptor gamma2 subunit R43Q mutation linked to childhood absence epilepsy and febrile seizures causes retention of alpha1beta2gamma2S receptors in the endoplasmic reticulum. J Neurosci 24:8672–8677

Kellaway P (1985) Sleep and epilepsy. Epilepsia 26 Suppl 1:S15–30

Kellaway P, Frost JD, Crawley JW (1980) Time modulation of spike-and-wave activity in generalized epilepsy. Ann Neurol 8:491–500

Kelly KM (2004) Spike-wave discharges: absence or not, a common finding in common laboratory rats. Epilepsy Curr 4:176–177

Kennard JTT, Barmanray R, Sampurno S, Ozturk E, Reid CA, Paradiso L, D'Abaco GM, Kaye AH, Foote SJ, O'Brien TJ, Powell KL (2011) Stargazin and AMPA receptor membrane expression is increased in the somatosensory cortex of Genetic Absence Epilepsy Rats from Strasbourg. Neurobiol Dis 42:48–54

Khan Z, Jinnah HA (2002) Paroxysmal dyskinesias in the lethargic mouse mutant. J Neurosci 22:8193–8200

Khosravani H, Altier C, Simms B, Hamming KS, Snutch TP, Mezeyova J, McRory JE, Zamponi GW (2004) Gating effects of mutations in the Cav3.2 T-type calcium channel associated with childhood absence epilepsy. J Biol Chem 279:9681–9684

Khosravani H, Bladen C, Parker DB, Snutch TP, McRory JE, Zamponi GW (2005) Effects of Cav3.2 channel mutations linked to idiopathic generalized epilepsy. Ann Neurol 57:745–749

Kim D, Song I, Keum S, Lee T, Jeong MJ, Kim SS, McEnery MW, Shin H (2001) Lack of the burst firing of thalamocortical relay neurons and resistance to absence seizures in mice lacking alpha(1G) T-type Ca(2+) channels. Neuron 31:35–45

Kim U, McCormick DA (1998) Functional and ionic properties of a slow afterhyperpolarization in ferret perigeniculate neurons in vitro. J Neurophysiol 80:1222–1235

Knight AR, Bowery NG (1992) GABA receptors in rats with spontaneous generalized nonconvulsive epilepsy. J Neural Transm Suppl 35:189–196

Koerner C, Danober L, Boehrer A, Marescaux C, Vergnes M (1996) Thalamic NMDA transmission in a genetic model of absence epilepsy in rats. Epilepsy Res 25:11–19

Kostopoulos GK (2000) Spike-and-wave discharges of absence seizures as a transformation of sleep spindles: the continuing development of a hypothesis. Clin Neurophysiol 111 Suppl :S27–38

Kostopoulos GK (2001) Involvement of the thalamocortical system in epileptic loss of consciousness. Epilepsia 42 Suppl 3:13–19

Kostopoulos GK, Gloor P, Pellegrini A, Gotman J, Siatitsas I (1981a) A study of the transition from spindles to spike and wave discharge in feline generalized penicillin epilepsy: microphysiological features. Exp Neurol 73:55–77

Kostopoulos GK, Gloor P, Pellegrini A, Siatitsas I (1981b) A study of the transition from spindles to spike and wave discharge in feline generalized penicillin epilepsy: EEG features. Exp Neurol 73:43–54

Kumaresan S, David J, Joseph T (2000) Comparative profiles of sodium valproate and ethosuximide on electro-behavioural correlates in gamma-hydroxybutyrate and pentylenetetrazol induced absence seizures in rats. Indian J Physiol Pharmacol 44:411–418

Kyuyoung CL, Huguenard JR (2014) Modulation of Short-Term Plasticity in the Corticothalamic Circuit by Group III Metabotropic Glutamate Receptors. J Neurosci 34:675–687

Labate a, Briellmann RS, Abbott DF, Waites a B, Jackson GD (2005) Typical childhood absence seizures are associated with thalamic activation. Epileptic Disord 7:373–377

Lannes B, Micheletti G, Vergnes M, Marescaux C, Depaulis A, Warter JM (1988) Relationship between spike-wave discharges and vigilance levels in rats with spontaneous petit mal-like epilepsy. Neurosci Lett 94:187–191

Larkum ME, Zhu JJ (2002) Signaling of layer 1 and whisker-evoked Ca2+ and Na+ action potentials in distal and terminal dendrites of rat neocortical pyramidal neurons in vitro and in vivo. J Neurosci 22:6991–7005

Laufs H, Lengler U, Hamandi K, Kleinschmidt A, Krakow K (2006) Linking generalized spike-and-wave discharges and resting state brain activity by using EEG/fMRI in a patient with absence seizures. Epilepsia 47:444–448

Lee KH, McCormick DA (1997) Modulation of spindle oscillations by acetylcholine, cholecystokinin and 1S,3R-ACPD in the ferret lateral geniculate and perigeniculate nuclei in vitro. Neuroscience 77:335–350

Leresche N, Jassik-gerschenfeld D, Haby M, Soltesz I, Crunelli V (1990) Pacemaker-like and other types of spontaneous membrane potential oscillations of thalamocortical cells. Neurosci Lett 113:72–77

Leresche N, Lambert RC, Errington AC, Crunelli V (2012) From sleep spindles of natural sleep to spike and wave discharges of typical absence seizures: is the hypothesis still valid? Pflugers Arch 463:201–212

Leresche N, Lightowler S, Soltesz I, Jassik-gerschenfeld D, Crunelli V (1991) Low-frequency oscillatory activities intrinsic to rat and cat thalamocortical cells. J Physiol 441:155–174

Leresche N, Parri HR, Erdemli G, Guyon a, Turner JP, Williams SR, Asprodini E, Crunelli V (1998) On the action of the anti-absence drug ethosuximide in the rat and cat thalamus. J Neurosci 18:4842–4853

Letts V a, Felix R, Biddlecome GH, Arikkath J, Mahaffey CL, Valenzuela a, Bartlett FS, Mori Y, Campbell KP, Frankel WN (1998) The mouse stargazer gene encodes a neuronal Ca2+-channel gamma subunit. Nat Genet 19:340–347

Leutmezer F, Lurger S, Baumgartner C (2002) Focal features in patients with idiopathic generalized epilepsy. Epilepsy Res 50:293–300

Liang J, Zhang Y, Chen Y, Wang J, Pan H, Wu H, Xu K, Liu X, Jiang Y, Shen Y, Wu X (2007) Common polymorphisms in the CACNA1H gene associated with childhood absence epilepsy in Chinese Han population. Ann Hum Genet 71:325–335

Liang J, Zhang Y, Wang J, Pan H, Wu H, Xu K, Liu X, Jiang Y, Shen Y, Wu X (2006) New variants in the CACNA1H gene identified in childhood absence epilepsy. Neurosci Lett 406:27–32

Liao W, Zhang Z, Mantini D, Xu Q, Ji G-J, Zhang H, Wang J, Wang Z, Chen G, Tian L, Jiao Q, Zang Y-F, Lu G (2013) Dynamical intrinsic functional architecture of the brain during absence seizures. Brain Struct Funct

Liu X-B, Coble J, van Luijtelaar G, Jones EG (2007) Reticular nucleus-specific changes in alpha3 subunit protein at GABA synapses in genetically epilepsy-prone rats. Proc Natl Acad Sci U S A 104:12512–12517

Liu XB, Honda CN, Jones EG (1995) Distribution of four types of synapse on physiologically identified relay neurons in the ventral posterior thalamic nucleus of the cat. J Comp Neurol 352:69–91

Liu XB, Jones EG (1999) Predominance of corticothalamic synaptic inputs to thalamic reticular nucleus neurons in the rat. J Comp Neurol 414:67–79

Liu Z, Vergnes M, Depaulis A (1992) Involvement of intrathalamic GABA< sub> b</sub> neurotransmission in the control of absence seizures in the rat. Neuroscience 48:87–93

Liu Z, Vergnes M, Depaulis A, Marescaux C (1991) Evidence for a critical role of GABAergic transmission within the thalamus in the genesis and control of absence seizures in the rat. 545:1–7.

Llinás RR, Choi S, Urbano FJ, Shin H-S (2007) Gamma-band deficiency and abnormal thalamocortical activity in P/Q-type channel mutant mice. Proc Natl Acad Sci U S A 104:17819–17824

Llinás RR, Jahnsen H (1982) Electrophysiology of mammalian thalamic neurones in vitro. Nature 297:406–408

Llinás RR, Yarom Y (1981) Properties and distribution of ionic conductances generating electroresponsiveness of mammalian inferior olivary neurones in vitro. J Physiol 315:569–584

Loiseau J, Loiseau P, Guyot M, Duche B, Dartigues JF, Aublet B (1990) Survey of seizure disorders in the French southwest. I. Incidence of epileptic syndromes. Epilepsia 31:391–396

Loiseau P (1992) Human absence epilepsies. J Neural Transm Suppl 35:1–6

Loiseau P, Duche B (1995) Childhood absence epilepsy. In: Typical Absences and Related Epileptic Syndromes (Duncan J, Panayiotopoulos CP, eds), pp 299–309. London: Churchill Livingstone.

Lourenço Neto F, Schadrack J, Berthele A, Zieglgänsberger W, Tölle TR, Castro-Lopes JM (2000) Differential distribution of metabotropic glutamate receptor subtype mRNAs in the thalamus of the rat. Brain Res 854:93–105

Lu J, Chen Y, Zhang Y, Pan H, Wu H, Xu K, Liu X, Jiang Y, Bao X, Ding K, Shen Y, Wu X (2002) Mutation screen of the GABA(A) receptor gamma 2 subunit gene in Chinese patients with childhood absence epilepsy. Neurosci Lett 332:75–78

Lübke J, Egger V, Sakmann B, Feldmeyer D (2000) Columnar organization of dendrites and axons of single and synaptically coupled excitatory spiny neurons in layer 4 of the rat barrel cortex. J Neurosci 20:5300–5311

Maitre M (1997) The gamma-hydroxybutyrate signalling system in brain: organization and functional implications. Prog Neurobiol 51:337–361

Maljevic S, Krampfl K, Cobilanschi J, Tilgen N, Beyer S, Weber YG, Schlesinger F, Ursu D, Melzer W, Cossette P, Bufler J, Lerche H, Heils A (2006) A mutation in the GABA(A) receptor alpha(1)-subunit is associated with absence epilepsy. Ann Neurol 59:983–987

Manning J (2004) Cortical-area specific block of genetically determined absence seizures by ethosuximide. Neuroscience 123:5–9

Marcus RJ, Winters WD, Mori K, Spooner CE (1967) EEG and behavioral comparison of the effects of gamma-hydroxybutyrate, gamma-butyrolactone and short chain fatty acids in the rat. Int J Neuropharmacol 6:175–185

Marescaux C, Micheletti G, Vergnes M, Depaulis A, Rumbach L, Warter JM (1984a) A model of chronic spontaneous petit mal-like seizures in the rat: comparison with pentylenetetrazol-induced seizures. Epilepsia 25:326–331

Marescaux C, Vergnes M, Depaulis A (1992a) Genetic absence epilepsy in rats from Strasbourg--a review. J Neural Transm Suppl 35:37–69

Marescaux C, Vergnes M, Depaulis A (1992b) Neurotransmission in rats' spontaneous generalized nonconvulsive epilepsy. Epilepsy Res Suppl 8:335–343

Marescaux C, Vergnes M, Micheletti G, Depaulis A, Reis J, Rumbach L, Warter JM, Kurtz D (1984b) Une forme génétique d'absences petit mal chez le rat Wistar. Rev Neurol (Paris) 140:63–66

Markram H, Sakmann B (1994) Calcium transients in dendrites of neocortical neurons evoked by single subthreshold excitatory postsynaptic potentials via low-voltage-activated calcium channels. Proc Natl Acad Sci U S A 91:5207–5211

McCormick DA (1992) Neurotransmitter actions in the thalamus and cerebral cortex and their role in neuromodulation of thalamocortical activity. Prog Neurobiol 39:337–388

McCormick DA, Huguenard JR (1992) A model of the electrophysiological properties of thalamocortical relay neurons. J Neurophysiol 68:1384–1400

McCormick DA, Pape H-C (1990a) Properties of a hyperpolarization-activated cation current and its role in rhythmic oscillation in thalamic relay neurones. J Physiol 431:291–318

McCormick DA, Pape H-C (1990b) Noradrenergic and serotonergic modulation of a hyperpolarization-activated cation current in thalamic relay neurones. J Physiol 840:319–342

McCormick DA, Prince DA (1987) Actions of acetylcholine in the guinea-pig and cat medial and lateral geniculate nuclei, in vitro. J Physiol:147–165

McKay BE, McRory JE, Molineux ML, Hamid J, Snutch TP, Zamponi GW, Turner RW (2006) Ca(V)3 T-type calcium channel isoforms differentially distribute to somatic and dendritic compartments in rat central neurons. Eur J Neurosci 24:2581–2594

McLachlan RS, Gloor P, Avoli M (1984) Differential participation of some “specific” and “non-specific” thalamic nuclei in generalized spike and wave discharges of feline generalized penicillin epilepsy. Brain Res 307:277–287

Meeren HKM, Pijn JPM, Van Luijtelaar ELJM, Coenen AML, Lopes da Silva FH (2002) Cortical focus drives widespread corticothalamic networks during spontaneous absence seizures in rats. J Neurosci 22:1480–1495

Meeren HKM, Veening JG, Möderscheim T a E, Coenen AML, van Luijtelaar G (2009) Thalamic lesions in a genetic rat model of absence epilepsy: dissociation between spike-wave discharges and sleep spindles. Exp Neurol 217:25–37

Mirsky AF, Van Buren JM (1965) On the nature of the “absence” in centrencephalic epilepsy: A study of some behavioral, electroencephalographic and autonomic factors. Electroencephalogr Clin Neurophysiol 18:334–348

Moeller F, Siebner HR, Wolff S, Muhle H, Boor R, Granert O, Jansen O, Stephani U, Siniatchkin M (2008) Changes in activity of striato-thalamo-cortical network precede generalized spike wave discharges. Neuroimage 39:1839–1849

Niedermeyer E (1996) Primary (idiopathic) generalized epilepsy and underlying mechanisms. Clin Electroencephalogr 27:1–21

Nilius B, Talavera K, Verkhratsky A (2006) T-type calcium channels: the never ending story. Cell Calcium 40:81–88

Noebels JL (2006) Spontaneous Epileptic Mutations in the Mouse. In: Models of Seizure and Epilepsy (Pitkanen A, Schwartzkroin PA, Moshé S, eds), pp 223–232. International: Elsevier Academic Press.

Noebels JL, Qiao X, Bronson RT, Spencer C, Davisson MT (1990) Stargazer: a new neurological mutant on chromosome 15 in the mouse with prolonged cortical seizures. Epilepsy Res 7:129–135

Noebels JL, Sidman RL (1979) Inherited epilepsy: spike-wave and focal motor seizures in the mutant mouse tottering. Science 204:1334–1336

Ohara PT (1988) Synaptic organization of the thalamic reticular nucleus. J Electron Microsc Tech 10:283–292

Ohara PT, Lieberman AR (1993) Some aspects of the synaptic circuitry underlying inhibition in the ventrobasal thalamus. J Neurocytol 22:815–825

Panayiotopoulos CP (1997) Absence Epilepsies. In: Epilepsy: a Comprehensive Textbook (Engel J, Pedley T, eds). Philadelphia: Lippincott-Raven.

Panayiotopoulos CP, Agathonikou A, Sharoqi IA, Parker AP (1997) Vigabatrin aggravates absences and absence status. Neurology 49:1467

Panayiotopoulos CP, Obeid T, Waheed G (1989a) Differentiation of typical absence seizures in epileptic syndromes. A video EEG study of 224 seizures in 20 patients. Brain 112 (Pt 4:1039–1056

Panayiotopoulos CP, Obeid T, Waheed G (1989b) Differentiation of Typical Absence Seizures in Epileptic Syndromes. Brain 112:1039–1056

Pape HC, Budde T, Mager R, Kisvárday ZF (1994) Prevention of Ca(2+)-mediated action potentials in GABAergic local circuit neurones of rat thalamus by a transient K+ current. J Physiol 478 Pt 3:403–422

Parker AP, Agathonikou a, Robinson RO, Panayiotopoulos CP (1998) Inappropriate use of carbamazepine and vigabatrin in typical absence seizures. Dev Med Child Neurol 40:517–519

Parri HR, Crunelli V (1998) Sodium current in rat and cat thalamocortical neurons: role of a non-inactivating component in tonic and burst firing. J Neurosci 18:854–867

Partridge L, Swandulla D (1988) Calcium-activated non-specific cation channels. Trends Neurosci 11:69–72.

Patel IH, Levy RH, Rapport RL (1977) Distribution characteristics of ethosuximide in discrete areas of rat brain. Epilepsia 18:533–541

Patsalos PN, Perucca E (2003a) Clinically important drug interactions in epilepsy: general features and interactions between antiepileptic drugs. Lancet Neurol 2:473–481

Patsalos PN, Perucca E (2003b) Clinically important drug interactions in epilepsy: interactions between antiepileptic drugs and other drugs. Lancet Neurol 2:473–481

Pavone P, Bianchini R, Trifiletti RR, Incorpora G, Pavone A, Parano E, Ronen GM, Meaney BF, Cunningham C (2001) Neuropsychological assessment in children with absence epilepsy. Neurology 56:1047–1051

Paxinos G, Watson C (2008) The Rat Brain in Stereotaxic Coordinates: Compact 6th Edition. Academic Press Inc. Available at: http://www.amazon.co.uk/The-Rat-Brain-Stereotaxic-Coordinates/dp/0123742439 [Accessed July 25, 2012].

Paz J, Bryant A, Peng K, Fenno L, Yizhar O, Frankel WN, Deisseroth K, Huguenard JR (2011) A new mode of corticothalamic transmission revealed in the Gria4-/-model of absence epilepsy. Nat Neurosci

Pedreira C, Martinez J, Ison MJ, Quian Quiroga R (2012) How many neurons can we see with current spike sorting algorithms? J Neurosci Methods 211:58–65

Peeters BW, Cheung KS, Vossen JM, Coenen AM (1992a) Some solvents for antiepileptics have proepileptic potencies in the WAG/Rij rat model for absence epilepsy. Brain Res Bull 29:515–517

Peeters BW, Kerbusch JM, Coenen AM, Vossen JM, van Luijtelaar EL (1992b) Genetics of spike-wave discharges in the electroencephalogram (EEG) of the WAG/Rij inbred rat strain: a classical mendelian crossbreeding study. Behav Genet 22:361–368

Peeters BW, van Rijn CM, Vossen JM, Coenen AM (1989) Effects of GABA-ergic agents on spontaneous non-convulsive epilepsy, EEG and behaviour, in the WAG/RIJ inbred strain of rats. Life Sci 45:1171–1176

Pellegrini A, Gloor P, Sherwin AL (1978) Effect of valproate sodium on generalized penicillin epilepsy in the cat. Epilepsia 19:351–360

Perez-Reyes E (1999) Three for T: molecular analysis of the low voltage-activated calcium channel family. Cell Mol Life Sci 56:660–669

Perez-Reyes E (2003) Molecular physiology of low-voltage-activated t-type calcium channels. Physiol Rev 83:117–161

Perez-Reyes E (2006) Molecular characterization of T-type calcium channels. Cell Calcium 40:89–96

Perucca E, Gram L, Avanzini G, Dulac O (1998) Antiepileptic drugs as a cause of worsening seizures. Epilepsia 39:5–17

Pfrieger FW, Veselovsky NS, Gottmann K, Lux HD (1992) Pharmacological characterization of calcium currents and synaptic transmission between thalamic neurons in vitro. J Neurosci 12:4347–4357

Pifl C, Hornykiewicz O, Blesa J, Adánez R, Cavada C, Obeso JA (2013) Reduced noradrenaline, but not dopamine and serotonin in motor thalamus of the MPTP primate: relation to severity of parkinsonism. J Neurochem 125:657–662

Pinault D (2003) Cellular interactions in the rat somatosensory thalamocortical system during normal and epileptic 5-9 Hz oscillations. J Physiol 552:881–905

Pinault D (2004) The thalamic reticular nucleus: structure, function and concept.

Pinault D, Deschênes M (1992) Voltage-dependent 40-Hz oscillations in rat reticular thalamic neurons in vivo. Neuroscience 51:245–258

Pinault D, Deschênes M (1998) Projection and innervation patterns of individual thalamic reticular axons in the thalamus of the adult rat: a three-dimensional, graphic, and morphometric analysis. J Comp Neurol 391:180–203

Pinault D, Leresche N, Charpier S, Deniau J-M, Marescaux C, Vergnes M, Crunelli V (1998) Intracellular recordings in thalamic neurones during spontaneous spike and wave discharges in rats with absence epilepsy. J Physiol 509 (Pt 2:449–456

Pinault D, Slézia A, Acsády L (2006) Corticothalamic 5-9 Hz oscillations are more pro-epileptogenic than sleep spindles in rats. J Physiol 574:209–227

Pinault D, Smith Y, Deschênes M (1997) Dendrodendritic and axoaxonic synapses in the thalamic reticular nucleus of the adult rat. J Neurosci 17:3215–3233

Pinault D, Vergnes M, Marescaux C (2001) Medium-voltage 5-9-Hz oscillations give rise to spike-and-wave discharges in a genetic model of absence epilepsy: in vivo dual extracellular recording of thalamic relay and reticular neurons. Neuroscience 105:181–201

Plock N, Kloft C (2005) Microdialysis--theoretical background and recent implementation in applied life-sciences. Eur J Pharm Sci 25:1–24

Polack P-O, Charpier S (2006) Intracellular activity of cortical and thalamic neurones during high-voltage rhythmic spike discharge in Long-Evans rats in vivo. J Physiol 571:461–476

Polack P-O, Guillemain I, Hu E, Deransart C, Depaulis A, Charpier S (2007) Deep layer somatosensory cortical neurons initiate spike-and-wave discharges in a genetic model of absence seizures. J Neurosci 27:6590–6599

Polack P-O, Mahon S, Chavez M, Charpier S (2009) Inactivation of the somatosensory cortex prevents paroxysmal oscillations in cortical and related thalamic neurons in a genetic model of absence epilepsy. Cereb Cortex 19:2078–2091

Portas CM, Thakkar M, Rainnie D, McCarley RW (1996) Microdialysis perfusion of 8-hydroxy-2-(di-n-propylamino)tetralin (8-OH-DPAT) in the dorsal raphe nucleus decreases serotonin release and increases rapid eye movement sleep in the freely moving cat. J Neurosci 16:2820–2828

Posner E, Mohamed K, Marson A (2010) Ethosuximide, sodium valproate or lamotrigine for absence seizures in children and adolescents. Cochrane Database Syst Rev

Pouzat C, Mazor O, Laurent G (2002) Using noise signature to optimize spike-sorting and to assess neuronal classification quality. J Neurosci Methods 122:43–57

Powell KL, Cain SM, Ng C, Sirdesai S, David LS, Kyi M, Garcia E, Tyson JR, Reid C a, Bahlo M, Foote SJ, Snutch TP, O'Brien TJ (2009) A Cav3.2 T-type calcium channel point mutation has splice-variant-specific effects on function and segregates with seizure expression in a polygenic rat model of absence epilepsy. J Neurosci 29:371–380

Powell KL, Kyi M, Reid CA, Paradiso L, D'Abaco GM, Kaye AH, Foote SJ, O'Brien TJ (2008) Genetic absence epilepsy rats from Strasbourg have increased corticothalamic expression of stargazin. Neurobiol Dis 31:261–265

Prevett MC, Duncan JS, Jones T, Fish DR, Brooks DJ (1995) Demonstration of thalamic activation during typical absence seizures using H2(15)O and PET. Neurology 45:1396–1402

Prince DA, Farrell D (1969) "Centrencephalic" spike wave discharges following parenteral penicillin injection in the cat. Neurology:309–310.

Princivalle AP, Richards DA, Duncan JS, Spreafico R, Bowery NG (2003) Modification of GABA(B1) and GABA(B2) receptor subunits in the somatosensory cerebral cortex and thalamus of rats with absence seizures (GAERS). Epilepsy Res 55:39–51

Pumain R, Louvel J, Gastard M, Kurcewicz I, Vergnes M (1992) Responses to N-methyl-D-aspartate are enhanced in rats with petit mal-like seizures. J Neural Transm Suppl 35:97–108

Ragsdale DS, Avoli M (1998) Sodium channels as molecular targets for antiepileptic drugs. Brain Res Brain Res Rev 26:16–28

Rankovic V, Landgraf P, Kanyshkova T, Ehling P, Meuth SG, Kreutz MR, Budde T, Munsch T (2011) Modulation of calcium-dependent inactivation of L-type Ca2+ channels via β-adrenergic signaling in thalamocortical relay neurons. PLoS One 6:e27474

Rateau Y, Ropert N (2006) Expression of a functional hyperpolarization-activated current (Ih) in the mouse nucleus reticularis thalami. J Neurophysiol 95:3073–3085

Renier WO, Coenen AML (2000) Human absence epilepsy: The WAG/Rij rat as a model. Neurosci Res Commun 26:181–191

Richards D a, Lemos T, Whitton PS, Bowery NG (1995) Extracellular GABA in the ventrolateral thalamus of rats exhibiting spontaneous absence epilepsy: a microdialysis study. J Neurochem 65:1674–1680

Richards D a, Manning J, Barnes D, Rombola L, Bowery NG, Caccia S, Leresche N, Crunelli V (2003) Targeting thalamic nuclei is not sufficient for the full anti-absence action of ethosuximide in a rat model of absence epilepsy. Epilepsy Res 54:97–107

Richens A (1995) Ethosuximide and valproate. In: Typical Absences and Related Epileptic Syndromes (Duncan JS, Panayiotopoulos CP, eds). London: Churchill Livingstone.

Rigoulot M-A, Boehrer A, Nehlig A (2003) Effects of topiramate in two models of genetically determined generalized epilepsy, the GAERS and the Audiogenic Wistar AS. Epilepsia 44:14–19

Roth RH, Giarman NJ (1969) Conversion in vivo of gamma-aminobutyric to gamma-hydroxybutyric acid in the rat. Biochem Pharmacol 18:247–250

Sadleir LG, Farrell K, Smith S, Connolly MB, Scheffer IE (2006) Electroclinical features of absence seizures in childhood absence epilepsy. Neurology 67:413–418

Sadleir LG, Scheffer IE, Smith S, Carstensen B, Carlin J, Connolly MB, Farrell K (2008) Factors influencing clinical features of absence seizures. Epilepsia 49:2100–2107

Sadleir LG, Scheffer IE, Smith S, Carstensen B, Farrell K, Connolly MB (2009) EEG features of absence seizures in idiopathic generalized epilepsy: impact of syndrome, age, and state. Epilepsia 50:1572–1578

Salek-Haddadi A, Lemieux L, Merschhemke M, Friston KJ, Duncan JS, Fish DR (2003) Functional magnetic resonance imaging of human absence seizures. Ann Neurol 53:663–667

Salt TE (1987) Excitatory amino acid receptors and synaptic transmission in the rat ventrobasal thalamus. J Physiol 391:499–510

Salt TE, Turner JP, Kingston AE (1999) Evaluation of agonists and antagonists acting at Group I metabotropic glutamate receptors in the thalamus in vivo. Neuropharmacology 38:1505–1510

Sanchez-Vives M V, Bal T, McCormick DA (1997) Inhibitory interactions between perigeniculate GABAergic neurons. J Neurosci 17:8894–8908

Sander J (1995) The epidemiology and prognosis of typical absence seizures. In: Typical Absences and Related Epileptic Syndromes (Duncan J, Panayiotopoulos CP, eds), pp 135–144. London: Churchill Livingstone.

Sayer RJ, Schwindt PC, Crill WE (1990) High- and low-threshold calcium currents in neurons acutely isolated from rat sensorimotor cortex. Neurosci Lett 120:175–178

Schachter S (1997) Treatment of Seizures. In: The Comprehensive Evaluation and Treatment of Epilepsy (Schachter S, Schomer D, eds). Academic Press.

Schapel G, Chadwick D (1996) Tiagabine and non-convulsive status epilepticus. Seizure 5:153–156

Schiff ND (2008) Central thalamic contributions to arousal regulation and neurological disorders of consciousness. Ann N Y Acad Sci 1129:105–118

Schofield CM, Kleiman-Weiner M, Rudolph U, Huguenard JR (2009) A gain in GABAA receptor synaptic strength in thalamus reduces oscillatory activity and absence seizures. Proc Natl Acad Sci U S A 106:7630–7635

Schuler V et al. (2001) Epilepsy, hyperalgesia, impaired memory, and loss of pre- and postsynaptic GABA(B) responses in mice lacking GABA(B(1)). Neuron 31:47–58

Seidenbecher T, Staak R, Pape H-C (1998) Relations between cortical and thalamic cellular activities during absence seizures in rats. Eur J Neurosci 10:1103–1112

Shaw F-Z (2004) Is spontaneous high-voltage rhythmic spike discharge in Long Evans rats an absence-like seizure activity? J Neurophysiol 91:63–77

Sherman SM (2001) Tonic and burst firing: dual modes of thalamocortical relay. Trends Neurosci 24:122–126

Sherman SM, Guillery RW (1996) Functional organization of thalamocortical relays. J Neurophysiol 76:1367–1395

Shimazono Y, Hirai T, Okuma T, Fukuda T, Yamamasu E (1953) Disturbance of Conciousness in Petit Mai Epilepsy. Epilepsia C2:49–55

Shipe WD et al. (2008) Design, synthesis, and evaluation of a novel 4-aminomethyl-4-fluoropiperidine as a T-type Ca2+ channel antagonist. J Med Chem 51:3692–3695

Shippenberg TS, Thompson AC (2001) Overview of microdialysis. Curr Protoc Neurosci Chapter 7:Unit7.1

Singh B, Monteil A, Bidaud I, Sugimoto Y, Suzuki T, Hamano S, Oguni H, Osawa M, Alonso ME, Delgado-Escueta A V, Inoue Y, Yasui-Furukori N, Kaneko S, Lory P, Yamakawa K (2007) Mutational analysis of CACNA1G in idiopathic generalized epilepsy. Mutation in brief #962. Online. Hum Mutat 28:524–525

Sitnikova E, van Luijtelaar G (2004) Cortical control of generalized absence seizures: effect of lidocaine applied to the somatosensory cortex in WAG/Rij rats. Brain Res 1012:127–137

Slaght SJ, Leresche N, Deniau J-M, Crunelli V, Charpier S (2002) Activity of thalamic reticular neurons during spontaneous genetically determined spike and wave discharges. J Neurosci 22:2323–2334 Available at: http://www.ncbi.nlm.nih.gov/pubmed/11896171.

Snead OC (1988) γ-Hydroxybutyrate Model of Generalized Absence Seizures: Further Characterization and Comparison with Other Absence Models. Epilepsia 29:361–368

Snead OC (1990) The ontogeny of GABAergic enhancement of the gamma-hydroxybutyrate model of generalized absence seizures. Epilepsia 31:363–368

Snead OC (1991) The gamma-hydroxybutyrate model of absence seizures: correlation of regional brain levels of gamma-hydroxybutyric acid and gamma-butyrolactone with spike wave discharges. Neuropharmacology 30:161–167

Snead OC (1992a) Pharmacological models of generalized absence seizures in rodents. J Neural Transm Suppl 35:7–19

Snead OC (1992b) Evidence for GABAB-mediated mechanisms in experimental generalized absence seizures. Eur J Pharmacol 213:343–349

Snead OC (1996) Antiabsence seizure activity of specific GABAB and gamma-Hydroxybutyric acid receptor antagonists. Pharmacol Biochem Behav 53:73–79

Snead OC, Banerjee P, Burnham M, Hampson D (2000) Modulation of Absence Seizures by the GABA A Receptor : A Critical Role for Metabotropic Glutamate Receptor 4 (mGluR4). J Neurosci 20:6218–6224.

Snead OC, Depaulis A, Vergnes M, Marescaux C (1999) Absence epilepsy: advances in experimental animal models. Adv Neurol 79:253–278

Sohal VS, Huguenard JR (2003) Inhibitory interconnections control burst pattern and emergent network synchrony in reticular thalamus. J Neurosci 23:8978–8988

Soltesz I, Lightowler S, Leresche N, Jassik-gerschenfeld D, Pollard CE, Crunelli V (1991) Two inward currents and the transformation of low-frequency oscillations of rat and cat thalamocortical cells. J Physiol:175–197

Song I, Kim D, Choi S, Sun M, Kim Y, Shin H-S (2004) Role of the alpha1G T-type calcium channel in spontaneous absence seizures in mutant mice. J Neurosci 24:5249–5257

Spain WJ, Schwindt PC, Crill WE (1991) Post-inhibitory excitation and inhibition in layer V pyramidal neurones from cat sensorimotor cortex. J Physiol 434:609–626

Spreafico R, Mennini T, Danober L, Cagnotto A, Regondi MC, Miari A, De Blas A, Vergnes M, Avanzini G (1993) GABAA receptor impairment in the genetic absence epilepsy rats from Strasbourg (GAERS): an immunocytochemical and receptor binding autoradiographic study. Epilepsy Res 15:229–238

Stefan H, Snead OC (1997) Absence Seizures. In: Epilepsy: a Comprehensive Textbook (Engel J, Pedley TA, eds), pp 579–590. Philadelphia: Lippincott-Raven.

Steriade M, Contreras D (1995) Relations between cortical and thalamic cellular events during transition from sleep patterns to paroxysmal activity. J Neurosci 15:623–642

Steriade M, Contreras D (1998) Spike-wave complexes and fast components of cortically generated seizures. I. Role of neocortex and thalamus. J Neurophysiol 80:1439–1455

Steriade M, Curro Dossi R, Nuñez A, Curró Dossi R (1991) Network modulation of a slow intrinsic oscillation of cat thalamocortical neurons implicated in sleep delta waves: cortically induced synchronization and brainstem cholinergic suppression. J Neurosci 11:3200–3217

Steriade M, Domich L, Oakson G (1986) Reticularis thalami neurons revisited: activity changes during shifts in states of vigilance. J Neurosci 6:68–81

Steriade M, Jones EG, McCormick DA (1997) Thalamus: Organisation and Function. Oxford: Elsevier Science.

Steriade M, McCormick DA, Sejnowski TJ (1993) Thalamocortical oscillations in the sleeping and aroused brain. Science 262:679–685

Sutch RJ, Davies CC, Bowery NG (1999) GABA release and uptake measured in crude synaptosomes from Genetic Absence Epilepsy Rats from Strasbourg (GAERS). Neurochem Int 34:415–425

Talavera K, Nilius B (2006) Biophysics and structure-function relationship of T-type Ca2+ channels. Cell Calcium 40:97–114

Talley EM, Cribbs LL, Lee JH, Daud a N, Perez-Reyes E, Bayliss D a (1999) Differential distribution of three members of a gene family encoding low voltage-activated (T-type) calcium channels. J Neurosci 19:1895–1911

Tan HO, Reid C a, Single FN, Davies PJ, Chiu C, Murphy S, Clarke AL, Dibbens L, Krestel H, Mulley JC, Jones M V, Seeburg PH, Sakmann B, Berkovic SF, Sprengel R, Petrou S (2007) Reduced cortical inhibition in a mouse model of familial childhood absence epilepsy. Proc Natl Acad Sci U S A 104:17536–17541

Tanaka M, Olsen RW, Medina MT, Schwartz E, Alonso ME, Duron RM, Castro-ortega R, Martinez-juarez IE, Pascual-castroviejo I, Machado-salas J, Silva R, Bailey JN, Bai D, Ochoa A, Jara-Prado A, Pineda G, Macdonald RL, Delgado-escueta A V (2008) Hyperglycosylation and reduced GABA currents of mutated GABRB3 polypeptide in remitting childhood absence epilepsy. Am J Hum Genet 82:1249–1261

Tarasenko AN, Kostyuk PG, Eremin A V, Isaev DS (1997) Two types of low-voltage-activated Ca2+ channels in neurones of rat laterodorsal thalamic nucleus. J Physiol 499 (Pt 1:77–86

Taylor-Courval D, Gloor P (1984) Behavioral alterations associated with generalized spike and wave discharges in the EEG of the cat. Exp Neurol 83:167–186

Tenney JR, Fujiwara H, Horn PS, Jacobson SE, Glauser TA, Rose DF (2013) Focal corticothalamic sources during generalized absence seizures: A MEG study. Epilepsy Res

Tóth TI, Hughes SW, Crunelli V (1998) Analysis and biophysical interpretation of bistable behaviour in thalamocortical neurons. Neuroscience 87:519–523

Touret M, Parrot S, Denoroy L, Belin M-F, Didier-Bazes M (2007) Glutamatergic alterations in the cortex of genetic absence epilepsy rats. BMC Neurosci 8:69

Tracey D (2004) Somatosensory System. In: The Rat Nervous System, 3rd ed. (Paxinos G, ed), pp 797–815. International: Elsevier Academic Press.

Tringham E, Powell KL, Cain SM, Kuplast K, Mezeyova J, Weerapura M, Eduljee C, Jiang X, Smith P, Morrison J-L, Jones NC, Braine E, Rind G, Fee-Maki M, Parker D, Pajouhesh H, Parmar M, O'Brien TJ, Snutch TP (2012) T-type calcium channel blockers that attenuate thalamic burst firing and suppress absence seizures. Sci Transl Med 4:121ra19

Tscherter A, David F, Ivanova T, Deleuze C, Renger JJ, Uebele VN, Shin H-S, Bal T, Leresche N, Lambert RC (2011) Minimal alterations in T-type calcium channel gating markedly modify physiological firing dynamics. J Physiol 589:1707–1724

Turner JP, Salt TE (2000) Synaptic activation of the group I metabotropic glutamate receptor mGlu1 on the thalamocortical neurons of the rat dorsal lateral geniculate nucleus in vitro. Neuroscience 100:493–505

Ulrich D, Huguenard JR (1996a) GABAB receptor-mediated responses in GABAergic projection neurones of rat nucleus reticularis thalami in vitro. J Physiol 493 (Pt 3:845–854

Ulrich D, Huguenard JR (1996b) Gamma-aminobutyric acid type B receptor-dependent burst-firing in thalamic neurons: a dynamic clamp study. Proc Natl Acad Sci U S A 93:13245–13249

Ulrich D, Huguenard JR (1997) GABA(A)-receptor-mediated rebound burst firing and burst shunting in thalamus. J Neurophysiol 78:1748–1751

Urak L, Feucht M, Fathi N, Hornik K, Fuchs K (2006) A GABRB3 promoter haplotype associated with childhood absence epilepsy impairs transcriptional activity. Hum Mol Genet 15:2533–2541

Van de Bovenkamp-Janssen MC, Scheenen WJJM, Kuijpers-Kwant FJ, Kozicz T, Veening JG, van Luijtelaar ELJM, McEnery MW, Roubos EW (2004) Differential expression of high voltage-activated Ca2+ channel types in the rostral reticular thalamic nucleus of the absence epileptic WAG/Rij rat. J Neurobiol 58:467–478

Van Der Loos H (1976) Barreloids in mouse somatosensory thalamus. Neurosci Lett 2:1–6

Van der Staay FJ, Arndt SS, Nordquist RE (2009) Evaluation of animal models of neurobehavioral disorders. Behav Brain Funct 5:11

Van Luijtelaar EL, Ates N, Coenen AM (1995) Role of L-type calcium channel modulation in nonconvulsive epilepsy in rats. Epilepsia 36:86–92

Van Luijtelaar EL, Coenen AM (1986) Two types of electrocortical paroxysms in an inbred strain of rats. Neurosci Lett 70:393–397

Van Luijtelaar ELJM, Drinkenburg WHIM, van Rijn CM, Coenen AML (2002) Rat models of genetic absence epilepsy: what do EEG spike-wave discharges tell us about drug effects? Methods Find Exp Clin Pharmacol 24 Suppl D:65–70

Van Raay L, Jovanovska V, Morris MJ, O'Brien TJ (2012) Focal administration of neuropeptide Y into the S2 somatosensory cortex maximally suppresses absence seizures in a genetic rat model. Epilepsia 53:477–484

Vandecasteele M, M S, Royer S, Belluscio M, Berényi A, Diba K, Fujisawa S, Grosmark A, Mao D, Mizuseki K, Patel J, Stark E, Sullivan D, Watson B, Buzsáki G (2012) Large-scale recording of neurons by movable silicon probes in behaving rodents. J Vis Exp:e3568

Varga C, Sík A, Lavallée P, Deschênes M (2002) Dendroarchitecture of relay cells in thalamic barreloids: a substrate for cross-whisker modulation. J Neurosci 22:6186–6194

Veinante P, Lavallée P, Deschênes M (2000) Corticothalamic projections from layer 5 of the vibrissal barrel cortex in the rat. J Comp Neurol 424:197–204

Velasco M, Velasco F, Velasco AL, Luján M, Vázquez del Mercado J (1989) Epileptiform EEG activities of the centromedian thalamic nuclei in patients with intractable partial motor, complex partial, and generalized seizures. Epilepsia 30:295–306

Vergnes M, Boehrer A, He X, Greney H, Dontenwill M, Cook J, Marescaux C (2001) Differential sensitivity to inverse agonists of GABA(A)/benzodiazepine receptors in rats with genetic absence-epilepsy. Epilepsy Res 47:43–53

Vergnes M, Boehrer A, Reibel S, Simler S, Marescaux C (2000) Selective susceptibility to inhibitors of GABA synthesis and antagonists of GABA(A) receptor in rats with genetic absence epilepsy. Exp Neurol 161:714–723

Vergnes M, Boehrer A, Simler S, Bernasconi R, Marescaux C (1997) Opposite effects of GABA B receptor antagonists on absences and convulsive seizures. :245–255.

Vergnes M, Marescaux C (1992) Cortical and thalamic lesions in rats with genetic absence epilepsy. J Neural Transm Suppl 35:71–83

Vergnes M, Marescaux C, Depaulis A (1990) Mapping of spontaneous spike and wave discharges in Wistar rats with genetic generalized non-convulsive epilepsy. Brain Res 523:87–91

Vergnes M, Marescaux C, Depaulis A, Micheletti G, Warter J (1986) Short Communications Ontogeny of spontaneous petit mal-like seizures in Wistar rats. 30:85–87.

Vergnes M, Marescaux C, Depaulis A, Micheletti G, Warter JM (1987) Spontaneous spike and wave discharges in thalamus and cortex in a rat model of genetic petit mal-like seizures. Exp Neurol 96:127–136

Vergnes M, Marescaux C, Micheletti G, Reis J (1982) Spontaneous paroxysmal electroclinical patterns in rat: a model of generalized non-convulsive epilepsy. Neurosci Lett 33:0–4

Vitko I, Bidaud I, Arias JM, Mezghrani A, Lory P, Perez-Reyes E (2007) The I-II loop controls plasma membrane expression and gating of Ca(v)3.2 T-type Ca2+ channels: a paradigm for childhood absence epilepsy mutations. J Neurosci 27:322–330

Vitko I, Chen Y, Arias JM, Shen Y, Wu X-R, Perez-Reyes E (2005) Functional characterization and neuronal modeling of the effects of childhood absence epilepsy variants of CACNA1H, a T-type calcium channel. J Neurosci 25:4844–4855

Von Krosigk M, Bal T, McCormick DA (1993) Cellular mechanisms of a synchronized oscillation in the thalamus. Science (80-) 261:361–364

Wakamori M, Yamazaki K, Matsunodaira H, Teramoto T, Tanaka I, Niidome T, Sawada K, Nishizawa Y, Sekiguchi N, Mori E, Mori Y, Imoto K (1998) Single tottering mutations responsible for the neuropathic phenotype of the P-type calcium channel. J Biol Chem 273:34857–34867

Wallace RH, Marini C, Petrou S, Harkin L a, Bowser DN, Panchal RG, Williams DA, Sutherland GR, Mulley JC, Scheffer IE, Berkovic SF (2001) Mutant GABA(A) receptor gamma2-subunit in childhood absence epilepsy and febrile seizures. Nat Genet 28:49–52

Wang J, You X, Wu W, Guillen MR, Cabrerizo M, Sullivan J, Donner E, Bjornson B, Gaillard WD, Adjouadi M (2013) Classification of fMRI patterns-A study of the language network segregation in pediatric localization related epilepsy. Hum Brain Mapp

Wang J, Zhang Y, Liang J, Pan H, Wu H, Xu K, Liu X, Jiang Y, Shen Y, Wu X (2006) CACNA1I is not associated with childhood absence epilepsy in the Chinese Han population. Pediatr Neurol 35:187–190

Wester JC, Contreras D (2013) Differential modulation of spontaneous and evoked thalamocortical network activity by acetylcholine level in vitro. J Neurosci 33:17951–17966

Wiest MC, Nicolelis MAL (2003) Behavioral detection of tactile stimuli during 7-12 Hz cortical oscillations in awake rats. Nat Neurosci 6:913–914

Williams D (1953) A study of thalamic and cortical rhythms in petit mal. Brain 76:50–69

Williams SR, Tóth TI, Turner JP, Hughes SW, Crunelli V (1997a) The "window" component of the low threshold Ca2+ current produces input signal amplification and bistability in cat and rat thalamocortical neurones. J Physiol 505 (Pt 3:689–705

Williams SR, Turner JP, Hughes SW, Crunelli V (1997b) On the nature of anomalous rectification in thalamocortical neurones of the cat ventrobasal thalamus in vitro. J Physiol 505 (Pt 3:727–747

Willner P (1984) The validity of animal models of depression. Psychopharmacology (Berl) 83:1–16

Wirrell EC, Camfield CS, Camfield PR, Dooley JM, Gordon KE, Smith B (1997) Long-term psychosocial outcome in typical absence epilepsy. Sometimes a wolf in sheeps' clothing. Arch Pediatr Adolesc Med 151:152–158

Woermann FG, Sisodiya SM, Free SL, Duncan JS (1998) Quantitative MRI in patients with idiopathic generalized epilepsy. Evidence of widespread cerebral structural changes. Brain 121 (Pt 9:1661–1667

Yalçın O (2012) Genes and molecular mechanisms involved in the epileptogenesis of idiopathic absence epilepsies. Seizure 21:79–86

Yang Y-C, Hu C-C, Huang C-S, Chou P-Y (2013) Thalamic synaptic transmission of sensory information modulated by synergistic interaction of adenosine and serotonin. J Neurochem

Yang Z-Q et al. (2008) Discovery of 1,4-substituted piperidines as potent and selective inhibitors of T-type calcium channels. J Med Chem 51:6471–6477

Yeni SN, Kabasakal L, Yalçinkaya C, Nişli C, Dervent A (2000) Ictal and interictal SPECT findings in childhood absence epilepsy. Seizure 9:265–269

Zaman T, Lee K, Park C, Paydar A, Choi JH, Cheong E, Lee CJ, Shin H-S (2011) Cav2.3 channels are critical for oscillatory burst discharges in the reticular thalamus and absence epilepsy. Neuron 70:95–108

Zhan XJ, Cox CL, Rinzel J, Sherman SM (1999) Current clamp and modeling studies of low-threshold calcium spikes in cells of the cat's lateral geniculate nucleus. J Neurophysiol 81:2360–2373

Zhan XJ, Cox CL, Sherman SM (2000) Dendritic depolarization efficiently attenuates low-threshold calcium spikes in thalamic relay cells. J Neurosci 20:3909–3914

Zhang SJ, Huguenard JR, Prince DA (1997) GABAA receptor-mediated Cl- currents in rat thalamic reticular and relay neurons. J Neurophysiol 78:2280–2286

Zhang X, Ju G, Le Gal La Salle G (1991) Fos expression in GHB-induced generalized absence epilepsy in the thalamus of the rat. Neuroreport 2:469–472

Zhang Y, Mori M, Burgess DL, Noebels JL (2002) Mutations in high-voltage-activated calcium channel genes stimulate low-voltage-activated currents in mouse thalamic relay neurons. J Neurosci 22:6362–6371

Zhang Y, Vilaythong AP, Yoshor D, Noebels JL (2004) Elevated thalamic low-voltage-activated currents precede the onset of absence epilepsy in the SNAP25-deficient mouse mutant coloboma. J Neurosci 24:5239–5248

Zhang Z-W, Deschenes M (1997) Intracortical Axonal Projections of Lamina VI Cells of the Primary Somatosensory Cortex in the Rat: A Single-Cell Labeling Study. J Neurosci 17:6365–6379

Zhang ZW, Deschênes M (1997) Intracortical axonal projections of lamina VI cells of the primary somatosensory cortex in the rat: a single-cell labeling study. J Neurosci 17:6365–6379

Zhong X, Liu JR, Kyle JW, Hanck D a, Agnew WS (2006) A profile of alternative RNA splicing and transcript variation of CACNA1H, a human T-channel gene candidate for idiopathic generalized epilepsies. Hum Mol Genet 15:1497–1512

Zhou Q, Godwin DW, O'Malley DM, Adams PR (1997) Visualization of calcium influx through channels that shape the burst and tonic firing modes of thalamic relay cells. J Neurophysiol 77:2816–2825

Zhu JJ, Uhlrich DJ, Lytton WW (1999) Burst firing in identified rat geniculate interneurons. Neuroscience 91:1445–1460

Zhu L, Blethyn KL, Cope DW, Tsomaia V, Crunelli V, Hughes SW (2006) Nucleus- and species-specific properties of the slow (<1 Hz) sleep oscillation in thalamocortical neurons. Neuroscience 141:621–636

Zhuravleva SO, Kostyuk PG, Shuba YM (2001) Subtypes of low voltage-activated Ca 2+ channels in laterodorsal thalamic neurons: possible localization and physiological roles. Pflugers Arch Eur J Physiol 441:832–839